Impact of Prokaryotic Phospholipid Translocation on Antimicrobial Resistance

Dissertation

der Mathematisch-Naturwissenschaftlichen Fakultät

der Eberhard Karls Universität Tübingen

zur Erlangung des Grades eines

Doktors der Naturwissenschaften

(Dr. rer. nat.)

vorgelegt von

Janna Nadine Hauser

aus Friedrichshafen

Tübingen

2022

Gedruckt mit Genehmigung der Mathematisch-Naturwissenschaftlichen Fakultät der Eberhard Karls Universität Tübingen.

Tag der mündlichen Qualifikation:	22.11.2022
Dekan:	Prof. Dr. Thilo Stehle
1. Berichterstatter:	Prof. Dr. Andreas Peschel
2. Berichterstatter:	Prof. Dr. Friedrich Götz

Table of contents

Abstract

The increasing rates of multi-resistant bacteria represent a major human health threat. Therefore, development of novel anti-infective strategies and understanding of antimicrobial resistance mechanisms is crucial. The clinically relevant pathogen *Staphylococcus aureus* uses the 'Multiple Peptide Resistance Factor' (MprF) to resist treatment with daptomycin, a calcium-dependent antibiotic of last resort whose mode of action is still not fully understood. To gain resistance, MprF synthetizes the positively charged lipid lysyl-phosphatidylglycerol (Lys-PG) and translocates it from the inner to the outer cytoplasmic leaflet. This process leads to an increase in cell surface charge, and thereby repulsion of cationic antimicrobial peptides (CAMP) and CAMP-like antibiotics.

During daptomycin treatment, single nucleotide polymorphisms in the *mprF* gene frequently take place, which can lead to a further increase in resistance and thereby a failure in treatment of *S. aureus* infections. Here, we analyze frequently found mutations, mediating a daptomycin-resistant phenotype. According to our data, we conclude that in a genetically defined background T345A may alter the substrate range of the MprF flippase to directly translocate daptomycin, because Lys-PG synthesis, translocation or cell surface charge were not affected while mutated MprF exhibited weakened intramolecular domain interaction.

Since MprF is not an essential protein but a critical virulence factor, we developed monoclonal antibodies (mAB) targeting several epitopes of potential extracellular loops of MprF. Here, we describe a mAB which rendered *S. aureus* susceptible to combinational treatment with antibiotics or antimicrobial peptides and reduces the survival in human polymorphonuclear leukocytes (PMN) treatment. Furthermore, we demonstrate novel mechanistical insights into the translocation process of bacterial phospholipids, which we conclude from the proof of the targeted loop being exposed at both sides of the membrane leaflet.

Apart from MprF, bacterial flippase proteins translocating phospholipids between the leaflets of the cytoplasmic membrane have remained largely unknown. Here, we demonstrate the widespread presence of the MprF flippase domain in Bacteria and Archaea. This domain can be found fused to different types of enzymes or encoded as a separate protein. The interaction with many phospholipid-synthetic enzymes and the impact on membrane fluidity and fitness in *Escherichia coli* led us to name this domain 'Prokaryotic Phospholipid Translocator' (PplT) and to propose a critical role in cellular homeostasis.

Our findings highlight novel mechanistical insights into the translocation process of bacterial membrane lipids, which may instruct new anti-infective approaches to eradicate or disarm invading pathogens.

Zusammenfassung

Die Zunahme multiresistenter Bakterien stellt eine große Bedrohung für die menschliche Gesundheit dar, daher ist die Entwicklung neuartiger antiinfektiöser Strategien und das Verständnis antimikrobieller Resistenzmechanismen von entscheidender Bedeutung. Der klinisch relevante Erreger *Staphylococcus aureus* nutzt den 'Multiple Peptide Resistance Factor' (MprF), um die Behandlung mit Daptomycin, einem kalziumabhängigen Reserveantibiotikum mit bislang unvollständig aufgeklärter Wirkungsweise, zu kompromittieren. Um Resistenz zu erlangen, synthetisiert MprF das positiv geladene Lipid Lysyl-Phosphatidylglycerin (Lys-PG) und transloziert es von der inneren zur äußeren Schicht der Zytoplasmamembran. Dieser Prozess führt zu einer Erhöhung der Zelloberflächenladung und stößt dadurch kationische antimikrobielle Peptide (KAMP) und KAMP-ähnliche Antibiotika ab.

Während der Behandlung mit Daptomycin kommt es häufig zu Einzelnukleotid-Polymorphismen im *mprF* Gen, die zu einer zusätzlichen Resistenzsteigerung und somit zu einem Therapieversagen bei Infektionen durch *S. aureus* führen können. Wir untersuchen einige der häufig gefundenen Mutationen, die einen Daptomycin-resistenten Phänotyp vermitteln. Gemäß der unbeeinflussten Lys-PG-Synthese, -Translokation und Zelloberflächenladung schlussfolgern wir, dass die Mutation T345A in einem genetisch-definierten Stammhintergrund in der Lage ist, die Substratspezifität der MprF-Flippase zu ändern, wodurch Daptomycin direkt transloziert werden könnte. Hierfür spricht ebenfalls die gezeigte geschwächte intramolekulare Interaktion der einzelnen Domänen, die durch die Mutation hervorgerufen wird.

MprF ist kein essentielles Protein, jedoch ein kritischer Virulenzfaktor. Daher haben wir monoklonale Antikörper (mAK) gegen verschiedene Epitope potentiell extrazellulär-gelegener Schleifen des MprF-Proteins entwickelt. *S. aureus* zeigt eine erhöhte Sensitivität gegenüber einer der untersuchten mAK während der Kombinationsbehandlung mit Antibiotika oder antimikrobiellen Peptiden, sowie die Reduktion der Überlebensrate während der Behandlung mit humanen polymorphkernigen Leukozyten. Darüber hinaus demonstrieren wir neue mechanistische Einblicke in den Translokationsprozess bakterieller Phospholipide, die wir aus der Exposition der vom mAK gebundenen Schleifen des MprF-Proteins an beiden Membranseiten schlussfolgern.

Mit Ausnahme von MprF sind bakterielle Flippase-Proteine, die Phospholipide zwischen den beiden Schichten der Zytoplasmamembran transportieren, noch weitgehend unbekannt. Wir

demonstrieren die weite Verbreitung der MprF-Flippase-Domäne in Bakterien und Archaeen, welches mit verschiedenen Enzymen fusioniert oder als separat kodiertes Protein vorgefunden werden kann. Die Interaktionsfähigkeit mit verschiedenen Enzymen der Phospholipid-Biosynthese, sowie die Auswirkungen auf die Membranfluidität und Fitness in *Escherichia coli* lassen uns die Domäne ’Prokaryotic Phospholipid Translocator“ (PplT) nennen und eine entscheidende Rolle in der zellulären Homöostase vermuten.

Unsere Ergebnisse bieten neue mechanistische Einblicke in den Translokationsprozess bakterieller Membranlipide und beleuchten potenzielle Ansatzpunkte zur Entwicklung antiinfektiöser Strategien zur Eradikation eindringender Erreger.

Chapter 1

Prokaryotic Phospholipid Translocation in Cytoplasmic Membranes

Janna N. Hauser[1,2,3], Christoph J. Slavetinsky[1,2,3,4], Andreas Peschel[1,2,3]

[1]Interfaculty Institute of Microbiology and Infection Medicine Tübingen, Infection Biology Section, University of Tübingen, Germany.
[2]German Center for Infection Research (DZIF), partner site Tübingen, Germany.
[3]Cluster of Excellence EXC2124 Controlling Microbes to Fight Infection, University of Tübingen, Germany
[4]Pediatric Surgery and Urology, University Children's Hospital Tübingen, University of Tübingen, Germany.

Ready for submission

1. Prokaryotic phospholipids - building blocks of membranes

Bacteria are constantly challenged by external hazards, like nutrient starvation, changes in osmolarity, exposure to surfactant molecules, and antibiotic treatment. Because outer and cytoplasmic membranes represent an intersection between cytoplasm and extracellular surrounding, a fast and continuous adaptation of bacterial membranes to environmental conditions is crucial for survival [1].

Most prokaryotic membranes are composed of amphipathic phospholipids, consisting of two lipophilic fatty acid chains, a phosphate group, a glycerol moiety, and a variable polar head group [2]. To form a bilayered cytoplasmic membrane, the polar head groups of the inner leaflet are faced to the cytoplasm, while the head groups of the outer leaflet are directed outward. Although cytoplasmic membranes differ between bacterial species, they are usually composed of the three major phospholipids, named phosphatidylglycerol (PG), phosphatidylethanolamine (PE), and cardiolipin (CL). The cytoplasmic membrane of *Escherichia coli* and most Enterobacteriaceae harbors about 75% PE, 20% PG and up to 5% CL [3, 4], whereas some Firmicutes like staphylococci, enterococci and streptococci lack PE in their membranes, rendering PG the main phospholipid [5]. Beside the three major ones, minor phospholipids like phosphatidylserine (PS), and phosphatidylinositol (PI) can be found integrated in bacterial cytoplasmic membranes [6, 7]. In *E. coli* and other γ-proteobacteria, PG, PE, PS, and CL are synthesized via the Kennedy pathway [8]. This pathway, starting with CDP-diacylglycerol (CDP-DAG), splits into two arms, which either results in synthesis of PG and CL with phosphatidylglycerolphosphate as intermediate, or formation of PS, PE and CL [8]. To increase the variety, many bacteria modify their membrane phospholipids. The head group of PG and CL can be modified by aminoacylation (aaPG, aaCL) in both, Gram-positive and Gram-negative bacteria [9-12]. Therefor one amino acid like lysine, alanine, arginine, and ornithine, donated by an aminoacyl tRNA [13, 14], is linked to one PG or CL molecule, resulting in formation of aaPG or aaCL (Lys-PG, Lys-CL, Ala-PG, Ala-CL, Arg-PG, Orn-PG), respectively [9-12, 15-18]. The formation of aaPG is mediated by homologs of the 'Multiple Peptide Resistance Factor' MprF [9, 11, 12, 14], while the pathway for synthesis of aaCL has been less studied yet. Based on findings in *Listeria monocytogenes*, it was speculated that the aaPGS could have a relaxed substrate specificity, accepting PG and CL [19], or that the condensation of one PG and one aaPG molecule, like in the CL synthase (Cls)-mediated synthesis of unmodified CL [20], results in aaCL formation. The formation of acyl-PG by transfer of an acyl group to the glycerol moiety of PG further diversifies the lipid composition in some *Salmonella* species [21]. Although this type of PG modification was already described in the early 1970s, the responsible acyltransferase remains unknown. Methylation of PE is another example, utilized by some bacteria to increase the phospholipid diversity. Formation of monomethyl-PE (MMPE), dimethyl-PE (DMPE) and trimethyl-PE, better known as phosphatidylcholine (PC), is

synthesized by phospholipid N-methyltransferases (Pmts), which uses S-adenosylmethionine as methyl donor [22-24]. Some bacteria harbor an alternative PC synthesis mechanism, where the phosphatidylcholine synthase (Pcs) condensates CDP-DAG with exogenous, often host-derived choline [25, 26]. Although methylated PE derivatives occur as intermediates during PC synthesis in most PC synthesizing bacteria, some species end up with MMPE or DMPE as adequate membrane incorporated lipids [2, 27, 28]. Instead of modification by adding additional groups, deacylation of phospholipids further diversifies the membrane lipid repertoire. In most Gram-negatives, the synthesis of lysophospholipids occurs as metabolic intermediate during N-acetyltransferase (Lnt)-mediated acyl group transfer from PE, PG, or CL donors to the major outer membrane lipoprotein Lpp, which results in formation of lysophospholipids (Lyso-PE, Lyso-CL, Lyso-PG) [29-31]. Mostly, lysophospholipids get recycled immediately by reacylation [31]. Nevertheless, Lyso-PE can also be found accumulated in the cytoplasmic membrane of some highly specialized bacterial genera, like *Neisseria* and *Helicobacter* [32, 33]. The role of lysophospholipids, besides being a metabolic intermediate, is poorly understood in prokaryotes, but it is found to be a potent chemoattractant [34], stimulation factor [35, 36] and biomarker for diseases [37, 38] in eukaryotes.

Beside possessing a cytoplasmic membrane, Gram-negative bacteria are covered by an additional and differently structured membrane, the outer membrane. This special type of membrane is constructed as a highly asymmetric bilayer, where phospholipids like PG and PE form its inner leaflet, while the outer layer is shapes by the glycolipid Lipid A [39, 40]. Lipid A is also known as the membrane anchor of the lipopolysaccharide (LPS), which consists of Lipid A and a long polysaccharide chain, called O-antigen. Since the focus of this Review is on phospholipids, Lipid A will not be further discussed in this section.

2. Prokaryotic lipid translocases - enigmatic proteins

2.1 Flipping, flopping, and scrambling - subclasses of translocases

In prokaryotes, phospholipid biosynthesis is facilitated at the inner leaflet of the cytoplasmic membrane bilayer [4]. To keep membranes intact even in fast changing or unfavorable conditions, a high level of phospholipid homeostasis and turnover in both leaflets is necessary [9, 11, 41, 42]. While the in-plane distribution within one membrane layer occurs at high rates via spontaneous lateral diffusion (diffusion coefficient $D=10^{-8}$ cm^2/s) [43], due to the amphiphilicity of phospholipids the transverse movement between the leaflets seems to be less efficient. Transverse diffusion (Fig. 1A), also known as flip-flop, happens independently of the phospholipid head group and does not need metabolic energy [44]. Yet, phospholipid translocation would need half-times of hours to weeks ($D=10^{-15}$ s^{-1}), if spontaneous flip-flop would be the only mechanism of distribution [43]. *In vivo* studies in the Gram-positive bacterium *Bacillus megaterium* revealed a 30,000 times faster translocation of freshly synthesized

phospholipids as theoretically calculated for flip-flop [45]. Interestingly, *in vitro* assays with isolated vesicles from cytoplasmic membranes of *B. megaterium* and *E. coli* confirmed a fast translocation, with half-times of seconds to minutes [46, 47]. Hence, phospholipid translocation in biological membranes and intact bacteria must be an enzyme-driven process.

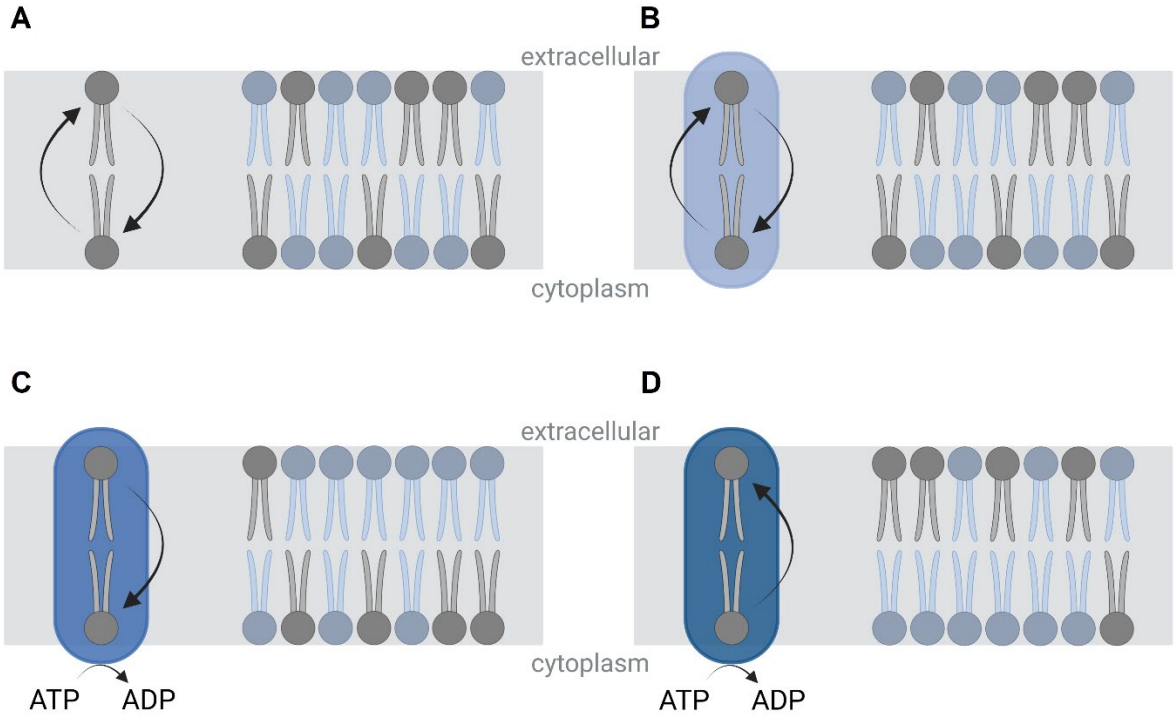

Figure 1: Subclasses of phospholipid translocases and their schematic translocation mechanisms, based on the eukaryotic concept. Translocation by transverse diffusion (A), scrambling (B), flipping (C), and flopping (D) are shown. The phospholipid distribution within the membrane is indicated by the lipid of interest (grey lipid) and other phospholipids (blue lipids). Blue ellipses indicate the use of a protein for the translocation process, black arrows the direction of translocation.

The term “flippase” was established in the 1970’s by Mark Bretscher, who referred to putative enzymes that catalyze the transmembrane distribution of freshly synthesized choline phospholipids in natural membranes [48]. Nowadays, the term “flippase” and its equivalent “translocase” is still used and defined as a membrane embedded protein that promote the transverse translocation of (phospho-)lipids between the membrane leaflets, independent from the direction of transport. The knowledge of phospholipid translocation is well established in membranes of erythrocytes, Golgi apparatus, and the endoplasmic reticulum, therefore the different principles of flippase proteins will be explained based on the eukaryotic status quo. Translocases can be divided into three subgroups (I) “flippases”, (II) “floppases”, and (III) “scramblases”, based on their direction of phospholipid translocation and the required energy source (Fig. 1).

(I) Proteins of the subgroup “flippases” move phospholipids from the outer leaflet to the cytoplasmic one, therefor energy in form of ATP is required (Fig. 1C). The hydrolysis of one molecule ATP per transported phospholipid [49] allows to transfer lipids against a concentration gradient and thereby generating an asymmetrical lipid distribution. The best

studied representatives of this subgroup belong to the P-type ATPase superfamily, which can be divided into five classes (P_1 to P_5), based on their structural differences [50]. So far, P_4-ATPases are the only known class with specificity to lipids as substrate. Although lipid-translocating P_4-ATPases could be identified in mammals, plants, and yeasts, only little is known about the process of flipping. Some of the lipid-flipping P_4-ATPases seem to have a substrate specificity to PS, but also PE and PC translocating examples can be found in this group of flippases [51-56].

(II) Proteins of the subgroup “floppases” translocate lipids from the inner to the outer leaflet of the membrane in an ATP-dependent manner (Fig. 1D). Due to the usage of ATP, the translocation process of floppases can also generate a concentration gradient of the translocated lipid. Typical examples for floppases can be found in the ATP-binding cassette (ABC) superfamily, which play a role in many cellular processes, but are also known to transport various substrates including ions, drugs, sugars, and peptides [57]. Because of their pathophysiology and the importance in treatment of diseases, probably the best studied ABC transporters are the human and murine ones. In humans, 48 ABC transporters could be identified and, according to phylogenetic properties, grouped into seven families (ABCA to ABCG) [58]. Although several of the human ABC transporters could be associated to lipid-linked diseases with abnormal transport and homeostasis [59-65], the defined substrate and the proof of lipid translocation has only been provided for a minority of proteins. One of the first hints for a role of ABC transporters in direct lipid translocation was observed in a mouse model, where the mutation of the murine ABCB4 (also known as MDR2 in mice and MDR3 in humans) leads to an absence of PC in the bile [66]. Although ABC transporters can be grouped by sequence similarities, the substrate specificity and affinity can be diverse within one group. An example can be found in the ABCB group, where ABCB4 was found to be highly specific for PC, while the closely related ABCB1 (also known as MDR1) ABC transporter is able to translocate a variety of lipids [67]. The behavioral diversity within this group makes it hard to draw conclusions from one member to the other.

(III) In contrast to flippases and floppases, proteins belonging to the subgroup “scramblases” translocate phospholipids in a substrate-unspecific, energy-independent, but calcium-dependent manner bidirectionally between both membrane leaflets (Fig. 1B) [68, 69]. The translocation process is driven by a concentration gradient generated by the lipid to be transported and stops if an equilibrium is accomplished, indicating an importance in randomization of lipid asymmetry generated during biosynthesis or ATP-dependent translocation [69]. Lipid translocation by scramblases has been described in many eukaryotic membranes, like those of platelets, erythrocytes, and many other cell types [68, 70-72]. Beside constitutively active scramblases, which are especially important for the lipid distribution during biosynthesis and normal cell function [73], inducible scramblase proteins play a particular role

in apoptosis and cell activation [74-77]. Typically, an increase in intracellular calcium activates the inducible scramblase, most likely by a calcium-induced conformational change [78]. Of note, since hydrolysis of ATP is not required for scramblase-mediated phospholipid translocation, it is much faster than transport by flippases or floppases [49, 79, 80].

2.2 Between the layers - mechanisms of transverse lipid translocation

Although the term 'flippase' has been established for five decades and lipid distribution of biological and artificial membrane leaflets can be investigated by various methods, it is still hard to follow the explicit lipid movement mediated by one of the different translocases. Although phospholipid translocating proteins clearly differ in dependence on metabolic energy, substrate specificity, and direction of translocation, the amphipathic property of membrane lipids could probably unite common transport mechanisms. During the translocation process, the lipophilic fatty acid chains remain in the hydrophobic part of the membrane and only change their orientation, while the polar head group must somehow transit the lipophilic part. Until the final proof provides a defined mechanism, the mode of lipid movement through the membrane leaflets remains only partially evidence based.

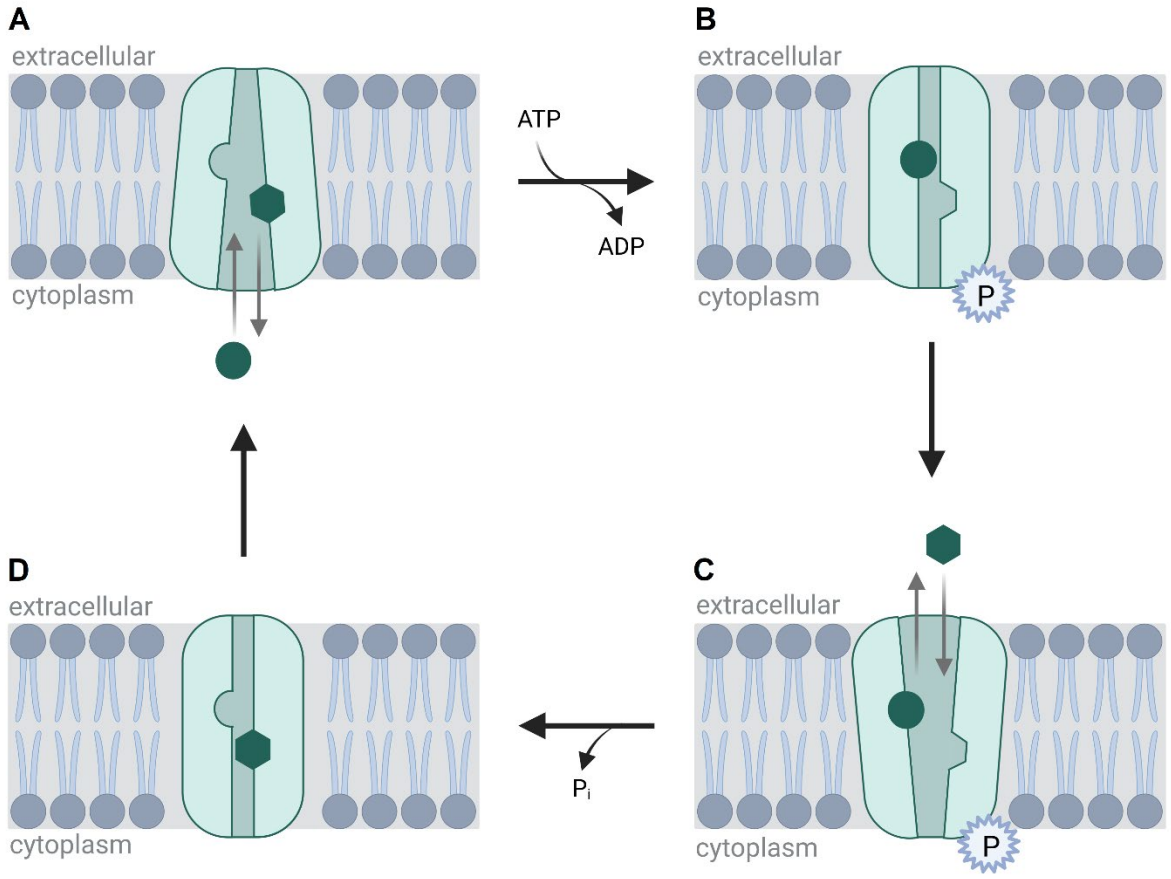

Figure 2: Ion transport through the membrane by P-type ATPases. (A) The first ion (green circle) enters the transporter (turquoise), which is in the E_1 state, from the cytoplasmic side. Phosphorylation of the transporter (blue star, E_1P state) by ATP hydrolysis initiates a conformational change to the E_2P position (B) and ion release to the extracellular side via a canonical channel-like structure (dark turquoise), while a second ion (green hexagon) enters

the transporter (C). (D) The dephosphorylation of the transporter (E_2 state) triggers the transformation to the initial position and the release of the second ion into the cytoplasm.

One approach to get an idea how the translocation process could take place, is the transfer of knowledge of well characterized transporters of the same protein family with already known transport mechanisms. During the catalytic cycle of Na^+K^+-ATPases (P_2ATPase), which takes place as postulated by the Post-Albers model [81], the transport of Na^+ out of the cell triggers the autophosphorylation of the ATPase by ATP hydrolysis (Fig. 2A, B), and the subsequent dephosphorylation initiates the transport of K^+ ions into the cytoplasm (Fig. 2C, D). During transport, the ATPase consists in one of two confirmations (E_1 and E_2) [80] and the canonical substrate binding pocket, where the ion can pass through the membrane, is located within a channel-like region formed by transmembrane segments (TMS) of the protein [82].

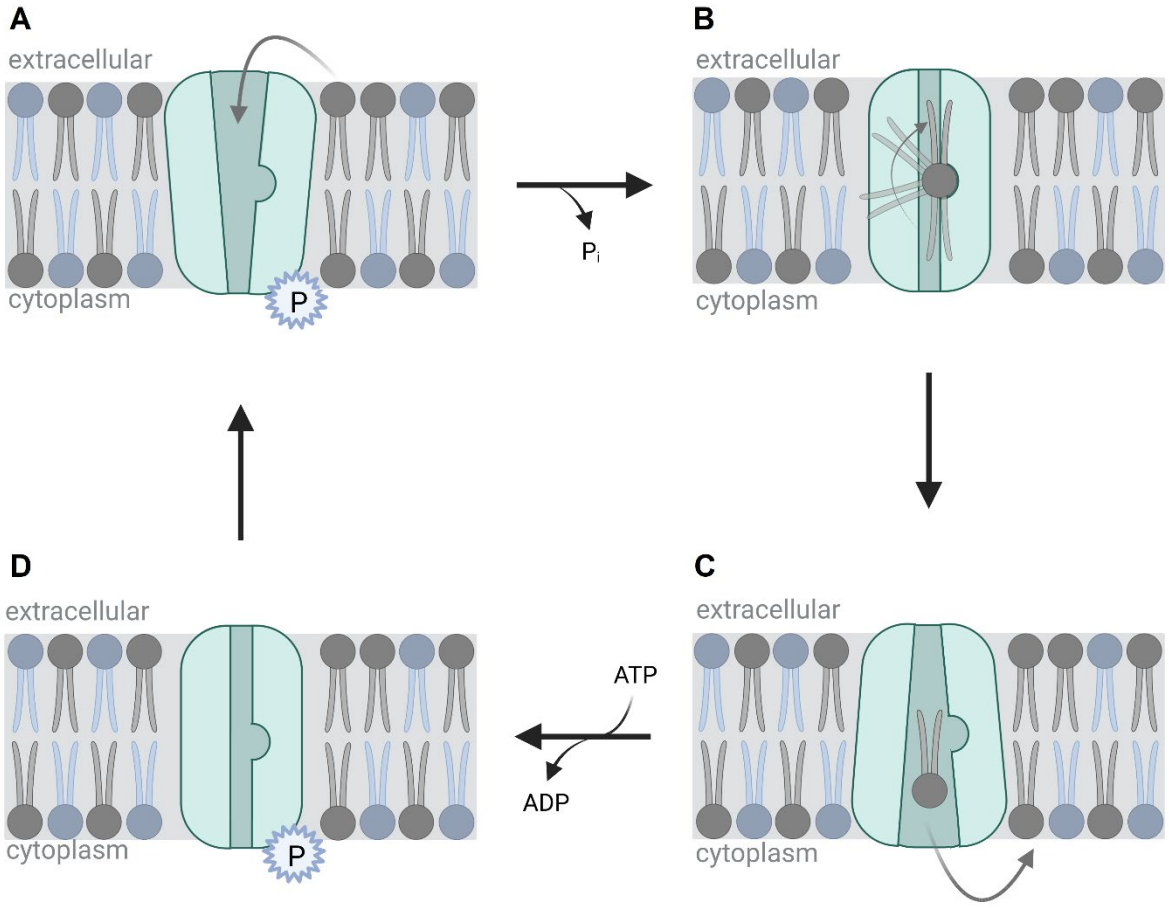

Figure 3: Presumed phospholipid translocation mechanism by P_4ATPases, deviated by well-established transporters of the P-type ATPase protein family. (A) The phospholipid of interest (grey) enters the transporter (turquoise) in the E2P state from the outer leaflet of the membrane. Dephosphorylation initiates a conformational change of the transporter (B) to the E1 state and lipid release into the inner leaflet of the same membrane (C). The transporter converts back while autophosphorylation by ATP hydrolysis (D).

Indeed, P_4ATPases also show a catalytic mechanism of ATP-mediated autophosphorylation, like Na^+K^+-ATPases. In contrast to P_2-ATPases, P_4ATPase-mediated flipping of PS through the membrane has been linked to dephosphorylation, and so far, there is no evidence for the need of a counter-transported ion as trigger (Fig. 3) [80, 83]. In agreement with this possible mode of phospholipid translocation, mutation of the TMS that form the canonical ion binding

pocket showed an altered substrate specificity of the P_4ATPase [80], indicating that these segments are involved in substrate recognition. Although P_2ATPases show a high similarity in sequence and catalytic mechanism of ATP hydrolysis, the properties of the transported ions differ from lipid substrates of P_4ATPases. The larger size of lipids (e.g., dipalmitoylphosphatidylcholine 18.9 Å [84], ellipsoid head radii 4.27-7.63 Å [85]) compared to an ion (ionic radii K^+ 1.37-1.64, Na^+ 0.99-1.39 [86]) and the necessary reorientation of the phospholipid substrate during the translocation process makes it hard to imagine a universal transport mechanism for phospholipids and ions. This difficulty is known as “giant substrate problem” [87] and can be circumvented by the so-called two-gate mechanism [88] as potential transport method.

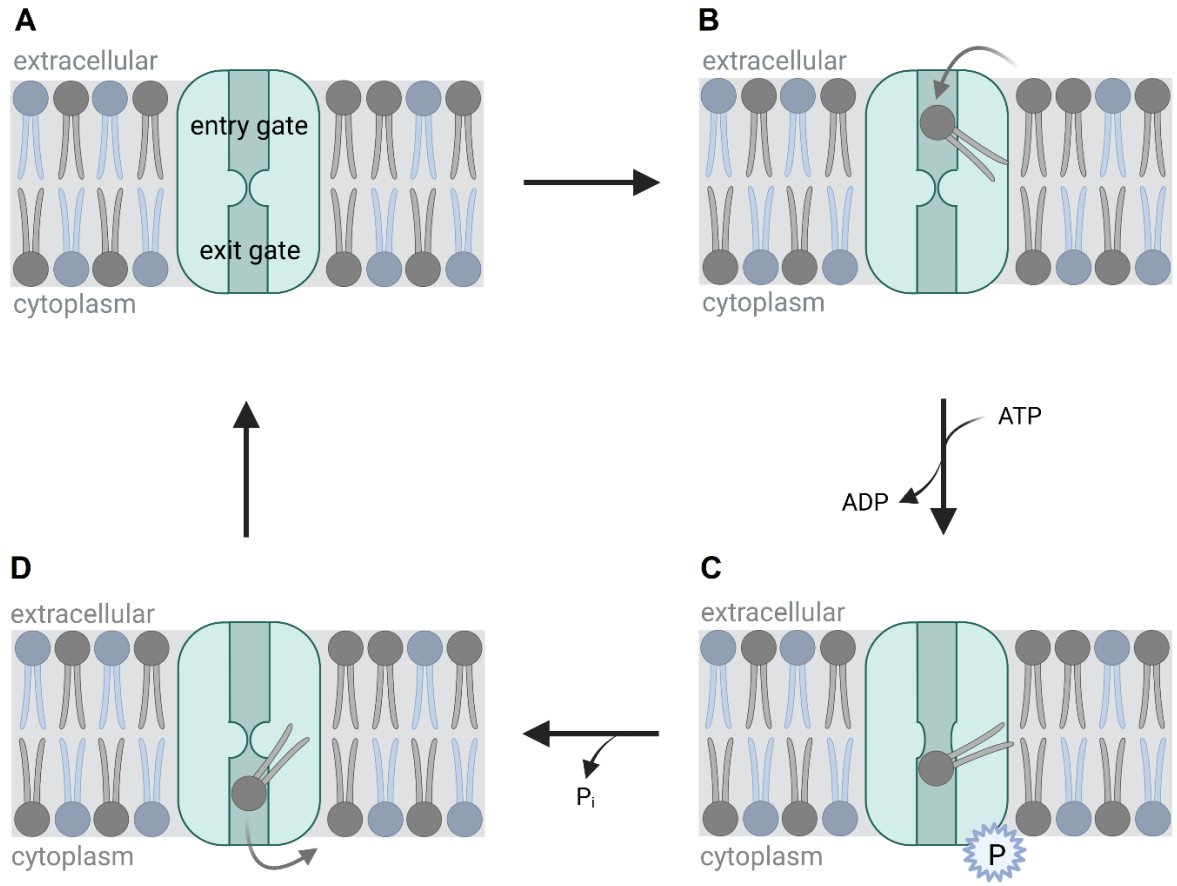

Figure 4: Two-gate model of P_4ATPases for phospholipid translocation. (A) The transporter (turquoise) harbors a noncanonical grove (dark turquoise), which is divided into an entry gate and exit gate. (B) The lipid of interest (grey) enters the entry gate at the outer leaflet of the membrane. The autophosphorylation of the transporter opens a connection between the two gates, that the phospholipid can pass the inner leaflet-located exit gate (C) and gets released (D).

The two-gate model proposes a second so-called “noncanonical pathway” within the P_4ATPases, where the lipid is specifically recognized at the outer leaflet-located “entry gate” (Fig. 4B), translocated upon a slight conformational change (Fig. 4C), and released to the cytoplasmic leaflet through the there located “exit gate” (Fig. 4D) [88]. This hypothesis is supported by mutational experiments of two P_4ATPases in yeast, where mutations correlated to substrate recognition in the proposed entry or exit gate [87, 88]. Of note, the P_4ATPase

undergo the same phosphorylation states during the noncanonical transport as described for the canonical translocation. Currently published cryo-electron microscopy (cryo-EM) data from MprF in *Rhizobium tropici* suggest a similar mechanism for the translocation of aaPGs from the inner to the outer leaflet of the cytoplasmic membrane, as proposed by the two-gate model [89]. In agreement with the two-gate model, aaPGs are specifically recognized at the inner leaflet by the entry gate of MprF (referred as cavity C), translocated by a transiently opened putative channel connection and released to the outer leaflet by the exit gate (referred as cavity P) [89] (for detailed information see section 2.3.1). In comparison to the two-gate model proposed for the P_4ATPase mediated translocation, MprF does not require ATP for the translocation of phospholipids [89, 90].

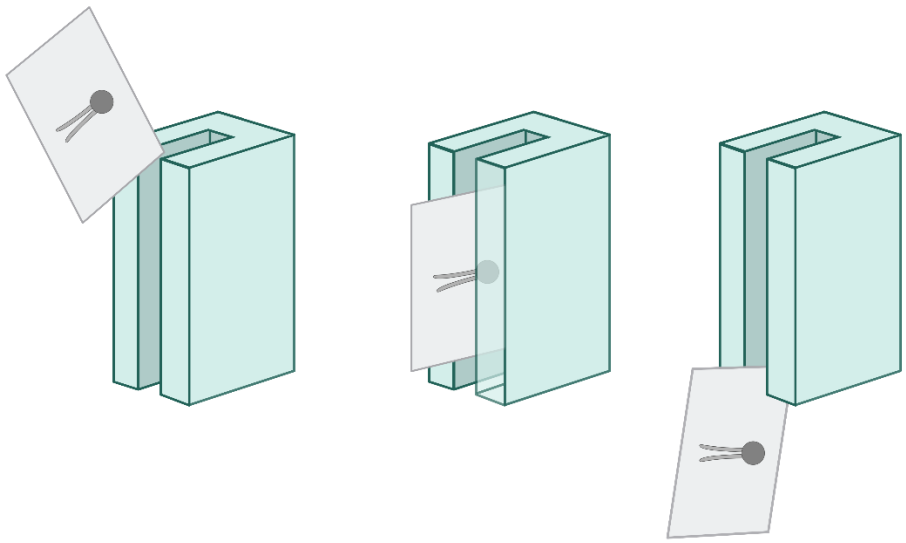

Figure 5: Phospholipid translocation via the credit card model. Only the phospholipid head group (dark grey) enters the protein spanning cleft, formed by the transporter (turquoise), while the lipophilic fatty acid chains (slight grey) remain outside. The method remembers a magnetic strip of a credit card, being pulled through the card reader. Figure adapted from [91].

Another possible and slightly different transport mechanism could be the so-called “credit card model” [91], which is abstracted from the magnetic strip of a credit card being pulled through the card reader (Fig. 5). Here, the translocase only interacts with the polar head group of the phospholipid. A first proof for this model could be found in the crystal structure of the scramblase TMEM16. Crystallization revealed a protein spanning cleft at the bilayer-exposed intersection with a strongly hydrophilic surface at the inner side, which could house the polar head group during phospholipid translocation, while the lipophilic fatty acid chains remain in the hydrophobic layer of the membrane [92]. In accordance with the credit card model, the crystal structure of a plant membrane proton pump (P_3ATPase) showed a large central cavity in a transmembrane domain of the protein, shaped by conserved hydrophilic and charged residues and probably filled with water [93]. Also, P_4ATPases exhibited such a grove in structural homology modeling and molecular simulations [94, 95]. Although the credit card model seems to be an interesting mode of translocation, especially the aspects of substrate

recognition and specificity remain unexplained. Overall, it is probably unlikely that all types of phospholipid translocating proteins share exactly the same mechanism of translocation, especially because they differ in structure, direction of translocation, substrate recognition, and dependence on ATP. Nevertheless, the presence of pore-forming membrane spanning compartments with hydrophilic residues on the inner surface, found in different types of translocases of diverse origins, could hint at the existence of one basic mechanism, probably modified during the evolution of the phospholipid flipping proteins.

2.3 Uncover the scarce - examples of prokaryotic lipid translocases

2.3.1 MprF/PplT domain

Beside the synthase function (see section 1), MprF is able to translocate freshly synthesized aaPGs from the inner to the outer leaflet of the cytoplasmic membrane [90], thereby acting as the first discovered prokaryotic phospholipid translocase. But how does MprF translocate aaPGs through the membrane? Biochemical and structural studies consistently revealed an oligomerization of MprF, most likely as homodimers or homotetramers [89, 96]. The vicinity of MprF homo-oligomers may help to enrich Lys-PG levels in the surrounding leaflet to form a local gradient, which could improve the translocation by the flippase domain. According to the cryo-EM data in *R. tropici* [89], the complex structure of the membrane-imbedded flippase domain forms two deep cavities, separated by a potential channel-like structure (Fig. 6). The aminoacyl head groups of aaPGs are specifically recognized by residues within the first cavity (referred to as cavity C), located at the inner membrane leaflet (Fig. 6C). A trigger, which is not known yet, transiently opens the channel-like connection between the two cavities and the aaPG migrates through the second cavity (referred to as cavity P), which is located close to the outer membrane leaflet, and gets released (Fig. 6D) [89]. The exact mechanisms of Lys-PG entrance in and release out of the cavities still need to be elucidated, but electrostatic repulsive forces between aaPGs and the surface of the cavities could be involved [89]. Two conserved amino acids within the channel-like structure turned out to be essential for the opening and thereby correct translocase-function of the *R. tropici* MprF [89]. In addition, also the interface between synthase domain and flippase domain of MprF seems to be crucial for translocation, since mutations within this area often cause either loss-of-function or gain-of-function of the flippase [89, 97].

It is still unclear if MprF translocates LysPG to create a membrane equilibrium as literature is quite controversial, demonstrating LysPG being present either symmetrically or asymmetrically distributed between the membrane leaflets [90, 98]. Since LysPG is synthesized and thereby inserted in higher concentrations into the inner leaflet, the MprF flippase domain could either act as a scramblase to equilibrate the membrane asymmetry or due to the directed transport

to the outer membrane leaflet, act as a floppase. According to a directed transport, *Pseudomonas aeruginosa* and *Enterococcus faecium* harbor aaPG hydrolases, cleaving off the aminoacyl residue of LysPG to lower the concentration in the outer membrane leaflet [99, 100]. In contrast to ABC transporters, which are classical examples of floppases in eukaryotes, the MprF flippase domain neither has ATP binding motifs nor any reported ATPase activity. This indicates that MprF is not an active primary transporter that translocates aaPGs under ATP consumption. In support of this notion, bioinformatic analysis of MprF suggests a relation to the so-called major facilitator superfamily (MFS) [101], a diverse group of α-helical transmembrane segment-containing transporters, that facilitate diffusion or cation-dependent secondary transport [102]. Beside a similar structure, proton-dependent members of the MFS share a conserved ExxER/K motif and two pairs of salt bridges [103]. The cryo-EM structure of MprF in *R. tropici* revealed at least one of these salt bridges [89], but neither the ExxER/K motif nor a dependence of MprF-mediated transport on proton-motive force (pmf) as energy source could be identified yet.

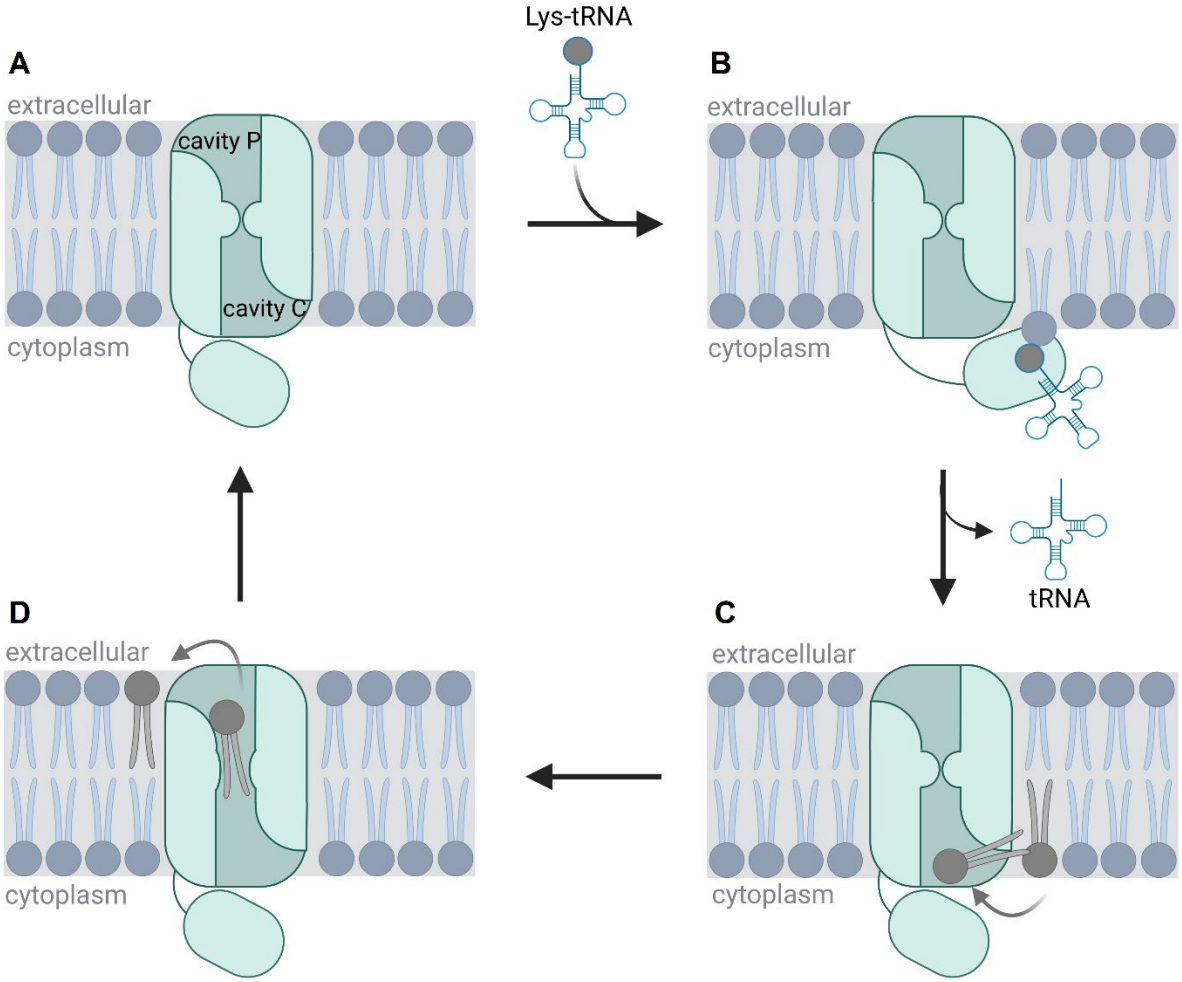

Figure 6: Proposed phospholipid translocation mechanism by MprF in *Rhizobium tropici* [89]. (A) The flippase domain of MprF forms a membrane spanning channel-like structure, divided into two cavities (dark turquoise). (B) The synthase domain of MprF transfers an amino acid residue (lysine) from a charged tRNA (blue cloverleaf structure with dark grey circle attached) to a PG molecule (blue lipid), to generate a Lys-PG molecule (grey lipid). (C) The freshly synthesized Lys-PG enters MprF via the inner membrane-located cavity C. The transiently opened

channel-like connection allows the translocation of the lysinylated phospholipid through cavity P and release into the outer leaflet of the cytoplasmic membrane (D).

The flippase domain seems to have a rather broad substrate specificity, since *S. aureus* MprF have shown the capacity to translocate both Lys-PG and Ala-PG [104], although the organism lacks the ability to produce Ala-PG under natural conditions. In agreement with this finding, cryo-EM data and structure simulations supported the substrate acceptance of both, Lys-PG and Ala-PG also for the *R. tropici* MprF flippase domain, but mentioned the interaction with PG, CL, PE and PS as unfavorable, because of the smaller size and anionic properties of the head groups [89]. Furthermore, our recent publication demonstrates the presence of MprF-homologous flippase domains, referred to as 'prokaryotic phospholipid translocator' (PplT), widespread in Bacteria and Archaea, either encoded as a single protein or fused to different types of enzymes, most likely to fulfill a general role in membrane homeostasis [105]. These findings clearly indicate that MprF flippase domains and probably all PplT domain-containing proteins may not have evolved for the transport of one defined substrate, but for a broader range of lipids.

2.3.2 MsbA

According to sequence identity, the highly conserved MsbA is assigned to the ABC transporter superfamily and is required for the translocation of Lipid A, the membrane anchor of LPS, from the inner to the outer leaflet of the cytoplasmic membrane of Gram-negative bacteria [106]. In *E. coli*, MsbA is the only essential ABC transporter, since mutation cause a lethal accumulation of Lipid A in the cytoplasmic leaflet of the inner membrane [107].

The overall organization of the functional MsbA transporter is consistent with most bacterial members of the ABC superfamily, composed of two transmembrane domains (TMD) and two highly conserved nucleotide binding domains (NBD) at the C-terminal end, important for binding and hydrolysis of ATP [108]. Of note, the *msbA* gene encodes only for one half of the transporter, while the functional protein requires homodimerization which has been solved by crystal structure for some Gram-negative organisms [109]. The exact mode of action and substrate acquisition for MsbA-mediated Lipid A translocation still need to be elucidated. Nevertheless, crystal structures in diverse conformations [108-110] suggest that in the inward-opened state, the TMDs of the MsbA homodimer forms a V-shaped chamber opened to the inner leaflet of the cytoplasmic membrane (Fig. 7A), where Lipid A can enter the port. Of note, the inner surface of MsbA forms a hydrophobic pocket which houses the acyl chains, and a hydrophilic cavity in which the head group of Lipid A is placed [108]. The integration of Lipid A into the binding pocket triggers a slight motion of the two NBDs towards each other to form the inward-occluded state of MsbA, which allows an ATP molecule to interact with these domains (Fig. 7B). Thus, vicinity of the two NBDs and the hydrolysis of the ATP leads to a rearranged

packing of the transmembrane helices of the TMDs and thereby results in an outward-facing V-shaped outward-opened conformation of MsbA and the release of Lipid A (Fig. 7C). MsbA has been shown to have a high ATPase activity [111], which seems to be important for the translocation process, since addition of ATP increased the movement of membrane lipids, while ATP depletion reduced it in a lipid translocation study [112]. Interestingly, ATPase activity of the NBD could be increased 4 to 5 times in the presence of a Lipid A homolog, demonstrating MsbA as a lipid-activated translocase [111].

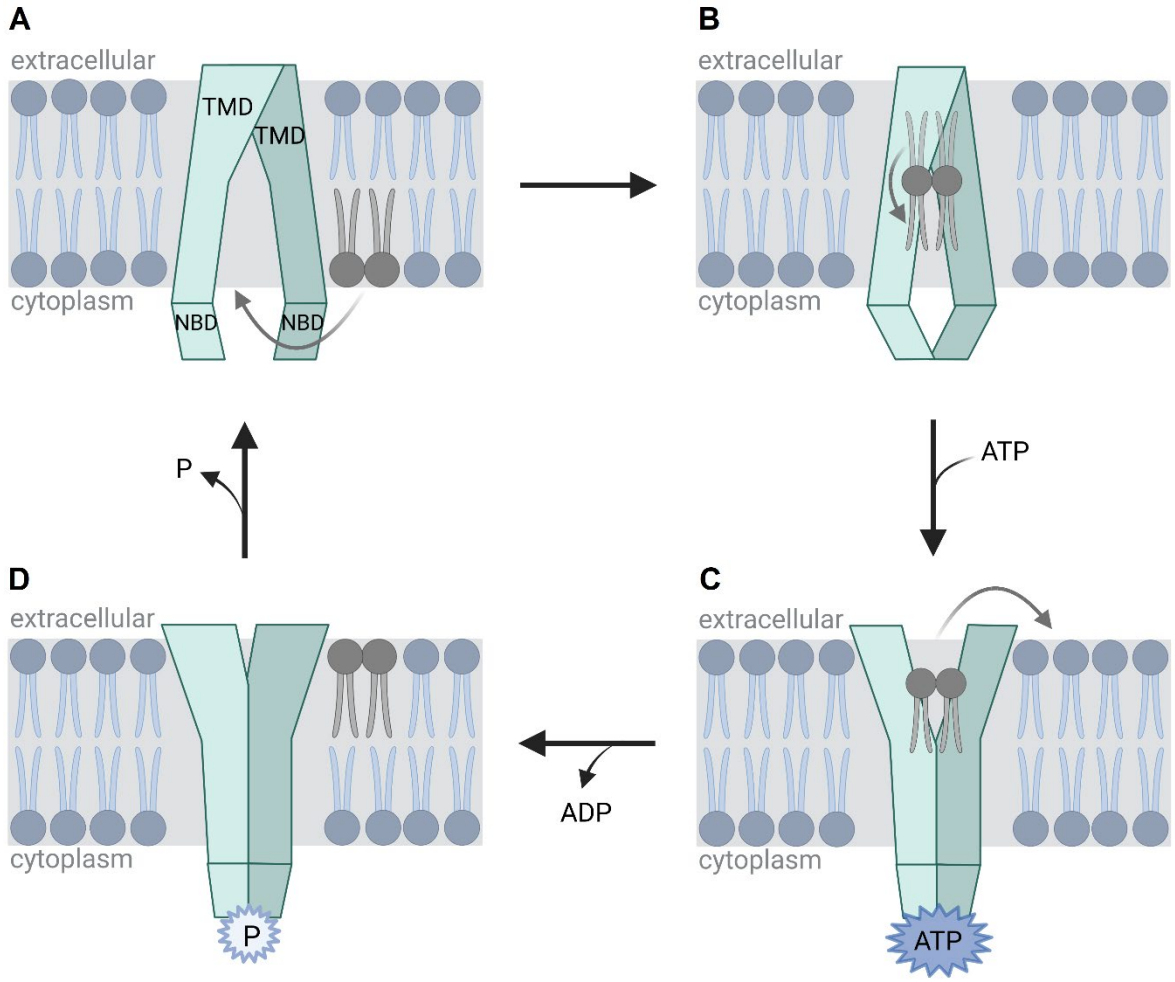

Figure 7: MsbA mediated translocation of Lipid A in the cytoplasmic membrane of Gram-negative bacteria. The functional MsbA consists of a homodimer (indicated in turquoise and dark turquoise), which is formed by two transmembrane domains (TMD) and two nucleotide binding domains (NBD). (A) In the inside-opened state, the two TMDs form a V-shaped chamber, opened to the inner leaflet. Lipid A (grey double-lipid) binding forces the inside-closed formation (B), which allows binding of ATP by the two NBDs. Binding of ATP triggers the conformational change to the outward-opened formation, which allows the release of Lipid A into the outer leaflet (C). (D) Autophosphorylation by ATP hydrolysis mediates the outward-closed formation of MsbA, while dephosphorylation cause another conformational change into the initial position. For a better overview, only the membrane anchor Lipid A is drawn, although LPS would be the target of this translocation process.

Literature shows an abundance of evidence for MsbA being involved specifically in the translocation of Lipid A. However, the substrate specificity seems to be wider, because temperature-induced functional inactivation of MsbA leads to an inhibited transport of all major membrane lipids [113], suggesting a general role in lipid translocation. In agreement with these findings, translocation studies revealed a high translocase activity for the common bacterial

membrane phospholipids PE, PG, and PS, which was significantly lowered up to 45% if the perceived substrate Lipid A was added as competitor [112, 114]. Due to the affiliation to the same superfamily as well-known drug efflux systems, one could speculate that there may be further substrates, like antibiotics for MsbA. At this point the literature is quite controversial, if compounds like daunorubicin, verapamil, or vinblastine could stimulate the MsbA activity and therefore operate as a potential substrate [111, 114-116]. Unaffected from this matter of dispute, the sequence identity to transporters causing bacterial multi-drug resistance can be seen as a hint for the origin of efficient drug-exporting mechanisms in basic lipid homeostasis systems.

2.3.3 Lipid II translocases FtsW/ MurJ/ AmJ

Lipid II, a key intermediate in biosynthesis of the cell wall building block peptidoglycan, is synthetized in the cytoplasm and has to be translocated through the membrane, where it becomes available for the incorporation into the growing cell wall [117]. Lipid II consists of an undecaprenyl pyrophosphate carrier, a N-acetylglucosamine-N-acetylmuramic acid disaccharide and a pentapeptide [118]. Undecaprenyl pyrophosphate is a lipid-like structure with a long C_{55} isoprenoid component anchored in the cytoplasmic membrane. The undecaprenyl pyrophosphate facilitates the universal translocation of glycan or sugar strands across the cytoplasmic membrane and is therefore involved in the biosynthesis of peptidoglycan [118], wall teichoic acids [119], and O-antigen of the lipopolysaccharide [120]. It has been proposed that the Lipid II metabolism is a fast and continuous process, since only a few hundred molecules have been found in the membrane of one cell [121]. Nevertheless, undecaprenyl pyrophosphate-mediated translocation of Lipid II must be a protein-dependent process, because spontaneous flip-flop of lipid bound glycans remains kinetically unfavorable and has been shown to not occur [122]. Moreover, Lipid II translocation experiments on *E. coli*-derived membrane vesicles implied an ATP and pmf-independent mechanism [122]. Potential candidates for the Lipid II translocation have been controversy discussed in the past with main focus on the three proteins FtsW [123], MurJ [124], and AmJ [125].

FtsW came up as a potential Lipid II translocase because the encoding gene is located in the same operon as genes involved in peptidoglycan biosynthesis [123, 126, 127]. Together with its homologs RodA and SpoVE, FtsW is a member of the shape, elongation, division, and sporulation (SEDS) family, with at least one representative of the protein family present in all types of bacteria, synthesizing peptidoglycan [128, 129]. FtsW is an essential membrane imbedded protein, proposed to be composed of 10 TMSs, but a crystal structure still needs to be elucidated [130]. *In vitro* studies with purified protein incorporated into membrane-derived vesicles suggested FtsW not to be head group specific, because FtsW was able to translocate Lipid II and membrane phospholipids, like PG, PE, and PC [123, 131]. These findings also hint

to a generally relaxed substrate specificity of FtsW, because the C_{55} segment of the undecaprenyl phosphate carrier is much longer than the fatty acid residues of membrane phospholipids, which have C_{16}-C_{18} acyl chains. Although FtsW consists of 10 TMSs, experiments revealed a functional protein even if TMS 5-10 are truncated [131]. In agreement with these findings, especially the TMS 4 is suggested to be important for the translocase function, since a full-length FtsW containing amino acid substitutions within this segment failed in Lipid II movement [131]. Interestingly, the substitution-containing protein was still able to translocate phospholipids, which indicates two different mechanisms for translocation of Lipid II and membrane lipids. As mentioned above, the role of FtsW as Lipid II translocase is still controversial, a recent publication mentioned FtsW as glycosyltransferase, involved in the peptidoglycan polymerization during cell division [132].

MurJ, also known as mouse virulence factor N (MviN), was identified as potential Lipid II translocase candidate through a bioinformatic screening [133] and experimental evidences [124]. MurJ is a membrane embedded protein, necessary for viability, shape, and integrity of bacterial cells [133, 134]. Biosynthesis of peptidoglycan is disturbed in a *murJ* depleted mutant, indicated by a decrease of mature peptidoglycan and accumulation of intermediates, like lipid and nucleotide precursors [134]. Due to structural homology, MurJ belongs to the multidrug/ oligosaccharidyl-lipid/ polysaccharide (MOP) exporter superfamily, of which members are already known to translocate undecaprenyl diphosphate carriers across the membrane [135]. Indeed, MurJ showed Lipid II translocase activity in *in vivo* translocation assays with *E. coli* and spheroplasts [124]. A recently published crystal structure of MurJ revealed a composition of 14 TMSs, 12 TMSs form the classical transporter core common to all MOP proteins, while two additional TMSs are unique to MurJ [136]. Of note, the 12 TMSs, that are common to all MOP transporters, are divided into two lobes, the N-lobe is formed by TMS 1-6 and the C-lobe, which consists of TMS 7-12 [136]. A combination of homology modelling with other MOP transporters, mutagenesis studies, and the recently published crystal structure proposed a solvent-exposed central cavity formed by TMS 1-12, and an additional lateral hydrophobic groove shaped by TMS 13-14, both are connected by a gate [136-138] (Fig. 8A). Both structures seem to be essential for Lipid II translocase activity [136-138]. Based on these findings [136-139], the following mechanism for MurJ mediated Lipid II translocation has been proposed: Lipid II enters MurJ in the inward-opened state (Fig. 8A), placing the undecaprenyl pyrophosphate tail in the hydrophobic groove and the disaccharide-pentapeptide part in the inner cleft of the central cavity (Fig. 8B). Binding of Lipid II triggers the inward-occluded state of MurJ, which is able to bind an external sodium ion and perform the outward transition (Fig. 8C). Probably due to the conformational change and the size of the outward-facing cleft, Lipid II is released to the periplasmic space. Binding of an external chloride ion sets MurJ to the inward-closed position (Fig. 8D), while the release of the bound ions to the cytoplasm facilitates

the restorage of the inward-opened state. Actually, not much is known about the substrate specificity of MurJ, but high-throughput mutagenesis revealed the importance of conserved amino acids in the hydrophobic groove, central cavity and connection gate, indicating the importance of the electrostatic interactions with Lipid II for the translocase activity [137, 138, 140].

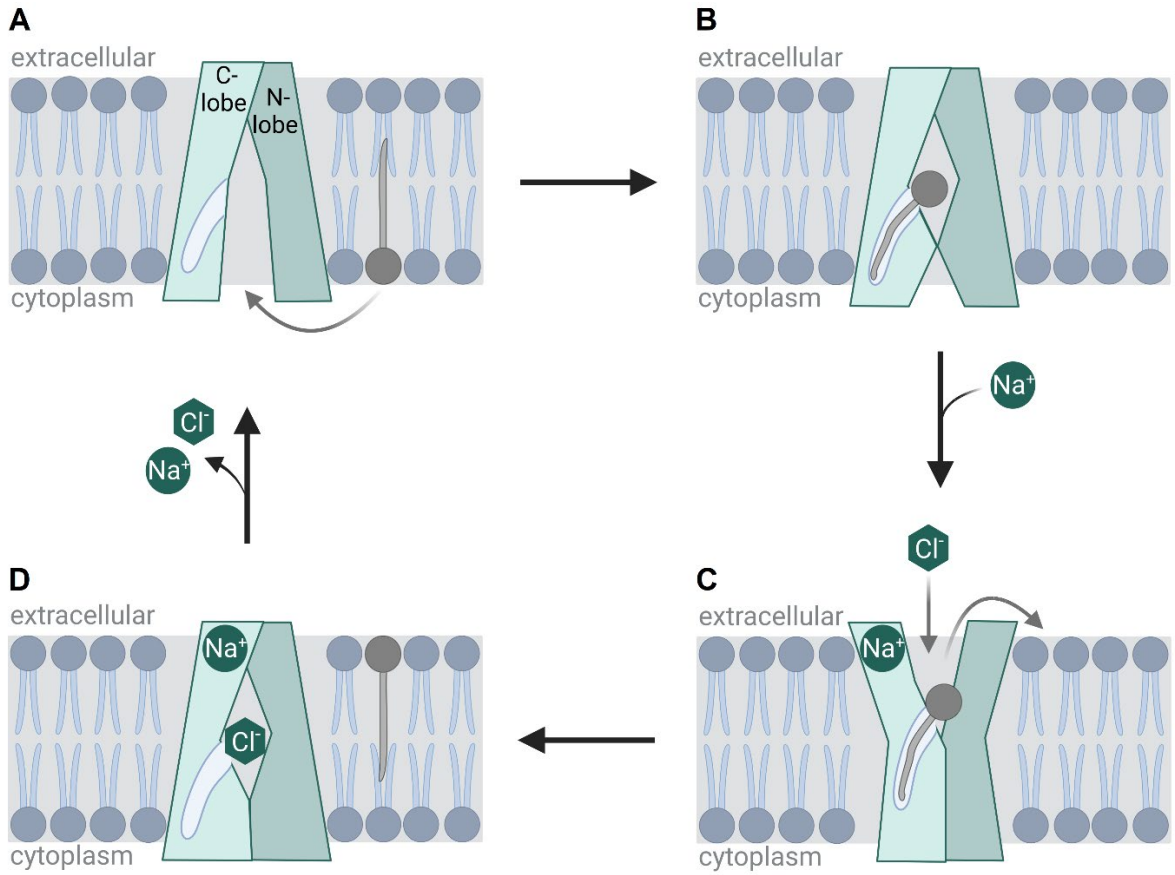

Figure 8: Proposed mechanism of Lipid II (grey lipid) translocation by MurJ (turquoise). For a better overview, only the undecaprenyl pyrophosphate without any cargo is shown. (A) The undecaprenyl pyrophosphate enters the central cavity of the inward-opened MurJ, which is formed by TMS 1-12 arranged into two lobes (indicated in shades of turquoise). Lipid II places its undecaprenyl pyrophosphate tail into a second grove (blue), formed by TMS 13 + 14, while the head group remains in the central cavity. Lipid II binding triggers formation of the inside-occluded state (B), while binding of an external sodium ion (green circle) induces the outward transition, which results in the Lipid II release (C). Binding of an external chloride ion (green hexagon) moves MurJ into the inward-closed state (D) and release of both ions results in the initial inward-opened position of MurJ.

AmJ, formerly YdaH, is the third highly controversly discussed potential Lipid II translocase candidate, which became of interest as it was shown to be functionally redundant with YtgP, the MurJ ortholog in *Bacillus subtilis* [125]. Interestingly, AmJ does not possess the typical MOP exporter structure or any sequence similarity to MurJ. In addition, AmJ is not essential and in contrast to MurJ only present in a subset of bacteria [125]. The transcriptional regulation mediated by σ^M, a sigma factor important during cell wall stress, leads to hypothesize that AmJ becomes of benefit under conditions inhibiting MurJ, which is in agreement with increased expression in the absence of MurJ [125, 141]. AmJ is predicted to consist of six TMSs and half of the size of representative MOP superfamily members, which leads to speculations of homodimerization of AmJ to form a MurJ-like structure [125] and thereby facilitating Lipid II

translocation in the same way [139]. Since AmJ does not belong to the MOP superfamily and lacks similarity to other known transporter superfamilies, one could propose AmJ as the first member of a new class of transporters, mediating the translocation of sugars [125]. Another hypothesis is that AmJ is the transporter of a yet unknown undecaprenyl phosphate-linked substrate and capriciously translocate Lipid II, like already shown for the O-antigen translocase Wzx [142].

2.3.4 LplT

As mentioned in section 1, some prokaryotes are able to generate lysophospholipids, like Lyso-PE, by transfer of one acyl chain from PE to the outer membrane lipoprotein Lpp [31]. After generation at the outer leaflet of the cytoplasmic membrane, Lyso-PE is transferred back to the inner layer of the cytoplasmic membrane by the lysophospholipid transporter LplT [143]. LplT belongs to the major facilitator superfamily (MFS) [143], a diverse group of transporters [102]. Like the other members of the group, LplT modelling shows the typical structure composed of 12 α-helical TMSs [143, 144] which are arranged into two bundles, the N- and C-domain [145]. LplT was the first member of the MFS, identified as lipid transporter [143].

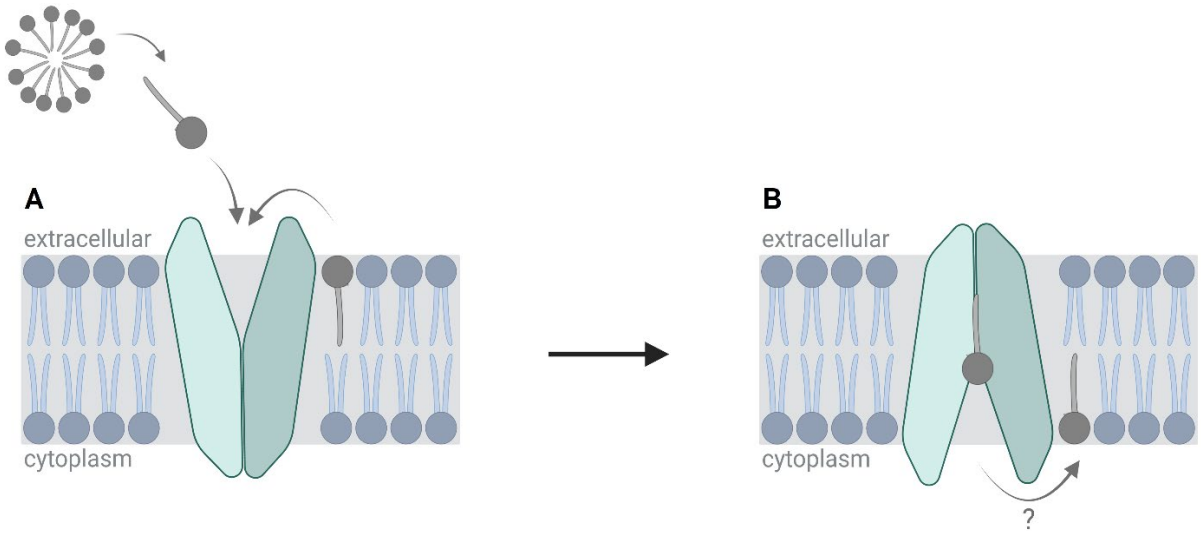

Figure 9: LplT mediated transport of lysophospholipids through the cytoplasmic membrane of Gram-negative bacteria. (A) The 12 α-helical TMSs of LplT are arranged into the C- and N-domain (shades of turquoise) and form a substrate binding pocket, opened to the outer leaflet. Lysophospholipids (grey lipid), origins from Lpp synthesis or external source, are recognized and bound in the central cavity, which mediates the conformational change into the inward opened conformation and thereby lipid release (B). The hypothesized release distinct from the central cavity is indicated by a question mark.

Based on the present literature, the LplT mediated transport of lysophospholipids through the cytoplasmic membrane is pure speculation, adapted from transport mechanisms and crystal structures known of other members of the superfamily and computational modelling of LplT in *Klebsiella pneumoniae* [144-146]. Based on the mechanism of a eukaryotic lysophosphatidylcholine transporter [146], the mode of lysophospholipid translocation was proposed to start with LplT, which forms a substrate binding pocket opened to the periplasmic side of the cytoplasmic membrane (Fig. 9A). Interestingly, LplT seems to have a dual substrate

accessing mechanism, meaning both, freshly synthesized lysophospholipids from Lpp synthesis and extracellular lysophospholipids can be bound and translocated [143, 145]. It is hypothesized, that LplT forms a large elongated central cavity, spanning the whole protein. If opened to the outer leaflet of the cytoplasmic membrane, modelled LplT creates two V-shaped grooves formed by TMS 2 + 11 and TMS 5 + 8, probably serving as entry points for lysophospholipids [145]. Due to the binding of the lysophospholipid, a conformational change of LplT could open the cytoplasmic site of the transporter and allow the substrate to get released (Fig. 9B) [144]. Of note, computational analysis in combination with *in vitro* mutation experiments indicate the release of the lysophospholipids distinct from the central groove, probably through an unknown separated exit gate [145].

Interaction studies using lyso-forms of the major bacterial membrane lipids found Lyso-PE, Lyso-PG, and Lyso-CL, but not Lyso-PS, lysophosphatidic acid (Lyso-PA) or Lyso-PC as potential substrates [147], indicating a head group specificity. Nevertheless, also the fatty acyl chain seems to be important for the translocation of lysophospholipids because the discriminatory capability of LplT diminished with reduced acyl chain length [145]. Since LplT shows no sequence homology to any eukaryotic transporter used as example for the transport mechanism, the suggested mode of action remains speculative and further investigations are highly recommended.

3. Being adaptive – the impact of phospholipid translocation

The process of lipid translocation is crucial for bacterial propagation and survival. The most obvious application of lipid translocation is the incorporation and distribution of newly synthesized phospholipids to maintain membrane homeostasis and allow cell division. Of note, all bacterial phospholipids are synthesized at the inner leaflet of the cytoplasmic membrane, causing an asymmetric distribution [4, 44]. To create lipid symmetry across both leaflets or to accumulate appropriate phospholipids at one layer, translocase-mediated transport is crucial. Beside the lipid diversity among bacterial species, also the composition within one species can differ dependent on external factors. The adaptation of lipid composition in response to the environment allows bacteria to survive unfavorable conditions [9, 11, 41, 42]. Therefore, the adaptation can occur in two basic mechanisms, (I) the degradation of existing phospholipids and incorporation of freshly synthesized lipids with altered characteristics or (II) the modification of existing lipids to obtain different properties. While (I) allows the exchange against different types of lipids and therefore covers a wide range of conditions, (II) is a mechanism to cope with rapid changes. During acidification, *S. aureus* induce the synthesis of CL resulting in an accumulation in the cytoplasmic membrane while contemporaneously the MprF-mediated modification of PG to Lys-PG is enhanced [148, 149]. Increased levels of aaPGs in correlation to acidic conditions were also reported for *P. aeruginosa*, although the

incorporation of Ala-PG represents a minor change in membrane composition with an elevation from 1% to 6% [11]. In response to osmotic stress, an increase in CL has been reported to be favorable in diverse bacteria, like *E. coli* [150], *Bacillus subtilis* [151] and *S. aureus* [152]. Also restricting conditions, like phosphate starvation or nutrient limitation, are drivers of membrane adaptation. Especially soil bacteria, like *Methylosinus trichosporium*, *Agrobacterium tumefaciens* and *Sinorhizobium meliloti* replace their membrane phospholipids PE and PC with phosphorous-free versions, thereby restoring the phosphate for other cellular processes [42, 153, 154]. This remodeling represents a major change in membrane composition, since the phosphorous-free lipids increase up to 60% [154]. Another kind of harsh and fast changing condition represents the treatment with antibiotics, wherewith especially human commensals and pathogens have to cope. The human pathogen *S. aureus* uses MprF to synthesize and translocate Lys-PG to the outer leaflet of the cytoplasmic membrane, where Lys-PG acts protective against host-derived cationic antimicrobial peptides (CAMP) and CAMP-like antibiotics like daptomycin, but also bacteriocins, vancomycin and gentamycin [9, 155]. The protective effect could be further confirmed for many other bacterial species [11, 12, 156, 157], heterologous expression of Ala-PG in *S. aureus* membranes [104], and the incorporation of aaPGs in artificial phospholipid bilayers [158]. Of note, the level of resistance is not proportional to the amount of Lys-PG after a certain threshold [90]. The protective effect of aaPGs against CAMPs and CAMP-like antibiotics is based on electrostatic repulsion of cationic compounds, caused by the reduction of the negative net charge of the cytoplasmic membrane that goes along with the insertion of Lys-PG or Ala-PG [9].

Another important reason for selective translocation is the creation of specialized microdomains and so-called “lipid rafts”, which are regions of the cytoplasmic membrane that differ in lipid composition. The first identified bacterial microdomains were CL domains in the two model organisms *E. coli* and *B. subtilis*, whose CL is especially localized at the poles and the septal region [159-162]. Currently, it is not clear how CL domains are formed, but it has been hypothesized that either the curvature of the membrane facilitates the accumulation of CL at the poles or the localization of the Cls at the pole region remains responsible for the increased appearance [163, 164]. Nevertheless, CL domains have been shown to be important insertion sites for membrane-associated proteins, like the pole localized osmoregulatory protein ProP [165], the chromosomal DNA replication initiator DnaA [166], or the septal oriented cell division machinery [161]. Beside CL domains, also the existence of PG domains has been described, found to be distributed in helical patterns within the whole cell [162, 167, 168]. Presumably, PG domains serve as landmark for the localization of the key cell division proteins FtsA and FtsZ, which have been found to arrange in dynamic helical structures before the Z ring formation occurs at midcell [169]. Lipid rafts, first described in eukaryotic cells, consists of particular lipids like cholesterol and sphingolipids, and harbor a number of proteins

related to membrane trafficking, cytoskeleton rearrangement, and signal transduction [170]. In contrast, bacteria were considered as too simple organisms to harbor lipid rafts, but recent publications confirmed the existence of these structures, also referred to as ‘functional membrane microdomains’, in prokaryotic cells [171]. Bacterial lipid rafts are heterogeneously distributed, and the punctual appearance seems to be independent of PG or CL domains [171]. In contrast to eukaryotes, prokaryotes lack cholesterol and sphingolipids, therefore lipid rafts contain polyisoprenoid lipids, acting as sterol surrogates [170, 171]. Bacterial lipid rafts play a key role in enabling important cellular processes, like sporulation via FtsH recruitment, signal transduction by insertion of the biofilm formation sensor kinase KinC, or protein secretion mediated by incorporation of the Sec system into the cytoplasmic membrane [170]. For the recruitment of proteins into bacterial lipid rafts, the membrane-bound chaperon flotillin and flotillin-like proteins are required, like as already known for eukaryotic counterparts [171].

Shedding of extracellular vesicles (EV) is another process based on the directed translocation of bacterial membrane lipids. EVs have already been reported in all of the three domains of life, Eukarya, Archaea, and Bacteria [172]. Both, Gram-positive and Gram-negative bacteria are able to produce EVs. While Gram-negative EVs origin from the outer membrane and therefore consist of a heterogenic phospholipid-LPS bilayer that encapsulates periplasmic proteins, toxins, ribonucleic acids, cytoplasmic proteins, and small biological active compounds, EVs of Gram-positive bacteria are formed by a homogenous bilayer generated by the cytoplasmic membrane and contains the same cargo as Gram-negative EVs, except for periplasmic proteins [173]. Since the EVs origin from different membranes, the biogenesis in Gram-positives differs from Gram-negatives. In Gram-negatives, EVs are formed by the so-called ‘membrane blebbing’. In this process, the positive curvature of the outer membrane, for example facilitated by the accumulation of phospholipids, but also disturbed crosslinking to peptidoglycan or accumulation of misfolded proteins in combination with the turgor pressure results in the formation of a spherical membranous body that will pinch-off from the mother cell [173]. The EV generation in Gram-positives is less well understood and much more complex. The cytoplasmic membrane blebbing in the Gram-positive bacterium *S. aureus* is facilitated by the incorporation of phenol-soluble modulins (PSMs), which increase the local fluidity and thereby allow the formation of vesicles via osmotic forces [174]. Since the tight structure of the multiple peptidoglycan layers that form the thick cell wall, would prohibit the release of EVs, it was demonstrated that Gram-positives modify their cell wall for vesicle release by peptidoglycan-degrading enzymes [173, 175]. But what is the purpose of EVs after release? EVs are of diverse functions, especially in the three main categories (I) bacterial (self-)defense, (II) interbacterial communication and (III) inter-kingdom communication.

(I) Some EVs remain associated with the mother cell and act like an armor, therefore shield from external hazards. Hence, EVs can either contain proteins that promote resistance by

degradation and modification or operate as sacrificial membranes that act as decoy against harmful substances [176-180]. But not only abiotic hazards can be battled by vesicle release. Bacteriocin-containing EVs of *Lactobacillus acidophilus* are mainly produced to eliminate other bacterial residents in the same niche, competing for nutrients and other limited resources [181]. Beside external hazards, bacteria have to cope with internal risks as well. Especially bacterial envelope stress triggers the accumulation of misfolded proteins within the membrane, which disturb important cellular processes. Therefore, misfolded proteins are vesiculated and released to eliminate potential harmful material and increase bacterial survival [173, 182]. Another serious enemy especially human pathogens have to deal with, is the host's immune response. Many pathogen-derived EVs carry virulence factors, important for immune evasion and circumvention of host mediated clearance. While EVs of staphylococci harbor the pore-forming toxins α-toxin (hla) and Panton-Valentine leucocidin (PVL) for escape of non-professional phagocytes [183], neisserial vesicles trigger the loss of membrane potential and the activation of apoptotic caspases, resulting in apoptosis of host cells by the oligomeric pore formation protein PorB [184], and *Listeria* uses EV-embedded listeriolysin O for phagosomal escape [185].

(II) Beside self-defense, EVs play an important role in interbacterial communication. Therefore, EVs can either contain DNA, which is transferred to other bacterial species and displays a role in horizontal gene transfer [186-189], or traffic signals to trigger coordinated activities via quorum sensing [190, 191]. Examples for vesicle-mediated quorum sensing are for instance the hydrophobic 'pseudomonas quinolone signal' (PQS), which is used by the opportunistic human pathogen *P. aeruginosa* to control group behavior, like biofilm formation or the generation of proteases, hemolysins and cytotoxins [191, 192].

(III) But also, inter-kingdom communication is mediated by EVs. Currently, several reports on pathogens using EVs for interaction with human pathogen recognition receptors (PRR), important for immune modulation, have been published and reviewed [174, 193-196]. For example, *S. aureus* uses EVs to transfer its lipoproteins to the PRR 'Toll-like receptor 2' (TLR2), presented on the surface of host cells, to mediate inflammation [174]. A similar TLR2-dependent induction of inflammation has been described for EVs of *Mycobacterium tuberculosis* [194]. Likewise, EVs can transport several natural agonists to PRR for immune modulation, like the enterohemorrhagic *E. coli* (EHEC) H7 flagellin to TLR5 [195], EHEC LPS to TLR4 [195], or peptidoglycan fragments of *P. aeruginosa*, *Helicobacter pylori*, and *Neisseria gonorrhoeae* to the 'nucleotide binding oligomerization domain 1' (NOD1) [196]. Interestingly, NOD1 is represented intracellularly, which infers either a pathogen invasion or the penetration of host cells by released EVs. It has been proposed that bacterial EVs can cross eukaryotic barriers, like the intestinal epithelium and the vascular endothelium to reach distant locations within the human body [197]. Hence, the potential role of vesicles in health maintenance and

infection therapy is highly discussed in the community. At the beginning of beneficial vesicle studies, it has been proposed that EVs produced mainly by probiotic bacteria might train the immune system by representation of possible bacterial targets. Nowadays, our knowledge is far beyond EVs just seeing as a trainer of the human immune system, nevertheless only a few insights into the great potential of EVs as possible therapeutic could be gained. To mention some examples, EVs of the commensal bacterium *Bacteroides fragilis* contains a capsular polysaccharide, which was able to enhance regulatory T cells and the production of anti-inflammatory cytokines in a TLR2-dependent manner and therefore prevented animals in a murine model for colitis [198]. Also, reports on disease treatment experiments in a murine alcohol-associated liver disease (ALD) model revealed beneficial effects of EVs [199]. Typical disease pattern of ALD is a gut barrier-dysfunction induced translocation of bacteria, which contributes to pathogenesis. Experimental treatment with EVs of the probiotic bacterium *Lactobacillus rhamnosus* increased the expression of the tight junction proteins in epithelial cells and thereby protected the intestine of ALD mice from bacterial translocation by reinforcing the intestinal barrier function [199]. Even mental health has been proposed to be influenced by bacterial derived EVs, since several publications implemented the gut microbiota as main player in modulation of anxiety and behavioral disorders via the ‘gut microbiota brain axis’ [200-202]. Because of their stability and mobility within the human body, engineered EVs have been investigated for their application as drug delivery vehicle and vaccine. An interesting approach with orally administered EVs against *Vibrio cholera* elicited robust IgG and IgA responses in a murine model, comparable to levels yielded by immunization with a commercially available vaccine [203]. Also, the usage of vesicles as drug delivery vehicles, as naturally exemplified by e.g. bacteriocin-containing EVs of lactobacilli [181], has been successfully demonstrated in mice with intestinal infections [204]. Beside the reduction of bacterial loads in the intestine and feces, the oral administration of EVs benefits a long disposition of the antibiotic in the intestine without a systemic spread [204]. Nevertheless, further studies concerning biosafety, biocompatibility, antimicrobial effectivity, and scope of application of EVs in bacterial infections have to be done in future.

1. Zhang YM, Rock CO. Membrane lipid homeostasis in bacteria. Nat Rev Microbiol. 2008;6(3):222-33. doi: 10.1038/nrmicro1839. PubMed PMID: 18264115.
2. Sohlenkamp C, Geiger O. Bacterial membrane lipids: diversity in structures and pathways. FEMS Microbiol Rev. 2016;40(1):133-59. Epub 2015/04/12. doi: 10.1093/femsre/fuv008. PubMed PMID: 25862689.
3. Raetz CR, Dowhan W. Biosynthesis and function of phospholipids in Escherichia coli. J Biol Chem. 1990;265(3):1235-8. Epub 1990/01/25. PubMed PMID: 2404013.
4. Cronan JE, Jr., Rock CO. Biosynthesis of Membrane Lipids. EcoSal Plus. 2008;3(1). Epub 2008/09/01. doi: 10.1128/ecosalplus.3.6.4. PubMed PMID: 26443744.
5. Ratledge C, Wilkinson SG. Microbial lipids: Academic press; 1988.
6. Makula RA, Finnerty WR. Phospholipid composition of Desulfovibrio species. J Bacteriol. 1974;120(3):1279-83. Epub 1974/12/01. doi: 10.1128/jb.120.3.1279-1283.1974. PubMed PMID: 4436257; PubMed Central PMCID: PMCPMC245912.
7. Jackson M, Crick DC, Brennan PJ. Phosphatidylinositol is an essential phospholipid of mycobacteria. J Biol Chem. 2000;275(39):30092-9. Epub 2000/07/13. doi: 10.1074/jbc.M004658200. PubMed PMID: 10889206.
8. Dowhan W, Bogdanov M. Eugene P. Kennedy's Legacy: Defining Bacterial Phospholipid Pathways and Function. Front Mol Biosci. 2021;8:666203. Epub 2021/04/13. doi: 10.3389/fmolb.2021.666203. PubMed PMID: 33842554; PubMed Central PMCID: PMCPMC8027125.
9. Peschel A, Jack RW, Otto M, Collins LV, Staubitz P, Nicholson G, et al. Staphylococcus aureus resistance to human defensins and evasion of neutrophil killing via the novel virulence factor MprF is based on modification of membrane lipids with l-lysine. J Exp Med. 2001;193(9):1067-76. Epub 2001/05/09. doi: 10.1084/jem.193.9.1067. PubMed PMID: 11342591; PubMed Central PMCID: PMCPMC2193429.
10. Fischer W, Leopold K. Polar lipids of four Listeria species containing L-lysylcardiolipin, a novel lipid structure, and other unique phospholipids. Int J Syst Bacteriol. 1999;49 Pt 2:653-62. Epub 1999/07/17. doi: 10.1099/00207713-49-2-653. PubMed PMID: 10408878.
11. Klein S, Lorenzo C, Hoffmann S, Walther JM, Storbeck S, Piekarski T, et al. Adaptation of Pseudomonas aeruginosa to various conditions includes tRNA-dependent formation of alanyl-phosphatidylglycerol. Mol Microbiol. 2009;71(3):551-65. Epub 2008/12/18. doi: 10.1111/j.1365-2958.2008.06562.x. PubMed PMID: 19087229.
12. Sohlenkamp C, Galindo-Lagunas KA, Guan Z, Vinuesa P, Robinson S, Thomas-Oates J, et al. The lipid lysyl-phosphatidylglycerol is present in membranes of Rhizobium tropici CIAT899 and confers increased resistance to polymyxin B under acidic growth conditions. Mol Plant Microbe Interact. 2007;20(11):1421-30. Epub 2007/11/06. doi: 10.1094/mpmi-20-11-1421. PubMed PMID: 17977153.
13. Staubitz P, Neumann H, Schneider T, Wiedemann I, Peschel A. MprF-mediated biosynthesis of lysylphosphatidylglycerol, an important determinant in staphylococcal defensin resistance. FEMS Microbiol Lett. 2004;231(1):67-71. Epub 2004/02/11. doi: 10.1016/s0378-1097(03)00921-2. PubMed PMID: 14769468.
14. Roy H, Ibba M. RNA-dependent lipid remodeling by bacterial multiple peptide resistance factors. Proc Natl Acad Sci U S A. 2008;105(12):4667-72. Epub 2008/02/29. doi: 10.1073/pnas.0800006105. PubMed PMID: 18305156; PubMed Central PMCID: PMCPMC2290796.
15. Slavetinsky C, Kuhn S, Peschel A. Bacterial aminoacyl phospholipids - Biosynthesis and role in basic cellular processes and pathogenicity. Biochim Biophys Acta Mol Cell Biol Lipids. 2017;1862(11):1310-8. Epub 2016/12/13. doi: 10.1016/j.bbalip.2016.11.013. PubMed PMID: 27940309.
16. Peter-Katalinic J, Fischer W. alpha-d-glucopyranosyl-, d-alanyl- and l-lysylcardiolipin from gram-positive bacteria: analysis by fast atom bombardment mass spectrometry. J Lipid Res. 1998;39(11):2286-92. Epub 1998/11/04. PubMed PMID: 9799815.
17. Khuller GK, Subrahmanyam D. On the ornithinyl ester of phosphatidylglycerol of Mycobacterium 607. J Bacteriol. 1970;101(2):654-6. Epub 1970/02/01. doi: 10.1128/jb.101.2.654-656.1970. PubMed PMID: 5414606; PubMed Central PMCID: PMCPMC284955.

18. Roy H, Ibba M. Broad range amino acid specificity of RNA-dependent lipid remodeling by multiple peptide resistance factors. J Biol Chem. 2009;284(43):29677-83. doi: 10.1074/jbc.M109.046367. PubMed PMID: 19734140; PubMed Central PMCID: PMCPMC2785599.
19. Thedieck K, Hain T, Mohamed W, Tindall BJ, Nimtz M, Chakraborty T, et al. The MprF protein is required for lysinylation of phospholipids in listerial membranes and confers resistance to cationic antimicrobial peptides (CAMPs) on Listeria monocytogenes. Mol Microbiol. 2006;62(5):1325-39. Epub 2006/10/18. doi: 10.1111/j.1365-2958.2006.05452.x. PubMed PMID: 17042784.
20. Short SA, White DC. Biosynthesis of cardiolipin from phosphatidylglycerol in Staphylococcus aureus. J Bacteriol. 1972;109(2):820-6. Epub 1972/02/01. doi: 10.1128/jb.109.2.820-826.1972. PubMed PMID: 5058454; PubMed Central PMCID: PMCPMC285211.
21. Olsen RW, Ballou CE. Acyl phosphatidylglycerol. A new phospholipid from Salmonella typhimurium. J Biol Chem. 1971;246(10):3305-13. Epub 1971/05/25. PubMed PMID: 4930058.
22. Kleetz J, Welter L, Mizza AS, Aktas M, Narberhaus F. Phospholipid N-Methyltransferases Produce Various Methylated Phosphatidylethanolamine Derivatives in Thermophilic Bacteria. Appl Environ Microbiol. 2021;87(19):e0110521. Epub 2021/07/22. doi: 10.1128/aem.01105-21. PubMed PMID: 34288711; PubMed Central PMCID: PMCPMC8432528.
23. Sohlenkamp C, López-Lara IM, Geiger O. Biosynthesis of phosphatidylcholine in bacteria. Prog Lipid Res. 2003;42(2):115-62. Epub 2003/01/28. doi: 10.1016/s0163-7827(02)00050-4. PubMed PMID: 12547654.
24. Kaneshiro T, Law JH. PHOSPHATIDYLCHOLINE SYNTHESIS IN AGROBACTERIUM TUMEFACIENS. I. PURIFICATION AND PROPERTIES OF A PHOSPHATIDYLETHANOLAMINE N-METHYLTRANSFERASE. J Biol Chem. 1964;239:1705-13. Epub 1964/06/01. PubMed PMID: 14217872.
25. Palusinska-Szysz M, Szuster-Ciesielska A, Kania M, Janczarek M, Chmiel E, Danikiewicz W. Legionella dumoffii utilizes exogenous choline for phosphatidylcholine synthesis. Int J Mol Sci. 2014;15(5):8256-79. Epub 2014/05/14. doi: 10.3390/ijms15058256. PubMed PMID: 24821544; PubMed Central PMCID: PMCPMC4057730.
26. Comerci DJ, Altabe S, de Mendoza D, Ugalde RA. Brucella abortus synthesizes phosphatidylcholine from choline provided by the host. J Bacteriol. 2006;188(5):1929-34. doi: 10.1128/jb.188.5.1929-1934.2006. PubMed PMID: 16484204; PubMed Central PMCID: PMCPMC1426538.
27. Goldfine H, Ellis ME. N-METHYL GROUPS IN BACTERIAL LIPIDS. J Bacteriol. 1964;87(1):8-15. Epub 1964/01/01. doi: 10.1128/jb.87.1.8-15.1964. PubMed PMID: 14102879; PubMed Central PMCID: PMCPMC276954.
28. Tornabene TG. Lipid composition of selected strains of Yersinia pestis and Yersinia pseudotuberculosis. Biochim Biophys Acta. 1973;306(2):173-85. Epub 1973/05/24. doi: 10.1016/0005-2760(73)90223-3. PubMed PMID: 4351505.
29. Gupta SD, Dowhan W, Wu HC. Phosphatidylethanolamine is not essential for the N-acylation of apolipoprotein in Escherichia coli. J Biol Chem. 1991;266(15):9983-6. PubMed PMID: 2033085.
30. Sankaran K, Wu HC. Lipid modification of bacterial prolipoprotein. Transfer of diacylglyceryl moiety from phosphatidylglycerol. J Biol Chem. 1994;269(31):19701-6. PubMed PMID: 8051048.
31. López-Lara IM, Geiger O. Bacterial lipid diversity. Biochim Biophys Acta Mol Cell Biol Lipids. 2017;1862(11):1287-99. Epub 2016/10/26. doi: 10.1016/j.bbalip.2016.10.007. PubMed PMID: 27760387.
32. Senff LM, Wegener WS, Brooks GF, Finnerty WR, Makula RA. Phospholipid composition and phospholipase A activity of Neisseria gonorrhoeae. J Bacteriol. 1976;127(2):874-80. Epub 1976/08/01. doi: 10.1128/jb.127.2.874-880.1976. PubMed PMID: 821921; PubMed Central PMCID: PMCPMC232996.

33. Tannaes T, Grav HJ, Bukholm G. Lipid profiles of Helicobacter pylori colony variants. Apmis. 2000;108(5):349-56. Epub 2000/08/11. doi: 10.1034/j.1600-0463.2000.d01-67.x. PubMed PMID: 10937772.
34. Whetton AD, Lu Y, Pierce A, Carney L, Spooncer E. Lysophospholipids synergistically promote primitive hematopoietic cell chemotaxis via a mechanism involving Vav 1. Blood. 2003;102(8):2798-802. Epub 2003/06/28. doi: 10.1182/blood-2002-12-3635. PubMed PMID: 12829605.
35. Yamamoto N, Willett NP, Lindsay DD. Participation of serum proteins in the inflammation-primed activation of macrophages. Inflammation. 1994;18(3):311-22. Epub 1994/06/01. doi: 10.1007/bf01534272. PubMed PMID: 8088927.
36. Sim MS, Kim HJ, Jo SH, Kim C, Chung IY. Lysophosphatidylserine Induces MUC5AC Production via the Feedforward Regulation of the TACE-EGFR-ERK Pathway in Airway Epithelial Cells in a Receptor-Independent Manner. Int J Mol Sci. 2022;23(7). Epub 2022/04/13. doi: 10.3390/ijms23073866. PubMed PMID: 35409225; PubMed Central PMCID: PMCPMC8999057.
37. Mills GB, Eder A, Fang X, Hasegawa Y, Mao M, Lu Y, et al. Critical role of lysophospholipids in the pathophysiology, diagnosis, and management of ovarian cancer. Cancer Treat Res. 2002;107:259-83. Epub 2002/01/05. doi: 10.1007/978-1-4757-3587-1_12. PubMed PMID: 11775454.
38. Nariai M, Abe H, Hoshioka Y, Makino Y, Iwase H. Biomarker profiling of postmortem blood for diabetes mellitus and discussion of possible applications of metabolomics for forensic casework. Int J Legal Med. 2022;136(4):1075-90. Epub 2022/01/21. doi: 10.1007/s00414-021-02767-w. PubMed PMID: 35050412.
39. Kamio Y, Nikaido H. Outer membrane of Salmonella typhimurium: accessibility of phospholipid head groups to phospholipase c and cyanogen bromide activated dextran in the external medium. Biochemistry. 1976;15(12):2561-70. Epub 1976/06/15. doi: 10.1021/bi00657a012. PubMed PMID: 820368.
40. Henderson JC, Zimmerman SM, Crofts AA, Boll JM, Kuhns LG, Herrera CM, et al. The Power of Asymmetry: Architecture and Assembly of the Gram-Negative Outer Membrane Lipid Bilayer. Annu Rev Microbiol. 2016;70:255-78. Epub 2016/07/01. doi: 10.1146/annurev-micro-102215-095308. PubMed PMID: 27359214.
41. Cronan JE, Jr., Gelmann EP. Physical properties of membrane lipids: biological relevance and regulation. Bacteriol Rev. 1975;39(3):232-56. doi: 10.1128/br.39.3.232-256.1975. PubMed PMID: 1100043; PubMed Central PMCID: PMCPMC413917.
42. Scanlan J, Guillonneau R, Cunningham MR, Najmin S, Mausz MA, Murphy A, et al. The Proteobacterial Methanotroph Methylosinus trichosporium OB3b Remodels Membrane Lipids in Response to Phosphate Limitation. mBio. 2022:e0024722. Epub 2022/05/17. doi: 10.1128/mbio.00247-22. PubMed PMID: 35575546.
43. Sharom FJ. Flipping and flopping--lipids on the move. IUBMB Life. 2011;63(9):736-46. Epub 2011/07/28. doi: 10.1002/iub.515. PubMed PMID: 21793163.
44. Kol MA, de Kroon AI, Killian JA, de Kruijff B. Transbilayer movement of phospholipids in biogenic membranes. Biochemistry. 2004;43(10):2673-81. Epub 2004/03/10. doi: 10.1021/bi036200f. PubMed PMID: 15005602.
45. Rothman JE, Kennedy EP. Rapid transmembrane movement of newly synthesized phospholipids during membrane assembly. Proc Natl Acad Sci U S A. 1977;74(5):1821-5. Epub 1977/05/01. doi: 10.1073/pnas.74.5.1821. PubMed PMID: 405668; PubMed Central PMCID: PMCPMC431015.
46. Hrafnsdóttir S, Nichols JW, Menon AK. Transbilayer movement of fluorescent phospholipids in Bacillus megaterium membrane vesicles. Biochemistry. 1997;36(16):4969-78. Epub 1997/04/22. doi: 10.1021/bi962513h. PubMed PMID: 9125519.
47. Huijbregts RP, de Kroon AI, de Kruijff B. Rapid transmembrane movement of newly synthesized phosphatidylethanolamine across the inner membrane of Escherichia coli. J Biol Chem. 1998;273(30):18936-42. Epub 1998/07/21. doi: 10.1074/jbc.273.30.18936. PubMed PMID: 9668071.
48. Bretscher MS. Some aspects of membrane structure. Perspectives in Membrane Biology: Academic Press New York; 1974. p. 3-24.

49. Beleznay Z, Zachowski A, Devaux PF, Navazo MP, Ott P. ATP-dependent aminophospholipid translocation in erythrocyte vesicles: stoichiometry of transport. Biochemistry. 1993;32(12):3146-52.
50. Palmgren MG, Axelsen KB. Evolution of P-type ATPases. Biochim Biophys Acta. 1998;1365(1-2):37-45. doi: 10.1016/s0005-2728(98)00041-3. PubMed PMID: 9693719.
51. Soupene E, Kemaladewi DU, Kuypers FA. ATP8A1 activity and phosphatidylserine transbilayer movement. J Receptor Ligand Channel Res. 2008;1:1-10. Epub 2008/01/01. doi: 10.2147/jrlcr.s3773. PubMed PMID: 20224745; PubMed Central PMCID: PMCPMC2835971.
52. Coleman JA, Kwok MC, Molday RS. Localization, purification, and functional reconstitution of the P4-ATPase Atp8a2, a phosphatidylserine flippase in photoreceptor disc membranes. J Biol Chem. 2009;284(47):32670-9. Epub 2009/09/26. doi: 10.1074/jbc.M109.047415. PubMed PMID: 19778899; PubMed Central PMCID: PMCPMC2781682.
53. Naito T, Takatsu H, Miyano R, Takada N, Nakayama K, Shin HW. Phospholipid Flippase ATP10A Translocates Phosphatidylcholine and Is Involved in Plasma Membrane Dynamics. J Biol Chem. 2015;290(24):15004-17. Epub 20150506. doi: 10.1074/jbc.M115.655191. PubMed PMID: 25947375; PubMed Central PMCID: PMCPMC4463445.
54. Gomès E, Jakobsen MK, Axelsen KB, Geisler M, Palmgren MG. Chilling tolerance in Arabidopsis involves ALA1, a member of a new family of putative aminophospholipid translocases. Plant Cell. 2000;12(12):2441-54. Epub 2001/01/10. PubMed PMID: 11148289; PubMed Central PMCID: PMCPMC102229.
55. Zhou X, Graham TR. Reconstitution of phospholipid translocase activity with purified Drs2p, a type-IV P-type ATPase from budding yeast. Proc Natl Acad Sci U S A. 2009;106(39):16586-91. Epub 2009/10/07. doi: 10.1073/pnas.0904293106. PubMed PMID: 19805341; PubMed Central PMCID: PMCPMC2757829.
56. Pomorski T, Lombardi R, Riezman H, Devaux PF, van Meer G, Holthuis JC. Drs2p-related P-type ATPases Dnf1p and Dnf2p are required for phospholipid translocation across the yeast plasma membrane and serve a role in endocytosis. Mol Biol Cell. 2003;14(3):1240-54. doi: 10.1091/mbc.e02-08-0501. PubMed PMID: 12631737; PubMed Central PMCID: PMCPMC151593.
57. Lage H. An overview of cancer multidrug resistance: a still unsolved problem. Cell Mol Life Sci. 2008;65(20):3145-67. Epub 2008/06/27. doi: 10.1007/s00018-008-8111-5. PubMed PMID: 18581055.
58. Vasiliou V, Vasiliou K, Nebert DW. Human ATP-binding cassette (ABC) transporter family. Hum Genomics. 2009;3(3):281-90. Epub 2009/05/01. doi: 10.1186/1479-7364-3-3-281. PubMed PMID: 19403462; PubMed Central PMCID: PMCPMC2752038.
59. Gonzales E, Davit-Spraul A, Baussan C, Buffet C, Maurice M, Jacquemin E. Liver diseases related to MDR3 (ABCB4) gene deficiency. Front Biosci (Landmark Ed). 2009;14(11):4242-56. Epub 20090101. doi: 10.2741/3526. PubMed PMID: 19273348.
60. Whitsett JA, Wert SE, Weaver TE. Alveolar surfactant homeostasis and the pathogenesis of pulmonary disease. Annu Rev Med. 2010;61:105-19. Epub 2009/10/15. doi: 10.1146/annurev.med.60.041807.123500. PubMed PMID: 19824815; PubMed Central PMCID: PMCPMC4127631.
61. Macé S, Cousin E, Ricard S, Génin E, Spanakis E, Lafargue-Soubigou C, et al. ABCA2 is a strong genetic risk factor for early-onset Alzheimer's disease. Neurobiol Dis. 2005;18(1):119-25. Epub 2005/01/15. doi: 10.1016/j.nbd.2004.09.011. PubMed PMID: 15649702.
62. Lee BH, Taylor MG, Robinet P, Smith JD, Schweitzer J, Sehayek E, et al. Dysregulation of cholesterol homeostasis in human prostate cancer through loss of ABCA1. Cancer Res. 2013;73(3):1211-8. Epub 20121211. doi: 10.1158/0008-5472.Can-12-3128. PubMed PMID: 23233737; PubMed Central PMCID: PMCPMC3563867.
63. Tsybovsky Y, Molday RS, Palczewski K. The ATP-binding cassette transporter ABCA4: structural and functional properties and role in retinal disease. Adv Exp Med Biol. 2010;703:105-25. Epub 2010/08/17. doi: 10.1007/978-1-4419-5635-4_8. PubMed PMID: 20711710; PubMed Central PMCID: PMCPMC2930353.

64. Vree JMLd, Jacquemin E, Sturm E, Cresteil D, Bosma PJ, Aten J, et al. Mutations in the MDR3 gene cause progressive familial intrahepatic cholestasis. Proceedings of the National Academy of Sciences. 1998;95(1):282-7. doi: doi:10.1073/pnas.95.1.282.
65. Stieger B, Fattinger K, Madon J, Kullak-Ublick GA, Meier PJ. Drug-and estrogen-induced cholestasis through inhibition of the hepatocellular bile salt export pump (Bsep) of rat liver. Gastroenterology. 2000;118(2):422-30.
66. Smit JJ, Schinkel AH, Oude Elferink RP, Groen AK, Wagenaar E, van Deemter L, et al. Homozygous disruption of the murine mdr2 P-glycoprotein gene leads to a complete absence of phospholipid from bile and to liver disease. Cell. 1993;75(3):451-62. Epub 1993/11/05. doi: 10.1016/0092-8674(93)90380-9. PubMed PMID: 8106172.
67. van Helvoort A, Smith AJ, Sprong H, Fritzsche I, Schinkel AH, Borst P, et al. MDR1 P-glycoprotein is a lipid translocase of broad specificity, while MDR3 P-glycoprotein specifically translocates phosphatidylcholine. Cell. 1996;87(3):507-17. Epub 1996/11/01. doi: 10.1016/s0092-8674(00)81370-7. PubMed PMID: 8898203.
68. Williamson P, Kulick A, Zachowski A, Schlegel RA, Devaux PF. Calcium induces transbilayer redistribution of all major phospholipids in human erythrocytes. Biochemistry. 1992;31(27):6355-60.
69. Williamson P, Bevers EM, Smeets EF, Comfurius P, Schlegel RA, Zwaal RF. Continuous analysis of the mechanism of activated transbilayer lipid movement in platelets. Biochemistry. 1995;34(33):10448-55. Epub 1995/08/22. doi: 10.1021/bi00033a017. PubMed PMID: 7654698.
70. Bevers EM, Comfurius P, van Rijn JL, Hemker HC, Zwaal RF. Generation of prothrombin-converting activity and the exposure of phosphatidylserine at the outer surface of platelets. Eur J Biochem. 1982;122(2):429-36. Epub 1982/02/01. doi: 10.1111/j.1432-1033.1982.tb05898.x. PubMed PMID: 7060583.
71. Bratton DL, Fadok VA, Richter DA, Kailey JM, Guthrie LA, Henson PM. Appearance of phosphatidylserine on apoptotic cells requires calcium-mediated nonspecific flip-flop and is enhanced by loss of the aminophospholipid translocase. Journal of Biological Chemistry. 1997;272(42):26159-65.
72. Suzuki J, Umeda M, Sims PJ, Nagata S. Calcium-dependent phospholipid scrambling by TMEM16F. Nature. 2010;468(7325):834-8. Epub 20101124. doi: 10.1038/nature09583. PubMed PMID: 21107324.
73. Goren MA, Morizumi T, Menon I, Joseph JS, Dittman JS, Cherezov V, et al. Constitutive phospholipid scramblase activity of a G protein-coupled receptor. Nat Commun. 2014;5:5115. Epub 2014/10/09. doi: 10.1038/ncomms6115. PubMed PMID: 25296113; PubMed Central PMCID: PMCPMC4198942.
74. Suzuki J, Denning DP, Imanishi E, Horvitz HR, Nagata S. Xk-related protein 8 and CED-8 promote phosphatidylserine exposure in apoptotic cells. Science. 2013;341(6144):403-6. Epub 2013/07/13. doi: 10.1126/science.1236758. PubMed PMID: 23845944.
75. Sivagnanam U, Palanirajan SK, Gummadi SN. The role of human phospholipid scramblases in apoptosis: An overview. Biochim Biophys Acta Mol Cell Res. 2017;1864(12):2261-71. Epub 20170824. doi: 10.1016/j.bbamcr.2017.08.008. PubMed PMID: 28844836.
76. Lentz BR. Exposure of platelet membrane phosphatidylserine regulates blood coagulation. Progress in lipid research. 2003;42(5):423-38.
77. Wu N, Song H, Veillette A. Plasma membrane lipid scrambling causing phosphatidylserine exposure negatively regulates NK cell activation. Cell Mol Immunol. 2021;18(3):686-97. Epub 20210119. doi: 10.1038/s41423-020-00600-9. PubMed PMID: 33469162; PubMed Central PMCID: PMCPMC8027605.
78. Stout JG, Bassé F, Luhm RA, Weiss HJ, Wiedmer T, Sims PJ. Scott syndrome erythrocytes contain a membrane protein capable of mediating Ca2+-dependent transbilayer migration of membrane phospholipids. The Journal of clinical investigation. 1997;99(9):2232-8.
79. Marx U, Lassmann G, Holzhütter HG, Wüstner D, Müller P, Höhlig A, et al. Rapid flip-flop of phospholipids in endoplasmic reticulum membranes studied by a stopped-flow

approach. Biophys J. 2000;78(5):2628-40. Epub 2000/04/25. doi: 10.1016/s0006-3495(00)76807-x. PubMed PMID: 10777759; PubMed Central PMCID: PMCPMC1300852.
80. Coleman JA, Vestergaard AL, Molday RS, Vilsen B, Andersen JP. Critical role of a transmembrane lysine in aminophospholipid transport by mammalian photoreceptor P4-ATPase ATP8A2. Proc Natl Acad Sci U S A. 2012;109(5):1449-54. Epub 2012/02/07. doi: 10.1073/pnas.1108862109. PubMed PMID: 22307598; PubMed Central PMCID: PMCPMC3277108.
81. Post RL, Hegyvary C, Kume S. Activation by adenosine triphosphate in the phosphorylation kinetics of sodium and potassium ion transport adenosine triphosphatase. J Biol Chem. 1972;247(20):6530-40. Epub 1972/10/25. PubMed PMID: 4263199.
82. Shinoda T, Ogawa H, Cornelius F, Toyoshima C. Crystal structure of the sodium-potassium pump at 2.4 A resolution. Nature. 2009;459(7245):446-50. Epub 2009/05/22. doi: 10.1038/nature07939. PubMed PMID: 19458722.
83. Bai L, You Q, Jain BK, Duan HD, Kovach A, Graham TR, et al. Transport mechanism of P4 ATPase phosphatidylcholine flippases. Elife. 2020;9. Epub 20201215. doi: 10.7554/eLife.62163. PubMed PMID: 33320091; PubMed Central PMCID: PMCPMC7773333.
84. Kucerka N, Tristram-Nagle S, Nagle JF. Closer look at structure of fully hydrated fluid phase DPPC bilayers. Biophys J. 2006;90(11):L83-5. Epub 20060414. doi: 10.1529/biophysj.106.086017. PubMed PMID: 16617085; PubMed Central PMCID: PMCPMC1459514.
85. Mashaghi A, Partovi-Azar P, Jadidi T, Nafari N, Maass P, Tabar MR, et al. Hydration strongly affects the molecular and electronic structure of membrane phospholipids. J Chem Phys. 2012;136(11):114709. doi: 10.1063/1.3694280. PubMed PMID: 22443792.
86. Shannon RD. Revised effective ionic radii and systematic studies of interatomic distances in halides and chalcogenides. Acta crystallographica section A: crystal physics, diffraction, theoretical and general crystallography. 1976;32(5):751-67.
87. Baldridge RD, Graham TR. Identification of residues defining phospholipid flippase substrate specificity of type IV P-type ATPases. Proc Natl Acad Sci U S A. 2012;109(6):E290-8. Epub 2012/02/07. doi: 10.1073/pnas.1115725109. PubMed PMID: 22308393; PubMed Central PMCID: PMCPMC3277569.
88. Baldridge RD, Graham TR. Two-gate mechanism for phospholipid selection and transport by type IV P-type ATPases. Proc Natl Acad Sci U S A. 2013;110(5):E358-67. Epub 2013/01/11. doi: 10.1073/pnas.1216948110. PubMed PMID: 23302692; PubMed Central PMCID: PMCPMC3562821.
89. Song D, Jiao H, Liu Z. Phospholipid translocation captured in a bifunctional membrane protein MprF. Nat Commun. 2021;12(1):2927. Epub 2021/05/20. doi: 10.1038/s41467-021-23248-z. PubMed PMID: 34006869; PubMed Central PMCID: PMCPMC8131360.
90. Ernst CM, Staubitz P, Mishra NN, Yang SJ, Hornig G, Kalbacher H, et al. The bacterial defensin resistance protein MprF consists of separable domains for lipid lysinylation and antimicrobial peptide repulsion. PLoS Pathog. 2009;5(11):e1000660. Epub 2009/11/17. doi: 10.1371/journal.ppat.1000660. PubMed PMID: 19915718; PubMed Central PMCID: PMCPMC2774229.
91. Pomorski T, Menon AK. Lipid flippases and their biological functions. Cell Mol Life Sci. 2006;63(24):2908-21. Epub 2006/11/15. doi: 10.1007/s00018-006-6167-7. PubMed PMID: 17103115.
92. Brunner JD, Lim NK, Schenck S, Duerst A, Dutzler R. X-ray structure of a calcium-activated TMEM16 lipid scramblase. Nature. 2014;516(7530):207-12. Epub 2014/11/11. doi: 10.1038/nature13984. PubMed PMID: 25383531.
93. Pedersen BP, Buch-Pedersen MJ, Morth JP, Palmgren MG, Nissen P. Crystal structure of the plasma membrane proton pump. Nature. 2007;450(7172):1111-4. Epub 2007/12/14. doi: 10.1038/nature06417. PubMed PMID: 18075595.
94. Vestergaard AL, Coleman JA, Lemmin T, Mikkelsen SA, Molday LL, Vilsen B, et al. Critical roles of isoleucine-364 and adjacent residues in a hydrophobic gate control of phospholipid transport by the mammalian P4-ATPase ATP8A2. Proc Natl Acad Sci U S A. 2014;111(14):E1334-43. Epub 2014/04/08. doi: 10.1073/pnas.1321165111. PubMed PMID: 24706822; PubMed Central PMCID: PMCPMC3986137.

95. Jensen MS, Costa SR, Duelli AS, Andersen PA, Poulsen LR, Stanchev LD, et al. Phospholipid flipping involves a central cavity in P4 ATPases. Sci Rep. 2017;7(1):17621. Epub 20171215. doi: 10.1038/s41598-017-17742-y. PubMed PMID: 29247234; PubMed Central PMCID: PMCPMC5732287.
96. Ernst CM, Kuhn S, Slavetinsky CJ, Krismer B, Heilbronner S, Gekeler C, et al. The lipid-modifying multiple peptide resistance factor is an oligomer consisting of distinct interacting synthase and flippase subunits. mBio. 2015;6(1). Epub 2015/01/30. doi: 10.1128/mBio.02340-14. PubMed PMID: 25626904; PubMed Central PMCID: PMCPMC4324311.
97. Ernst CM, Slavetinsky CJ, Kuhn S, Hauser JN, Nega M, Mishra NN, et al. Gain-of-Function Mutations in the Phospholipid Flippase MprF Confer Specific Daptomycin Resistance. MBio. 2018;9(6). Epub 2018/12/20. doi: 10.1128/mBio.01659-18. PubMed PMID: 30563904; PubMed Central PMCID: PMCPMC6299216.
98. Mishra NN, Yang S-J, Sawa A, Rubio A, Nast CC, Yeaman MR, et al. Analysis of cell membrane characteristics of in vitro-selected daptomycin-resistant strains of methicillin-resistant Staphylococcus aureus. Antimicrobial agents and chemotherapy. 2009;53(6):2312-8.
99. Smith AM, Harrison JS, Sprague KM, Roy H. A conserved hydrolase responsible for the cleavage of aminoacylphosphatidylglycerol in the membrane of Enterococcus faecium. J Biol Chem. 2013;288(31):22768-76. Epub 2013/06/25. doi: 10.1074/jbc.M113.484402. PubMed PMID: 23793054; PubMed Central PMCID: PMCPMC3829361.
100. Arendt W, Groenewold MK, Hebecker S, Dickschat JS, Moser J. Identification and characterization of a periplasmic aminoacyl-phosphatidylglycerol hydrolase responsible for Pseudomonas aeruginosa lipid homeostasis. J Biol Chem. 2013;288(34):24717-30. Epub 2013/06/25. doi: 10.1074/jbc.M113.482935. PubMed PMID: 23792962; PubMed Central PMCID: PMCPMC3750168.
101. Wang SC, Davejan P, Hendargo KJ, Javadi-Razaz I, Chou A, Yee DC, et al. Expansion of the Major Facilitator Superfamily (MFS) to include novel transporters as well as transmembrane-acting enzymes. Biochimica et Biophysica Acta (BBA)-Biomembranes. 2020;1862(9):183277.
102. Pao SS, Paulsen IT, Saier MH, Jr. Major facilitator superfamily. Microbiol Mol Biol Rev. 1998;62(1):1-34. Epub 1998/04/08. doi: 10.1128/mmbr.62.1.1-34.1998. PubMed PMID: 9529885; PubMed Central PMCID: PMCPMC98904.
103. Newstead S. Recent advances in understanding proton coupled peptide transport via the POT family. Curr Opin Struct Biol. 2017;45:17-24. Epub 2016/11/20. doi: 10.1016/j.sbi.2016.10.018. PubMed PMID: 27865112; PubMed Central PMCID: PMCPMC5628733.
104. Slavetinsky CJ, Peschel A, Ernst CM. Alanyl-phosphatidylglycerol and lysyl-phosphatidylglycerol are translocated by the same MprF flippases and have similar capacities to protect against the antibiotic daptomycin in Staphylococcus aureus. Antimicrob Agents Chemother. 2012;56(7):3492-7. Epub 2012/04/12. doi: 10.1128/aac.00370-12. PubMed PMID: 22491694; PubMed Central PMCID: PMCPMC3393434.
105. Hauser JN, Tchoupa AK, Zabel S, Nieselt K, Ernst CM, Slavetinsky CJ, et al. Prokaryotic phospholipid translocation by ubiquitous PplT domain proteins. bioRxiv. 2022:2022.03.11.483950. doi: 10.1101/2022.03.11.483950.
106. Doerrler WT, Gibbons HS, Raetz CR. MsbA-dependent translocation of lipids across the inner membrane of Escherichia coli. J Biol Chem. 2004;279(43):45102-9. Epub 2004/08/12. doi: 10.1074/jbc.M408106200. PubMed PMID: 15304478.
107. Karow M, Georgopoulos C. The essential Escherichia coli msbA gene, a multicopy suppressor of null mutations in the htrB gene, is related to the universally conserved family of ATP-dependent translocators. Mol Microbiol. 1993;7(1):69-79. Epub 1993/01/01. doi: 10.1111/j.1365-2958.1993.tb01098.x. PubMed PMID: 8094880.
108. Mi W, Li Y, Yoon SH, Ernst RK, Walz T, Liao M. Structural basis of MsbA-mediated lipopolysaccharide transport. Nature. 2017;549(7671):233-7. Epub 20170906. doi: 10.1038/nature23649. PubMed PMID: 28869968; PubMed Central PMCID: PMCPMC5759761.

109. Ward A, Reyes CL, Yu J, Roth CB, Chang G. Flexibility in the ABC transporter MsbA: Alternating access with a twist. Proc Natl Acad Sci U S A. 2007;104(48):19005-10. Epub 2007/11/21. doi: 10.1073/pnas.0709388104. PubMed PMID: 18024585; PubMed Central PMCID: PMCPMC2141898.
110. Kehlenbeck DM, Traore DAK, Josts I, Sander S, Moulin M, Haertlein M, et al. Cryo-EM structure of MsbA in saposin-lipid nanoparticles (Salipro) provides insights into nucleotide coordination. Febs j. 2022;289(10):2959-70. Epub 20211227. doi: 10.1111/febs.16327. PubMed PMID: 34921499.
111. Doerrler WT, Raetz CR. ATPase activity of the MsbA lipid flippase of Escherichia coli. J Biol Chem. 2002;277(39):36697-705. Epub 2002/07/18. doi: 10.1074/jbc.M205857200. PubMed PMID: 12119303.
112. Eckford PD, Sharom FJ. The reconstituted Escherichia coli MsbA protein displays lipid flippase activity. Biochem J. 2010;429(1):195-203. Epub 2010/04/24. doi: 10.1042/bj20100144. PubMed PMID: 20412049; PubMed Central PMCID: PMCPMC2888566.
113. Doerrler WT, Reedy MC, Raetz CR. An Escherichia coli mutant defective in lipid export. J Biol Chem. 2001;276(15):11461-4. Epub 2001/03/30. doi: 10.1074/jbc.C100091200. PubMed PMID: 11278265.
114. Guo D, Singh H, Shimoyama A, Guffick C, Tang Y, Rowe SM, et al. Energetics of lipid transport by the ABC transporter MsbA is lipid dependent. Commun Biol. 2021;4(1):1379. Epub 20211209. doi: 10.1038/s42003-021-02902-8. PubMed PMID: 34887543; PubMed Central PMCID: PMCPMC8660845.
115. Reuter G, Janvilisri T, Venter H, Shahi S, Balakrishnan L, van Veen HW. The ATP binding cassette multidrug transporter LmrA and lipid transporter MsbA have overlapping substrate specificities. J Biol Chem. 2003;278(37):35193-8. Epub 2003/07/05. doi: 10.1074/jbc.M306226200. PubMed PMID: 12842882.
116. Eckford PD, Sharom FJ. Functional characterization of Escherichia coli MsbA: interaction with nucleotides and substrates. J Biol Chem. 2008;283(19):12840-50. Epub 2008/03/18. doi: 10.1074/jbc.M708274200. PubMed PMID: 18344567.
117. Kumar S, Mollo A, Kahne D, Ruiz N. The Bacterial Cell Wall: From Lipid II Flipping to Polymerization. Chem Rev. 2022;122(9):8884-910. Epub 2022/03/12. doi: 10.1021/acs.chemrev.1c00773. PubMed PMID: 35274942; PubMed Central PMCID: PMCPMC9098691.
118. van Heijenoort J. Formation of the glycan chains in the synthesis of bacterial peptidoglycan. Glycobiology. 2001;11(3):25r-36r. Epub 2001/04/26. doi: 10.1093/glycob/11.3.25r. PubMed PMID: 11320055.
119. Brown S, Santa Maria JP, Jr., Walker S. Wall teichoic acids of gram-positive bacteria. Annu Rev Microbiol. 2013;67:313-36. Epub 2013/09/13. doi: 10.1146/annurev-micro-092412-155620. PubMed PMID: 24024634; PubMed Central PMCID: PMCPMC3883102.
120. Valvano MA. Export of O-specific lipopolysaccharide. Front Biosci. 2003;8:s452-71. Epub 2003/04/18. doi: 10.2741/1079. PubMed PMID: 12700099.
121. van Heijenoort J. Lipid intermediates in the biosynthesis of bacterial peptidoglycan. Microbiol Mol Biol Rev. 2007;71(4):620-35. Epub 2007/12/08. doi: 10.1128/mmbr.00016-07. PubMed PMID: 18063720; PubMed Central PMCID: PMCPMC2168651.
122. van Dam V, Sijbrandi R, Kol M, Swiezewska E, de Kruijff B, Breukink E. Transmembrane transport of peptidoglycan precursors across model and bacterial membranes. Mol Microbiol. 2007;64(4):1105-14. Epub 2007/05/16. doi: 10.1111/j.1365-2958.2007.05722.x. PubMed PMID: 17501931.
123. Mohammadi T, van Dam V, Sijbrandi R, Vernet T, Zapun A, Bouhss A, et al. Identification of FtsW as a transporter of lipid-linked cell wall precursors across the membrane. Embo j. 2011;30(8):1425-32. Epub 2011/03/10. doi: 10.1038/emboj.2011.61. PubMed PMID: 21386816; PubMed Central PMCID: PMCPMC3102273.
124. Sham LT, Butler EK, Lebar MD, Kahne D, Bernhardt TG, Ruiz N. Bacterial cell wall. MurJ is the flippase of lipid-linked precursors for peptidoglycan biogenesis. Science. 2014;345(6193):220-2. Epub 2014/07/12. doi: 10.1126/science.1254522. PubMed PMID: 25013077; PubMed Central PMCID: PMCPMC4163187.

125. Meeske AJ, Sham LT, Kimsey H, Koo BM, Gross CA, Bernhardt TG, et al. MurJ and a novel lipid II flippase are required for cell wall biogenesis in Bacillus subtilis. Proc Natl Acad Sci U S A. 2015;112(20):6437-42. Epub 2015/04/29. doi: 10.1073/pnas.1504967112. PubMed PMID: 25918422; PubMed Central PMCID: PMCPMC4443310.
126. Miyakawa T, Matsuzawa H, Matsuhashi M, Sugino Y. Cell wall peptidoglycan mutants of Escherichia coli K-12: existence of two clusters of genes, mra and mrb, for cell wall peptidoglycan biosynthesis. J Bacteriol. 1972;112(2):950-8. Epub 1972/11/01. doi: 10.1128/jb.112.2.950-958.1972. PubMed PMID: 4563986; PubMed Central PMCID: PMCPMC251507.
127. Ishino F, Jung HK, Ikeda M, Doi M, Wachi M, Matsuhashi M. New mutations fts-36, lts-33, and ftsW clustered in the mra region of the Escherichia coli chromosome induce thermosensitive cell growth and division. J Bacteriol. 1989;171(10):5523-30. Epub 1989/10/01. doi: 10.1128/jb.171.10.5523-5530.1989. PubMed PMID: 2676977; PubMed Central PMCID: PMCPMC210392.
128. Ikeda M, Sato T, Wachi M, Jung HK, Ishino F, Kobayashi Y, et al. Structural similarity among Escherichia coli FtsW and RodA proteins and Bacillus subtilis SpoVE protein, which function in cell division, cell elongation, and spore formation, respectively. J Bacteriol. 1989;171(11):6375-8. Epub 1989/11/01. doi: 10.1128/jb.171.11.6375-6378.1989. PubMed PMID: 2509435; PubMed Central PMCID: PMCPMC210516.
129. Henriques AO, Glaser P, Piggot PJ, Moran CP, Jr. Control of cell shape and elongation by the rodA gene in Bacillus subtilis. Mol Microbiol. 1998;28(2):235-47. Epub 1998/06/11. doi: 10.1046/j.1365-2958.1998.00766.x. PubMed PMID: 9622350.
130. Lara B, Ayala JA. Topological characterization of the essential Escherichia coli cell division protein FtsW. FEMS Microbiol Lett. 2002;216(1):23-32. Epub 2002/11/09. doi: 10.1111/j.1574-6968.2002.tb11409.x. PubMed PMID: 12423747.
131. Mohammadi T, Sijbrandi R, Lutters M, Verheul J, Martin NI, den Blaauwen T, et al. Specificity of the transport of lipid II by FtsW in Escherichia coli. J Biol Chem. 2014;289(21):14707-18. Epub 2014/04/09. doi: 10.1074/jbc.M114.557371. PubMed PMID: 24711460; PubMed Central PMCID: PMCPMC4031526.
132. Taguchi A, Welsh MA, Marmont LS, Lee W, Sjodt M, Kruse AC, et al. FtsW is a peptidoglycan polymerase that is functional only in complex with its cognate penicillin-binding protein. Nat Microbiol. 2019;4(4):587-94. Epub 2019/01/30. doi: 10.1038/s41564-018-0345-x. PubMed PMID: 30692671; PubMed Central PMCID: PMCPMC6430707.
133. Ruiz N. Bioinformatics identification of MurJ (MviN) as the peptidoglycan lipid II flippase in Escherichia coli. Proc Natl Acad Sci U S A. 2008;105(40):15553-7. Epub 2008/10/04. doi: 10.1073/pnas.0808352105. PubMed PMID: 18832143; PubMed Central PMCID: PMCPMC2563115.
134. Inoue A, Murata Y, Takahashi H, Tsuji N, Fujisaki S, Kato J. Involvement of an essential gene, mviN, in murein synthesis in Escherichia coli. J Bacteriol. 2008;190(21):7298-301. Epub 2008/08/19. doi: 10.1128/jb.00551-08. PubMed PMID: 18708495; PubMed Central PMCID: PMCPMC2580715.
135. Hvorup RN, Winnen B, Chang AB, Jiang Y, Zhou XF, Saier MH, Jr. The multidrug/oligosaccharidyl-lipid/polysaccharide (MOP) exporter superfamily. Eur J Biochem. 2003;270(5):799-813. Epub 2003/02/27. doi: 10.1046/j.1432-1033.2003.03418.x. PubMed PMID: 12603313.
136. Kuk AC, Mashalidis EH, Lee SY. Crystal structure of the MOP flippase MurJ in an inward-facing conformation. Nat Struct Mol Biol. 2017;24(2):171-6. Epub 2016/12/27. doi: 10.1038/nsmb.3346. PubMed PMID: 28024149; PubMed Central PMCID: PMCPMC5382020.
137. Butler EK, Davis RM, Bari V, Nicholson PA, Ruiz N. Structure-function analysis of MurJ reveals a solvent-exposed cavity containing residues essential for peptidoglycan biogenesis in Escherichia coli. J Bacteriol. 2013;195(20):4639-49. Epub 2013/08/13. doi: 10.1128/jb.00731-13. PubMed PMID: 23935042; PubMed Central PMCID: PMCPMC3807429.
138. Butler EK, Tan WB, Joseph H, Ruiz N. Charge requirements of lipid II flippase activity in Escherichia coli. J Bacteriol. 2014;196(23):4111-9. Epub 2014/09/17. doi: 10.1128/jb.02172-14. PubMed PMID: 25225268; PubMed Central PMCID: PMCPMC4248868.

139. Kuk ACY, Hao A, Lee S-Y. Structure and Mechanism of the Lipid Flippase MurJ. Annual Review of Biochemistry. 2022;91(1):null. doi: 10.1146/annurev-biochem-040320-105145. PubMed PMID: 35320686.
140. Zheng S, Sham LT, Rubino FA, Brock KP, Robins WP, Mekalanos JJ, et al. Structure and mutagenic analysis of the lipid II flippase MurJ from Escherichia coli. Proc Natl Acad Sci U S A. 2018;115(26):6709-14. Epub 2018/06/13. doi: 10.1073/pnas.1802192115. PubMed PMID: 29891673; PubMed Central PMCID: PMCPMC6042122.
141. Jervis AJ, Thackray PD, Houston CW, Horsburgh MJ, Moir A. SigM-responsive genes of Bacillus subtilis and their promoters. J Bacteriol. 2007;189(12):4534-8. Epub 2007/04/17. doi: 10.1128/jb.00130-07. PubMed PMID: 17434969; PubMed Central PMCID: PMCPMC1913368.
142. Elhenawy W, Davis RM, Fero J, Salama NR, Felman MF, Ruiz N. The O-Antigen Flippase Wzk Can Substitute for MurJ in Peptidoglycan Synthesis in Helicobacter pylori and Escherichia coli. PLoS One. 2016;11(8):e0161587. Epub 2016/08/19. doi: 10.1371/journal.pone.0161587. PubMed PMID: 27537185; PubMed Central PMCID: PMCPMC4990322.
143. Harvat EM, Zhang YM, Tran CV, Zhang Z, Frank MW, Rock CO, et al. Lysophospholipid flipping across the Escherichia coli inner membrane catalyzed by a transporter (LplT) belonging to the major facilitator superfamily. J Biol Chem. 2005;280(12):12028-34. Epub 2005/01/22. doi: 10.1074/jbc.M414368200. PubMed PMID: 15661733.
144. Zheng L, Lin Y, Lu S, Zhang J, Bogdanov M. Biogenesis, transport and remodeling of lysophospholipids in Gram-negative bacteria. Biochim Biophys Acta Mol Cell Biol Lipids. 2017;1862(11):1404-13. Epub 2016/12/14. doi: 10.1016/j.bbalip.2016.11.015. PubMed PMID: 27956138; PubMed Central PMCID: PMCPMC6162059.
145. Lin Y, Deepak R, Zheng JZ, Fan H, Zheng L. A dual substrate-accessing mechanism of a major facilitator superfamily protein facilitates lysophospholipid flipping across the cell membrane. J Biol Chem. 2018;293(51):19919-31. Epub 2018/10/31. doi: 10.1074/jbc.RA118.005548. PubMed PMID: 30373772; PubMed Central PMCID: PMCPMC6314139.
146. Quek DQ, Nguyen LN, Fan H, Silver DL. Structural Insights into the Transport Mechanism of the Human Sodium-dependent Lysophosphatidylcholine Transporter MFSD2A. J Biol Chem. 2016;291(18):9383-94. Epub 2016/03/06. doi: 10.1074/jbc.M116.721035. PubMed PMID: 26945070; PubMed Central PMCID: PMCPMC4850279.
147. Lin Y, Bogdanov M, Tong S, Guan Z, Zheng L. Substrate Selectivity of Lysophospholipid Transporter LplT Involved in Membrane Phospholipid Remodeling in Escherichia coli. J Biol Chem. 2016;291(5):2136-49. Epub 2015/11/29. doi: 10.1074/jbc.M115.700419. PubMed PMID: 26613781; PubMed Central PMCID: PMCPMC4732200.
148. Ohniwa RL, Kitabayashi K, Morikawa K. Alternative cardiolipin synthase Cls1 compensates for stalled Cls2 function in Staphylococcus aureus under conditions of acute acid stress. FEMS microbiology letters. 2013;338(2):141-6.
149. Gould RM, Lennarz W. Metabolism of phosphatidylglycerol and lysyl phosphatidylglycerol in Staphylococcus aureus. Journal of Bacteriology. 1970;104(3):1135-44.
150. Tsatskis Y, Khambati J, Dobson M, Bogdanov M, Dowhan W, Wood JM. The osmotic activation of transporter ProP is tuned by both its C-terminal coiled-coil and osmotically induced changes in phospholipid composition. Journal of Biological Chemistry. 2005;280(50):41387-94.
151. López CS, Heras H, Garda H, Ruzal S, Sánchez-Rivas C, Rivas E. Biochemical and biophysical studies of Bacillus subtilis envelopes under hyperosmotic stress. Int J Food Microbiol. 2000;55(1-3):137-42. Epub 2000/05/03. doi: 10.1016/s0168-1605(00)00171-9. PubMed PMID: 10791732.
152. Kanemasa Y, Yoshioka T, Hayashi H. Alteration of the phospholipid composition of Staphylococcus aureus cultured in medium containing NaCl. Biochimica et biophysica acta. 1972;280(3):444-50.

153. Geske T, Vom Dorp K, Dörmann P, Hölzl G. Accumulation of glycolipids and other non-phosphorous lipids in Agrobacterium tumefaciens grown under phosphate deprivation. Glycobiology. 2013;23(1):69-80.
154. Geiger O, Röhrs V, Weissenmayer B, Finan TM, Thomas-Oates JE. The regulator gene phoB mediates phosphate stress-controlled synthesis of the membrane lipid diacylglyceryl-N,N,N-trimethylhomoserine in Rhizobium (Sinorhizobium) meliloti. Mol Microbiol. 1999;32(1):63-73. Epub 1999/04/27. doi: 10.1046/j.1365-2958.1999.01325.x. PubMed PMID: 10216860.
155. Nishi H, Komatsuzawa H, Fujiwara T, McCallum N, Sugai M. Reduced content of lysyl-phosphatidylglycerol in the cytoplasmic membrane affects susceptibility to moenomycin, as well as vancomycin, gentamicin, and antimicrobial peptides, in Staphylococcus aureus. Antimicrobial Agents and Chemotherapy. 2004;48(12):4800-7.
156. Samant S, Hsu F-F, Neyfakh AA, Lee H. The Bacillus anthracis protein MprF is required for synthesis of lysylphosphatidylglycerols and for resistance to cationic antimicrobial peptides. Journal of bacteriology. 2009;191(4):1311-9.
157. Arendt W, Hebecker S, Jäger S, Nimtz M, Moser J. Resistance phenotypes mediated by aminoacyl-phosphatidylglycerol synthases. Journal of bacteriology. 2012;194(6):1401-16.
158. Andrä J, Goldmann T, Ernst CM, Peschel A, Gutsmann T. Multiple peptide resistance factor (MprF)-mediated Resistance of Staphylococcus aureus against antimicrobial peptides coincides with a modulated peptide interaction with artificial membranes comprising lysyl-phosphatidylglycerol. J Biol Chem. 2011;286(21):18692-700. Epub 2011/04/09. doi: 10.1074/jbc.M111.226886. PubMed PMID: 21474443; PubMed Central PMCID: PMCPMC3099686.
159. Mileykovskaya E, Dowhan W. Cardiolipin membrane domains in prokaryotes and eukaryotes. Biochimica et Biophysica Acta (BBA)-Biomembranes. 2009;1788(10):2084-91.
160. Dowhan W, Mileykovskaya E, Bogdanov M. Diversity and versatility of lipid–protein interactions revealed by molecular genetic approaches. Biochimica et Biophysica Acta (BBA)-Biomembranes. 2004;1666(1-2):19-39.
161. Kawai F, Shoda M, Harashima R, Sadaie Y, Hara H, Matsumoto K. Cardiolipin domains in Bacillus subtilis marburg membranes. Journal of bacteriology. 2004;186(5):1475-83.
162. Barák I, Muchová K. The role of lipid domains in bacterial cell processes. International journal of molecular sciences. 2013;14(2):4050-65.
163. Mukhopadhyay R, Huang KC, Wingreen NS. Lipid localization in bacterial cells through curvature-mediated microphase separation. Biophysical Journal. 2008;95(3):1034-49.
164. Wood JM. Perspective: challenges and opportunities for the study of cardiolipin, a key player in bacterial cell structure and function. Curr Genet. 2018;64(4):795-8. Epub 2018/02/11. doi: 10.1007/s00294-018-0811-2. PubMed PMID: 29427078.
165. Mileykovskaya E. Subcellular localization of Escherichia coli osmosensory transporter ProP: focus on cardiolipin membrane domains. Molecular microbiology. 2007;64(6):1419-22.
166. Saxena R, Fingland N, Patil D, Sharma AK, Crooke E. Crosstalk between DnaA protein, the initiator of Escherichia coli chromosomal replication, and acidic phospholipids present in bacterial membranes. Int J Mol Sci. 2013;14(4):8517-37. Epub 2013/04/19. doi: 10.3390/ijms14048517. PubMed PMID: 23595001; PubMed Central PMCID: PMCPMC3645759.
167. Barák I, Muchová K, Wilkinson AJ, O'Toole PJ, Pavlendová N. Lipid spirals in Bacillus subtilis and their role in cell division. Molecular microbiology. 2008;68(5):1315-27.
168. Muchová K, Wilkinson AJ, Barák I. Changes of lipid domains in Bacillus subtilis cells with disrupted cell wall peptidoglycan. FEMS microbiology letters. 2011;325(1):92-8.
169. Peters PC, Migocki MD, Thoni C, Harry EJ. A new assembly pathway for the cytokinetic Z ring from a dynamic helical structure in vegetatively growing cells of Bacillus subtilis. Molecular microbiology. 2007;64(2):487-99.
170. Lopez D. Molecular composition of functional microdomains in bacterial membranes. Chem Phys Lipids. 2015;192:3-11. Epub 2015/09/01. doi: 10.1016/j.chemphyslip.2015.08.015. PubMed PMID: 26320704.
171. López D, Kolter R. Functional microdomains in bacterial membranes. Genes & development. 2010;24(17):1893-902.

172. Deatherage BL, Cookson BT. Membrane vesicle release in bacteria, eukaryotes, and archaea: a conserved yet underappreciated aspect of microbial life. Infect Immun. 2012;80(6):1948-57. Epub 2012/03/14. doi: 10.1128/iai.06014-11. PubMed PMID: 22409932; PubMed Central PMCID: PMCPMC3370574.
173. Villageliu DN, Samuelson DR. The Role of Bacterial Membrane Vesicles in Human Health and Disease. Front Microbiol. 2022;13:828704. Epub 2022/03/19. doi: 10.3389/fmicb.2022.828704. PubMed PMID: 35300484; PubMed Central PMCID: PMCPMC8923303.
174. Schlatterer K, Beck C, Hanzelmann D, Lebtig M, Fehrenbacher B, Schaller M, et al. The Mechanism behind Bacterial Lipoprotein Release: Phenol-Soluble Modulins Mediate Toll-Like Receptor 2 Activation via Extracellular Vesicle Release from Staphylococcus aureus. mBio. 2018;9(6). Epub 2018/11/22. doi: 10.1128/mBio.01851-18. PubMed PMID: 30459192; PubMed Central PMCID: PMCPMC6247081.
175. Bose S, Aggarwal S, Singh DV, Acharya N. Extracellular vesicles: An emerging platform in gram-positive bacteria. Microb Cell. 2020;7(12):312-22. Epub 2020/12/19. doi: 10.15698/mic2020.12.737. PubMed PMID: 33335921; PubMed Central PMCID: PMCPMC7713254.
176. Lee EY, Choi DY, Kim DK, Kim JW, Park JO, Kim S, et al. Gram-positive bacteria produce membrane vesicles: proteomics-based characterization of Staphylococcus aureus-derived membrane vesicles. Proteomics. 2009;9(24):5425-36. Epub 2009/10/17. doi: 10.1002/pmic.200900338. PubMed PMID: 19834908.
177. Brown L, Kessler A, Cabezas-Sanchez P, Luque-Garcia JL, Casadevall A. Extracellular vesicles produced by the Gram-positive bacterium Bacillus subtilis are disrupted by the lipopeptide surfactin. Mol Microbiol. 2014;93(1):183-98. Epub 2014/05/16. doi: 10.1111/mmi.12650. PubMed PMID: 24826903; PubMed Central PMCID: PMCPMC4079059.
178. Manning AJ, Kuehn MJ. Contribution of bacterial outer membrane vesicles to innate bacterial defense. BMC Microbiol. 2011;11:258. Epub 2011/12/03. doi: 10.1186/1471-2180-11-258. PubMed PMID: 22133164; PubMed Central PMCID: PMCPMC3248377.
179. Stentz R, Horn N, Cross K, Salt L, Brearley C, Livermore DM, et al. Cephalosporinases associated with outer membrane vesicles released by Bacteroides spp. protect gut pathogens and commensals against β-lactam antibiotics. J Antimicrob Chemother. 2015;70(3):701-9. Epub 2014/11/30. doi: 10.1093/jac/dku466. PubMed PMID: 25433011; PubMed Central PMCID: PMCPMC4319488.
180. Andreoni F, Toyofuku M, Menzi C, Kalawong R, Mairpady Shambat S, François P, et al. Antibiotics Stimulate Formation of Vesicles in Staphylococcus aureus in both Phage-Dependent and -Independent Fashions and via Different Routes. Antimicrob Agents Chemother. 2019;63(2). Epub 2018/12/05. doi: 10.1128/aac.01439-18. PubMed PMID: 30509943; PubMed Central PMCID: PMCPMC6355553.
181. Dean SN, Rimmer MA, Turner KB, Phillips DA, Caruana JC, Hervey WJt, et al. Lactobacillus acidophilus Membrane Vesicles as a Vehicle of Bacteriocin Delivery. Front Microbiol. 2020;11:710. Epub 2020/05/20. doi: 10.3389/fmicb.2020.00710. PubMed PMID: 32425905; PubMed Central PMCID: PMCPMC7203471.
182. McBroom AJ, Kuehn MJ. Release of outer membrane vesicles by Gram-negative bacteria is a novel envelope stress response. Mol Microbiol. 2007;63(2):545-58. Epub 2006/12/14. doi: 10.1111/j.1365-2958.2006.05522.x. PubMed PMID: 17163978; PubMed Central PMCID: PMCPMC1868505.
183. Moldovan A, Fraunholz MJ. In or out: Phagosomal escape of Staphylococcus aureus. Cell Microbiol. 2019;21(3):e12997. Epub 2018/12/24. doi: 10.1111/cmi.12997. PubMed PMID: 30576050.
184. Deo P, Chow SH, Hay ID, Kleifeld O, Costin A, Elgass KD, et al. Outer membrane vesicles from Neisseria gonorrhoeae target PorB to mitochondria and induce apoptosis. PLoS Pathog. 2018;14(3):e1006945. Epub 2018/03/31. doi: 10.1371/journal.ppat.1006945. PubMed PMID: 29601598; PubMed Central PMCID: PMCPMC5877877.
185. Cossart P, Vicente MF, Mengaud J, Baquero F, Perez-Diaz JC, Berche P. Listeriolysin O is essential for virulence of Listeria monocytogenes: direct evidence obtained by gene complementation. Infect Immun. 1989;57(11):3629-36. Epub 1989/11/01. doi:

10.1128/iai.57.11.3629-3636.1989. PubMed PMID: 2509366; PubMed Central PMCID: PMCPMC259877.
186. Aktar S, Okamoto Y, Ueno S, Tahara YO, Imaizumi M, Shintani M, et al. Incorporation of Plasmid DNA Into Bacterial Membrane Vesicles by Peptidoglycan Defects in Escherichia coli. Front Microbiol. 2021;12:747606. Epub 2021/12/17. doi: 10.3389/fmicb.2021.747606. PubMed PMID: 34912309; PubMed Central PMCID: PMCPMC8667616.
187. Hua Y, Wang J, Huang M, Huang Y, Zhang R, Bu F, et al. Outer membrane vesicles-transmitted virulence genes mediate the emergence of new antimicrobial-resistant hypervirulent Klebsiella pneumoniae. Emerg Microbes Infect. 2022;11(1):1281-92. Epub 2022/04/20. doi: 10.1080/22221751.2022.2065935. PubMed PMID: 35437096; PubMed Central PMCID: PMCPMC9132476.
188. Li C, Wen R, Mu R, Chen X, Ma P, Gu K, et al. Outer Membrane Vesicles of Avian PathogenicEscherichia coli Mediate the Horizontal Transmission of bla(CTX-M-55). Pathogens. 2022;11(4). Epub 2022/04/24. doi: 10.3390/pathogens11040481. PubMed PMID: 35456156; PubMed Central PMCID: PMCPMC9025603.
189. Dell'Annunziata F, Dell'Aversana C, Doti N, Donadio G, Dal Piaz F, Izzo V, et al. Outer Membrane Vesicles Derived from Klebsiella pneumoniae Are a Driving Force for Horizontal Gene Transfer. Int J Mol Sci. 2021;22(16). Epub 2021/08/28. doi: 10.3390/ijms22168732. PubMed PMID: 34445438; PubMed Central PMCID: PMCPMC8395779.
190. Zhao Z, Wang L, Miao J, Zhang Z, Ruan J, Xu L, et al. Regulation of the formation and structure of biofilms by quorum sensing signal molecules packaged in outer membrane vesicles. Sci Total Environ. 2022;806(Pt 4):151403. Epub 2021/11/08. doi: 10.1016/j.scitotenv.2021.151403. PubMed PMID: 34742801.
191. Mashburn LM, Whiteley M. Membrane vesicles traffic signals and facilitate group activities in a prokaryote. Nature. 2005;437(7057):422-5. Epub 2005/09/16. doi: 10.1038/nature03925. PubMed PMID: 16163359.
192. Lin J, Cheng J, Wang Y, Shen X. The Pseudomonas Quinolone Signal (PQS): Not Just for Quorum Sensing Anymore. Front Cell Infect Microbiol. 2018;8:230. Epub 2018/07/20. doi: 10.3389/fcimb.2018.00230. PubMed PMID: 30023354; PubMed Central PMCID: PMCPMC6039570.
193. Sultan S, Mottawea W, Yeo J, Hammami R. Gut Microbiota Extracellular Vesicles as Signaling Molecules Mediating Host-Microbiota Communications. Int J Mol Sci. 2021;22(23). Epub 2021/12/11. doi: 10.3390/ijms222313166. PubMed PMID: 34884969; PubMed Central PMCID: PMCPMC8658398.
194. Prados-Rosales R, Baena A, Martinez LR, Luque-Garcia J, Kalscheuer R, Veeraraghavan U, et al. Mycobacteria release active membrane vesicles that modulate immune responses in a TLR2-dependent manner in mice. J Clin Invest. 2011;121(4):1471-83. Epub 2011/03/03. doi: 10.1172/jci44261. PubMed PMID: 21364279; PubMed Central PMCID: PMCPMC3069770.
195. Bielaszewska M, Marejková M, Bauwens A, Kunsmann-Prokscha L, Mellmann A, Karch H. Enterohemorrhagic Escherichia coli O157 outer membrane vesicles induce interleukin 8 production in human intestinal epithelial cells by signaling via Toll-like receptors TLR4 and TLR5 and activation of the nuclear factor NF-κB. Int J Med Microbiol. 2018;308(7):882-9. Epub 2018/06/24. doi: 10.1016/j.ijmm.2018.06.004. PubMed PMID: 29934223.
196. Kaparakis M, Turnbull L, Carneiro L, Firth S, Coleman HA, Parkington HC, et al. Bacterial membrane vesicles deliver peptidoglycan to NOD1 in epithelial cells. Cell Microbiol. 2010;12(3):372-85. Epub 2009/11/06. doi: 10.1111/j.1462-5822.2009.01404.x. PubMed PMID: 19888989.
197. Stentz R, Carvalho AL, Jones EJ, Carding SR. Fantastic voyage: the journey of intestinal microbiota-derived microvesicles through the body. Biochem Soc Trans. 2018;46(5):1021-7. Epub 2018/08/30. doi: 10.1042/bst20180114. PubMed PMID: 30154095; PubMed Central PMCID: PMCPMC6195637.
198. Shen Y, Giardino Torchia ML, Lawson GW, Karp CL, Ashwell JD, Mazmanian SK. Outer membrane vesicles of a human commensal mediate immune regulation and disease protection. Cell Host Microbe. 2012;12(4):509-20. Epub 2012/09/25. doi:

10.1016/j.chom.2012.08.004. PubMed PMID: 22999859; PubMed Central PMCID: PMCPMC3895402.
199. Gu Z, Li F, Liu Y, Jiang M, Zhang L, He L, et al. Exosome-Like Nanoparticles From Lactobacillus rhamnosusGG Protect Against Alcohol-Associated Liver Disease Through Intestinal Aryl Hydrocarbon Receptor in Mice. Hepatol Commun. 2021;5(5):846-64. Epub 2021/05/25. doi: 10.1002/hep4.1679. PubMed PMID: 34027273; PubMed Central PMCID: PMCPMC8122379.
200. Bravo JA, Forsythe P, Chew MV, Escaravage E, Savignac HM, Dinan TG, et al. Ingestion of Lactobacillus strain regulates emotional behavior and central GABA receptor expression in a mouse via the vagus nerve. Proc Natl Acad Sci U S A. 2011;108(38):16050-5. Epub 2011/08/31. doi: 10.1073/pnas.1102999108. PubMed PMID: 21876150; PubMed Central PMCID: PMCPMC3179073.
201. Nikolova VL, Cleare AJ, Young AH, Stone JM. Updated Review and Meta-Analysis of Probiotics for the Treatment of Clinical Depression: Adjunctive vs. Stand-Alone Treatment. J Clin Med. 2021;10(4). Epub 2021/02/12. doi: 10.3390/jcm10040647. PubMed PMID: 33567631; PubMed Central PMCID: PMCPMC7915600.
202. Pirolli NH, Bentley WE, Jay SM. Bacterial Extracellular Vesicles and the Gut-Microbiota Brain Axis: Emerging Roles in Communication and Potential as Therapeutics. Adv Biol (Weinh). 2021;5(7):e2000540. Epub 2021/04/16. doi: 10.1002/adbi.202000540. PubMed PMID: 33857347.
203. Sedaghat M, Siadat SD, Mirabzadeh E, Keramati M, Vaziri F, Shafiei M, et al. Evaluation of antibody responses to outer membrane vesicles (OMVs) and killed whole cell of Vibrio cholerae O1 El Tor in immunized mice. Iran J Microbiol. 2019;11(3):212-9. Epub 2019/09/17. PubMed PMID: 31523404; PubMed Central PMCID: PMCPMC6711870.
204. Huang W, Zhang Q, Li W, Yuan M, Zhou J, Hua L, et al. Development of novel nanoantibiotics using an outer membrane vesicle-based drug efflux mechanism. J Control Release. 2020;317:1-22. Epub 2019/11/19. doi: 10.1016/j.jconrel.2019.11.017. PubMed PMID: 31738965.

Figures were created with Biorender.com

Chapter 2

Gain-of-Function Mutations in the Phospholipid Flippase MprF Confer Specific Daptomycin Resistance

Christoph M. Ernst,[a,b*] Christoph J. Slavetinsky,[a,b,e] Sebastian Kuhn,[a,b] Janna N. Hauser,[a,b] Mulugeta Nega,[a,b] Nagendra N. Mishra,[c,d] Cordula Gekeler,[a,b] Arnold S. Bayer,[c,d] Andreas Peschel[a,b]

[a]Interfaculty Institute of Microbiology and Infection Medicine, Infection Biology, University of Tübingen, Tübingen, Germany

[b]German Centre for Infection Research (DZIF), Partner Site Tübingen, Tübingen, Germany

[c]Los Angeles Biomedical Research Institute at Harbor-UCLA Medical Center, Torrance, California, USA

[d]David Geffen School of Medicine at UCLA, Los Angeles, California, USA

[e]Department of General Pediatrics, Oncology/Hematology, University Children's Hospital Tübingen, Tübingen, Germany

*Present address: Christoph M. Ernst, Department of Molecular Biology and Center for Computational and Integrative Biology, Massachusetts General Hospital, Harvard Medical School, Boston, Massachusetts, USA

C.M.E. and C.J.S. contributed equally to this article

mBio. 2018 Dec 18;9(6):e01659-18. doi: 10.1128/mBio.01659-18.

Abstract

Daptomycin, a calcium-dependent lipopeptide antibiotic whose full mode of action is still not entirely understood, has become a standard-of-care agent for treating methicillin-resistant *Staphylococcus aureus* (MRSA) infections. Daptomycin-resistant (DAP-R) S. aureus mutants emerge during therapy, featuring isolates which in most cases possess point mutations in the *mprF* gene. MprF is a bifunctional bacterial resistance protein that synthesizes the positively charged lipid lysyl-phosphatidylglycerol (LysPG) and translocates it subsequently from the inner membrane leaflet to the outer membrane leaflet. This process leads to increased positive *S. aureus* surface charge and reduces susceptibility to cationic antimicrobial peptides and cationic antibiotics. We characterized the most commonly reported MprF mutations in DAP-R *S. aureus* strains in a defined genetic background and found that only certain mutations, including the frequently reported T345A single nucleotide polymorphism (SNP), can reproducibly cause daptomycin resistance. Surprisingly, T345A did not alter LysPG synthesis, LysPG translocation, or the *S. aureus* cell surface charge. MprF-mediated DAP-R relied on a functional flippase domain and was restricted to daptomycin and a related cyclic lipopeptide antibiotic, friulimicin B, suggesting that the mutations modulate specific interactions with these two antibiotics. Notably, the T345A mutation led to weakened intramolecular domain interactions of MprF, suggesting that daptomycin and friulimicin resistance-conferring mutations may alter the substrate range of the MprF flippase to directly translocate these lipopeptide antibiotics or other membrane components with crucial roles in the activity of these antimicrobials. Our study points to a new mechanism used by *S. aureus* to resist calcium-dependent lipopeptide antibiotics and increases our understanding of the bacterial phospholipid flippase MprF.

Importance

Ever since daptomycin was introduced to the clinic, daptomycin- resistant isolates have been reported. In most cases, the resistant isolates harbor point mutations in MprF, which produces and flips the positively charged phospholipid LysPG. This has led to the assumption that the resistance mechanism relies on the overproduction of LysPG, given that increased LysPG production may lead to increased electrostatic repulsion of positively charged antimicrobial compounds, including daptomycin. Here we show that the resistance mechanism is highly specific and relies on a different process that involves a functional MprF flippase, suggesting that the resistance-conferring mutations may enable the flippase to accommodate daptomycin or an unknown component that is crucial for its activity. Our report provides a new perspective on the mechanism of resistance to a major antibiotic.

Keywords

daptomycin, MRSA, MprF, Staphylococcus aureus, antibiotic resistance, flippase

Introduction

The opportunistic pathogens Staphylococcus aureus, Enterococcus faecalis, and *Enterococcus faecium* are responsible for a large percentage of invasive infections, particularly in hospitalized and immunocompromised patients (1). These often life-threatening infections are complicated by the high prevalence of methicillin-resistant *S. aureus* (MRSA) and vancomycin-resistant enterococci (VRE) (1, 2), resulting in the frequent use of the lipopeptide antibiotic daptomycin, which has remained effective against drug-resistant isolates. Yet, an increasing number of reports on mutations emerging during daptomycin therapy, leading to increased daptomycin minimal inhibitory concentrations (MICs), have been reported (3–5). This phenomenon has raised concerns about the future of daptomycin therapy for such pathogens and has led to demands for in-depth investigations on the resistance mechanisms as well as counter-measures (6, 7).

Daptomycin is the first approved drug of a new class of calcium-dependent lipopeptide antibiotics, whose entire mode of action is still not fully understood (6, 8). It interacts with phosphatidylglycerol (PG) and interferes with bacterial fluid membrane microdomains, which leads to inhibition of cell wall synthesis (9). However, it is unclear if its activity requires a specific docking molecule in the membrane (9, 10). How point mutations in different *S. aureus* proteins contribute to or cause DAP-R remains equally elusive (6). Several proteins involved in the synthesis, regulation, or maintenance of cell surface molecules have been reported to be mutated during prolonged exposure to daptomycin (6). The characterization of such mutants has led, in part, to conflicting findings of potentially altered bacterial cell surface charge, lipid composition, or cell wall thickness (3, 4, 11–15). In *S. aureus*, distinct mutations in the phospholipid (PL) synthase and flippase, MprF, have repeatedly been found to affect daptomycin susceptibility (6) and to be among the first to emerge during exposure of *S. aureus* to serial passage in increasing sublethal daptomycin concentrations (16). MprF links lysine to negatively charged PG (17) and translocates the resulting positively charged lysyl-PG (LysPG) to the outer leaflet of the cytoplasmic membrane (CM) (18), resulting in electrostatic repulsion of cationic antimicrobial peptides (CAMPs), including human defensins and bacterial lantibiotics (17, 18). Daptomycin resembles CAMPs following its binding to calcium ions, an event absolutely required for its microbiologic activity (19). Chromosomal deletion of MprF leads to CAMP and daptomycin hyper susceptibility, while an intact MprF protein confers a basic level of DAP-R, which is usually low enough to enable effective therapy with daptomycin (18).

MprF is the first example of a bacterial phospholipid flippase. Recent studies have revealed important details about its membrane topology and domain organization (20). It is still unclear which lipid molecules can be translocated by MprF, although its substrate range has been found to include the zwitterionic lipid alanyl-PG (AlaPG) in addition to LysPG (21). Of note, DAP-R-conferring point mutations in MprF are often found in distinct regions of the protein and do not seem to affect conserved amino acid positions (6, 18, 20).

In this study, we characterized the most frequently reported DAP-R-associated MprF point mutations in a defined genetic background, in order to exclude potentially contributing activities of additional mutations and accessory elements. We found that only some of the widely reported mutations associated with DAP-R can reproducibly cause DAP-R and that they do not affect LysPG synthesis and translocation or any other process affecting the *S. aureus* cell surface charge. MprF-mediated DAP-R led to cross-resistance only to the structurally related cyclic lipopeptide friulimicin B, which has a different target than daptomycin (10, 22), indicating that the resistance mechanism is based on specific interactions with the drug rather than the target molecule. We found that DAP-R relied on a functional flippase domain and was associated with reduced intramolecular domain interactions of MprF, suggesting that alteration of the protein structure modulates the substrate range of the flippase to accommodate daptomycin or another membrane-embedded substrate that is crucial for daptomycin activity.

Results

Distinct point mutations at the junction of MprF synthase and flippase lead to DAP-R. The most frequently identified MprF mutations associated with DAP-R are located at the junction of the flippase domain and synthase domain or in the synthase domain of the protein (Fig. 1A; see also Table S1 in the supplemental material). These strains often contain additional point mutations in other chromosomal loci, such as *yycFG* (*walKR*), *rpoB*, *rpoC*, *vraS*, and *dltA* (6, 7), raising the issue of whether the documented MprF mutations are in fact sufficient for mediating the DAP-R phenotype. In order to elucidate the contribution of individual mutations to DAP-R in a defined genetic background, the most frequently identified mutations were introduced into mprF harbored on a plasmid, which was then transferred to the *S. aureus* 113 (SA113) *mprF* mutant. Two mutations at the junction between the flippase domain and the synthase domain (T345A and V351E) led to significantly increased, clinically relevant DAP-R (MIC of 3 µg/ml) compared to the parental MprF sequence (MIC of 1 µg/ml) (Fig. 1B). In contrast, other mutations in this region of the protein (S295L, P314L, and S337L) and two mutations in the synthase domain (I420N and L826F) did not alter daptomycin susceptibility, suggesting that these mutations contribute to DAP-R only in combination with additional

mutations. Thus, specific mutations at the junction between the synthase domain and the flippase domain of MprF can reproducibly confer DAP-R in *S. aureus*.

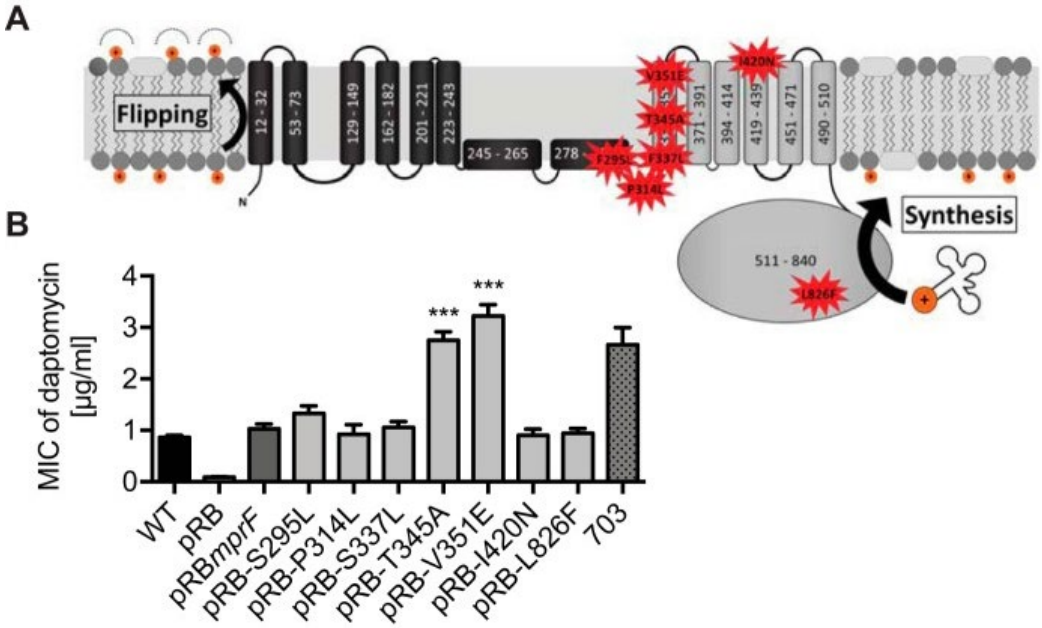

Fig 1: Specific mutations at the junction of the flippase domain and synthase domain of MprF confer daptomycin resistance. (A) Topology of most frequent DAP-R-associated point mutations in MprF (Table S1). The MprF synthase and flippase domains are shown in gray and black, respectively. (B) Impact of daptomycin resistance-associated point mutations expressed in the *S. aureus ΔmprF* mutant on daptomycin susceptibility. The recently characterized clinical daptomycin-resistant isolate, strain 703 (4), served as a control and reference for clinically relevant daptomycin MICs. Values that are significantly different from the values determined for the *S. aureus ΔmprF* mutant expressing wild-type MprF (pRB*mprF*) are indicated (***, $P < 0.0001$). The means plus standard errors of the means (SEM) of results from at least five independent experiments are shown. WT, wild type.

DAP-R-conferring point mutations in MprF do not alter the cellular LysPG level or membrane leaflet distribution. Basal levels of CAMP resistance mediated by MprF depend on the protein's capacity to synthesize LysPG and translocate a substantial amount of this lipid to the outer membrane leaflet, where it repulses harmful cationic proteins by electrostatic interaction (17, 18, 23, 24). In order to elucidate if the DAP-R-associated point mutations at the junction between the synthase domain and the flippase domain (Fig. 1B) might lead to increased activity of one of the two protein domains, the levels of LysPG production and distribution between the inner and outer membrane leaflets of *S. aureus* with native versus mutated *mprF* were compared. LysPG contents were determined by thin-layer chromatography (TLC) and staining of LysPG with the phosphate group-specific dye molybdenum blue (20, 21). None of the *S. aureus* strains expressing a mutated *mprF* gene exhibited altered LysPG production (Fig. 2A), indicating that these point mutations confer DAP-R via a mechanism other than increasing LysPG synthesis. Of note, the expression of the cloned *mprF* variants was controlled by the constitutive *Bacillus subtilis* promoter *vegII*, which may explain why they displayed slightly reduced LysPG production compared to the wild type. The localization of LysPG in the cytoplasmic membrane was determined by incubating intact *S. aureus* cells expressing MprF with wild-type sequence or with the T345A mutation with the

fluorescent dye fluorescamine, which reacts with the free amino group of LysPG at the outer membrane leaflet but cannot access the inner leaflet. Thin-layer chromatography and quantification of fluorescamine-labeled versus nonlabeled LysPG allowed inner-leaflet and outer-leaflet LysPG to be distinguished (25, 26). Experiments performed with wild-type MprF and T345A-MprF led to the same percentage of LysPG in the outer membrane (ca. 40%) (Fig. 2B), indicating that DAP-R is not associated with an increased capacity of MprF to translocate LysPG. Thus, the signature mutations in MprF leading to DAP-R do not seem to alter either of the two documented activities of MprF.

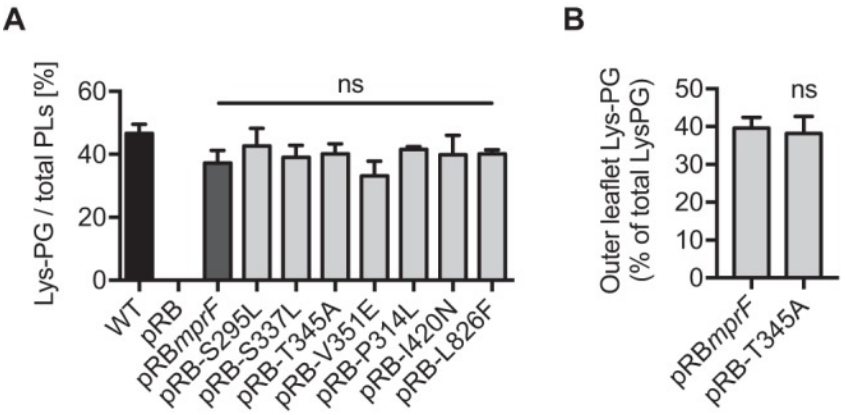

Fig 2: Signature DAP-R mutations in MprF do not alter known functions of MprF. (A) Percentages of LysPG production in relation to total phospholipid (PL) content. (B) Percentages of LysPG located in the outer leaflet of the membrane. Values that are not significantly different from the values determined for the *S. aureus ΔmprF* mutant expressing wild-type MprF (pRB*mprF*) are indicated (ns). The means plus SEM of results from three independent experiments are shown.

The DAP-R-conferring MprF point mutation T345A does not alter the *S. aureus* surface charge. Daptomycin is thought to integrate into the bacterial cytoplasmic membrane upon binding of calcium ions in a manner similar to that seen with many typical CAMPs (19). Most bacteria achieve protection against a broad range of CAMPs by introduction of positive charges that modify the bacterial surface charge and diminish the affinity for CAMPs, thereby allowing bacteria to tolerate substantial CAMP concentrations (27). Aside from the modification of membrane phospholipids with lysine or other amino acids, the neutralization of negatively charged teichoic acids (TAs) with D-alanine is a particularly widespread CAMP repulsion mechanism found in several bacterial divisions (27, 28). D-Alanylation of teichoic acids is mediated by the DltABCD system, which is composed of four proteins responsible for activation, transfer, and linkage of cytosolic D-alanine residues onto the backbone of teichoic acids (29). In order to determine if mutated, DAP-R-conferring MprF affects the Dlt system, we quantified the teichoic acid D-alanylation of *S. aureus* expressing wild-type MprF compared to T345A-MprF (Fig. 3A). While a *dltA* knockout mutant serving as a negative control showed the complete absence of D-alanylation, we did not observe a difference between strains expressing wild-type MprF and strains expressing T345A-MprF. In order to analyze if the daptomycin resistance-causing point mutations in MprF could some- how affect the overall *S.*

aureus surface charge in a LysPG or wall teichoic acid (WTA) alanylation-independent manner, the capacities of *S. aureus* expressing MprF with wild-type sequence or a T345A mutation to bind the cationic protein cytochrome c or calcium-bound annexin V was compared. These model proteins were proven to allow a sensitive assessment of changes in the surface charge of *S. aureus* in several previous studies (17, 18, 21, 30). The lack of *mprF* had a profound impact on the capacity of *S. aureus* to bind cytochrome c or annexin V (Fig. 3B), demonstrating the suitability of the assays. However, the T345A mutation did not alter the binding behavior of annexin V significantly (Fig. 3C), and both DAP-R-conferring mutations (T345A and V351E) did not alter the binding of cytochrome c (Fig. 3B). Thus, the DAP-R-conferring point mutations in MprF do not lead to a general alteration of the cell surface charge.

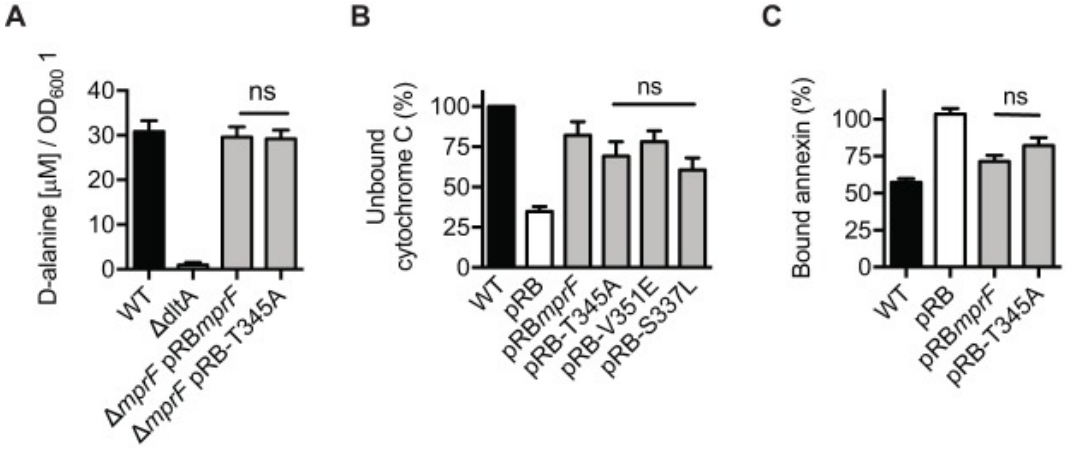

Fig 3: The DAP-R-conferring point mutations T345A and V351E do not affect cell surface charge. (A) Quantification of teichoic acid d-alanylation. The SA113 *dltA* deletion mutant served as a negative control (43). (B) Percentages of repulsed cytochrome *c* normalized to the wild type. The *mprF* deletion mutant was used as a negative control. (C) Percentages of bound annexin V normalized to the *ΔmprF* mutant harboring the empty plasmid (pRB). The *mprF* deletion mutant was used as a negative control. Values that are not significantly different from the values determined for the *S. aureus ΔmprF* mutant expressing wild-type MprF (pRB*mprF*) are indicated (ns). The means plus SEM of results from three independent experiments are shown.

MprF point mutation T345A causes cross-resistance only to daptomycin and the related lipopeptide antibiotic friulimicin B. The DAP-R-conferring point mutations in MprF do not seem to be based on a canonical CAMP resistance strategy, which raises the issue of how specific the resistance mechanism may be. A variety of cationic, membrane-active antibiotics from different classes and with different modes of action, including the calcium-dependent lipopeptides daptomycin and friulimicin B, the calcium-independent lipopeptide polymyxin B, the nonlipidated peptide bacitracin, the glycopeptide vancomycin, and the lantibiotics nisin and gallidermin (31, 32), were analyzed for their capacity to inhibit growth of *S. aureus* expressing MprF with wild-type sequence or a T345A mutation. The ability of these compounds to inhibit *S. aureus* growth was reduced in the presence of a functional MprF protein (Fig. 4A), which indicates that surface charge alterations have a strong impact on the capacity of these agents to inhibit *S. aureus*. In contrast, the neutral antibiotic oxacillin was not affected by MprF. However, the T345A and V351E mutations in MprF exclusively led to cross-resistance to friulimicin B, which is the closest relative of daptomycin among the tested antibiotics (Fig. 4)

but has a different target (10). Of note, the addition of calcium to calcium-independent antibiotics did not lead to differences in the levels of inhibition of *S. aureus* expressing wild-type versus T345A-MprF by any of these compounds (Fig. S1). Thus, mprF-mediated DAP-R does not lead to broad-spectrum cross-resistance to cationic antibiotics and antimicrobial peptides but is restricted to compounds with a specific, daptomycin-related structure. Moreover, the different targets of daptomycin and friulimicin B suggest that the resistance mechanism does not involve the target of daptomycin.

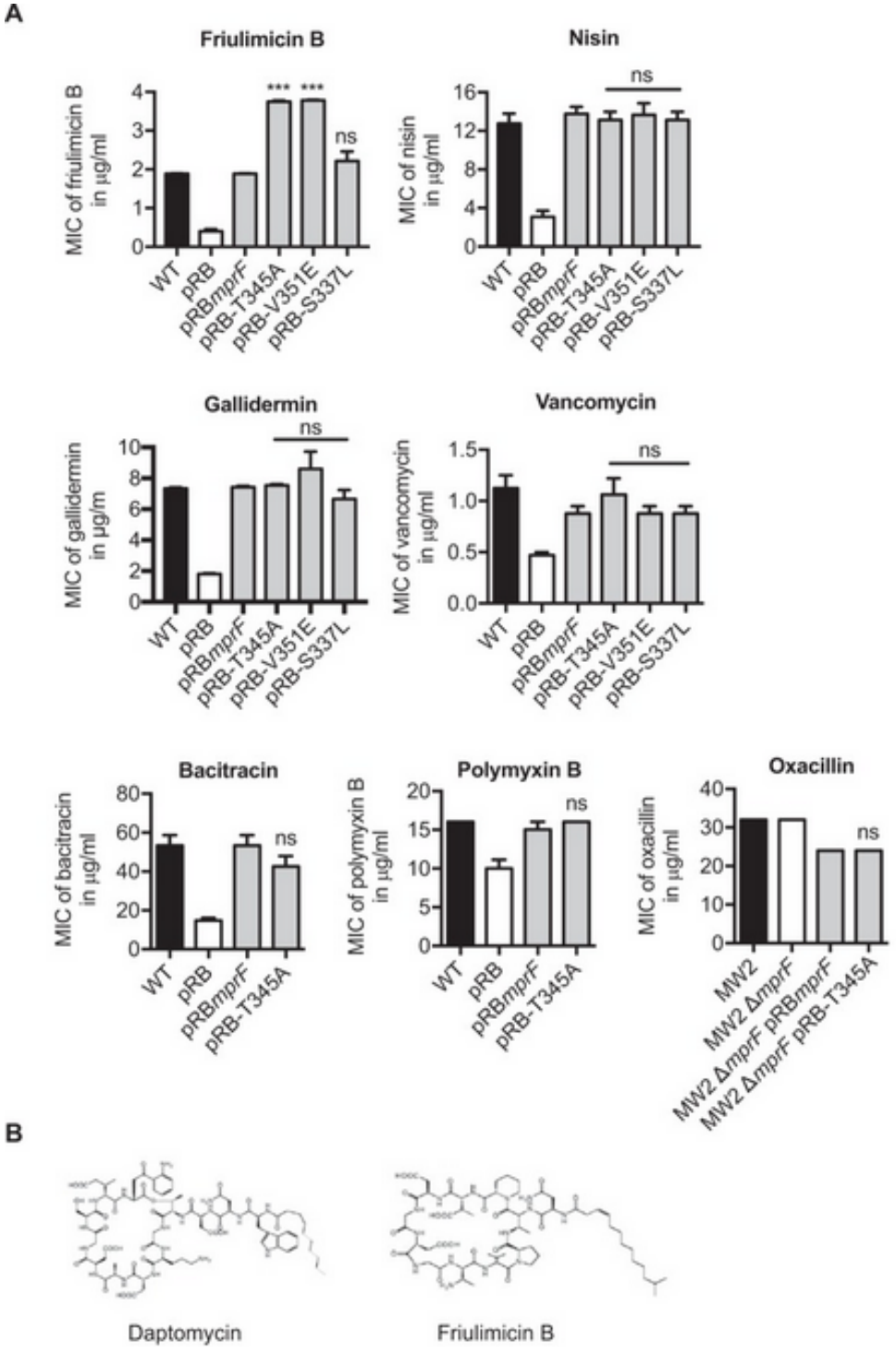

Fig 4: MprF-mediated daptomycin resistance leads to cross-resistance to friulimicin B. (A) MICs of antibiotics as indicated. The *mprF* deletion mutant served as a negative control. (B) Structures of friulimicin B and daptomycin

(22). Values that are significantly different from the values determined for the *S. aureus ΔmprF* mutant expressing wild-type MprF (pRB*mprF*) are indicated (***, $P < 0.0001$). Values that are not significantly different from the values determined for the *S. aureus ΔmprF* mutant expressing wild-type MprF (pRB*mprF*) are indicated (ns). The means plus SEM of results from three independent experiments are shown.

T345A-mediated DAP-R depends on the presence of a functional MprF flippase domain. The T345A point mutation does not alter the LysPG flippase activity of MprF, but it may enable the flippase to translocate other substrate molecules in addition to LysPG. We have previously identified conserved amino acids in the flippase domains of MprF proteins and have shown that they are essential for flippase activity (20). The ability of T345A to increase the MIC of daptomycin in the presence of the flippase-inactivating mutations D71A, R112A, and E206A was investigated. All the resulting strains were hypersusceptible to the CAMP bacitracin compared to strains expressing a functional MprF (Fig. 5A), which confirms that LysPG could not be translocated from the inner layer to the outer layer of the cell membrane in these strains. T345A was not able to increase the daptomycin MIC in combination with mutations D71A and R206A and led to an only slightly increased MIC with mutation R112A (Fig. 5B), indicating that the functionality of the MprF flippase is crucial for the capacity of T345A to confer DAP-R.

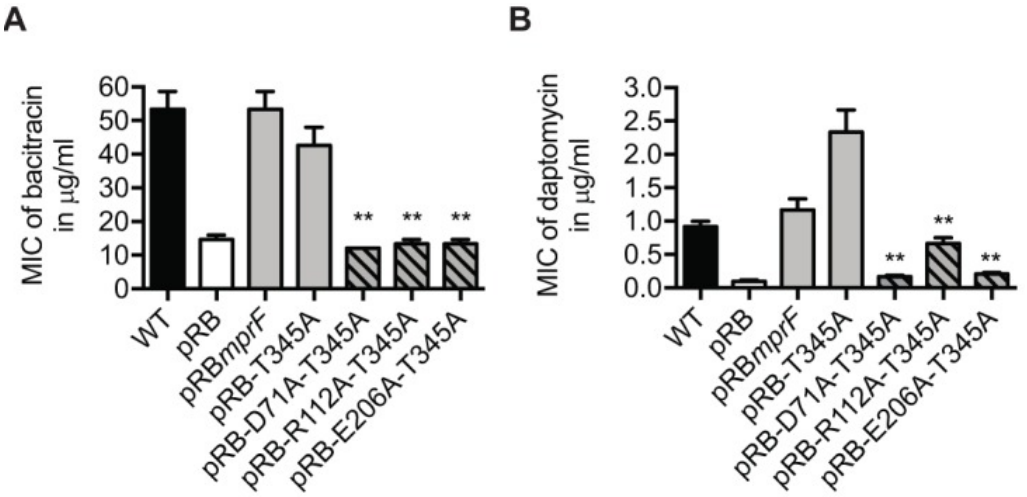

Fig 5: The functionality of the MprF flippase is required for MprF-mediated DAP-R. (A) MIC of bacitracin as indicator of flippase activity. (B) MIC of daptomycin. The means plus SEM of results from three independent experiments are shown. Values that are significantly different from the values determined for the *S. aureus ΔmprF* mutant expressing T345A-MprF (pRB-T345A) are indicated (**, $P < 0.01$).

The T345A point mutation reduces intramolecular interactions of MprF domains. The point mutations in MprF leading to DAP-R do not occur at conserved amino acid positions, but they involve a variety of sites at the junction of the LysPG synthase and flippase domains (Fig. 1B). The various domains of MprF have been found to undergo several complex intramolecular interactions (20), which may be altered by the T345A point mutation. In order to test this hypothesis, the impact of T345A on the capacities of full-length MprF or of the synthase and flippase domains to interact were compared in the bacterial two-hybrid system, which has been proven to be suitable for elucidating intramolecular MprF interactions (20). Full-length MprF proteins with native sequence and those with the T345A point mutation showed similar capacities to interact (Fig. 6A). However, the flippase domain and an extended version of the

flippase domain, which was previously shown to be required for full flippase activity (20), interacted with the synthase domain much less efficiently when the T345A mutation was present. Thus, the T345A mutations in MprF (leading to specific resistance to structurally related lipopeptide antibiotics) are associated with reduced intramolecular interactions. Such mutations do not seem to affect the efficiency of the flippase functionality but might instead extend the range of molecules that the flippase is able to translocate (Fig. 6B).

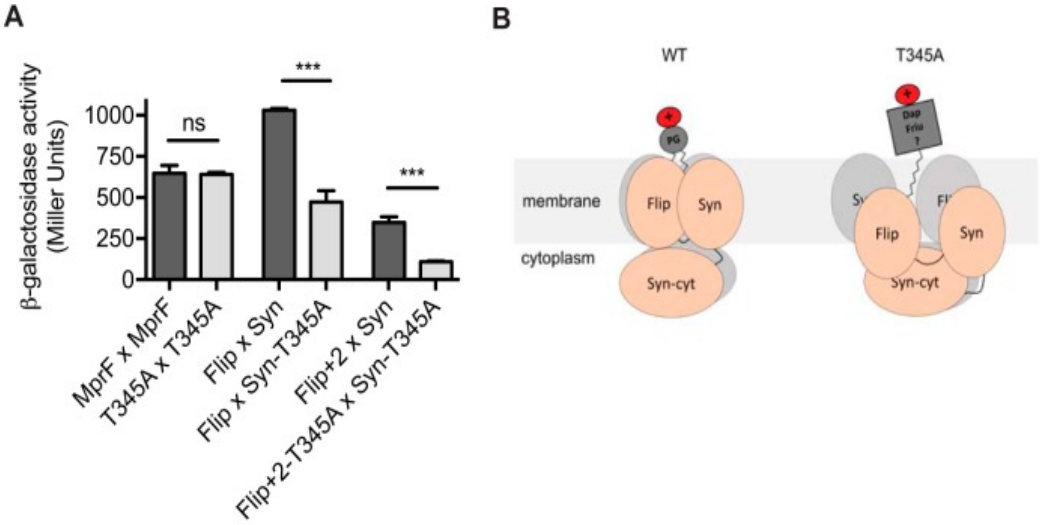

Fig 6: The DAP-R-conferring point mutation T345A reduces intramolecular interactions of MprF domains. The T345A mutation is located in the hydrophobic part of the synthase domain, which was previously shown to specifically interact with the flippase domain (20). β-Galactosidase activity of *E. coli* cells expressing full-length MprF (MprF), the flippase domain encompassing amino acids 1 to 320 (Flip), the extended flippase domain encompassing amino acids 1 to 393 (Flip + 2), and the synthase domain encompassing amino acids 328 to 840 (Syn) and T345A variants. The extended flippase domain consists of two additional transmembrane segments (TMS) of the synthase domain, which were previously shown to be required for full flippase activity (20). β-Galactosidase activity is displayed as Miller units. Values that are significantly different from those determined for the T345A variants are indicated (***, $P < 0.0001$). Values that are not significantly different from those determined for the T345A variants are indicated (ns). The means plus SEM of results from three independent experiments are shown. (B) Proposed model for MprF-mediated daptomycin resistance. MprF forms oligomers with distinct intradomain interactions (20), resulting in the formation of a translocation channel, which enables the flipping of bacterial phospholipids (LysPG and AlaPG) (21). Daptomycin resistance-conferring SNPs (e.g., T345A) reduce intradomain interactions, enabling the channel to accommodate daptomycin and friulimicin or a membrane-embedded molecule that is crucial for the activity of the two structurally related antibiotics. Flip, flippase domain; Syn, synthase domain; Syn-cyt, cytosolic part of the synthase domain; Dap, daptomycin; Friu, friulimicin B; ?, potential other membrane-embedded molecule that is crucial for daptomycin and friulimicin B activity; WT, wild type.

Discussion

Point mutations leading to resistance to antibiotics are a common phenomenon occurring during therapy with almost any antimicrobial compound (33). Resistance levels conferred by such mutations often lead to only moderately increased MICs; however, these can be sufficient to compromise the efficacy of antibiotic therapies. The mechanisms of antibiotic resistance are diverse, ranging from modified target molecules to decreased uptake or gain of function of enzymes that inactivate the antimicrobial compound (33). Elucidation of how the signature DAP-R-associated point mutations compromise the antibiotic's activity has remained elusive (6). Since such mutations often occur within MprF, a protein which is known to electrostatically

repulse CAMPs by synthesizing and translocating cationic LysPG (24), it is tempting to speculate that an increase of LysPG levels in the outer leaflet of the cytoplasmic membrane may be the major consequence of these DAP-R-conferring point mutations. By introducing the most frequently identified *mprF* mutations among clinically derived DAP-R strains into an *S. aureus* strain with a defined genetic background, we found, surprisingly, that many of them were not able to cause DAP-R. Yet it is possible that such mutations contribute to DAP-R in a more complex manner involving, for instance, additional changes in multiple genetic loci. Notably, our study results indicate that DAP-R- conferring point mutations at the junction of the flippase and synthase domains of MprF such as T345A and V351E do not alter the level or translocation of LysPG. Other research groups have reported the association of altered LysPG production and/or translocation with these reported *mprF* point mutations (3, 4, 14, 34). However, since most of those studies analyzed strains that had been under *in vitro* or *in vivo* selection pressure, it is possible that they harbored additional point mutations that either preexisted in the parental isolates or were acquired during daptomycin exposure that could have influenced MprF activity and DAP-R, for example, by additional modifications of the cell envelope or by other, less obvious modifications (see Table S2 in the supplemental material) (35).

The T345A point mutation was selected for more-detailed analyses and was found to not alter LysPG production or translocation, D-alanylation of teichoic acids, or the overall cell surface charge. T345A conferred resistance to only two structurally related lipopeptide antibiotics, namely, daptomycin and friulimicin B, whereas the activity of other lipopeptide or peptide antibiotics was not affected. Since daptomycin and friulimicin B do not share the same target (10), the resistance mechanism appears to be based on specific interactions of MprF with the structurally related lipopeptide antibiotics rather than with a target molecule. Moreover, T345A could confer resistance only when the flippase domain was functional, suggesting that flippase functionality may have been extended (rather than compromised), leading to DAP-R. We have previously shown that the MprF flippase is capable of flipping two different phospholipids species, Ala-PG and LysPG (21), which indicated that the flippase has relaxed substrate specificity for similar substrates. As proposed for other phospholipid flippases (36) and as suggested by our recent structural investigation of MprF (20), the membrane-integrated domains of MprF likely associate to form a channel in order to accommodate phospholipid substrate molecules and to facilitate their translocation. Thus, the affinity of MprF domains for each other may determine the substrate specificity of the channel and, in the case of reduced domain interactions, may extend the substrate specificity of the flippase to accommodate and translocate either daptomycin and friulimicin B or another membrane-embedded molecule whose orientation in the membrane is crucial for the activity of these antibiotics (Fig. 6B). A change in MprF flippase specificity would be in agreement with all of our findings; however,

this is particularly difficult to demonstrate directly because it would likely affect the orientation of substrate molecules in the membrane rather than their presence or absence. Moreover, as shown previously for other phospholipid transporters (36), the translocation process is probably very fast and may be reversible. Indeed, all our attempts to demonstrate that T345A-mutated MprF affects the membrane integration or orientation of daptomycin led to inconclusive results. Thus, future highly sophisticated and time-consuming biophysical technology performed with in vitro-reconstituted MprF-containing membrane vesicles will likely be necessary to study MprF-mediated altered daptomycin translocation dynamics in the membrane.

Our finding that T345A does not alter the LysPG synthase and flippase activity of MprF was unexpected and points to a novel resistance mechanism against daptomycin, which warrants further in-depth investigation. MprF is the first bacterial phospholipid flippase to have been described, but its mode of action remains only superficially understood. Our study reveals critical details of its role in a novel resistance mechanism with important implications for basic bacterial membrane-associated processes and for the development of inhibitors which may block DAP-R to maintain the efficacy of this important therapeutic compound.

Materials and Methods

Bacterial strains and mutagenesis of mprF. The common laboratory strain, methicillin-susceptible *S. aureus* SA113 (ATCC 35556) and its *mprF* knockout derivative SA113Δ*mprF* have been described recently (17). Point mutations in *mprF* were introduced by site-directed mutagenesis in *Escherichia coli* using *E. coli*/*S. aureus* shuttle vector pRB474 bearing *mprF* via the use of a QuikChange kit (Stratagene, La Jolla, CA, USA) (see Table S3 in the supplemental material), as described recently (20). Mutated derivatives of *mprF* were cloned in pRB474*mprF* and transferred into strain SA113Δ*mprF*. Expression of the pRB474*mprF* variants was mediated by the use of constitutive *Bacillus subtilis* promoter *vegII*. Plasmids were maintained with 10 μg/ml chloramphenicol in all studies, with the exception of the MIC assays. Plasmids used in this study are given in Table S3. Primers used in this study are given in Table S4.

Prediction of MprF structure. The transmembrane topology of MprF was predicted with the TOPCONS program (http://topcons.cbr.su.se/) combined with our latest experimental results (20).

Determination of susceptibility to antimicrobial agents. The MICs of daptomycin, bacitracin, polymyxin B, vancomycin, and oxacillin were determined with MIC test strips from Liofilchem according to the manufacturer's advice. The MICs of friulimicin B, nisin, and gallidermin were determined by broth microdilution in Mueller-Hinton broth (MHB) in a 24-well plate under shaking conditions. Friulimicin B and daptomycin MICs were determined in the

presence of 50 mg/liter $CaCl_2$. Other MICs were determined in the presence of 50 mg/liter $CaCl_2$ when indicated.

Isolation and quantification of polar lipids. Phospholipids were isolated and quantified as described recently (20, 21). Bacterial overnight cultures grown in MHB to an optical density at 600 nm (OD_{600}) of 0.05 were incubated in 100 ml fresh MHB until the exponential-growth phase (OD_{600} of 0.5 to 1) was reached. After adjusting *S. aureus* strains to equal optical densities, the Bligh-Dyer method (37) was used to extract lipids with a chloroform-methanol-sodium acetate buffer (20 mM, pH 4.6) mixture (1:1:1 [vol/vol/vol]). Isolated lipids were vacuum dried, resuspended in chloroform-methanol (2:1 [vol/ vol), and spotted onto silica gel 60 F254 high-performance thin-layer chromatography (HPTLC) plates (Merck, Darmstadt, Germany) with a Linomat 5 sample application unit (Camag, Berlin, Germany). Polar lipids were separated in an ADC 2 developing chamber (Camag, Berlin, Germany) with a chloroform- methanol-water (65:25:4 [vol/vol/vol]) running solvent. Phospholipids were detected by staining of phosphate groups with molybdenum blue, and the LysPG content was determined in relation to the total phospholipid content by densitometry analysis performed with ImageJ (http://rsbweb.nih.gov/ij/docs/ guide/index.html) as described recently (20, 21).

Translocation of LysPG. The distribution of LysPG in the inner leaflet and outer leaflet of the membrane was determined as described recently (26). Briefly, *S. aureus* overnight cultures were diluted 1:100 and grown for 12 h in brain heart infusion (BHI) medium. Cells were harvested and washed several times, and the cell pellet was incubated with the membrane-impermeative, amino-reactive dye fluorescamine (0.52 M) to specifically label outer-leaflet LysPG. The reaction was stopped after 30 s, and after several washing steps, the phospholipids were extracted and separated in two dimensions via thin-layer chromatography. Fluorescamine-labeled outer-leaflet LysPG was identified with a UV lamp, while unlabeled inner-leaflet LysPG was identified with amino-group reactive ninhydrin. Both lipid species were extracted from the TLC plates and digested with perchloric acid for 3 h in order to liberate and quantify the phosphate content with a colorimetric agent and to quantify the phospholipid content spectrophotometrically at a wavelength of 660 nm.

Quantification of D-alanine from teichoic acids. Bacteria were grown to early stationary phase in basal medium (BM) complemented with 0.36% glucose for 6 h and washed twice with ammonium acetate buffer (20 mM, pH 4.8, 4°C) as described recently (38). A 1-ml volume of a suspension with an OD_{600} of 30 was incubated with NaOH (0.1 M; final volume of 100 µl) for 1 h of shaking at 37°C to hydrolyze the D-alanine esters. HCl (100 µl) served as a stopping reagent, and cell debris was removed by centrifugation and sterile filtration. The D-alanine content of the teichoic acid polymers was assayed by high-performance liquid chromatography (HPLC) upon precolumn derivatization of the amino acid by the use of ortho-phthalaldehyde (OPA). The sample and reagent (OPA diluted 1:10 in 1 M sodium borate buffer, pH 10.7) were

drawn into the autosampler injection needle (Agilent 1200 HPLC system; Waldbronn, Germany) and shaken for 90 s before injection. The amino acid derivatives were separated on a reversed-phase column (Grom-Sil OPA-1; Alltech-Grom GmbH, Rottenburg-Hailfingen, Germany) (150 mm by 4.6 mm, 3-μm pore size) at a flow rate of 1.1 ml/min using a linear-gradient elution from 0% to 60% buffer B for 15 min and were detected at 340 nm. Buffer A was 25 mM phosphate buffer (pH 7.2) containing 0.75% tetrahydrofuran (THF), while buffer B was composed of 35% MeOH–15% acetonitrile (ACN)–25 mM phosphate buffer. A minimum of three independent runs were performed. Peak areas were quantified based on a D-alanine standard curve.

Repulsion of cationic cytochrome c. Differences in the bacterial capacity to repulse cationic proteins were determined by comparing the levels of binding of the red-colored cationic protein cytochrome c as described previously (18, 39). Exponential-phase bacteria were harvested and washed twice with sodium acetate buffer (20 mM, pH 4.6), and the bacterial cell suspension was adjusted to an OD_{600} of 3. Aliquots of 1.5 ml were pelleted, resuspended in 750 μl cytochrome c solution (Sigma; 0.25 mg/ml in sodium acetate buffer), and incubated at 37°C with shaking for 15 min. Suspensions were pelleted, the resulting supernatant was diluted 1:5 with sodium acetate buffer, and absorbance was measured at 410 nm.

Binding of annexin V to negatively charged phospholipids. To validate the experimentation of the phospholipids, particularly for the assay examining translocation of LysPG, we performed the annexin V-Ca^{++} assay, which measures the levels of binding to phosphatidyl serine present on the outer layer of cell membrane (“flipped”) (40). This assay has been very commonly used in eukaryotic systems to unravel apoptotic reactions, because of the ability of annexin V-Ca^{++} to bind to and demonstrate the translocation of phosphatidylserine in the outer layer of the CM. We utilized this method as an indirect measure of the relative levels of outer CM-flipped, positively charged LysPG (the higher the level of positively charged LysPG that is flipped to the outer CM, the lower the level of negatively charged PL species that are available for annexin V-Ca^{++} binding) (40–42). Briefly, *S. aureus* cells were grown overnight in BHI broth. Post centrifugation, the cell pellet was washed twice and resuspended in binding buffer to adjust the OD_{600} to 0.5 (~10^8 CFU/ml). A 5-μl volume of allophycocyanin (APC) annexin V was added to the cells, and the cells were subjected to gentle vortex mixing and incubated at room temperature for 15 min in the dark (30). The cells were then quantified by flow cytometry for analysis of surface-bound fluorophore (30) (excitation and emission wavelengths of 650 nm and 660 nm, respectively; 10,000 events acquired). Data are represented in relative fluorescent units.

MprF domain interactions. MprF-domain interactions were analyzed with a bacterial two-hybrid kit (BACTH system kit; Euromedex), as described recently (20). Briefly, *E. coli* BTH101 was transformed with *mprF* variants (Table S1) and fused to adenylate cyclase fragments T25

and T18 of *Bordetella pertussis*, and protein interactions resulting in cyclic AMP (cAMP) production and subsequent expression of the *lac* and *mal* operons in *E. coli* were quantified by determining ß-galactosidase activity in triplicate (20).

Acknowledgement

This work was financed by grants from the German Research Foundation (TRR34, SFB766, and GRK1708) and from the German Center of Infection Research (DZIF) to A.P. A.S.B. was supported for this research in part by a grant from the U.S. National Institutes of Health (NIH-NIAID) (grant 5RO-1 AI039109-18). N.N.M. was supported by a LABiomed-Harbor UCLA intramural grant.

C.M.E. and C.J.S. cloned DAP-R-associated mutated MprF variants in S. aureus. C.M.E., C.G., and C.J.S. determined daptomycin MICs. C.M.E. established that T345A has no impact on LysPG synthesis, LysPG flipping, or cytochrome c repulsion and that its presence specifically leads to cross-resistance to friulimicin B. C.J.S. determined the impact of all DAP-R signature point mutations on LysPG production. C.J.S. and J.N.H. determined the impact of calcium addition on cross-resistance to calcium-independent antibiotics and validated the T345A findings by determining the impact of T345A, V351E, and S337L on cytochrome c binding and cross-resistance to antibiotics. C.M.E. cloned MprF double mutants to study the role of the flippase in MprF-mediated DAP-R. S.K. analyzed the impact of T345A on MprF domain interaction. M.N. and C.J.S. determined the impact of T345A on the D-alanylation of teichoic acids. N.N.M. deter- mined the impact of T345A on annexin V binding. A.S.B. and N.N.M. analyzed the annexin V binding data. C.M.E., C.J.S., and A.P. wrote the paper. N.N.M. and A.S.B. reviewed and revised draft versions of the paper.

We declare that we have no conflict of interest.

References

1. Weiner LM, Webb AK, Limbago B, Dudeck MA, Patel J, Kallen AJ, Edwards JR, Sievert DM. 2016. Antimicrobial-resistant pathogens associated with healthcare-associated infections: summary of data reported to the Na- tional Healthcare Safety Network at the Centers for Disease Control and Prevention, 2011–2014. Infect Control Hosp Epidemiol 37:1288 –1301. https://doi.org/10.1017/ice.2016.174.
2. CDC. 2013. Antibiotic resistance threats in the United States, 2013. CDC, Atlanta, GA.
3. Bayer AS, Mishra NN, Chen L, Kreiswirth BN, Rubio A, Yang SJ. 2015. Frequency and distribution of single-nucleotide polymorphisms within mprF in methicillin-resistant Staphylococcus aureus clinical isolates and their role in cross-resistance to daptomycin and host defense antimicro- bial peptides. Antimicrob Agents Chemother 59:4930 –4937. https://doi.org/10.1128/AAC.00970-15.
4. Jones T, Yeaman MR, Sakoulas G, Yang SJ, Proctor RA, Sahl HG, Schrenzel J, Xiong YQ, Bayer AS. 2008. Failures in clinical treatment of Staphylo- coccus aureus infection

with daptomycin are associated with alterations in surface charge, membrane phospholipid asymmetry, and drug bind- ing. Antimicrob Agents Chemother 52:269 –278. https://doi.org/10.1128/ AAC.00719-07.

5. Murthy MH, Olson ME, Wickert RW, Fey PD, Jalali Z. 2008. Daptomycin non-susceptible meticillin-resistant Staphylococcus aureus USA 300 isolate. J Med Microbiol 57:1036 –1038. https://doi.org/10.1099/jmm.0.2008/000588-0.

6. Bayer AS, Schneider T, Sahl HG. 2013. Mechanisms of daptomycin resis- tance in Staphylococcus aureus: role of the cell membrane and cell wall. Ann N Y Acad Sci 1277:139 –158. https://doi.org/10.1111/j.1749-6632.2012.06819.x.

7. Miller WR, Bayer AS, Arias CA. 2016. Mechanism of action and resis- tance to daptomycin in Staphylococcus aureus and enterococci. Cold Spring Harb Perspect Med 6:a026997. https://doi.org/10.1101/ cshperspect.a026997.

8. Tran TT, Munita JM, Arias CA. 2015. Mechanisms of drug resistance: daptomycin resistance. Ann N Y Acad Sci 1354:32–53. https://doi.org/10.1111/nyas.12948.

9. Muller A, Wenzel M, Strahl H, Grein F, Saaki TN, Kohl B, Siersma T, Bandow JE, Sahl HG, Schneider T, Hamoen LW. 2016. Daptomycin inhib- its cell envelope synthesis by interfering with fluid membrane microdo- mains. Proc Natl Acad Sci U S A 113:E7077–E7086. https://doi.org/10.1073/pnas.1611173113.

10. Schneider T, Gries K, Josten M, Wiedemann I, Pelzer S, Labischinski H, Sahl HG. 2009. The lipopeptide antibiotic friulimicin B inhibits cell wall biosynthesis through complex formation with bactoprenol phosphate. Antimicrob Agents Chemother 53:1610 –1618. https://doi.org/10.1128/ AAC.01040-08.

11. Bayer AS, Mishra NN, Cheung AL, Rubio A, Yang SJ. 2016. Dysregulation of mprF and dltABCD expression among daptomycin-non-susceptible MRSA clinical isolates. J Antimicrob Chemother 71:2100 –2104. https:// doi.org/10.1093/jac/dkw142.

12. Bayer AS, Mishra NN, Sakoulas G, Nonejuie P, Nast CC, Pogliano J, Chen KT, Ellison SN, Yeaman MR, Yang SJ. 2014. Heterogeneity of mprF sequences in methicillin-resistant Staphylococcus aureus clinical isolates: role in cross-resistance between daptomycin and host defense antimicrobial peptides. Antimicrob Agents Chemother 58:7462–7467. https://doi.org/10.1128/AAC.03422-14.

13. Rubio A, Moore J, Varoglu M, Conrad M, Chu M, Shaw W, Silverman JA. 2012. LC-MS/MS characterization of phospholipid content in daptomycin-susceptible and -resistant isolates of Staphylococcus aureus with mutations in mprF. Mol Membr Biol 29:1– 8. https://doi.org/10.3109/09687688.2011.640948.

14. Mishra NN, Bayer AS, Weidenmaier C, Grau T, Wanner S, Stefani S, Cafiso V, Bertuccio T, Yeaman MR, Nast CC, Yang SJ. 2014. Phenotypic and genotypic characterization of daptomycin-resistant methicillin-resistant Staphylococcus aureus strains: relative roles of mprF and dlt operons. PLoS One 9:e107426. https://doi.org/10.1371/journal.pone.0107426.

15. Mehta S, Cuirolo AX, Plata KB, Riosa S, Silverman JA, Rubio A, Rosato RR, Rosato AE. 2012. VraSR two-component regulatory system contributes to mprF-mediated decreased susceptibility to daptomycin in in vivo- selected clinical strains of methicillin-resistant Staphylococcus aureus. Antimicrob Agents Chemother 56:92–102. https://doi.org/10.1128/AAC.00432-10.

16. Friedman L, Alder JD, Silverman JA. 2006. Genetic changes that correlate with reduced susceptibility to daptomycin in Staphylococcus aureus. Antimicrob Agents Chemother 50:2137–2145. https://doi.org/10.1128/ AAC.00039-06.

17. Peschel A, Jack RW, Otto M, Collins LV, Staubitz P, Nicholson G, Kalbacher H, Nieuwenhuizen WF, Jung G, Tarkowski A, van Kessel KP, van Strijp JA. 2001. Staphylococcus aureus resistance to human defensins and evasion of neutrophil killing via the novel virulence factor MprF is based on modification of membrane lipids with L-lysine. J Exp Med 193: 1067–1076. https://doi.org/10.1084/jem.193.9.1067.

18. Ernst CM, Staubitz P, Mishra NN, Yang SJ, Hornig G, Kalbacher H, Bayer AS, Kraus D, Peschel A. 2009. The bacterial defensin resistance protein MprF consists of separable domains for lipid lysinylation and antimicro- bial peptide repulsion. PLoS Pathog 5:e1000660. https://doi.org/10.1371/journal.ppat.1000660.

19. Straus SK, Hancock RE. 2006. Mode of action of the new antibiotic for Gram-positive pathogens daptomycin: comparison with cationic antimi- crobial peptides and lipopeptides. Biochim Biophys Acta 1758: 1215–1223. https://doi.org/10.1016/j.bbamem.2006.02.009.

20. Ernst CM, Kuhn S, Slavetinsky CJ, Krismer B, Heilbronner S, Gekeler C, Kraus D, Wagner S, Peschel A. 2015. The lipid-modifying multiple pep- tide resistance factor is an oligomer consisting of distinct interacting synthase and flippase subunits. mBio 6:e02340-14. https://doi.org/10.1128/mBio.02340-14.

21. Slavetinsky CJ, Peschel A, Ernst CM. 2012. Alanyl-phosphatidylglycerol and lysyl-phosphatidylglycerol are translocated by the same MprF flip- pases and have similar capacities to protect against the antibiotic dap- tomycin in Staphylococcus aureus. Antimicrob Agents Chemother 56: 3492–3497. https://doi.org/10.1128/AAC.00370-12.

22. Wecke T, Zuhlke D, Mader U, Jordan S, Voigt B, Pelzer S, Labischinski H, Homuth G, Hecker M, Mascher T. 2009. Daptomycin versus friulimicin B: in-depth profiling of Bacillus subtilis cell envelope stress responses. Antimicrob Agents Chemother 53:1619 –1623. https://doi.org/10.1128/ AAC.01046-08.

23. Slavetinsky C, Kuhn S, Peschel A. 2017. Bacterial aminoacyl phospholip- ids—biosynthesis and role in basic cellular processes and pathogenicity. Biochim Biophys Acta 1862:1310 –1318. https://doi.org/10.1016/j.bbalip.2016.11.013.

24. Ernst CM, Peschel A. 2011. Broad-spectrum antimicrobial peptide resistance by MprF-mediated aminoacylation and flipping of phos- pholipids. Mol Microbiol 80:290 –299. https://doi.org/10.1111/j.1365-2958.2011.07576.x.

25. Mishra NN, Yang SJ, Sawa A, Rubio A, Nast CC, Yeaman MR, Bayer AS. 2009. Analysis of cell membrane characteristics of in vitro-selected daptomycin-resistant strains of methicillin-resistant Staphylococcus au- reus. Antimicrob Agents Chemother 53:2312–2318. https://doi.org/10.1128/AAC.01682-08.

26. Mukhopadhyay K, Whitmire W, Xiong YQ, Molden J, Jones T, Peschel A, Staubitz P, Adler-Moore J, McNamara PJ, Proctor RA, Yeaman MR, Bayer AS. 2007. In vitro susceptibility of Staphylococcus aureus to thrombin- induced platelet microbicidal protein-1 (tPMP-1) is influenced by cell membrane phospholipid composition and asymmetry. Microbiology 153:1187–1197. https://doi.org/10.1099/mic.0.2006/003111-0.

27. Peschel A, Sahl HG. 2006. The co-evolution of host cationic antimicrobial peptides and microbial resistance. Nat Rev Microbiol 4:529 –536. https:// doi.org/10.1038/nrmicro1441.

28. Weidenmaier C, Peschel A. 2008. Teichoic acids and related cell-wall glycopolymers in Gram-positive physiology and host interactions. Nat Rev Microbiol 6:276 –287. https://doi.org/10.1038/nrmicro1861.

29. Reichmann NT, Cassona CP, Grundling A. 2013. Revised mechanism of D-alanine incorporation into cell wall polymers in Gram-positive bacteria. Microbiology 159:1868 –1877. https://doi.org/10.1099/mic.0.069898-0.

30. Mishra NN, Yang S-J, Chen L, Muller C, Saleh-Mghir A, Kuhn S, Peschel A, Yeaman MR, Nast CC, Kreiswirth BN, Crémieux A-C, Bayer AS. 2013. Emergence of daptomycin resistance in daptomycin-naive rabbits with methicillin-resistant Staphylococcus aureus prosthetic joint infection is associated with resistance to host defense cationic peptides and mprF polymorphisms. PLoS One 8:e71151. https://doi.org/10.1371/journal.pone.0071151.

31. Perez F, Salata RA, Bonomo RA. 2008. Current and novel antibiotics against resistant Gram-positive bacteria. Infect Drug Resist 1:27– 44.

32. Bierbaum G, Sahl HG. 2009. Lantibiotics: mode of action, biosynthesis and bioengineering. Curr Pharm Biotechnol 10:2–18. https://doi.org/10.2174/138920109787048616.

33. Blair JM, Webber MA, Baylay AJ, Ogbolu DO, Piddock LJ. 2015. Molecular mechanisms of antibiotic resistance. Nat Rev Microbiol 13:42–51. https:// doi.org/10.1038/nrmicro3380.

34. Yang SJ, Mishra NN, Rubio A, Bayer AS. 2013. Causal role of single nucleotide polymorphisms within the mprF gene of Staphylococcus aureus in daptomycin resistance. Antimicrob Agents Chemother 57: 5658 –5664. https://doi.org/10.1128/AAC.01184-13.

35. Peleg AY, Miyakis S, Ward DV, Earl AM, Rubio A, Cameron DR, Pillai S, Moellering RC, Jr, Eliopoulos GM. 2012. Whole genome characterization of the mechanisms of daptomycin resistance in clinical and laboratory derived isolates of Staphylococcus aureus. PLoS One 7:e28316. https:// doi.org/10.1371/journal.pone.0028316.

36. Pomorski TG, Menon AK. 2016. Lipid somersaults: uncovering the mech- anisms of protein-mediated lipid flipping. Prog Lipid Res 64:69 – 84. https://doi.org/10.1016/j.plipres.2016.08.003.

37. Bligh EG, Dyer WJ. 1959. A rapid method of total lipid extraction and purification. Can J Biochem Physiol 37:911–917. https://doi.org/10.1139/ o59-099.

38. Vestergaard M, Nohr-Meldgaard K, Bojer MS, Krogsgard Nielsen C, Meyer RL, Slavetinsky C, Peschel A, Ingmer H. 2017. Inhibition of the ATP synthase eliminates the intrinsic resistance of Staphylococcus aureus towards polymyxins. mBio 8:e01114-17. https://doi.org/10.1128/mBio.01114-17.

39. Kraus D, Herbert S, Kristian SA, Khosravi A, Nizet V, Gotz F, Peschel A. 2008. The GraRS regulatory system controls Staphylococcus aureus sus- ceptibility to antimicrobial host defenses. BMC Microbiol 8:85. https:// doi.org/10.1186/1471-2180-8-85.

40. Yount NY, Kupferwasser D, Spisni A, Dutz SM, Ramjan ZH, Sharma S, Waring AJ, Yeaman MR. 2009. Selective reciprocity in antimicrobial activity versus cytotoxicity of hBD-2 and crotamine. Proc Natl Acad Sci U S A 106:14972–14977. https://doi.org/10.1073/pnas.0904465106.

41. Vermes I, Haanen C, Steffens-Nakken H, Reutelingsperger C. 1995. A novel assay for apoptosis. Flow cytometric detection of phosphatidyl- serine expression on early apoptotic cells using fluorescein labelled annexin V. J Immunol Methods 184:39 –51. https://doi.org/10.1016/0022-1759(95)00072-I.

42. Koopman G, Reutelingsperger CP, Kuijten GA, Keehnen RM, Pals ST, van Oers MH. 1994. Annexin V for flow cytometric detection of phosphati- dylserine expression on B cells undergoing apoptosis. Blood 84: 1415–1420.

43. Peschel A, Otto M, Jack RW, Kalbacher H, Jung G, Gotz F. 1999. Inacti- vation of the dlt operon in Staphylococcus aureus confers sensitivity to defensins, protegrins, and other antimicrobial peptides. J Biol Chem 274:8405– 8410. https://doi.org/10.1074/jbc.274.13.8405.

Supplemental Material

Supplemental material for this article may be found at https://doi.org/10.1128/mBio.01659-18.

Table S1: Frequency of reported point mutations in MprF. The frequency of the reported mutations is shown. A distinction is made between the frequency of mutations reported from *in vitro* passaging studies, and the frequency of mutations reported from studies with clinical isolates.

MprF point mutation	*In vitro* isolates	Clinical isolates	Reference
E44V	1	0	(1)
G61V	0	1	(2)
L291I	1	0	(3)
S295L	2	11	(1, 2, 4-18)
A302V	1	0	(5)
P314L	3	6	(3, 5, 6, 12, 17-21)
S337L	3	9	(2, 4, 5, 12, 17-24)
L338S	1	0	(24)
L341S	3	0	(8, 11, 12, 17-19, 25)
T345A/I/K	4	13	(2, 6, 9, 12, 14, 17, 18, 26-31)

M347R	1	1	(5, 12, 18)
V351E	1	1	(12, 18, 32)
H376Y	1	0	(5)
I420N/S/T	2	3	(1, 2, 8, 11, 33)
W424C	1	0	(5)
T472K	0	1	(12, 18)
I506M	1	0	(1)
E692Q	0	1	(20)
L776S	0	1	(17)
L826F/I	2	28	(2, 5, 6, 8, 10-12, 17-20, 25, 28, 34)

1. **Kosowska-Shick K, Clark C, Pankuch GA, McGhee P, Dewasse B, Beachel L, Appelbaum PC.** 2009. Activity of telavancin against staphylococci and enterococci determined by MIC and resistance selection studies. Antimicrob Agents Chemother **53:**4217-4224.
2. **Peleg AY, Miyakis S, Ward DV, Earl AM, Rubio A, Cameron DR, Pillai S, Moellering RC, Jr., Eliopoulos GM.** 2012. Whole genome characterization of the mechanisms of daptomycin resistance in clinical and laboratory derived isolates of Staphylococcus aureus. PLoS One **7:**e28316.
3. **Mishra NN, Yang SJ, Chen L, Muller C, Saleh-Mghir A, Kuhn S, Peschel A, Yeaman MR, Nast CC, Kreiswirth BN, Cremieux AC, Bayer AS.** 2013. Emergence of daptomycin resistance in daptomycin-naive rabbits with methicillin-resistant Staphylococcus aureus prosthetic joint infection is associated with resistance to host defense cationic peptides and mprF polymorphisms. PLoS One **8:**e71151.
4. **Quinn B, Hussain S, Malik M, Drlica K, Zhao X.** 2007. Daptomycin inoculum effects and mutant prevention concentration with Staphylococcus aureus. J Antimicrob Chemother **60:**1380-1383.
5. **Berti AD, Baines SL, Howden BP, Sakoulas G, Nizet V, Proctor RA, Rose WE.** 2015. Heterogeneity of genetic pathways toward daptomycin nonsusceptibility in Staphylococcus aureus determined by adjunctive antibiotics. Antimicrob Agents Chemother **59:**2799-2806.
6. **Friedman L, Alder JD, Silverman JA.** 2006. Genetic changes that correlate with reduced susceptibility to daptomycin in Staphylococcus aureus. Antimicrob Agents Chemother **50:**2137-2145.
7. **Jones T, Yeaman MR, Sakoulas G, Yang SJ, Proctor RA, Sahl HG, Schrenzel J, Xiong YQ, Bayer AS.** 2008. Failures in clinical treatment of Staphylococcus aureus Infection with daptomycin are associated with alterations in surface charge, membrane phospholipid asymmetry, and drug binding. Antimicrob Agents Chemother **52:**269-278.
8. **Mishra NN, McKinnell J, Yeaman MR, Rubio A, Nast CC, Chen L, Kreiswirth BN, Bayer AS.** 2011. In vitro cross-resistance to daptomycin and host defense cationic antimicrobial peptides in clinical methicillin-resistant Staphylococcus aureus isolates. Antimicrob Agents Chemother **55:**4012-4018.
9. **Mishra NN, Bayer AS, Weidenmaier C, Grau T, Wanner S, Stefani S, Cafiso V, Bertuccio T, Yeaman MR, Nast CC, Yang SJ.** 2014. Phenotypic and genotypic characterization of daptomycin-resistant methicillin-resistant Staphylococcus aureus strains: relative roles of mprF and dlt operons. PLoS One **9:**e107426.
10. **Bertsche U, Yang SJ, Kuehner D, Wanner S, Mishra NN, Roth T, Nega M, Schneider A, Mayer C, Grau T, Bayer AS, Weidenmaier C.** 2013. Increased cell wall teichoic acid production and D-alanylation are common phenotypes among daptomycin-resistant methicillin-resistant Staphylococcus aureus (MRSA) clinical isolates. PLoS One **8:**e67398.
11. **Mishra NN, Bayer AS.** 2013. Correlation of cell membrane lipid profiles with daptomycin resistance in methicillin-resistant Staphylococcus aureus. Antimicrob Agents Chemother **57:**1082-1085.
12. **Bayer AS, Mishra NN, Chen L, Kreiswirth BN, Rubio A, Yang SJ.** 2015. Frequency and Distribution of Single-Nucleotide Polymorphisms within mprF in Methicillin-Resistant Staphylococcus aureus Clinical Isolates and Their Role in Cross-Resistance to Daptomycin and Host Defense Antimicrobial Peptides. Antimicrob Agents Chemother **59:**4930-4937.
13. **Fischer A, Yang SJ, Bayer AS, Vaezzadeh AR, Herzig S, Stenz L, Girard M, Sakoulas G, Scherl A, Yeaman MR, Proctor RA, Schrenzel J, Francois P.** 2011. Daptomycin resistance mechanisms in

clinically derived Staphylococcus aureus strains assessed by a combined transcriptomics and proteomics approach. J Antimicrob Chemother **66:**1696-1711.

14. **Yang SJ, Mishra NN, Rubio A, Bayer AS.** 2013. Causal role of single nucleotide polymorphisms within the mprF gene of Staphylococcus aureus in daptomycin resistance. Antimicrob Agents Chemother **57:**5658-5664.
15. **Yang SJ, Kreiswirth BN, Sakoulas G, Yeaman MR, Xiong YQ, Sawa A, Bayer AS.** 2009. Enhanced expression of dltABCD is associated with the development of daptomycin nonsusceptibility in a clinical endocarditis isolate of Staphylococcus aureus. J Infect Dis **200:**1916-1920.
16. **Chen CJ, Huang YC, Chiu CH.** 2015. Multiple pathways of cross-resistance to glycopeptides and daptomycin in persistent MRSA bacteraemia. J Antimicrob Chemother **70:**2965-2972.
17. **Rubio A, Moore J, Varoglu M, Conrad M, Chu M, Shaw W, Silverman JA.** 2012. LC-MS/MS characterization of phospholipid content in daptomycin-susceptible and -resistant isolates of Staphylococcus aureus with mutations in mprF. Mol Membr Biol **29:**1-8.
18. **Bayer AS, Mishra NN, Cheung AL, Rubio A, Yang SJ.** 2016. Dysregulation of mprF and dltABCD expression among daptomycin-non-susceptible MRSA clinical isolates. J Antimicrob Chemother **71:**2100-2104.
19. **Mehta S, Cuirolo AX, Plata KB, Riosa S, Silverman JA, Rubio A, Rosato RR, Rosato AE.** 2012. VraSR two-component regulatory system contributes to mprF-mediated decreased susceptibility to daptomycin in in vivo-selected clinical strains of methicillin-resistant Staphylococcus aureus. Antimicrob Agents Chemother **56:**92-102.
20. **Steed ME, Hall AD, Salimnia H, Kaatz GW, Kaye KS, Rybak MJ.** 2013. Evaluation of Daptomycin Non-Susceptible Staphylococcus aureus for Stability, Population Profiles, mprF Mutations, and Daptomycin Activity. Infect Dis Ther **2:**187-200.
21. **Kang KM, Mishra NN, Park KT, Lee GY, Park YH, Bayer AS, Yang SJ.** 2017. Phenotypic and genotypic correlates of daptomycin-resistant methicillin-susceptible Staphylococcus aureus clinical isolates. J Microbiol **55:**153-159.
22. **Boyle-Vavra S, Jones M, Gourley BL, Holmes M, Ruf R, Balsam AR, Boulware DR, Kline S, Jawahir S, Devries A, Peterson SN, Daum RS.** 2011. Comparative genome sequencing of an isogenic pair of USA800 clinical methicillin-resistant Staphylococcus aureus isolates obtained before and after daptomycin treatment failure. Antimicrob Agents Chemother **55:**2018-2025.
23. **Cameron DR, Jiang JH, Abbott IJ, Spelman DW, Peleg AY.** 2015. Draft Genome Sequences of Clinical Daptomycin-Nonsusceptible Methicillin-Resistant Staphylococcus aureus Strain APS211 and Its Daptomycin-Susceptible Progenitor APS210. Genome Announc **3**.
24. **Patel D, Husain M, Vidaillac C, Steed ME, Rybak MJ, Seo SM, Kaatz GW.** 2011. Mechanisms of in-vitro-selected daptomycin-non-susceptibility in Staphylococcus aureus. Int J Antimicrob Agents **38:**442-446.
25. **Bayer AS, Mishra NN, Sakoulas G, Nonejuie P, Nast CC, Pogliano J, Chen KT, Ellison SN, Yeaman MR, Yang SJ.** 2014. Heterogeneity of mprF sequences in methicillin-resistant Staphylococcus aureus clinical isolates: role in cross-resistance between daptomycin and host defense antimicrobial peptides. Antimicrob Agents Chemother **58:**7462-7467.
26. **Yang SJ, Nast CC, Mishra NN, Yeaman MR, Fey PD, Bayer AS.** 2010. Cell wall thickening is not a universal accompaniment of the daptomycin nonsusceptibility phenotype in Staphylococcus aureus: evidence for multiple resistance mechanisms. Antimicrob Agents Chemother **54:**3079-3085.
27. **Murthy MH, Olson ME, Wickert RW, Fey PD, Jalali Z.** 2008. Daptomycin non-susceptible meticillin-resistant Staphylococcus aureus USA 300 isolate. J Med Microbiol **57:**1036-1038.
28. **Rubio A, Conrad M, Haselbeck RJ, G CK, Brown-Driver V, Finn J, Silverman JA.** 2011. Regulation of mprF by antisense RNA restores daptomycin susceptibility to daptomycin-resistant isolates of Staphylococcus aureus. Antimicrob Agents Chemother **55:**364-367.
29. **Capone A, Cafiso V, Campanile F, Parisi G, Mariani B, Petrosillo N, Stefani S.** 2016. In vivo development of daptomycin resistance in vancomycin-susceptible methicillin-resistant Staphylococcus aureus severe infections previously treated with glycopeptides. Eur J Clin Microbiol Infect Dis **35:**625-631.
30. **Lin YT, Tsai JC, Yamamoto T, Chen HJ, Hung WC, Hsueh PR, Teng LJ.** 2016. Emergence of a small colony variant of vancomycin-intermediate Staphylococcus aureus in a patient with septic arthritis during long-term treatment with daptomycin. J Antimicrob Chemother **71:**1807-1814.
31. **Mishra NN, Yang SJ, Sawa A, Rubio A, Nast CC, Yeaman MR, Bayer AS.** 2009. Analysis of cell membrane characteristics of in vitro-selected daptomycin-resistant strains of methicillin-resistant Staphylococcus aureus. Antimicrob Agents Chemother **53:**2312-2318.
32. **Yamaguchi T, Suzuki S, Okamura S, Miura Y, Tsukimori A, Nakamura I, Ito N, Masuya A, Shiina T, Matsumoto T.** 2015. Evolution and single-nucleotide polymorphisms in methicillin-resistant Staphylococcus aureus strains with reduced susceptibility to vancomycin and daptomycin, based on determination of the complete genome. Antimicrob Agents Chemother **59:**3585-3587.
33. **Julian K, Kosowska-Shick K, Whitener C, Roos M, Labischinski H, Rubio A, Parent L, Ednie L, Koeth L, Bogdanovich T, Appelbaum PC.** 2007. Characterization of a daptomycin-nonsusceptible vancomycin-intermediate Staphylococcus aureus strain in a patient with endocarditis. Antimicrob Agents Chemother **51:**3445-3448.
34. **Iwata Y, Satou K, Tsuzuku H, Furuichi K, Senda Y, Sakai-Takemori Y, Wada T, Fujita S, Miyake T, Yasuda H, Sakai N, Kitajima S, Toyama T, Shinozaki Y, Sagara A, Miyagawa T, Hara A, Shimizu M, Kamikawa Y, Kaneko S, Wada T.** 2017. Down-regulation of the two-component system and cell-wall

biosynthesis-related genes was associated with the reversion to daptomycin susceptibility in daptomycin non-susceptible methicillin-resistant Staphylococcus aureus. Eur J Clin Microbiol Infect Dis doi:10.1007/s10096-017-2999-3.

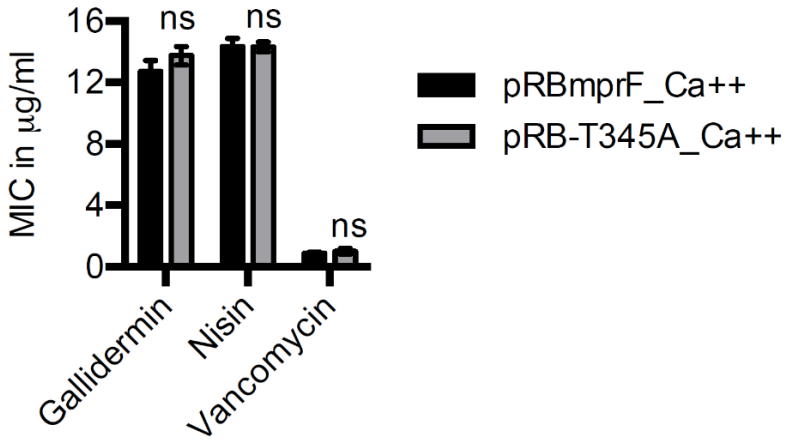

Fig S1: Calcium supplementation does not confer T345A-MprF mediated resistance to calcium-independent antibiotics.

Table S2: Phenotypes observed in DAP-R resistant isolates. The point mutations and the strain background (clinical or in vitro generated) is indicated, as well as the observed phenotypes.

MprF point mutation	Origins	Phenotypes	Reference
E44V	Serially passaged isolate	nd	(1)
G61V	Clinical isolate	nd	(2)
L291I	Isolate from passaging experiments in rabbits	Cross-resistance to AMPs; Increased production of LysPG; Cell wall thickening	(3)
S295L	Serially passaged and clinical isolates	Cross-resistance to AMPs; Increased production of LysPG; Increased translocation of LysPG; Increased positive surface charge; Increased D-alanylation of WTA; Cell wall thickening; Enhanced cell membrane fluidity; Reduced surface binding of daptomycin; Enhanced expression of *mprF* and *dltABCD*; Reduced carotenoid content; Enhanced biofilm formation	(1, 2, 4-18)
A302V	Serially passaged isolate	Increased positive surface charge	(5)

P314L	Serially passaged and clinical isolates, and from passaging experiments in rabbits	Cross-resistance to AMPs; Increased production of LysPG; Increased positive surface charge; Cell wall thickening; Enhanced expression of *mprF* and *dltA*	(3, 5, 6, 12, 17-21)
S337L	Serially passaged and clinical isolates	Cross-resistance to AMPs; Increased production of LysPG; Increased positive surface charge; Cell wall thickening; Enhanced expression of *mprF*, *dltA* and *vraS*; Downregulation of specific ORFs (e.g. PSMs, delta-hemolysin); Reduced autolysis and lysostaphin lysis	(2, 4, 5, 12, 17-24)
L338S	Serially passaged isolate	Increased positive surface charge, Enhanced expression of *vraS*	(24)
L341S	Clinical isolates	Cross-resistance to AMPs; Increased production of LysPG; Increased positive surface charge; Cell wall thickening; Reduced carotenoid content	(8, 11, 12, 17-19, 25)
T345A	Serially passaged and clinical isolates	Cross-resistance to AMPs; Increased production of LysPG; Increased positive surface charge; Reduced surface binding of daptomycin; Enhanced expression of *mprF*, *dltA* and *sceD*	(6, 12, 14, 18, 26-29)
T345I	Serially passaged and clinical isolates	Cross-resistance to AMPs; Increased production of LysPG; Increased positive surface charge; Increased D-alanylation of WTA; Increased WTA content; Cell wall thickening; Enhanced cell membrane fluidity; Enhanced expression of *mprF* and *dltABCD*; Shortening of membrane lipid fatty acids	(2, 6, 9, 12, 17, 18, 30, 31)
T345K	Clinical isolate	Increased positive surface charge	(12, 18)
M347R	Serially passaged and clinical isolates	Cross-resistance to AMPs; Increased positive surface charge;	(5, 12, 18)
V351E	Clinical isolates	Cross-resistance to AMPs; Increased production of LysPG; Increased positive surface charge; Enhanced expression of *mprF*, *dltA* and *graS*	(12, 18, 32)
H376Y	Serially passaged isolate	Increased positive surface charge	(5)
I420N	Clinical isolates	Cross-resistance to AMPs; Increased production of LysPG; Cell wall thickening; Reduced carotenoid content; Reduction in muramic acid *O*-acetylation	(2, 8, 11, 33)
I420S	Serially passaged isolate	nd	(1)
I420T	Serially passaged isolate	nd	(1)

W424C	Serially passaged isolate	Increased positive surface charge	(5)
T472K	Clinical isolate	Cross-resistance to AMPs; Increased positive surface charge	(12, 18)
I506M	Serially passaged isolate	nd	(1)
E692Q	Clinical isolate	nd	(20)
L776S	Clinical isolate	Increased production of LysPG	(17)
L826F	Serially passaged and clinical isolates	Cross-resistance to AMPs; Increased production of LysPG; Increased positive surface charge; Increased D-alanylation of WTA; Increased WTA content; Cell wall thickening; Enhanced cell membrane fluidity; Enhanced expression of *mprF*, *dltA*, *tagA*, *vraSR*, *yycG*, *graS* and other cell wall biosynthesis-related genes; Reduced carotenoid content; Reduced muropeptide cross-linkage	(2, 5, 6, 8, 10-12, 17-20, 25, 28, 34)
L826I	Serially passaged isolate	Increased positive surface charge	(5)

1. **Kosowska-Shick K, Clark C, Pankuch GA, McGhee P, Dewasse B, Beachel L, Appelbaum PC.** 2009. Activity of telavancin against staphylococci and enterococci determined by MIC and resistance selection studies. Antimicrob Agents Chemother **53:**4217-4224.
2. **Peleg AY, Miyakis S, Ward DV, Earl AM, Rubio A, Cameron DR, Pillai S, Moellering RC, Jr., Eliopoulos GM.** 2012. Whole genome characterization of the mechanisms of daptomycin resistance in clinical and laboratory derived isolates of Staphylococcus aureus. PLoS One **7:**e28316.
3. **Mishra NN, Yang SJ, Chen L, Muller C, Saleh-Mghir A, Kuhn S, Peschel A, Yeaman MR, Nast CC, Kreiswirth BN, Cremieux AC, Bayer AS.** 2013. Emergence of daptomycin resistance in daptomycin-naive rabbits with methicillin-resistant Staphylococcus aureus prosthetic joint infection is associated with resistance to host defense cationic peptides and mprF polymorphisms. PLoS One **8:**e71151.
4. **Quinn B, Hussain S, Malik M, Drlica K, Zhao X.** 2007. Daptomycin inoculum effects and mutant prevention concentration with Staphylococcus aureus. J Antimicrob Chemother **60:**1380-1383.
5. **Berti AD, Baines SL, Howden BP, Sakoulas G, Nizet V, Proctor RA, Rose WE.** 2015. Heterogeneity of genetic pathways toward daptomycin nonsusceptibility in Staphylococcus aureus determined by adjunctive antibiotics. Antimicrob Agents Chemother **59:**2799-2806.
6. **Friedman L, Alder JD, Silverman JA.** 2006. Genetic changes that correlate with reduced susceptibility to daptomycin in Staphylococcus aureus. Antimicrob Agents Chemother **50:**2137-2145.
7. **Jones T, Yeaman MR, Sakoulas G, Yang SJ, Proctor RA, Sahl HG, Schrenzel J, Xiong YQ, Bayer AS.** 2008. Failures in clinical treatment of Staphylococcus aureus Infection with daptomycin are associated with alterations in surface charge, membrane phospholipid asymmetry, and drug binding. Antimicrob Agents Chemother **52:**269-278.
8. **Mishra NN, McKinnell J, Yeaman MR, Rubio A, Nast CC, Chen L, Kreiswirth BN, Bayer AS.** 2011. In vitro cross-resistance to daptomycin and host defense cationic antimicrobial peptides in clinical methicillin-resistant Staphylococcus aureus isolates. Antimicrob Agents Chemother **55:**4012-4018.
9. **Mishra NN, Bayer AS, Weidenmaier C, Grau T, Wanner S, Stefani S, Cafiso V, Bertuccio T, Yeaman MR, Nast CC, Yang SJ.** 2014. Phenotypic and genotypic characterization of daptomycin-resistant methicillin-resistant Staphylococcus aureus strains: relative roles of mprF and dlt operons. PLoS One **9:**e107426.
10. **Bertsche U, Yang SJ, Kuehner D, Wanner S, Mishra NN, Roth T, Nega M, Schneider A, Mayer C, Grau T, Bayer AS, Weidenmaier C.** 2013. Increased cell wall teichoic acid production and D-alanylation are common phenotypes among daptomycin-resistant methicillin-resistant Staphylococcus aureus (MRSA) clinical isolates. PLoS One **8:**e67398.
11. **Mishra NN, Bayer AS.** 2013. Correlation of cell membrane lipid profiles with daptomycin resistance in methicillin-resistant Staphylococcus aureus. Antimicrob Agents Chemother **57:**1082-1085.

12. **Bayer AS, Mishra NN, Chen L, Kreiswirth BN, Rubio A, Yang SJ.** 2015. Frequency and Distribution of Single-Nucleotide Polymorphisms within mprF in Methicillin-Resistant Staphylococcus aureus Clinical Isolates and Their Role in Cross-Resistance to Daptomycin and Host Defense Antimicrobial Peptides. Antimicrob Agents Chemother **59:**4930-4937.
13. **Fischer A, Yang SJ, Bayer AS, Vaezzadeh AR, Herzig S, Stenz L, Girard M, Sakoulas G, Scherl A, Yeaman MR, Proctor RA, Schrenzel J, Francois P.** 2011. Daptomycin resistance mechanisms in clinically derived Staphylococcus aureus strains assessed by a combined transcriptomics and proteomics approach. J Antimicrob Chemother **66:**1696-1711.
14. **Yang SJ, Mishra NN, Rubio A, Bayer AS.** 2013. Causal role of single nucleotide polymorphisms within the mprF gene of Staphylococcus aureus in daptomycin resistance. Antimicrob Agents Chemother **57:**5658-5664.
15. **Yang SJ, Kreiswirth BN, Sakoulas G, Yeaman MR, Xiong YQ, Sawa A, Bayer AS.** 2009. Enhanced expression of dltABCD is associated with the development of daptomycin nonsusceptibility in a clinical endocarditis isolate of Staphylococcus aureus. J Infect Dis **200:**1916-1920.
16. **Chen CJ, Huang YC, Chiu CH.** 2015. Multiple pathways of cross-resistance to glycopeptides and daptomycin in persistent MRSA bacteraemia. J Antimicrob Chemother **70:**2965-2972.
17. **Rubio A, Moore J, Varoglu M, Conrad M, Chu M, Shaw W, Silverman JA.** 2012. LC-MS/MS characterization of phospholipid content in daptomycin-susceptible and -resistant isolates of Staphylococcus aureus with mutations in mprF. Mol Membr Biol **29:**1-8.
18. **Bayer AS, Mishra NN, Cheung AL, Rubio A, Yang SJ.** 2016. Dysregulation of mprF and dltABCD expression among daptomycin-non-susceptible MRSA clinical isolates. J Antimicrob Chemother **71:**2100-2104.
19. **Mehta S, Cuirolo AX, Plata KB, Riosa S, Silverman JA, Rubio A, Rosato RR, Rosato AE.** 2012. VraSR two-component regulatory system contributes to mprF-mediated decreased susceptibility to daptomycin in in vivo-selected clinical strains of methicillin-resistant Staphylococcus aureus. Antimicrob Agents Chemother **56:**92-102.
20. **Steed ME, Hall AD, Salimnia H, Kaatz GW, Kaye KS, Rybak MJ.** 2013. Evaluation of Daptomycin Non-Susceptible Staphylococcus aureus for Stability, Population Profiles, mprF Mutations, and Daptomycin Activity. Infect Dis Ther **2:**187-200.
21. **Kang KM, Mishra NN, Park KT, Lee GY, Park YH, Bayer AS, Yang SJ.** 2017. Phenotypic and genotypic correlates of daptomycin-resistant methicillin-susceptible Staphylococcus aureus clinical isolates. J Microbiol **55:**153-159.
22. **Boyle-Vavra S, Jones M, Gourley BL, Holmes M, Ruf R, Balsam AR, Boulware DR, Kline S, Jawahir S, Devries A, Peterson SN, Daum RS.** 2011. Comparative genome sequencing of an isogenic pair of USA800 clinical methicillin-resistant Staphylococcus aureus isolates obtained before and after daptomycin treatment failure. Antimicrob Agents Chemother **55:**2018-2025.
23. **Cameron DR, Jiang JH, Abbott IJ, Spelman DW, Peleg AY.** 2015. Draft Genome Sequences of Clinical Daptomycin-Nonsusceptible Methicillin-Resistant Staphylococcus aureus Strain APS211 and Its Daptomycin-Susceptible Progenitor APS210. Genome Announc **3**.
24. **Patel D, Husain M, Vidaillac C, Steed ME, Rybak MJ, Seo SM, Kaatz GW.** 2011. Mechanisms of in-vitro-selected daptomycin-non-susceptibility in Staphylococcus aureus. Int J Antimicrob Agents **38:**442-446.
25. **Bayer AS, Mishra NN, Sakoulas G, Nonejuie P, Nast CC, Pogliano J, Chen KT, Ellison SN, Yeaman MR, Yang SJ.** 2014. Heterogeneity of mprF sequences in methicillin-resistant Staphylococcus aureus clinical isolates: role in cross-resistance between daptomycin and host defense antimicrobial peptides. Antimicrob Agents Chemother **58:**7462-7467.
26. **Yang SJ, Nast CC, Mishra NN, Yeaman MR, Fey PD, Bayer AS.** 2010. Cell wall thickening is not a universal accompaniment of the daptomycin nonsusceptibility phenotype in Staphylococcus aureus: evidence for multiple resistance mechanisms. Antimicrob Agents Chemother **54:**3079-3085.
27. **Murthy MH, Olson ME, Wickert RW, Fey PD, Jalali Z.** 2008. Daptomycin non-susceptible meticillin-resistant Staphylococcus aureus USA 300 isolate. J Med Microbiol **57:**1036-1038.
28. **Rubio A, Conrad M, Haselbeck RJ, G CK, Brown-Driver V, Finn J, Silverman JA.** 2011. Regulation of mprF by antisense RNA restores daptomycin susceptibility to daptomycin-resistant isolates of Staphylococcus aureus. Antimicrob Agents Chemother **55:**364-367.
29. **Capone A, Cafiso V, Campanile F, Parisi G, Mariani B, Petrosillo N, Stefani S.** 2016. In vivo development of daptomycin resistance in vancomycin-susceptible methicillin-resistant Staphylococcus aureus severe infections previously treated with glycopeptides. Eur J Clin Microbiol Infect Dis **35:**625-631.
30. **Mishra NN, Yang SJ, Sawa A, Rubio A, Nast CC, Yeaman MR, Bayer AS.** 2009. Analysis of cell membrane characteristics of in vitro-selected daptomycin-resistant strains of methicillin-resistant Staphylococcus aureus. Antimicrob Agents Chemother **53:**2312-2318.
31. **Lin YT, Tsai JC, Yamamoto T, Chen HJ, Hung WC, Hsueh PR, Teng LJ.** 2016. Emergence of a small colony variant of vancomycin-intermediate Staphylococcus aureus in a patient with septic arthritis during long-term treatment with daptomycin. J Antimicrob Chemother **71:**1807-1814.
32. **Yamaguchi T, Suzuki S, Okamura S, Miura Y, Tsukimori A, Nakamura I, Ito N, Masuya A, Shiina T, Matsumoto T.** 2015. Evolution and single-nucleotide polymorphisms in methicillin-resistant Staphylococcus aureus strains with reduced susceptibility to vancomycin and daptomycin, based on determination of the complete genome. Antimicrob Agents Chemother **59:**3585-3587.

33. **Julian K, Kosowska-Shick K, Whitener C, Roos M, Labischinski H, Rubio A, Parent L, Ednie L, Koeth L, Bogdanovich T, Appelbaum PC.** 2007. Characterization of a daptomycin-nonsusceptible vancomycin-intermediate Staphylococcus aureus strain in a patient with endocarditis. Antimicrob Agents Chemother **51:**3445-3448.

34. **Iwata Y, Satou K, Tsuzuku H, Furuichi K, Senda Y, Sakai-Takemori Y, Wada T, Fujita S, Miyake T, Yasuda H, Sakai N, Kitajima S, Toyama T, Shinozaki Y, Sagara A, Miyagawa T, Hara A, Shimizu M, Kamikawa Y, Kaneko S, Wada T.** 2017. Down-regulation of the two-component system and cell-wall biosynthesis-related genes was associated with the reversion to daptomycin susceptibility in daptomycin non-susceptible methicillin-resistant Staphylococcus aureus. Eur J Clin Microbiol Infect Dis doi:10.1007/s10096-017-2999-3.

Table S3: Plasmids used in this study.

Plasmid	**Characteristics**	**Short name in figure**
pRB	*E. coli/S. aureus* shuttle vector pRB474 (Bruckner, 1992)	nd
pRBmprF	*mprF* cloned in *E. coli/S. aureus* shuttle vector pRB474 (Bruckner, 1992)	nd
pRB-S295L	Daptomycin resistance associated point mutations introduced in *mprF* by site directed mutagenesis and cloned in E. coli/S. aureus shuttle vector pRB474 (Bruckner, 1992)	nd
pRB-P314L		
pRB-S337L		
pRB-T345A		
pRB-V351E		
pRB-I420N		
pRB-L826F		
pRB-D71A-T345A	T345A and additional flippase loss-of-function point mutations introduced in *mprF* by site directed mutagenesis and cloned in E. coli/S. aureus shuttle vector pRB474 (Bruckner, 1992)	nd
pRB-R112A-T345A		
pRB-E206A-T345A		
pKT25-mprF	*mprF* gene encoding full length MprF C-terminally fused to adenylate cyclase fragment T25 in low copy vector pKT25 (Euromedex) (Ernst et al., 2015)	MprF (Fig. 6)
pKT25-T345A	*mprF-T345A* gene encoding full length MprF-T345A C-terminally fused to adenylate cyclase fragment T25 in low copy vector pKT25 (Euromedex)	MprF-T345A (Fig. 6)
pKT25-flip	Truncated *mprF* gene encoding amino acids 1-320 of MprF (Flippase) C-terminally fused to adenylate cyclase fragment T25 in low copy vector pKT25 (Euromedex) (Ernst et al., 2015)	Flip (Fig. 6)
pKT25-flip+2	Truncated *mprF* gene encoding amino acids 1-393 of MprF (Flippase plus 2 TMS of synthase) C-terminally fused to adenylate cyclase fragment T25 in low copy vector pKT25 (Euromedex) (Ernst et al., 2015)	Flip+2 (Fig. 6)

pKT25-flip+2-T345A	Truncated *mprF-T345A* gene encoding amino acids 1-393 of MprF (Flippase-T345A plus 2 TMS of synthase) C-terminally fused to adenylate cyclase fragment T25 in low copy vector pKT25 (Euromedex)	Flip+2-T345A (Fig. 6)
pUT18-mprF	*mprF* gene encoding full length MprF N-terminally fused to adenylate cyclase fragment T18 in high copy vector pUT18 (Euromedex) (Ernst et al., 2015)	MprF (Fig. 6)
pUT18-T345A	*mprF-T345A* gene encoding MprF-T345A N-terminally fused to adenylate cyclase fragment T18 in high copy vector pUT18 (Euromedex)	MprF-T345A (Fig. 6)
pUT18-syn	Truncated *mprF* gene encoding amino acids 328-840 of MprF (Synthase) N-terminally fused to adenylate cyclase fragment T18 in high copy vector pUT18 (Euromedex) (Ernst et al., 2015)	Syn (Fig. 6)
pUT18-syn-T345A	Truncated *mprF-T345A* gene encoding amino acids 328-840 of MprF-T345A (Synthase) N-terminally fused to adenylate cyclase fragment T18 in high copy vector pUT18 (Euromedex)	Syn-T345A (Fig. 6)

Bruckner R. 1992. A series of shuttle vectors for Bacillus subtilis and Escherichia coli. Gene **122:**187-192.

Ernst CM, Kuhn S, Slavetinsky CJ, Krismer B, Heilbronner S, Gekeler C, Kraus D, Wagner S, Peschel A.2015. The lipid-modifying multiple peptide resistance factor is an oligomer consisting of distinct interacting synthase and flippase subunits. MBio 6.

Table S4: Primers used in this study.

Name	5´ → 3´ sequence	Usage
D71Afw	GTTATTCTATCAATGTATGCTGTGATTTTATCTAGAGCT	Forward primer for construction of pRB-D71A-T345A by site directed mutagenesis
D71Arev	AGCTCTAGATAAAATCACAGCATACATTGATAGAATAAC	Reverse primer for construction of pRB-D71A-T345A by site directed mutagenesis
R112Afw	CAGGCGTTGCAGCAATGGTTTATAAAAACTATACGC	Forward primer for construction of pRB-R112A-T345A by site directed mutagenesis
R112Arev	GCGTATAGTTTTTATAAACCATTGCTGCAACGCCTG	Reverse primer for construction of pRB-R112A-T345A by site directed mutagenesis
E206Afw	ACTTTAGTGTCGTGTGTTGCATGGTTAGCAGCTGCAGTT	Forward primer for construction of pRB-E206A-T345A by site directed mutagenesis
E206Arev	AACTGCAGCTGCTAACCATGCAACACACGACACTAAAGT	Reverse primer for construction of pRB-E206A-T345A by site directed mutagenesis

S295Lfw	GTAATTATTGCATTAATTTTATCATTATTTGAATTTGGTACATCAGCTAAG	Forward primer for construction of pRB-S295L by site directed mutagenesis
S295Lrev	CTTAGCTGATGTACCAAATTCAAATAATGATAAAATTAATGCAATAATTAC	Reverse primer for construction of pRB-S295L by site directed mutagenesis
P314Lfw	GGGATCTAAATACTTTATTCTTGCTAAAGATGTTACG	Forward primer for construction of pRB-P314L by site directed mutagenesis
P314Lrev	CGTAACATCTTTAGCAAGAATAAAGTATTTAGATCCC	Reverse primer for construction of pRB-P314L by site directed mutagenesis
S337Lfw	AAAATTCCATCATTATTATTAGCAATTTTAGTA	Forward primer for construction of pRB-S337L by site directed mutagenesis
S337Lrev	TACTAAAATTGCTAATAATAATGATGGAATTTT	Reverse primer for construction of pRB-S337L by site directed mutagenesis
T345Afw	GCAATTTTAGTATTCTTTGCAAGTATGATCTTTTTT	Forward primer for construction of pRB-T345A, pKT25-T345A, pKT25-flip+2-T345A, pUT18-T345A, pUT18-syn-T345A by site directed mutagenesis
T345Arev	AAAAAAGATCATACTTGCAAAGAATACTAAAATTGC	Reverse primer for construction of pRB-T345A, pKT25-T345A, pKT25-flip+2-T345A, pUT18-T345A, pUT18-syn-T345A by site directed mutagenesis
V351Efw	AGTATGATCTTTTTTGAAAATAACTTAACGATT	Forward primer for construction of pRB-V351E by site directed mutagenesis
V351Erev	AATCGTTAAGTTATTTTCAAAAAAGATCATACT	Reverse primer for construction of pRB-V351E by site directed mutagenesis
I420Nfw	TTCTTCACTTACGCTTCATATAATTTAATAACATGGTTAGCTATT	Forward primer for construction of pRB-I420N by site directed mutagenesis
I420Nrev	AATAGCTAACCATGTTATTAAATTATATGAAGCGTAAGTGAAGAA	Reverse primer for construction of pRB-I420N by site directed mutagenesis

L826Ffw	ATCGTAAAGATAATTC GTTCTGGGAATCACTT TCTAAAG	Forward primer for construction of pRB-L826F by site directed mutagenesis
L826Frev	CTTTAGAAAGTGATTC CCAGAACGAATTATCT TTACGAT	Reverse primer for construction of pRB-L826F by site directed mutagenesis

Chapter 3

Sensitizing *Staphylococcus aureus* to antibacterial agents by decoding and blocking the lipid flippase MprF

Christoph J Slavetinsky[1,2,3,4,5*], Janna N Hauser[1,3,4], Cordula Gekeler[1,3,4], Jessica Slavetinsky[1,3,4], André Geyer[1,3], Alexandra Kraus[6], Doris Heilingbrunner[6], Samuel Wagner[3,4,7], Michael Tesar[6], Bernhard Krismer[1,3,4], Sebastian Kuhn[1,3], Christoph M Ernst[1,3*†], Andreas Peschel[1,3,4]

[1]Department of Infection Biology, Interfaculty Institute for Microbiology and Infection Medicine Tübingen (IMIT), Eberhard Karls University Tübingen, Tübingen, Germany
[2]Pediatric Gastroenterology and Hepatology, University Children's Hospital Tübingen, Eberhard Karls University Tübingen, Tübingen, Germany
[3]German Centre for Infection Research (DZIF), Partner Site Tübingen, Tübingen, Germany;
[4]Cluster of Excellence "Controlling Microbes to Fight Infections," University of Tübingen, Tübingen, Germany
[5]Pediatric Surgery and Urology, University Children's Hospital Tübingen, Eberhard Karls University Tübingen, Tübingen, Germany;
[6]MorphoSys AG, Planegg, Germany; 7Section of Cellular and Molecular Microbiology, Interfaculty Institute for Microbiology and Infection Medicine Tübingen (IMIT), University of Tübingen, Tübingen, Germany
*For correspondence: christoph.slavetinsky@med.uni-tuebingen.de (CJS); cmernst@broadinstitute.org (CME)
†Present address: Christoph M. Ernst, Department of Molecular Biology and Center for Computational and Integrative Biology, Massachusetts General Hospital, Harvard Medical School, Boston, United States

Elife. 2022 Jan 19;11:e66376. doi: 10.7554/eLife.66376.

Abstract

The pandemic of antibiotic resistance represents a major human health threat demanding new antimicrobial strategies. Multiple peptide resistance factor (MprF) is the synthase and flippase of the phospholipid lysyl-phosphatidylglycerol that increases virulence and resistance of methicillin-resistant *Staphylococcus aureus* (MRSA) and other pathogens to cationic host defense peptides and antibiotics. With the aim to design MprF inhibitors that could sensitize MRSA to antimicrobial agents and support the clearance of staphylococcal infections with minimal selection pressure, we developed MprF-targeting monoclonal antibodies, which bound and blocked the MprF flippase subunit. Antibody M-C7.1 targeted a specific loop in the flippase domain that proved to be exposed at both sides of the bacterial membrane, thereby enhancing the mechanistic understanding of bacterial lipid translocation. M-C7.1 rendered MRSA susceptible to host antimicrobial peptides and antibiotics such as daptomycin, and it impaired MRSA survival in human phagocytes. Thus, MprF inhibitors are recommended for new antivirulence approaches against MRSA and other bacterial pathogens.

Editor's evaluation

This study uses an innovative anti-virulence approach based on monoclonal antibodies that target the *Staphylococcus aureus* lipid flippase involved in tolerance to cationic peptides. The authors show that this strategy resensitizes antibiotic-resistant *S. aureus* and serves as a proof of principle for anti-virulence approaches to target bacterial infections.

Introduction

The continuous increase of antibiotic resistance rates undermines the significance and efficacy of available antibiotics against bacterial infections (Årdal et al., 2020). Several opportunistic antibiotic-resistant bacterial pathogens including methicillin-resistant *Staphylococcus aureus* (MRSA), vancomycin-resistant enterococci, and extended-spectrum beta-lactam or carbapenem-resistant proteobacteria impose a continuously growing pressure on modern healthcare systems (Tacconelli et al., 2018). MRSA is responsible for a large percentage of superficial and severe bacterial infections and the available last-resort antibiotics are much less effective than beta-lactams (Lee et al., 2018). Unfortunately, no new class of antibiotics has entered the clinical phase since the introduction of the lipopeptide antibiotic daptomycin in 2003 (Årdal et al., 2020). Novel anti-infective strategies that would circumvent on the one hand the difficulties in identifying new microbiota-preserving small-molecule antimicrobials and, on the other hand, the enormous selection pressures exerted by broad-spectrum antibiotics, are discussed as potential solutions against a looming postantibiotic era (Dickey et al., 2017). Such strategies could be based for instance on therapeutic antibodies or bacteriophages, which

usually have only a narrow activity spectrum. A possible direction could be the inhibition of bacterial targets that are of viable importance only during infection (Lakemeyer et al., 2018). Blocking such targets by so-called antivirulence or antifitness drugs would preserve microbiome integrity and create selection pressure for resistance-conferring mutations only on invading pathogens. Interfering with bacterial virulence factors should ameliorate the course of infection and enable more effective bacterial clearance by the immune system or by antibiotics.

Monoclonal antibodies (mABs) directed against antivirulence targets could be interesting alternatives provided the target can be reached by comparatively large antibody molecules. Therapeutic mABs are used in several malignant, inflammatory, and viral diseases (Qu et al., 2018; O'Brien et al., 2021) and have proven efficacy in toxin-mediated bacterial infections such as anthrax or clostridial toxin-mediated diseases (Dickey et al., 2017; Migone et al., 2009; Lowy et al., 2010). Apart from toxin neutralization, however, mABs have hardly been applied in antimicrobial development programs. Moreover, in-depth molecular studies are necessary to devise most promising targets for mABs and elucidate if and how mAB binding could disable pathogens to colonize and infect humans.

The multiple peptide resistance factor (MprF), a large integral membrane protein, is crucial for the capacity of bacterial pathogens such as *S. aureus* to resist cationic antimicrobial peptides (CAMPs) of the innate immune system and CAMP-like antibiotics such as daptomycin (Peschel et al., 2001; Ernst and Peschel, 2011; Slavetinsky et al., 2017). MprF is highly conserved and can be found in various Gram-positive or Gram-negative pathogens (Slavetinsky et al., 2017). MprF proteins proved to be crucial for *in vivo* virulence of various pathogens in infection models (Peschel et al., 2001; Thedieck et al., 2006; Maloney et al., 2009) and when exposed to human phagocytes as a result of increased resistance to phagocyte-derived antimicrobial agents such as CAMPs (Slavetinsky et al., 2017; Kristian et al., 2003). Some parts of the protein are located at the outer surface of the cytoplasmic membrane and could in principle be reached by mABs (Ernst et al., 2009; Ernst et al., 2015). MprF forms oligomers and it is a bifunctional enzyme, which can be separated into two distinct domains (Ernst et al., 2015). The C-terminal domain synthesizes positively charged lysyl-phosphatidylglycerol (LysPG) from a negatively charged phosphatidylglycerol (PG) acceptor and a Lys-tRNA donor substrate, while the N-terminal domain translocates newly synthesized LysPG from the inner to the outer leaflet of the cytoplasmic membrane and thus functions as a phospholipid flippase (Ernst et al., 2009; Roy and Ibba, 2009). The exposure of LysPG at the outer surface of the membrane reduces the affinity for CAMPs and other antimicrobials (Ernst et al., 2009). Notably, *mprF* is a major hot spot for gain-of-function point mutations that lead to daptomycin resistance, acquired during therapy of *S. aureus* infections (Ernst et al., 2018).

In order to assess the suitability of MprF as a target for antivirulence agents we developed mABs targeting several epitopes of potential extracellular loops of its transmembrane part and analyzed their capacity to bind specifically to *S. aureus* MprF. We identified a collection of mABs, which did not only bind to but also inhibited the LysPG flippase domain of MprF. Our results suggest that a specific loop between two of the transmembrane segments (TMSs) of MprF is exposed at both sides of the membrane suggesting an unusual, potentially flexible topology of this protein part, which may be involved in LysPG translocation. Accordingly, targeting this loop with a specific mAB inhibited the MprF flippase function, rendered *S. aureus* susceptible to killing by antimicrobial host peptides and daptomycin, and reduced *S. aureus* survival when challenged by human CAMP-producing polymorphonuclear leukocytes (PMNs).

Results

Generation of mABs binding to putative extracellular loops of MprF

The hydrophobic part of *S. aureus* MprF appears to include 14 TMS connected by loops with predicted lengths between 2 and 56 amino acids (Ernst et al., 2015). Several of the loops are located at the outer surface of the cytoplasmic membrane, accessible to mABs (Figure 1A). Peptides representing 4 loops with a minimum length of 13 amino acids were synthesized with N- and C-terminal cysteine residues to allow cyclization (Supplementary file 1a). The peptides corresponded to three loops predicted to be at the outer membrane surface (loops 1, 9, and 13) and loop 7, the location of which has remained ambiguous due to conflicting computational and experimental findings (Ernst et al., 2015). The N-terminal amino groups of cyclized peptides were linked to biotin to facilitate their recovery and detection. The antigen peptides were incubated with MorphoSys's Human Combinatorial Antibody Library (HuCAL), a phage display library expressing human Fab fragments with highly diverse variable regions at the phage surface (Prassler et al., 2011). Antigen-binding phages were enriched in three iterative rounds of panning in solution and antigen-phage complexes were captured with streptavidin-coated beads. The bound phages were extensively washed to remove unspecifically binding phages, eluted, and propagated in *Escherichia coli* for a subsequent panning round. Washing steps were prolonged and antigen concentrations reduced from round one to round three to increase stringency and discard antibodies with low specificity and affinity. DNA of the eluted, antigen-specific phages was isolated and subcloned in specific *E. coli* expression vectors to yield His-tagged fragment antigen-binding (Fab) molecules. 368 individual colonies per antigen were picked and Fab fragments were expressed and purified. A representative selection of 24 unique Fabs against all 4 peptides were converted to human IgG by cloning in an IgG1 expression vector system and expression in human HKB11 cells and IgGs were purified via

protein A chromatography, as recently described (Prassler et al., 2011) (see graphical workflow in Figure 1—figure supplement 1).

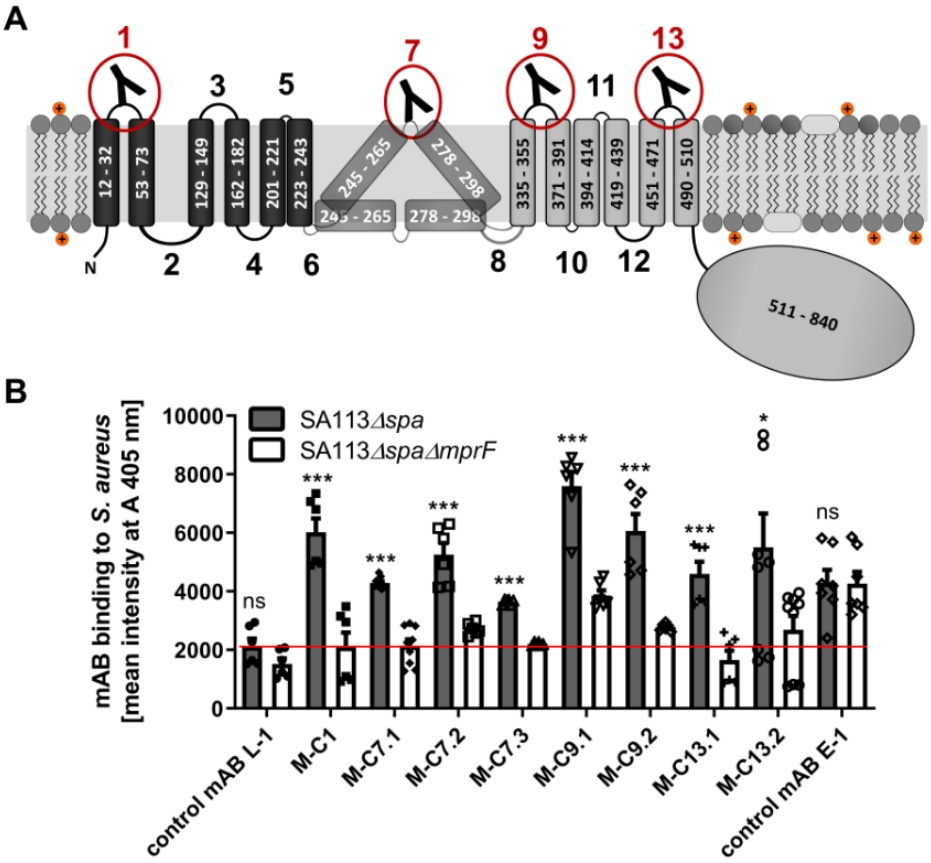

Figure 1: Multiple peptide resistance factor (MprF) topology and binding of monoclonal antibodies (mABs) to MprF-expressing *S. aureus* cells. (A) MprF membrane topology is given according to our recent study (Ernst et al., 2015) showing synthase and flippase domains in gray and black, respectively. Amino acid (aa) positions of transmembrane segment (TMS) and the C-terminal hydrophilic domain are indicated. TMSs from aa 245–265 and aa 278–298 are shown in two alternative positions as computational and experimental results of transmembrane topology have been contradictory (Ernst et al., 2015). Localizations of MprF's TMS-connecting loops are numbered starting from the N-terminus, antibody-targeted loops are indicated by red circles and antibody symbols. (B) Specific binding of mABs (100 nM) to *S. aureus* was analyzed by ELISA using SA113 strains deficient in the IgG-binding protein A (Spa) comparing the SA113 *spa* mutant (Δspa) and *spa mprF* double knockout mutant (Δ*spa*Δ*mprF*). The red line indicates the mean intensity measured at A 405 nm (affinity) of the isotype control mAB L-1 bound to *S. aureus* SA113Δ*spa*. Means and standard error of the mean (SEM) of at least three biological replicates are shown. Significant differences between SA113Δspa and SA113ΔspaΔ*mprF* were calculated by Student's paired t-test (ns, not significant; *p < 0.05; ***p < 0.0001).

The IgGs were analyzed for binding to the corresponding antigen peptides and also to the three noncognate peptides to assess their selectivity, by ELISA with streptavidin-coated microtiter plates (Figure 1—figure supplement 2). Peptide one bound IgGs developed against different antigen peptides indicating that it may bind antibodies with only low selectivity. Antibodies directed against the four targeted MprF loops were selected based on affinity and analyzed for binding to *S. aureus* SA113 cells expressing or not expressing MprF. Both, the 'wild-type' and *mprF* deletion mutant strains lacked the gene for protein A (*spa*), which would otherwise unspecifically bind to IgG (Kim et al., 2012). Bacteria were adsorbed to microtiter plates, blocked with bovine serum albumin, and incubated with IgGs, which were then detected with goat antihuman IgG after extensive washing. Antibodies M-C1, M-C7.1, M-C7.3, M-C9.1,

M-C13.1, and M-C13.2 bound significantly stronger to MprF-expressing *S. aureus* (SA113Δ*spa*) compared to MprF-deficient *S. aureus* (SA113Δ*spa*Δ*mprF*), while the humanized isotype control mAB L-1 showed no specific binding (Figure 1B). An additional mAB directed against the *S. aureus* surface protein EbpS served as positive control, showing equal affinity toward SA113Δ*spa* and SA113Δ*spa*Δ*mprF* (Figure 1B). These findings are in agreement with the location of the loops 1, 9, and 13 at the outer surface of the cytoplasmic membrane, confirming the overall topology of MprF (Figure 1A). Of note, loop 7 between potential TMS 7 and 8 whose location had previously remained controversial was detected by antibodies M-C7.1 and M-C7.3 (Figure 1B) indicating that loop 7 is accessible from the outside. Antibodies M-C1, M-C7.1, M-C9.1, and M-C13.1 showed the strongest binding to MprF.

The MprF epitope bound by M-C7.1 is located at both, outer, and inner surface of the cytoplasmic membrane

The MprF loop 7 between TMS 7 and 8 bound by M-C7.1 seemed to have an ambiguous position within the cytoplasmic membrane because the flanking TMS have a comparatively low content of hydrophobic amino acids. Accordingly, only some topology analysis algorithms predict its location at the outer surface of the cytoplasmic membrane and a previous experimental topology investigation using a set of translational fusions with enzymes that are active only at intracellular or extracellular location has revealed a preferential location at the inner cytoplasmic membrane surface in *E. coli* (Ernst et al., 2015). Since our M-C7.1- and M-C7.3-binding experiments indicated accessibility of loop 7 from the outside, we revisited its location in *S. aureus* with two experimental strategies.

To confirm that M-C7.1 has access to its cognate MprF antigen epitope at the outer surface of the cytoplasmic membrane in intact bacterial cells, *S. aureus* SA113Δ*spa*Δ*mprF*-expressing MprF (pRB-MprF) was grown in the presence of M-C7.1. Cells were then disrupted, membranes were solubilized by treatment with the mild nonionic detergent n-dodecyl-β-D-maltoside (DDM), and proteins were separated in nondenaturing PAGE gels (BN-PAGE). If M-C7.1 bound before cell disruption and remained tightly attached to MprF, it should shift the MprF bands in Western blots of the blue native gels and the MprF–M-C7.1 complex should be detectable after Western blotting with a human IgG- specific secondary antibody. In order to detect MprF independently of M-C7.1, an MprF variant translationally fused to green-fluorescent protein (MprF-GFP, expressed from plasmid pRB-MprF-GFP), which is detectable by a GFP-specific primary antibody (Ernst et al., 2015), was also used and treated in the same way. To detect potentially nonshifted MprF proteins in the native MprF variant (pRB-MprF), M-C7.1 was used as additional primary antibody. *S. aureus* SA113Δ*spa*Δ*mprF* bearing the empty vector (pRB) was used as a negative control. In addition to M-C7.1, all three *S. aureus* strains were also incubated with the control antibody L-1. *S. aureus* cells expressing either unmodified MprF or MprF-GFP yielded a protein band migrating at a molecular weight of around 900 kDa

when preincubated with M-C7.1 but not with L-1 or in cells with the empty-vector control (pRB) (Figure 2A; Figure 2—figure supplement 2). In contrast, the empty-vector control (pRB) strain showed an unspecific band at 300 kDa when preincubated with M-C7.1 or at 150 kDa when preincubated with L-1 but no MprF-specific band (Figure 2A; Figure 2—figure supplement 2). The 900 kDa band of MprF-GFP was detected by both, M-C7.1 and, with a weaker signal, anti-GFP, confirming the identity of MprF (Figure 2A; Figure 2—figure supplement 2). We could recently show that MprF forms oligomers in the staphylococcal membrane, which were migrating at ca. 300 and 600 kDa (Ernst et al., 2015). Bands migrating at similar heights (ca. 250 and 500 kDa) were detected specifically in the MprF-GFP lanes after preincubation with either M-C7.1 or L-1 (Figure 2A; Figure 2—figure supplement 2) suggesting that they represent the oligomerized but not the mAB-complexed MprF proteins (Ernst et al., 2015). Therefore, the 900 kDa bands probably represent a complex formed by MprF and M-C7.1, which confirms that M-C7.1 specifically binds MprF loop seven in live *S. aureus* cells. The fact, that M-C7.1 used as primary antibody was not able to detect 250 and 500 kDa bands of noncomplexed MprF proteins while the MprF–M-C7.1 complex can directly be detected via anti-human secondary antibody, suggests that M-C7.1 binding only occurs in the living staphylococcal cell. Of note, the MprF–M-C7.1 complex migrating at around 900 kDa indicates that higher-order MprF multimers were shifted by complex formation with M-C7.1.

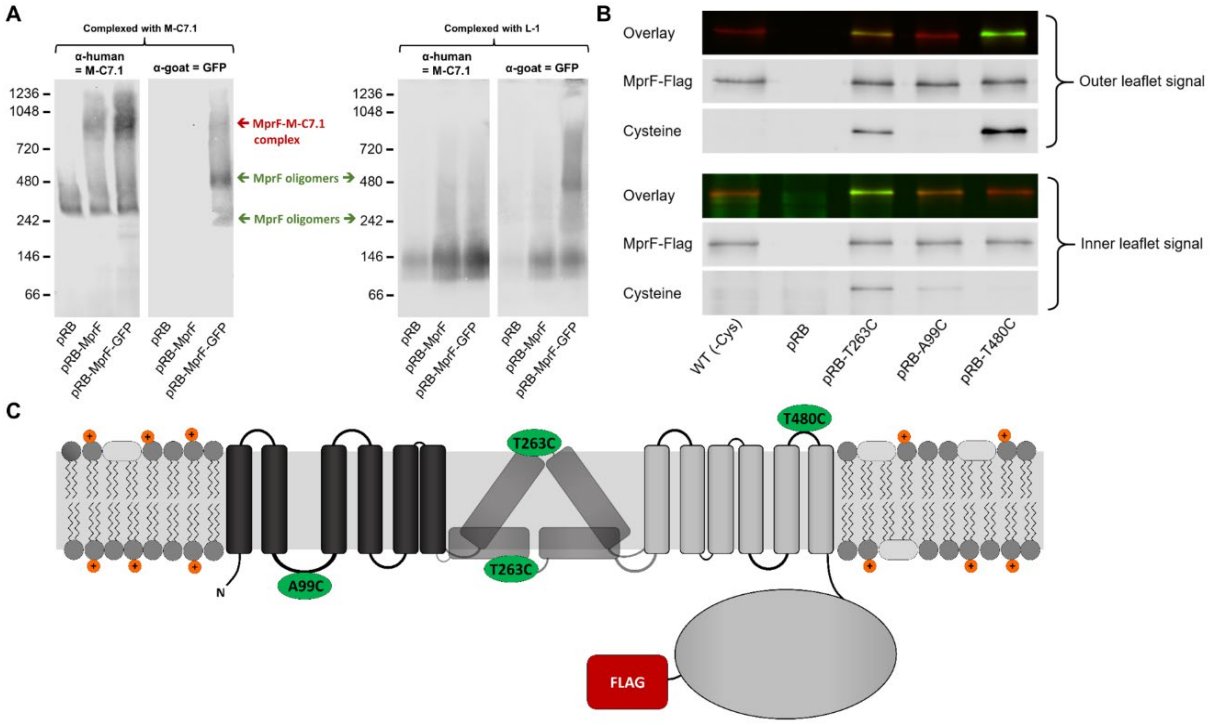

Figure 2: Binding of M-C7.1 to multiple peptide resistance factor (MprF) and membrane localization of the M-C7.1-targeted MprF loop 7. (A) Detection of M-C7.1 binding to MprF. Plasmid-encoded native and green fluorescent protein(GFP)-tagged MprF variants were expressed in *S. aureus* SA113Δ*spa*Δ*mprF* and living cells were preincubated with M-C7.1 or the isotype control monoclonal antibody (mAB) L-1 (in order to form MprF–mAB complexes). MprF variants complexed with M-C7.1 or control mAB L-1, respectively, were detected by blue native PAGE followed by Western blotting using two different primary (anti-GFP or M-C7.1) and corresponding secondary antibodies. SA113Δ*spa*Δ*mprF* expressing the empty vector (pRB) served as negative control. Molecular masses in kDa of marker proteins are given on the left of the blot. Arrows mark both the MprF–M-C7.1 complex at 900 kDa

and the MprF oligomers at 250 and 500 kDa, which were previously described (Ernst et al., 2015). (B) Cellular localization of the antigen epitope of M-C7.1 using the substituted cysteine accessibility method (SCAM) for specific loops between the MprF transmembrane segments (TMSs). The substituted cysteine T263C is localized in M-C7.1's target peptide sequence in MprF. Substitution of A99C served as inside control, substitution of T480C served as outside control (see topology model, part C). *S. aureus* SA113Δ*mprF* expressing the empty vector (pRB) and an MprF variant lacking all native cysteines (wild-type [WT] (-Cys)) served as additional negative controls. All MprF variants were plasmid-encoded, FLAG tagged at the C-terminus to allow immunoprecipitation and detection, and were expressed in *S. aureus* SA113Δ*mprF*. Substituted extracellular cysteine residues were labeled with Na*-(3-maleimidylpropionyl)-biocytin (MPB) (outer leaflet signal, green in overlay), while labeling of substituted internal cysteine with MPB was performed after the blocking of external cysteines with 4-acetamino-4′-maleimidylstilbene-2,2′-disulfonic acid (AMS) (inner leaflet signal, green in overlay). MprF was detected via antibody staining by an anti-FLAG antibody (red in overlay). (C) MprF topology showing location and amino acid exchanges of artificial cysteine residues for SCAM detection in green.

The position of MprF loop 7 was further investigated by inserting a cysteine residue into the loop and analyzing the capacity of the membrane-impermeable agent Na*-(3-maleimidylpropionyl)-biocytin (MPB) to label cysteines covalently, using the substituted cysteine accessibility method (SCAM) (Bogdanov et al., 2005). MPB treatment of intact *S. aureus* cells should only lead to labeling of extracellular protein portions while blocking cysteines at the outside with 4-acetamido-4′-maleim idylstilbene-2,2′-disulfonic acid (AMS), followed by cell homogenization and addition of MPB should allow to label only protein parts at the inner surface of the membrane according to a previously established method in *E. coli* (Bogdanov et al., 2005). An MprF variant lacking all native cysteine residues was generated to exclude background signals. Cysteine residues in MprF were exchanged against serine or alanine residues to minimize structural or functional changes. Native *S. aureus* MprF contains six cysteines none of which is conserved in MprF proteins from other bacteria suggesting that they do not have critical functions. The cysteine-deficient mutant protein was found to be indeed functional because it decreased the susceptibility of the *S. aureus* mprF mutant (SA113Δ*mprF*) to daptomycin (Figure 2—figure supplement 1), which depends on intact MprF synthase and flippase activities (Ernst et al., 2009). However, the mutated proteins conferred lower resistance levels than the wild-type protein, presumably because of less efficient protein folding or stability. Cysteines were then inserted into MprF loop seven (T263) and, as a control, into the first intracellular loop (loop 2, A99) and the last extracellular loop (loop 13, T480), the localization of which had been consistently confirmed by previous computational and experimental analyses (Ernst et al., 2015; Figures 1A and 2C). Amino acids for exchange were chosen according to a predicted weak effect for functional changes by respective substitution with cysteine using https://predictprotein.org (Yachdav et al., 2014). The prediction is based on a machine learning program integrating both evolutionary information and structural features such as predicted secondary structure and solvent accessibility to evaluate the effect of amino acid exchanges in a protein sequence (Yachdav et al., 2014). The SCAM approach further confirmed the topology of intracellular loop 2 and extracellular loop 13 (Figure 2B), thereby demonstrating that the technique can lead to reliable results in *S. aureus*. Notably, MprF loop 7 was found in both locations, at the inner and outer surface of the membrane. This

finding corroborates the ambiguous position of loop 7 and suggests that this loop may have some degree of mobility in the membrane, which may reflect the lipid translocation process. The finding also clarifies why M-C7.1 has the capacity to bind MprF loop 7 at the outer surface of the cytoplasmic membrane.

mABs binding to putative extracellular loops of MprF render *S. aureus* susceptible to CAMPs

MprF confers resistance to cationic antimicrobials such as the bacteriocin nisin by reducing the negative net charge of the membrane outer surface (Peschel et al., 2001; Ernst et al., 2009). If the mABs would not only bind to but also inhibit the function of MprF, *S. aureus* should become more susceptible to nisin. The six mABs with confirmed specific binding to MprF and the isotype control mAB L-1 were analyzed for their capacity to increase the susceptibility of *S. aureus* SA113 to nisin. For those initial screening experiments protein A (*spa*) mutants were used to diminish effects of unspecific IgG binding to protein A. Bacteria were grown in the presence of one of the mABs and then incubated with nisin at the IC_{50} followed by quantification of viable bacterial cells. Two of the MprF-specific mABs targeting loops 7 or 13 increased the sensitivity of *S. aureus* SA113Δ*spa* to nisin while the other mABs and the isotype control mAB L-1 had no significant impact (Figure 3A). mAB M-C7.1 caused the strongest sensitization (Figure 3A) and it synergized with nisin in a dose-dependent fashion (Figure 3— figure supplement 1). It was therefore selected for further analysis using the highly prevalent and virulent community-associated methicillin-resistant *S. aureus* (CA-MRSA) USA300 clone (Otto, 2013).

For all following experiments *S. aureus* wild-type (WT) strains with intact protein A were used to make sure that the observed sensitization to CAMPs was not affected by unspecific antibody binding to protein A.

M-C7.1 was found to also increase the susceptibility of USA300 WT to the human CAMP LL-37, a host defense peptide produced by epithelial and phagocyte cells (Pinheiro da Silva and Machado, 2017), and to daptomycin, a lipopeptide antibiotic in clinical use sharing physicochemical and anti- bacterial properties with CAMPs (Bayer et al., 2013), in addition to nisin (Figure 3B–D). M-C7.1 also increased the antimicrobial activity of daptomycin against the daptomycin-resistant (DAP-R) clinical CA-MRSA isolate 703 possessing the gain-of-function mutation S295L in MprF (Jones et al., 2008; Figure 3E). Of note, M-C7.1 could reduce daptomycin minimal inhibitory concentration (MIC) of both, *S. aureus* SA113 WT and the DAP-R strain 703 (Figure 3F), suggesting that M-C7.1 may potentially be able to overcome daptomycin resistance during therapy. M-C7.1 but not the isotype control mAB L-1 was able to inhibit growth of USA300 WT in the presence of subinhibitory concentrations of nisin (Figure 3G). Thus, mABs specific for certain extracellular loops of MprF may not only bind to MprF but also inhibit its function. When USA300 WT was passaged for several days through media with

M-C7.1 at 10 or 100 nM and with or without subinhibitory daptomycin (0.5 µg/ml), no point mutations in *mprF* were found suggesting that the MprF segment targeted by M-C7.1 is not prone to quickly occurring escape mutations.

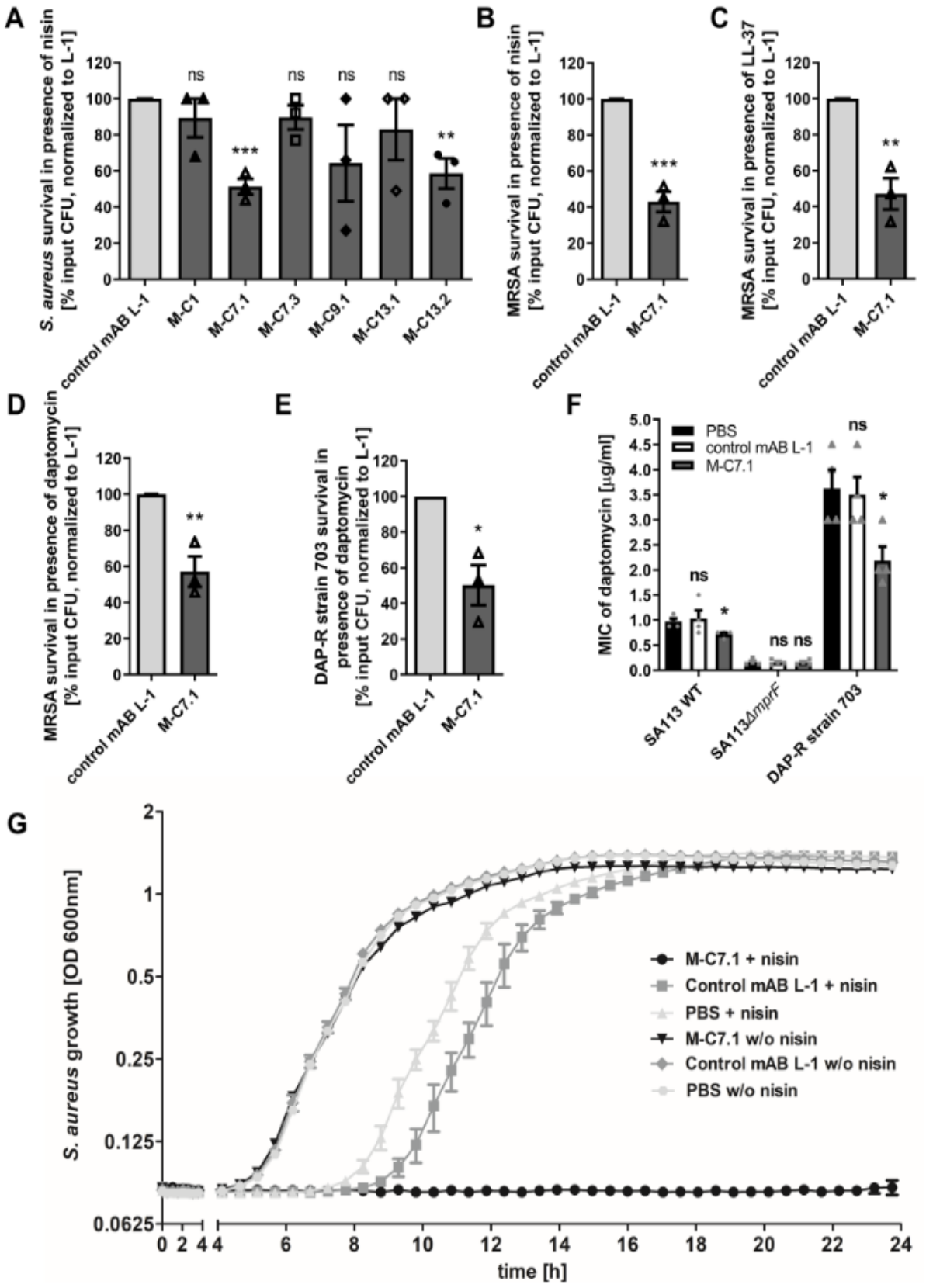

Figure 3: Killing and growth inhibition of *S. aureus* by antimicrobial peptides and antibiotics in the presence of M-C7.1. (A) Survival of *S. aureus* SA113Δ*spa* in the presence of nisin and 100 µg/ml anti-multiple peptide resistance

factor (MprF) antibodies compared to 100 µg/ml control monoclonal antibody (mAB) L-1. Surviving colony-forming units (CFU) of *S. aureus* incubated with one of the antibodies and nisin were analyzed after 2 hr incubation and the negative control (isotype mAB L-1) was set to 100% survival. (B) Survival of community-associated methicillin-resistant *S.* aureus (CA-MRSA) wild-type (WT) strain USA300 in the presence of nisin and 100 µg/ml M-C7.1 compared to the isotype control mAB L-1. (C) Survival of USA300 WT in the presence of LL-37 and 100 µg/ml M-C7.1 compared to the isotype control mAB L-1. (D) Survival of USA300 WT in the presence of daptomycin and 100 µg/ml M-C7.1 compared to the isotype control mAB L-1. (E) Survival of daptomycin-resistant (DAP-R) CA-MRSA strain 703 (Jones et al., 2008) in the presence of daptomycin and 100 µg/ml M-C7.1 compared to the isotype control mAB L-1. (F) Daptomycin MICs of SA113 WT, SA113Δ*mprF* and DAP-R strain 703 when pretreated with PBS compared to 100 µg/ml control mAB L-1 and to 100 µg/ml M-C7.1. (G) Growth inhibition of USA300 WT in the presence of 4 µg/ml nisin and 1 µM M-C7.1 compared to 1 µM isotype control mAB L-1. Wells without nisin and/or antibodies served as additional negative controls. The means + standard error of the mean (SEM) of results from at least three biological replicates are shown in (A)–(F). (G) shows means + SEM of technical triplicates from a representative experiment of three biological replicates. Values for M-C7.1 or other anti-MprF antibodies that were significantly different from those for the isotype control mAB L-1 in (A)–(F), calculated by Student's paired t-test are indicated (*$p < 0.05$; **$p < 0.01$; ***$p < 0.0001$).

M-C7.1 inhibits the flippase function of MprF

M-C7.1 binds MprF at the junction between the LysPG synthase and flippase domains (Figure 1). The lipid patterns of SA113 WT treated with M-C7.1 at concentrations that increased the susceptibility to nisin or with the isotype control mAB L-1 were compared but showed no differences indicating that the synthase function of MprF was not inhibited by M-C7.1 (Figure 4A). The flippase activity of MprF promotes the exposure of positively charged LysPG at the outer surface of the cytoplasmic membrane thereby reducing the affinity for the small cationic protein cytochrome C (Peschel et al., 1999), which binds preferentially to negatively charged PG, or for calcium-bound annexin V (Yount et al., 2009). These model proteins have been shown to allow a sensitive assessment of changes in the surface charge of *S. aureus* in several previous studies (Ernst et al., 2009; Ernst et al., 2018; Slavetinsky et al., 2012). Treatment of SA113 WT with M-C7.1 at concentrations that increased the susceptibility to nisin led to a significant increase in the capacity to bind cytochrome C or annexin V compared to SA113 WT without treatment or treated with isotype control mAB L-1 (Figure 4B, C) thereby indicating that M-C7.1 inhibits the flippase function of MprF. It is tempting to speculate that the protein region of MprF loop 7 and adjacent TMSs may accomplish a crucial function in the process of phospholipid translocation, as suggested by the dynamic localization of loop 7 on the cytoplasmic and external faces of the membrane.

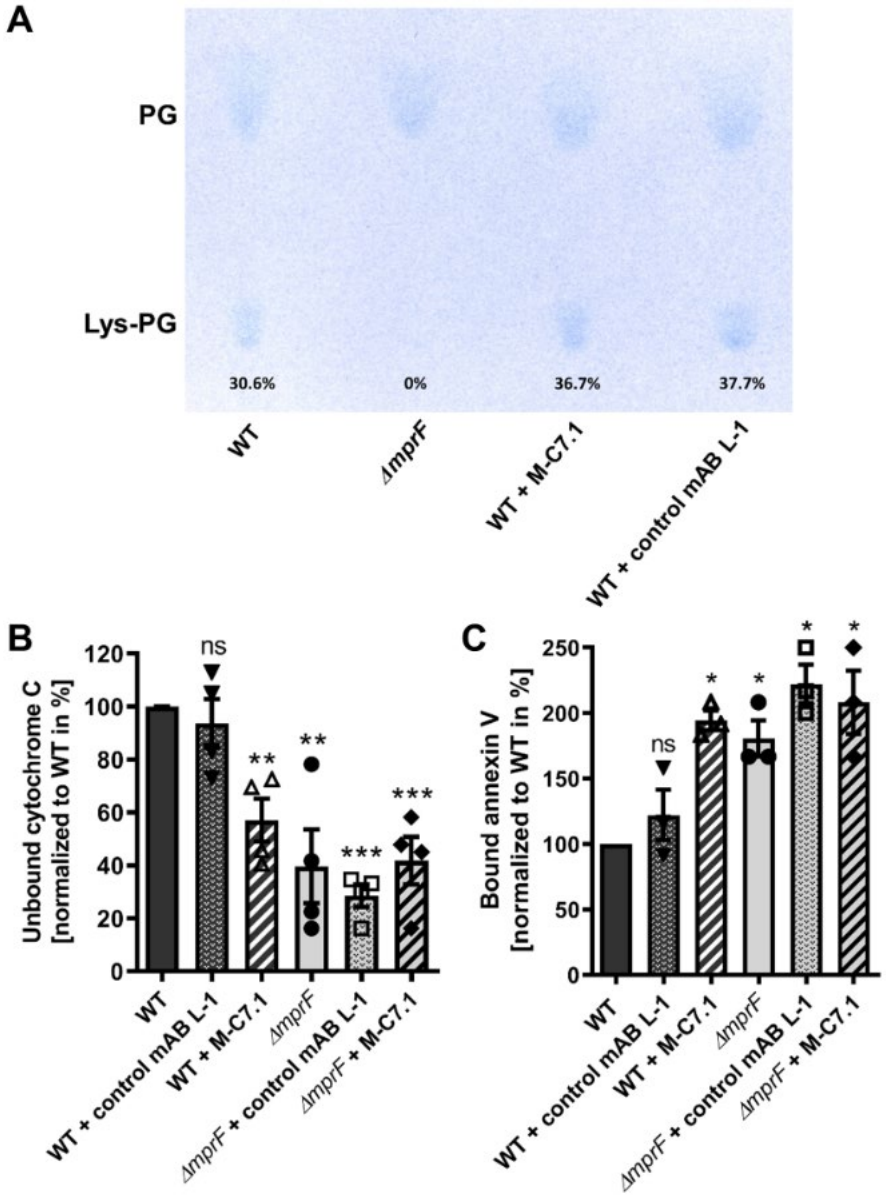

Figure 4: M-C7.1 inhibits the multiple peptide resistance factor (MprF) lysyl-phosphatidylglycerol (LysPG) flippase but not the LysPG synthase. (A) Detection of phospholipids from *S. aureus* SA113Δ*mprF* and wild-type (WT) treated or not treated with 100 µg/ml M-C7.1 or the isotype control monoclonal antibody (mAB) L-1. Polar lipids were separated by thin layer chromatography (TLC) and stained with the phosphate group-specific dye molybdenum blue to detect the well-documented phosphatidylglycerol (PG) and LysPG pattern of *S. aureus* WT and *mprF* deletion mutant (Slavetinsky et al., 2012). Percentages of LysPG in relation to total phospholipid content are given below LysPG spots. (B) The repulsion of positively charged cytochrome C corresponds to MprF LysPG synthase plus flippase activity while the synthase activity alone does not affect repulsion. To assess MprF flippase efficiency, unbound cytochrome C in the supernatant was quantified photometrically after incubation with the *S. aureus* SA113 WT without pretreatment, or with pretreated with M-C7.1 or the isotype control mAB L-1 (WT set to 100%). SA113Δ*mprF* with or without mAB pretreatment served as positive control. The means + standard error of the mean (SEM) of results from three biological replicates are shown. (C) Annexin V binding to *S. aureus* SA113 WT compared to incubation with M-C7.1 or the isotype control mAB L-1 was quantified by measuring cell-bound annexin V by fluorescence-activated cell sorting (FACS) and untreated WT samples were set to 100%. SA113Δ*mprF* with and without mAB incubation served as positive control. Data are expressed as % of untreated WT cells. The means + SEM of results from three biological replicates are shown in (B) and (C). Significant differences compared to WT samples were calculated by Student's paired t-test (*$p < 0.05$; **$p < 0.01$; ***$p < 0.0001$).

M-C7.1 treatment abrogates *S. aureus* survival in phagocytes

The capacity of PMNs to kill phagocytosed bacteria does not only rely on the oxidative burst but also on the activity of LL-37 and other CAMPs and antimicrobial proteins (Spaan et al.,

2013). Accordingly, *S. aureus mprF* mutants are more susceptible to PMN killing than the parental strains while their opsonization and phagocytosis by PMNs remains unaltered (Peschel et al., 2001; Kristian et al., 2003). The increased susceptibility of M-C7.1-treated *S. aureus* to CAMPs should therefore alter its survival ability in PMNs. CA-MRSA WT strain USA300 was pretreated with mABs, opsonized with normal human serum, and exposed to human PMNs. Treatment with M-C7.1 or the isotype control mAB L-1 did not alter the rate of PMN phagocytosis, but M-C7.1-treated USA300 cells were significantly more rapidly killed by PMNs than those treated with the isotype control antibody (Figure 5). This finding reflects our previous reports on reduced survival of MprF-deficient *S. aureus* in PMNs (Peschel et al., 2001; Kristian et al., 2003). Thus, *S. aureus* treatment with M-C7.1 might reduce the capacity to persist in infections and may help to blunt the virulence of *S. aureus* in invasive infections.

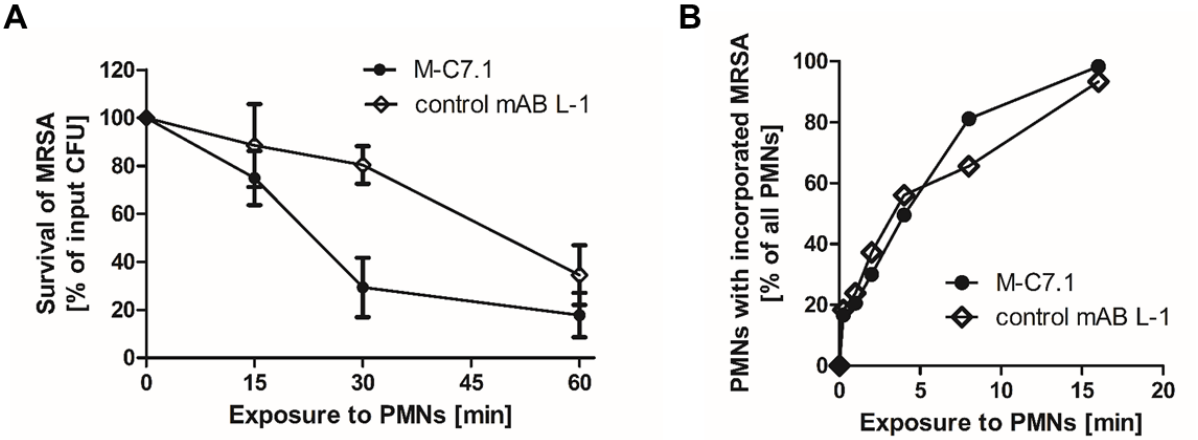

Figure 5: M-C7.1 supports *S. aureus* clearance by isolated human polymorphonuclear leukocytes (PMNs). (A) Kinetics of killing of community-associated methicillin-resistant *S. aureus* (CA-MRSA) strain USA300 wild-type (WT) treated with M-C7.1 compared to isotype control monoclonal antibody (mAB) L-1 by freshly isolated human PMNs. Viable bacteria (colony-forming units, CFU) after incubation with PMNs are shown as percentage of initial CFU counts. The means + standard error of the mean (SEM) of results from three biological replicates are shown. (B) Kinetics of phagocytosis of USA300 WT treated with M-C7.1 compared to isotype control mAB L-1 by freshly isolated human PMNs. Percentages of PMNs bearing fluorescein-5-isothiocyanate (FITC)-labeled USA300 are given. Means of three counts from a representative experiment are shown.

Discussion

Monoclonal therapeutic antibodies have proven efficacy for neutralization of bacterial toxins such as *Clostridium botulinum* or *Clostridioides difficile* toxins, and mAB-based therapies targeting the *S. aureus* alpha toxins and leukotoxins are currently developed (Dickey et al., 2017; Tabor et al., 2016). Moreover, therapeutic mABs binding to *S. aureus* surface molecules to promote opsonic phagocytosis have been assessed in preclinical and clinical trials (Missiakas and Schneewind, 2016). In contrast, mABs inhibiting crucial cellular mechanisms of bacterial pathogens have hardly been assessed so far (Zheng et al., 2019). We developed specific mABs, which can block the activity of *S. aureus* MprF, the first described bacterial phospholipid flippase. Our mABs did not mediate increased internalization of *S. aureus* cells, most probably because the bacterial cell wall is too thick to allow binding of the mAB FC part

to phagocyte FC receptors. However, the inhibition of MprF by M-C7.1 sensitized *S. aureus* to CAMPs and daptomycin and promoted killing by human PMNs, which use CAMPs as an important component of their antimicrobial arsenal. Specific inhibition of MprF could therefore promote the capacity of human host defense to clear or prevent a *S. aureus* infection and would, at the same time, increase the susceptibility of *S. aureus* to CAMP-like antibiotics such as daptomycin. Thus, targeting bacterial defense mechanisms provides a promising concept for antivirulence therapy. The capacity of antibodies to traverse the cell wall and reach the cytoplasmic membrane of *S. aureus* has remained controversial (Reichmann et al., 2014). However, other labs' and our findings demonstrate that specific antibodies can reach membrane-associated epitopes in *S. aureus* (Mishra et al., 2012; Weisman et al., 2009). A recent atomic-force microscopy-based study revealed large, irregular pores in the cell wall of *S. aureus*, which might allow large proteins such as antibodies to reach the cytoplasmic membrane (Pasquina-Lemonche et al., 2020). M-C7.1 sensitized *S. aureus* also in the presence of protein A indicating that the unspecific IgG binding by protein A does not interfere with the M-C7.1 capacity to block MprF.

Specific binding of MprF antibody M-C7.1 to the extracellular loop 7 inhibited the flippase function of MprF, which indicates that this loop plays a crucial role in the lipid translocation process. Loop 7 is located between predicted TMS 7 and 8, and its presence at the outer surface of the cytoplasmic membrane had remained elusive since computational and experimental analyses had yielded conflicting results (Ernst et al., 2015). Surprisingly, we found loop 7 to be accessible from both, the outside and inside of the cytoplasmic membrane. This suggests that the protein part formed by loop 7 and adjacent TMS 7 and 8 may change its position in the protein complex, moving between the two membrane surfaces to accomplish LysPG translocation (Figure 6), or it could be in a unique position of the large MprF protein complex that allows access from both sides. This protein part might represent the center of the MprF flippase establishing the previously reported MprF-dependent distribution of charged LysPG in the inner and outer leaflet of the cytoplasmic membrane of *S. aureus* (Ernst et al., 2009; Figure 6). While this manuscript was in revision, the three-dimensional structure of the MprF protein of *Rhizobium tropici* was reported. It demonstrates that the region corresponding to the *S. aureus* MprF loop 7 is part of a gate between two large protein cavities, which are accessible from the outer and inner surface of the cytoplasmic membrane and allow for the passage of LysPG molecules between the two membrane leaflets (Song et al., 2021). Song et al. suggest a mechanistic model where LysPG binding in the inner protein cavity of the MprF flippase results in a transient channel formation/gate opening allowing LysPG to diffuse into the outer protein cavity which would put the M-C7.1-binding site in the center of the flipping process. This model would explain why M-C7.1 binding to MprF seems to require the live *S. aureus* cell to achieve structural accessibility to MprF. Moreover, Song et al. confirmed that

MprF forms homodimers and larger oligomers. These structural data support our functional data and provide molecular explanations.

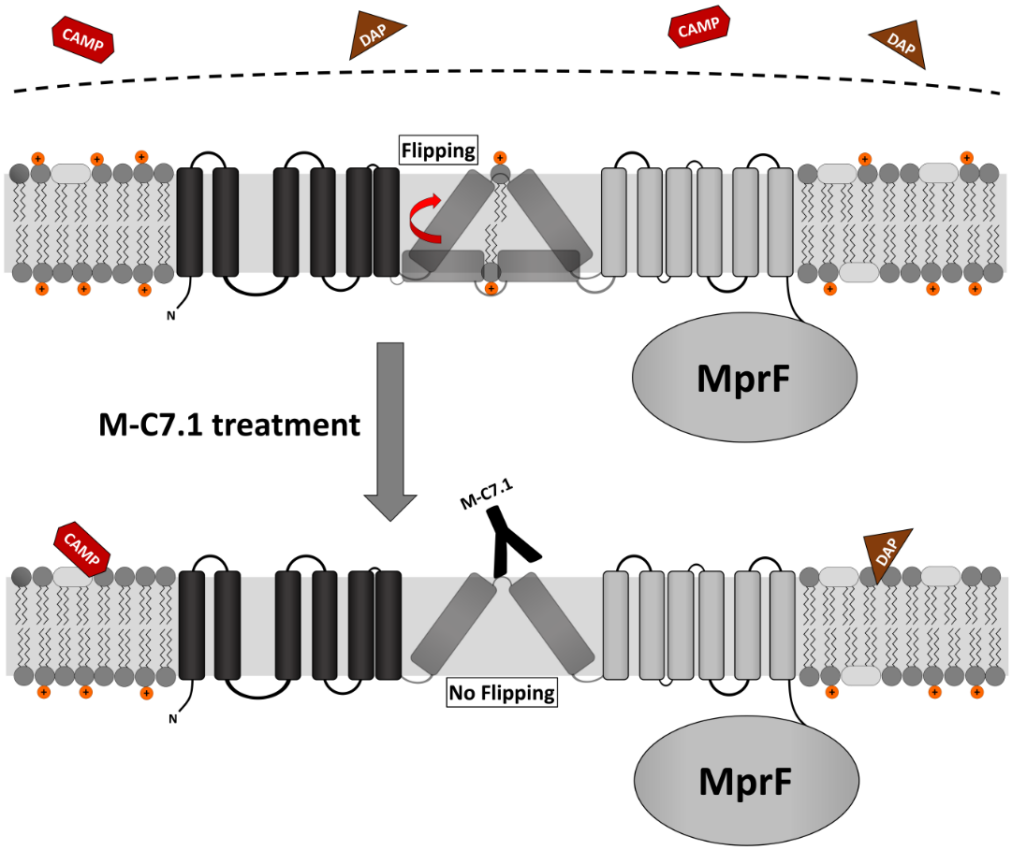

Figure 6: Proposed model for multiple peptide resistance factor (MprF) inhibition by M-C7.1. Flipping of positively charged lysyl-phosphatidylglycerol (LysPG) probably by transmembrane segment (TMS) 7 and 8 of MprF results in a more positively charged staphylococcal membrane, which is better able to repulse cationic antimicrobial peptides (CAMPs) or daptomycin (DAP). Binding of M-C7.1 to MprF loop 7 blocks the flippase, which results in a more negatively charged staphylococcal membrane and subsequently in an increased *S. aureus* membrane disruption by CAMPs and daptomycin.

Interestingly, in living staphylococcal cells, M-C7.1 bound to putative higher-order MprF multimers as shown via blue native Western blotting suggesting that such multimers might represent the active lipid translocating state of MprF. Replacement of conserved amino acids in the M-C7.1-targeted protein part has been shown to inhibit the flippase function of MprF (Ernst et al., 2015), which underscores the crucial function of this domain. Notably, one of the conserved and essential amino acids in TMS 7, D254, is negatively charged. It is tempting to speculate that D254 may interact with the positively charged head group of LysPG during the translocation process in the *S. aureus* MprF. Mutations on loop 7 and adjacent TMS have recently been found to cause specific resistance to the structurally related lipopeptide antibiotics daptomycin and friulimicin B but not to other antimicrobials (Ernst et al., 2018). Indirect evidence has suggested that these mutations allow the flippase to translocate these lipopeptide antibiotics instead of or together with LysPG (Ernst et al., 2018), which is in agreement with a direct role of loop 7 in the translocation process. A mAB-binding loop 13 also

sensitized *S. aureus* to nisin in a similar but less pronounced way as M-C7.1 suggesting that this loop may also have a critical role for MprF activity.

With the severe shortage of new antibiotic target and drug candidates, crucial cellular machineries conferring fitness benefits during infection rather than accomplishing essential cellular functions should be considered as targets for the development of new therapeutics. The phospholipid synthase and flippase MprF may become a role model for further targeting of bacterial defense mechanisms for such antifitness or antivirulence drugs. Compared to other potential targets, MprF has the advantage that essential parts of it are exposed at the external surface of the cytoplasmic membrane. Moreover, MprF is found in many other bacterial pathogens for which similar therapeutic mABs could be developed (Ernst et al., 2009). On the other hand, only a few amino acids in loop 7 are conserved in other bacteria, which would limit the impact of loop-7-directed mABs on other microbiome members thereby minimizing the resistance selection pressure and the risk of dysbiosis.

Materials and Methods

Bacterial strains, maintenance, and mutagenesis of mprF

We used commonly used strains, the methicillin-susceptible laboratory strain *S. aureus* SA113 (ATCC 35556), methicillin-resistant clinical clone *S. aureus* USA300, and the SA113 *mprF* knockout derivative SA113Δ*mprF*, which has been described recently (Peschel et al., 1999; Wang et al., 2007; Supplementary file 1b).

For the construction of a protein A mutant (Δ*spa*) the *E. coli*/*S. aureus* shuttle vector pKOR1 (Bae and Schneewind, 2006) was used, which allows allelic replacement with inducible counterselection in staphylococci. Flanking regions of spa were amplified from chromosomal DNA of S. aureus COL with primer pairs Spa-del_attB1 (ggggacaagtttgtacaaaaaagcaggccaatattccatggtccagaact; bold: spa sequence) and Spa-del for BglII (gtcgagatctataaaaacaaacaatacacaacg, restriction site italic) as well as Spa-del_attB2 (ggggaccactttgtacaagaaagctgggatcagcaagaaaacacacttcc; bold: spa flanking sequence) and Spa-del rev BglII (aaaagatctaacgaattatgtattgcaata, restriction site italic). Both PCR products were digested with BglII and subsequently ligated. Without further purification, the ligation product was mixed with equimolar amounts of pKOR1 and in vitro recombination was performed with BP clonase Mix (Invitrogen) according to the manufacturer's instructions. The recombination mixture was transferred to chemically competent *E. coli* DH5α and isolated plasmids from the resulting transformants were analyzed by restriction digest. The correct plasmid was isolated from *E. coli* DH5α and used to electroporate competent *S. aureus* RN4220 from which it was again isolated and transferred into *S. aureus* SA113 by electroporation. Allelic replacement was essentially conducted as previously described (Bae and Schneewind, 2006) and resulting deletion mutants were confirmed by PCR.

The *S. aureus* SA113 *spa mprF* double mutant (SA113Δ*spa*Δ*mprF*) was constructed by transducing the gene deletion cassette of the *S. aureus* SA113 *mprF* deletion mutant (SA113Δ*mprF*) to the marker-less spa-deficient *S. aureus* SA113 mutant (SA113Δ*spa*) using standard transduction protocols. The resulting *S. aureus* strain SA113Δ*spa*Δ*mprF* was identified by screening for erythromycin resistance conferred by the gene deletion cassette and confirmed by PCR of the deleted genome section. Bacteria were maintained on tryptic soy agar plates.

Cysteine substitutions in *mprF* were accomplished by site-directed mutagenesis in *E. coli* using *E. coli*/*S. aureus* shuttle vector pRB474 bearing *mprF*, using the QuickChange II Site-Directed Mutagenesis Kit (Agilent), as described recently (Ernst et al., 2018). Mutated *mprF* derivatives in pRB474*mprF* were transferred into SA113Δ*mprF* and *mprF* expression was mediated by the plasmid-encoded constitutive *Bacillus subtilis* promoter *vegII*. 10 µg/ml chloramphenicol served for maintenance in all plasmid-based studies. A99, T263, and T480 were chosen for exchange against a cysteine residue because of prediction of a weak effect on protein structure in an analysis of functional changes given a single point mutation according to https://predictprotein.org (Yachdav et al., 2014).

Plasmids and primers used in this study are given in Supplementary file 1c, d, respectively. Unless otherwise stated, bacteria were cultivated in Mueller-Hinton Broth (MHB, Sigma-Aldrich) with appropriate antibiotics for all experiments.

Antigen selection and antibody production

MprF-derived peptides of interest (Figure 1 and Supplementary file 1a) were custom synthesized by JPT Peptide Technologies GmbH (Berlin). An N-terminal and a C-terminal cysteine were added to enable cyclization. Biotin was coupled to the peptide via a 4,7,10-trioxa-1,13-tridecanediamine succinic acid (Ttds) linker (Ieronymaki et al., 2017). Cyclization and coupling of linker and biotin were performed by JPT Peptide Technologies.

Recombinant antibodies were generated from the HuCAL PLATINUM library, as described recently, by three iterative rounds of panning on the antigen peptides in solution and antigen-antibody-phage complexes were captured with streptavidin-coated beads (Dynal M-280) (Prassler et al., 2011; Tiller et al., 2013). Fab-encoding inserts of the selected HuCAL PLATINUM phagemids were cloned and expressed in *E. coli* TG1 F cells, purified chromatographically by IMAC (BioRad) and subcloned in an IgG1 expression vector system to obtain full-length IgG1s by expression in eukaryotic HKB11 cells, as described recently (Prassler et al., 2011). Identity has been identified by STR profiling. Regular mycoplasma contamination testing was performed throughout all mAB productions and were negative. IgGs were purified by protein A affinity chromatography (MabSelect SURE, GE Healthcare) (Prassler et al., 2011).

The humanized antibody MOR03207 (Neuber et al., 2014) directed against chicken lysozyme serves as isotype control and was called L-1 in this manuscript. The IgG MOR13182 generated with peptide QSIDTNSHQDHTEDVEKDQSE derived from the *S. aureus* surface protein elastin-binding protein of *S. aureus* (EbpS) served as positive control for whole-cell ELISAs and was called E-1 in this manuscript.

Peptide and whole-cell ELISAs of MprF-specific mABs

Overnight *S. aureus* SA113Δ*spa* or SA113Δ*spa*Δ*mprF* cultures grown in MHB were adjusted to OD_{600} 0.1 in fresh MHB and grown to OD_{600} of at least 1.0. Cells were harvested, adjusted to OD_{600} 0.5 with 0.9% NaCl, and used to coat 96 well NUNC Maxisorp Immuno Plates for 1 hr (50 µl/well). After three washing steps with Tris-buffered saline (TBS; 50 mM Tris, 150 mM NaCl in 800 ml of H2O, pH 7.4) containing 0.05% Tween 20 (TBS-T), the cells were blocked with PBS containing 1× ROTIBlock (Carl Roth) for 1 hr. Primary antibodies were added after three washing steps with TBS-T at an indicated final concentration of 1, 10, or 100 nM and incubated for 1 hr. After three more washing steps with TBS-T, antihuman IgG conjugated to alkaline phosphatase (Sigma-Aldrich A8542) diluted 1:10,000 in TBS-T was applied. Finally, after three washing steps with 2× TBS-T and 1× TBS, the cells were incubated with 100 µl p-nitrophenyl phosphate solution as advised by the manufacturer (Sigma-Aldrich N1891). Absorbance was measured at 405 nm.

Detection of antibody binding to MprF by blue native Western blotting

To detect binding of the anti-MprF antibody to MprF we performed blue native polyacrylamide gel electrophoresis (BN-PAGE) as previously described (Ernst et al., 2015) with slight modifications. Briefly, 20 ml of *S. aureus* cells grown in MHB with anti-MprF antibodies (100 µg/ml) to OD_{600} 1 were incubated with 750 µl of lysis buffer (100 mM ethylenediaminetetraacetic acid (EDTA) [pH 8.0], 1 mM MgCl2, 5 µg/ml lysostaphin, 10 µg/ml DNase, proteinase inhibitor [cocktail set III from Calbiochem] diluted 1:100 in PBS) for 30 min at 37°C and homogenized three times with 500 µl zirconia-silica beads (0.1 mm diameter from Carl-Roth) using a FastPrep 24 homogenizer (MP Biomedicals) for 30 s at a speed of 6.5 m/s. After removing the beads, cell lysate was centrifuged 20 min at 14,000 rpm and 4°C to sediment cell debris and supernatant was transferred to microcentrifuge polypropylene tubes (Beckman Coulter) and cytoplasmic membranes were precipitated by ultracentrifugation for 45 min at 55,000 rpm and 4°C (Beckman Coulter rotor TLA 55). Membrane fractions resuspended in resuspension buffer (750 mM aminocaproic acid, 50 mM Bis-Tris [pH 7.0]) were incubated with the MprF- or lysozyme-specific humanized IgG mAB and/or a GFP-specific rabbit IgG mAB (Invitrogen) for 30 min shaking at 37°C. Dodecyl maltoside was added to a final concentration of 1% for 1 hr at 4°C to solubilize MprF–antibody complexes. Insoluble material was removed by ultracentrifugation for 30 min at 40,000 rpm and 4°C. 20 µl supernatant was mixed 1:10 with 10× BN loading dye (5% [wt/ vol] Serva Blue G, 250 mM aminocaproic acid,

50% glycerol) and run on a Novex NativePAGE 4%–16% Bis-Tris gel (Invitrogen). Separated proteins were transferred to a polyvinyl difluoride membrane and detected via either, goat antihuman IgG DyLight 700 (Pierce) or goat antirabbit IgG DyLight 800 (Pierce) as secondary antibodies in an Odyssey imaging system from LI-COR.

SCAM to localize MprF loops in inner and/or outer membrane leaflet

SCAM was adapted for use in *S. aureus* from the protocol recently established for *E. coli* (Bogdanov et al., 2005). Variants of *S. aureus* SA113Δ*mprF* were expressing cysteine-deficient and/or -altered MprF derivatives bearing a FLAG tag at the C-terminus via the plasmid pRB474. Bacteria were grown at 37°C to an OD_{600} 0.7–0.8 in 100 ml TSB, split into two equal aliquots, and harvested. Pellets were resuspended in a mixture of buffer A (100 mM HEPES, 250 mM sucrose, 25 mM $MgCl_2$, 0.1 mM KCl [pH 7.5]) supplemented with 1 mM $MgSO_4$, 1 mM EDTA, 2.1 µg lysostaphin, 0.7 µg DNase, and 1% of a protease inhibitor cocktail (Roche) and incubated for 45 min at 37°C. For staining of cysteine residues in the outer leaflet of the cytoplasmic membrane, cells of the first aliquot were treated with N*-(3- maleimidylpropionyl)-biocytin (MPB, Thermo Scientific) at a final concentration of 107 µM for 20 min on ice. In the second aliquot, external cysteine residues were blocked with 107 µM (AMS Thermo Scientific) for 20 min on ice, bacterial cells were subsequently disrupted in a bead mill as described above and internal cysteines were labeled with MPB for 5 min. MPB labeling was quenched in both aliquots by the addition of 21 mM β-mercaptoethanol. Cell debris was removed by several centrifugation and washing steps, membrane fractions were collected via ultracentrifugation at 38,000 × g, and labeled membrane samples were stored at −80°C.

For protein enrichment and precipitation, labeled membrane samples were thawed on ice and suspended in 20 mM β-mercaptoethanol containing buffer A. Proteins were solubilized by the addition of an equal volume of solubilization buffer (50 mM Tris–HCl [pH 9], 1 mM EDTA, 2% SDS) and vigorous vortexing for 30 min at 4°C, followed by an incubation step of 30 min at 37°C and vortexing for 30 min at 4°C. After solubilization, one and a half volumes of immunoprecipitation buffer 1 (50 mM Tris–HCl [pH 9], 150 mM NaCl, 1 mM EDTA, 2% Thesit, 0.4% SDS [pH 8.1]) was added and samples were incubated for 2.5 hr with magnetic FLAGbeads (Sigma-Aldrich) in a rotation wheel at 4°C. After several washing steps with immunoprecipitation buffer one and immunoprecipitation buffer 2 (50 mM Tris–HCl [pH 9], 1 M NaCl, 1 mM EDTA, 2% Thesit, 0.4% SDS [pH 8.1]), FLAG-tagged MprF was eluted by the addition of 0.1 M glycine–HCl (pH 2.2) and neutralized by adding Tris–HCl (pH 9).

For detection of cysteine-labeled MprF, samples were analyzed by denaturing SDS–PAGE and Western blotting. To this end, 12 µl samples were mixed with 4× Laemmli sample buffer (BioRad), loaded onto a 10% polyacrylamide gel, and separated via electrophoresis. Proteins were transferred onto a polyvinylidene difluoride (PVDF) membrane (Immobilon-PSQ PVDF membrane, Merck) by semi-dry turbo Western blot procedure (Trans-Blot Turbo Transfer

System, BioRad). FLAG-tagged MprF was detected both by a mouse anti-FLAG primary antibody (Sigma-Aldrich) and goat antimouse secondary antibody (LI-COR) at 700 nm, while MBP-labeled cysteine residues were detected with streptavidin DyLight conjugate (Thermo Scientific) at 800 nm in an Odyssey imaging system from LI-COR.

Determination of susceptibility to antimicrobial agents

Overnight cultures of *S. aureus* SA113Δ*spa* or USA300 WT were diluted in fresh MHB and adjusted to OD_{600} 0.25 (~1.5 × 10^7 cells). Antibodies were adjusted to a concentration of 1 mg/ml and 10 µl per well of a 96-well plate were added to 90 µl of the adjusted cell suspension (final antibody concentration: 100 µg/ml). Cells were grown in the presence of the isotype control antibody L-1 or with the respective anti-MprF antibodies. After 3 hr of incubation at 37°C under shaking, optical density was determined, and cells were adjusted to OD_{600} 0.025 in 500 µl cold PBS. 80 µl of the adjusted cell suspension were mixed with 20 µl of antimicrobial substances to final concentrations of 22.5 µg/ ml nisin for SA113Δ*spa* or of 5 µg/ml nisin for USA300, 1.5 µg/ml daptomycin for USA300, 11 µg/ml daptomycin for DAP-R CA-MRSA strain 703, and 45 µg/ml LL-37 for USA300 or 20 µl PBS as control. After incubation for 2 hr under shaking at 37°C, the cell suspensions were diluted 1:200 and 100 µl of each duplicate was plated in triplicates on TSB agar plates to obtain a representative value of bacterial survival.

The capacity of M-C7.1 to reduce daptomycin MICs of *S. aureus* was analyzed by pretreatment of SA113 WT, SA113Δ*mprF*, and DAP-R CA-MRSA strain 703 with either PBS (1:10 diluted), control mAB L-1 (100 µg/ml), or M-C7.1 (100 µg/ml) in MHB, cultivation for 3 hr at 37°C under agitation. Subsequently, bacterial suspensions were adjusted to OD_{600} 0.05, and daptomycin MIC test strips (Liofilchem) were applied according to the manufacturer's advice.

To analyze the capacity of mAB M-C7.1 to inhibit *S. aureus* growth, overnight cultures of CA-MRSA strain USA300 grown in MHB medium were diluted to OD_{600} 0.01 with fresh MHB medium containing 1 µM of antibodies and 4 µg/ml nisin (Sigma-Aldrich) or PBS as a control in 96-well plates. Plates were incubated for 24 hr at 37°C under shaking conditions using a Bioscreen C (Oy Growth Curves Ab Ltd). Optical density at 600 nm was determined and compared to growth without nisin.

Determination of *in vitro* evolution of resistance to (combined daptomycin) M-C7.1 treatment in *S. aureus*

S. aureus USA300 was inoculated in a 48-well microtiter plate (Nunclon Delta surface, Thermo Scientific Nunc) with 500 µl MHB supplemented with 50 mg/l $CaCl_2$ at 37°C and shaking. It was combined with either (1) only subinhibitory concentrations of daptomycin (0.5 µg/ml), (2) the same daptomycin concentrations plus 10 nM or 100 nM M-C7.1, (3) only 10 nM or 100 nM M-C7.1 without daptomycin, or (4) no additional supplements. Cultures were passaged every 24 hr for 6 days in total. Control wells were included to check for sterility. To check for potential contaminations, 5 µl of each passage was streaked on Tryptic Soy Agar to detect single

colonies. To screen for potential mutations in *mprF* resulting from respective selection pressure, genomic DNA was isolated from each passage using NucleoSpin Microbial DNA Kit (Marchery-Nagel) according to the manufacturer's instructions. MprF was amplified with the primers MprF_USA300_fw and MprF_USA300_rev. Amplified mprF was sequenced by Sanger sequencing using primers MprF_USA300_fw, MprF_USA300_600, MprF_USA300_1200, MprF_USA300_1800, MprF_USA300_2200, MprF_USA300_800rev and MprF_USA300_rev by Eurofins Genomics Europe and analyzed for point mutations.

Isolation and quantification of polar lipids

S. aureus cultures (1 ml in MHB) were grown to the exponential phase (OD_{600} 1) in the presence of antibodies (final concentration: 100 µg/ml) as described above for the determination of susceptibility to antimicrobials. Polar lipids were extracted using the Bligh–Dyer method (Bligh and Dyer, 1959), with chloroform/methanol/sodium acetate buffer (20 mM) (1:1:1, by vol), vacuum-dried, and resuspended in chloroform/methanol (2:1, by vol). Extracts were filled into a 100 µl Hamilton syringe and spotted onto silica gel 60 F254 high-performance thin-layer chromatography plates (Merck) with a Linomat five sample application unit (Camag) and run in a developing chamber ADC 2 (Camag) with a running solution composed of chloroform–methanol–water (65:25:4, by vol). Phosphate group-containing lipids were detected by molybdenum blue staining and phospholipids were quantified in relation to total phospholipid content by determining lipid spot intensities densitometrically with ImageJ (http://rsbweb.nih.gov/ij/docs/guide/index.html) as described recently (Slavetinsky et al., 2012).

Determination of *S. aureus* cell surface charge

For analysis of the cytochrome C repulsion capacity of *S. aureus*, bacterial cells were grown in the presence of antibodies (100 µg/ml) as described above for the analysis of antimicrobial susceptibility. Bacteria were adjusted to OD_{600} 1 in 1 ml PBS, pelleted, resuspended in 100 µl 0.05 mg/ml cytochrome C (Sigma-Aldrich) followed by incubation at 37°C under shaking. The cells were then pelleted by centrifugation and absorption of the supernatant containing unbound cytochrome C was determined by measuring absorbance at 410 nm.

To determine annexin V binding to *S. aureus*, bacterial cells were grown in the presence of antibodies (100 µg/ml) as described above at 37°C with shaking for 3 hr, harvested, washed twice in PBS buffer, and resuspended in PBS containing $CaCl_2$ to OD_{600} 0.5 in 1 ml. Bacteria were gently mixed with 5 µl of allophycocyanin-labeled annexin V (Thermo Scientific) and incubated at room temperature for 15 min in the dark, as described recently (Ernst et al., 2018). At least 50,000 bacterial cells per antibody were analyzed by flow cytometry to quantify surface-bound fluorophore (FL-4).

Phagocytosis and killing of *S. aureus* by human (PMNs)

Human PMNs are the major human phagocytes to counteract bacterial infection and form the largest subgroup (~95%) of PMNs (Spaan et al., 2013). PMNs were isolated from fresh human blood of healthy volunteers by standard Ficoll/Histopaque gradient centrifugation as described recently (Hanzelmann et al., 2016). Cells were resuspended in Hanks' balanced salt solution (HBSS) containing 0.05% human serum albumin (HBSS-HSA; HBSS with 0.05% Albiomin, Biotest AG).

CA-MRSA strain USA300 was prepared for PMN experiments as described for the determination of susceptibility to antimicrobials, grown in the presence of antibodies (100 µg/ml) at 37°C under shaking for 3 hr, harvested, washed twice in HBSS, and adjusted to a density of 5×10^7 CFU/ml. Pooled serum from healthy human volunteers (blood bank of the University Hospital Tübingen) was added to a final concentration of 5% and bacteria were opsonized for 10 min at 37°C, as described recently (Peschel et al., 2001). Prewarmed bacteria and PMNs were mixed to final concentrations of 5×10^6 CFU/ml and 2.5×10^6 PMNs/ml in flat-bottom 96-well plates together with antibodies (final concentration 100 µg/ml). Samples of 50 µl were shaken at 37°C.

For analysis of the PMN killing capacity, incubation was stopped at different time points by the addition of 100-fold volumes of ice-cold distilled water to disrupt the PMNs. Triplets of appropriate sample volumes were spread on LB agar plates and colonies were counted after 24 hr incubation at 37°C. Numbers of live bacteria did not change during the 60 min incubation period in the absence of PMNs compared to the initial bacteria counts.

For phagocytosis studies, overnight cultures of bacteria were labeled with 0.1 mg/ml fluorescein- 5-isothiocyanate (FITC) at 37°C for 1 hr, as described previously (Peschel et al., 2001). After washing with PBS, the bacteria were resuspended in HBSS-HSA, adjusted to 5×10^6 CFU/ml, mixed with PMNs (2.5×10^6 PMNs/ml), and opsonized as described above (shaking at 37°C). Incubation was stopped by addition of 100 µl ice-cold 1% paraformaldehyde. The percentage of PMNs bearing FITC-labeled bacteria was determined by flow cytometric analysis of 20,000 cells.

Statistics

Statistical analyses were performed with the Prism 5.0 package (GraphPad Software) and group differences were analyzed for significance with the two-tailed Student’s t-test. A p value of ≤0.05 was considered statistically significant.

Acknowledgement

This work was financed by Grants from the Deutsche Forschungsgemeinschaft (DFG) (TRR34, SFB766, TRR156, TRR261, and GRK1708) to AP; and the German Center of Infection Research (DZIF) to AP. CJS was supported by the intramural Experimental Medicine

program of the Medical Faculty at the University of Tübingen and received grants from the DZIF and the DFG Cluster of Excellence EXC2124 'Controlling Microbes to Fight Infection' (CMFI). The authors acknowledge infrastructural support by the cluster of Excellence EXC2124 CMFI, project ID 390838134.

Additional information

Competing interests

Alexandra Kraus, Michael Tesar, Christoph M Ernst, Andreas Peschel: Antibodies disclosed in the manuscript are part of patent "Anti-staphylococcal antibodies" (US9873733B2/ EP2935324B1), assigned to the Universitaetsklinikum Tuebingen and MorphoSys AG. The authors have declared that no further conflict of interest exists. The other authors declare that no competing interests exist.

Funding

Funder	Grant reference number	Author
Deutsche Forschungsgemeinschaft	EXC-2124/project ID 390838134	Christoph J Slavetinsky Andreas Peschel
Deutsches Zentrum für Infektionsforschung	TTU 08.806	Andreas Peschel Christoph J Slavetinsky
Deutsche Forschungsgemeinschaft	SFB 766/1-3 TP A08	Andreas Peschel
Deutsche Forschungsgemeinschaft	TRR34	Andreas Peschel
Deutsche Forschungsgemeinschaft	TRR156	Andreas Peschel
Deutsche Forschungsgemeinschaft	TRR261	Andreas Peschel
Deutsche Forschungsgemeinschaft	GRK1708	Andreas Peschel
Universitätsklinikum Tübingen		Christoph J Slavetinsky
MorphoSys		Christoph M Ernst

Author contributions

Christoph J Slavetinsky, Conceptualization, Data curation, Formal analysis, Funding acquisition, Investigation, Methodology, Project administration, Supervision, Validation, Visualization, Writing – original draft, Writing – review and editing; Janna N Hauser, Formal analysis, Investigation, Methodology, Writing – review and editing; Cordula Gekeler, André Geyer, Doris Heilingbrunner, Investigation, Methodology; Jessica Slavetinsky, Investigation, Methodology, Visualization; Alexandra Kraus, Conceptualization, Data curation, Investigation, Methodology, Supervision, Writing – review and editing; Samuel Wagner, Concept and analysis of Blue-Native Western blotting, Conceptualization, Data curation, Methodology, Writing – review and editing; Michael Tesar, Conceptualization, Data curation, Methodology, Writing – review and editing; Bernhard Krismer, Investigation, Methodology, Writing – review

and editing; Sebastian Kuhn, Data curation, Methodology; Christoph M Ernst, Conceptualization, Data curation, Formal analysis, Investigation, Methodology, Project administration, Supervision, Validation, Writing – review and editing; Andreas Peschel, Conceptualization, Formal analysis, Funding acquisition, Project administration, Supervision, Writing – original draft, Writing – review and editing

References

- Årdal C, Balasegaram M, Laxminarayan R, McAdams D, Outterson K, Rex JH, Sumpradit N. 2020. Antibiotic development - economic, regulatory and societal challenges. Nature Reviews. Microbiology 18:267–274. DOI: https://doi.org/10.1038/s41579-019-0293-3, PMID: 31745330 Bae T, Schneewind O. 2006. Allelic replacement in Staphylococcus aureus with inducible counter-selection. Plasmid 55:58–63. DOI: https://doi.org/10.1016/j.plasmid.2005.05.005, PMID: 16051359
- Bayer AS, Schneider T, Sahl HG. 2013. Mechanisms of daptomycin resistance in Staphylococcus aureus: role of the cell membrane and cell wall. Annals of the New York Academy of Sciences 1277:139–158. DOI: https://doi. org/10.1111/j.1749-6632.2012.06819.x, PMID: 23215859
- Bligh EG, Dyer WJ. 1959. A rapid method of total lipid extraction and purification. Canadian Journal of Biochemistry and Physiology 37:911–917. DOI: https://doi.org/10.1139/o59-099, PMID: 13671378
- Bogdanov M, Zhang W, Xie J, Dowhan W. 2005. Transmembrane protein topology mapping by the substituted cysteine accessibility method (SCAM(TM)): application to lipid-specific membrane protein topogenesis. Methods 36:148–171. DOI: https://doi.org/10.1016/j.ymeth.2004.11.002, PMID: 15894490
- Dickey SW, Cheung GYC, Otto M. 2017. Different drugs for bad bugs: antivirulence strategies in the age of antibiotic resistance. Nature Reviews. Drug Discovery 16:457–471. DOI: https://doi.org/10.1038/nrd.2017.23, PMID: 28337021
- Ernst CM, Staubitz P, Mishra NN, Yang S-J, Hornig G, Kalbacher H, Bayer AS, Kraus D, Peschel A. 2009. The bacterial defensin resistance protein MprF consists of separable domains for lipid lysinylation and antimicrobial peptide repulsion. PLOS Pathogens 5:e1000660. DOI: https://doi.org/10.1371/journal.ppat.1000660, PMID: 19915718
- Ernst CM, Peschel A. 2011. Broad-spectrum antimicrobial peptide resistance by MprF-mediated aminoacylation and flipping of phospholipids. Molecular Microbiology 80:290–299. DOI: https://doi.org/10.1111/j.1365-2958. 2011.07576.x, PMID: 21306448

- Ernst CM, Kuhn S, Slavetinsky CJ, Krismer B, Heilbronner S, Gekeler C, Kraus D, Wagner S, Peschel A. 2015. The lipid-modifying multiple peptide resistance factor is an oligomer consisting of distinct interacting synthase and flippase subunits. MBio 6:e02340-14. DOI: https://doi.org/10.1128/mBio.02340-14, PMID: 25626904
- Ernst CM, Slavetinsky CJ, Kuhn S, Hauser JN, Nega M, Mishra NN, Gekeler C, Bayer AS, Peschel A. 2018. Gain-of-Function Mutations in the Phospholipid Flippase MprF Confer Specific Daptomycin Resistance. MBio 9:e01659-18. DOI: https://doi.org/10.1128/mBio.01659-18, PMID: 30563904
- Hanzelmann D, Joo H-S, Franz-Wachtel M, Hertlein T, Stevanovic S, Macek B, Wolz C, Götz F, Otto M, Kretschmer D, Peschel A. 2016. Toll-like receptor 2 activation depends on lipopeptide shedding by bacterial surfactants. Nature Communications 7:12304. DOI: https://doi.org/10.1038/ncomms12304, PMID: 27470911
- Ieronymaki M, Nuti F, Brancaccio D, Rossi G, Real-Fernández F, Cao Y, Monasson O, Larregola M, Peroni E, Uziel J, Sabatino G, Novellino E, Carotenuto A, Papini AM, Rovero P. 2017. Structure-Activity Relationship Studies, SPR Affinity Characterization, and Conformational Analysis of Peptides That Mimic the HNK-1 Carbohydrate Epitope. ChemMedChem 12:751–759. DOI: https://doi.org/10.1002/cmdc.201700042, PMID: 28403522
- Jones T, Yeaman MR, Sakoulas G, Yang S-J, Proctor RA, Sahl H-G, Schrenzel J, Xiong YQ, Bayer AS. 2008. Failures in clinical treatment of Staphylococcus aureus Infection with daptomycin are associated with alterations in surface charge, membrane phospholipid asymmetry, and drug binding. Antimicrobial Agents and Chemotherapy 52:269–278. DOI: https://doi.org/10.1128/AAC.00719-07, PMID: 17954690
- Kim HK, Thammavongsa V, Schneewind O, Missiakas D. 2012. Recurrent infections and immune evasion strategies of Staphylococcus aureus. Current Opinion in Microbiology 15:92–99. DOI: https://doi.org/10.1016/ j.mib.2011.10.012, PMID: 22088393
- Kristian SA, Dürr M, Van Strijp JAG, Neumeister B, Peschel A. 2003. MprF-mediated lysinylation of phospholipids in Staphylococcus aureus leads to protection against oxygen-independent neutrophil killing. Infection and Immunity 71:546–549. DOI: https://doi.org/10.1128/IAI.71.1.546-549.2003, PMID: 12496209
- Lakemeyer M, Zhao W, Mandl FA, Hammann P, Sieber SA. 2018. Thinking Outside the Box-Novel Antibacterials To Tackle the Resistance Crisis. Angewandte Chemie 57:14440–14475. DOI: https://doi.org/10.1002/anie.201804971, PMID: 29939462
- Lee AS, de Lencastre H, Garau J, Kluytmans J, Malhotra-Kumar S, Peschel A, Harbarth S. 2018. Methicillin- resistant Staphylococcus aureus. Nature Reviews.

Disease Primers 4:18033. DOI: https://doi.org/10.1038/nrdp. 2018.33, PMID: 29849094

- Lowy I, Molrine DC, Leav BA, Blair BM, Baxter R, Gerding DN, Nichol G, Thomas WD Jr, Leney M, Sloan S, Hay CA, Ambrosino DM. 2010. Treatment with monoclonal antibodies against Clostridium difficile toxins. The New England Journal of Medicine 362:197–205. DOI: https://doi.org/10.1056/NEJMoa0907635, PMID: 20089970
- Maloney E, Stankowska D, Zhang J, Fol M, Cheng Q-J, Lun S, Bishai WR, Rajagopalan M, Chatterjee D, Madiraju MV. 2009. The two-domain LysX protein of Mycobacterium tuberculosis is required for production of lysinylated phosphatidylglycerol and resistance to cationic antimicrobial peptides. PLOS Pathogens 5:e1000534. DOI: https://doi.org/10.1371/journal.ppat.1000534, PMID: 19649276
- Migone T-S, Subramanian GM, Zhong J, Healey LM, Corey A, Devalaraja M, Lo L, Ullrich S, Zimmerman J, Chen A, Lewis M, Meister G, Gillum K, Sanford D, Mott J, Bolmer SD. 2009. Raxibacumab for the treatment of inhalational anthrax. The New England Journal of Medicine 361:135–144. DOI: https://doi.org/10.1056/NEJMoa0810603, PMID: 19587338
- Mishra RPN, Mariotti P, Fiaschi L, Nosari S, Maccari S, Liberatori S, Fontana MR, Pezzicoli A, De Falco MG, Falugi F, Altindis E, Serruto D, Grandi G, Bagnoli F. 2012. Staphylococcus aureus FhuD2 is involved in the early phase of staphylococcal dissemination and generates protective immunity in mice. The Journal of Infectious Diseases 206:1041–1049. DOI: https://doi.org/10.1093/infdis/jis463, PMID: 22829645
- Missiakas D, Schneewind O. 2016. Staphylococcus aureus vaccines: Deviating from the carol. The Journal of Experimental Medicine 213:1645–1653. DOI: https://doi.org/10.1084/jem.20160569, PMID: 27526714
- Neuber T, Frese K, Jaehrling J, Jäger S, Daubert D, Felderer K, Linnemann M, Höhne A, Kaden S, Kölln J, Tiller T, Brocks B, Ostendorp R, Pabst S. 2014. Characterization and screening of IgG binding to the neonatal Fc receptor. MAbs 6:928–942. DOI: https://doi.org/10.4161/mabs.28744, PMID: 24802048
- Otto M. 2013. Community-associated MRSA: what makes them special? International Journal of Medical Microbiology 303:324–330. DOI: https://doi.org/10.1016/j.ijmm.2013.02.007, PMID: 23517691
- O'Brien MP, Forleo-Neto E, Musser BJ, Isa F, Chan K-C, Sarkar N, Bar KJ, Barnabas RV, Barouch DH, Cohen MS, Hurt CB, Burwen DR, Marovich MA, Hou P, Heirman I, Davis JD, Turner KC, Ramesh D, Mahmood A, Hooper AT, et al. 2021. Subcutaneous REGEN-COV Antibody Combination to Prevent Covid-19. The New England Journal of Medicine 385:1184–1195. DOI: https://doi.org/10.1056/NEJMoa2109682, PMID: 34347950

- Pasquina-Lemonche L, Burns J, Turner RD, Kumar S, Tank R, Mullin N, Wilson JS, Chakrabarti B, Bullough PA, Foster SJ, Hobbs JK. 2020. The architecture of the Gram-positive bacterial cell wall. Nature 582:294–297. DOI: https://doi.org/10.1038/s41586-020-2236-6, PMID: 32523118
- Peschel A, Otto M, Jack RW, Kalbacher H, Jung G, Götz F. 1999. Inactivation of the dlt operon in Staphylococcus aureus confers sensitivity to defensins, protegrins, and other antimicrobial peptides. The Journal of Biological Chemistry 274:8405–8410. DOI: https://doi.org/10.1074/jbc.274.13.8405, PMID: 10085071
- Peschel A, Jack RW, Otto M, Collins LV, Staubitz P, Nicholson G, Kalbacher H, Nieuwenhuizen WF, Jung G, Tarkowski A, van Kessel KP, van Strijp JA. 2001. Staphylococcus aureus resistance to human defensins and evasion of neutrophil killing via the novel virulence factor MprF is based on modification of membrane lipids with l-lysine. The Journal of Experimental Medicine 193:1067–1076. DOI: https://doi.org/10.1084/jem.193.9. 1067, PMID: 11342591
- Pinheiro da Silva F, Machado MCC. 2017. The dual role of cathelicidins in systemic inflammation. Immunology Letters 182:57–60. DOI: https://doi.org/10.1016/j.imlet.2017.01.004, PMID: 28082134
- Prassler J, Thiel S, Pracht C, Polzer A, Peters S, Bauer M, Nörenberg S, Stark Y, Kölln J, Popp A, Urlinger S, Enzelberger M. 2011. HuCAL PLATINUM, a synthetic Fab library optimized for sequence diversity and superior performance in mammalian expression systems. Journal of Molecular Biology 413:261–278. DOI: https://doi.org/10.1016/j.jmb.2011.08.012, PMID: 21856311
- Qu X, Tang Y, Hua S. 2018. Immunological Approaches Towards Cancer and Inflammation: A Cross Talk. Frontiers in Immunology 9:563. DOI: https://doi.org/10.3389/fimmu.2018.00563, PMID: 29662489
- Reichmann NT, Piçarra Cassona C, Monteiro JM, Bottomley AL, Corrigan RM, Foster SJ, Pinho MG, Gründling A. 2014. Differential localization of LTA synthesis proteins and their interaction with the cell division machinery in Staphylococcus aureus. Molecular Microbiology 92:273–286. DOI: https://doi.org/10.1111/mmi.12551, PMID: 24533796
- Roy H, Ibba M. 2009. Broad range amino acid specificity of RNA-dependent lipid remodeling by multiple peptide resistance factors. The Journal of Biological Chemistry 284:29677–29683. DOI: https://doi.org/10. 1074/jbc.M109.046367, PMID: 19734140
- Slavetinsky CJ, Peschel A, Ernst CM. 2012. Alanyl-phosphatidylglycerol and lysyl-phosphatidylglycerol are translocated by the same MprF flippases and have similar capacities to protect against the antibiotic daptomycin in Staphylococcus aureus.

Antimicrobial Agents and Chemotherapy 56:3492–3497. DOI: https:// doi.org/10.1128/AAC.00370-12, PMID: 22491694

- Slavetinsky C, Kuhn S, Peschel A. 2017. Bacterial aminoacyl phospholipids - Biosynthesis and role in basic cellular processes and pathogenicity. Biochimica et Biophysica Acta. Molecular and Cell Biology of Lipids 1862:1310–1318. DOI: https://doi.org/10.1016/j.bbalip.2016.11.013, PMID: 27940309
- Song D, Jiao H, Liu Z. 2021. Phospholipid translocation captured in a bifunctional membrane protein MprF. Nature Communications 12:2927. DOI: https://doi.org/10.1038/s41467-021-23248-z, PMID: 34006869
- Spaan AN, Surewaard BGJ, Nijland R, van Strijp JAG. 2013. Neutrophils versus Staphylococcus aureus: a biological tug of war. Annual Review of Microbiology 67:629–650. DOI: https://doi.org/10.1146/annurev-micro- 092412-155746, PMID: 23834243
- Tabor DE, Yu L, Mok H, Tkaczyk C, Sellman BR, Wu Y, Oganesyan V, Slidel T, Jafri H, McCarthy M, Bradford P, Esser MT. 2016. Staphylococcus aureus Alpha-Toxin Is Conserved among Diverse Hospital Respiratory Isolates Collected from a Global Surveillance Study and Is Neutralized by Monoclonal Antibody MEDI4893. Antimicrobial Agents and Chemotherapy 60:5312–5321. DOI: https://doi.org/10.1128/AAC.00357-16, PMID: 27324766
- Tacconelli E, Carrara E, Savoldi A, Harbarth S, Mendelson M, Monnet DL, Pulcini C, Kahlmeter G, Kluytmans J, Carmeli Y, Ouellette M, Outterson K, Patel J, Cavaleri M, Cox EM, Houchens CR, Grayson ML, Hansen P, Singh N, Theuretzbacher U, et al. 2018. Discovery, research, and development of new antibiotics: the WHO priority list of antibiotic-resistant bacteria and tuberculosis. The Lancet. Infectious Diseases 18:318–327. DOI: https://doi.org/10.1016/S1473-3099(17)30753-3, PMID: 29276051
- Thedieck K, Hain T, Mohamed W, Tindall BJ, Nimtz M, Chakraborty T, Wehland J, Jänsch L. 2006. The MprF protein is required for lysinylation of phospholipids in listerial membranes and confers resistance to cationic antimicrobial peptides (CAMPs) on Listeria monocytogenes. Molecular Microbiology 62:1325–1339. DOI: https://doi.org/10.1111/j.1365 2958.2006.05452.x, PMID: 17042784
- Tiller T, Schuster I, Deppe D, Siegers K, Strohner R, Herrmann T, Berenguer M, Poujol D, Stehle J, Stark Y, Heßling M, Daubert D, Felderer K, Kaden S, Kölln J, Enzelberger M, Urlinger S. 2013. A fully synthetic human Fab antibody library based on fixed VH/VL framework pairings with favorable biophysical properties. MAbs 5:445–470. DOI: https://doi.org/10.4161/mabs.24218, PMID: 23571156
- Wang R, Braughton KR, Kretschmer D, Bach T-HL, Queck SY, Li M, Kennedy AD, Dorward DW, Klebanoff SJ, Peschel A, DeLeo FR, Otto M. 2007. Identification of novel cytolytic peptides as key virulence determinants for community-associated MRSA.

Nature Medicine 13:1510–1514. DOI: https://doi.org/10.1038/nm1656, PMID: 17994102

- Weisman LE, Fischer GW, Thackray HM, Johnson KE, Schuman RF, Mandy GT, Stratton BE, Adams KM, Kramer WG, Mond JJ. 2009. Safety and pharmacokinetics of a chimerized anti-lipoteichoic acid monoclonal antibody in healthy adults. International Immunopharmacology 9:639–644. DOI: https://doi.org/10.1016/j. intimp.2009.02.008, PMID: 19268719
- Yachdav G, Kloppmann E, Kajan L, Hecht M, Goldberg T, Hamp T, Hönigschmid P, Schafferhans A, Roos M, Bernhofer M, Richter L, Ashkenazy H, Punta M, Schlessinger A, Bromberg Y, Schneider R, Vriend G, Sander C, Ben-Tal N, Rost B. 2014. PredictProtein--an open resource for online prediction of protein structural and functional features. Nucleic Acids Research 42:W337–W343. DOI: https://doi.org/10.1093/nar/gku366, PMID: 24799431
- Yount NY, Kupferwasser D, Spisni A, Dutz SM, Ramjan ZH, Sharma S, Waring AJ, Yeaman MR. 2009. Selective reciprocity in antimicrobial activity versus cytotoxicity of hBD-2 and crotamine. PNAS 106:14972–14977. DOI: https://doi.org/10.1073/pnas.0904465106, PMID: 19706485
- Zheng Y, Shang W, Peng H, Rao Y, Zhao X, Hu Z, Yang Y, Hu Q, Tan L, Xiong K, Li S, Zhu J, Hu X, Zhou R, Li M, Rao X. 2019. Virulence Determinants Are Required for Brain Abscess Formation Through Staphylococcus aureus Infection and Are Potential Targets of Antivirulence Factor Therapy. Frontiers in Microbiology 10:682. DOI: https://doi.org/10.3389/fmicb.2019.00682, PMID: 31024479

Supplemental Material

All data generated or analysed during this study are included in the manuscript and supporting files.

Supplementary file 1a: Antibodies.

Antibody	Antigen	Peptide sequence	Framework
M-C1	Cyclic peptide, loop TMS 1-2	ELSGINFKDTLVEFSKINR	VH3-23 kappa 3
M-C7.1	Cyclic peptide, loop TMS 7-8	LGFKTLGVPEEKV	VH1A kappa 1
M-C7.2	Cyclic peptide, loop TMS 7-8	LGFKTLGVPEEKV	VH3-23 kappa 1
M-C7.3	Cyclic peptide, loop TMS 7-8	LGFKTLGVPEEKV	VH1A kappa 1
M-C9.1	Cyclic peptide, loop TMS 9-10	DALYDGNHLT	VH1A kappa 1
M-C9.2	Cyclic peptide, loop TMS 9-10	DALYDGNHLT	VH3-23 kappa 1

M-C13.1	Cyclic peptide, loop TMS 13-14	DIYTIEMHTSVLR	VH1A kappa 1
M-C13.2	Cyclic peptide, loop TMS 13-14	DIYTIEMHTSVLR	VH1A kappa 1

Supplementary file 1b: Strains.

Strain name	**Characteristics**
S. aureus SA113 WT (ATCC 35556)	Restriction-deficient *S. aureus* strain derived from NCTC 8325 [1]
S. aureus SA113Δ*mprF*	*mprF* deletion mutant of SA113, gene replaced by erythromycin resistance cassette [2].
S. aureus SA113Δ*spa*	*spa* deletion mutant of SA113. Constructed in this study. Markerless.
S. aureus SA113Δ*spa*Δ*mprF*	*spa* and *mprF* double deletion mutant of SA113. Constructed in this study. Erm^r
S. aureus DAP-R MRSA 703	Daptomycin resistant clinical CA-MRSA isolate possessing a single point mutation in *mprF* (S295L) [3]
S. aureus USA300 LAC	CA-MRSA WT strain [4]
E. coli TG1	Strain for phage display usage [5]

Supplementary file 1c: Plasmids.

Plasmid	**Characteristics**	**Short name in figures**
pKOR1	*E. coli/S. aureus* shuttle vector to allow allelic replacement with inducible counter-selection in staphylococci [6]	-
pRB474	*E. coli/S. aureus* shuttle vector [7]	pRB
pRB474mprF	*mprF* cloned in *E. coli/S. aureus* shuttle vector pRB474 [2]	pRB-MprF
pRB474mprF-GFP	N-terminally GFP-tagged *mprF* cloned in *E. coli/S. aureus* shuttle vector pRB474 [8]	pRB-MprF-GFP
pRB474mprFdelCys flag	C-terminally FLAG®-tagged, cysteine codon-depleted *mprF* cloned in *E. coli/S. aureus* shuttle vector pRB474; constructed in this study	WT (-Cys)
pRB474mprFdelCys T263C flag	C-terminally FLAG®-tagged, cysteine codon-depleted *mprF* with artificial cysteine insertion cloned in *E. coli/S. aureus* shuttle vector pRB474; as indicated, each plasmid bears another amino	pRB-T263C
pRB474mprFdelCys A99C flag		pRB-A99C

pRB474mprFdelCys T480C flag	acid substituted against cysteine (T263C, A99C, or T480C)	pRB-T480C

Supplementary file 1d: Primers.

Primer	5' → 3' sequence	Usage
A99C fw	GCATTGAATTGTATTGTAGGTTTCGGTGG CTTTATTGGTGCAGGCG	Forward primer for construction of pRB-A99C by site-directed mutagenesis
A99C rev	CCGAAACCTACAATACAATTCAATGCATT GATGATATAACTTACTC	Reverse primer for construction of pRB-A99C by site-directed mutagenesis
T263C fw	GTTGTATTACTAGGATTTAAATGTTTAGGT GTCCCTGAGGAAAAAG	Forward primer for construction of pRB-T263C by site-directed mutagenesis
T263C rev	CTTTTTCCTCAGGGACACCTAAACATTTAA ATCCTAGTAATACAAC	Reverse primer for construction of pRB-T263C by site-directed mutagenesis
T480C fw	GGAACGTTATATGCATTAGATATTTATTGT ATTGAAATGCATACATCTGTATTGCG	Forward primer for construction of pRB-T480C by site-directed mutagenesis
T480C rev	CGCAATACAGATGTATGCATTTCAATACA ATAAATATCTAATGCATATAACGTTCC	Reverse primer for construction of pRB-T480C by site-directed mutagenesis
mprF C199+204S fw	TACTCTACTTTAGTGTCGTCTGTTGAATG GTTAGCAG	Primer for cysteine depletion of pRB474 encoded native *mprF* by site-directed mutagenesis
mprF C199+204S rev	AACAGACGACACTAAAGTAGAGTACAATC CTACAAAACG	
mprF C217A fw	TTCGCTGGTGTAATTGTTGACGC	
mprF C217A rev	ACCAGCGAAATATAATACAACTGC	
mprF C380A fw	GCTGCTTTATTACTTTTACTGAATGTAGTT GG	
mprF C380A rev	TAAAGCAGCACTAGTATGAATTGCC	
mprF C526S fw	GATAGCGAGGAGATTATTAATCAG	
mprF C526S rev	CTCGCTATCTTCAATTTTAGAAG	
mprF C717S fw	GTAATTGCATTTAGTAGTTTAATGCCAACA TACTTTAATGATG	
mprF C717S rev	CTACTAAATGCAATTACTTCATTTTCTTCA TTTCGCATTACACC	

Spa-del_attB1	GGGGACAAGTTTGTACAAAAAAGCAGGCCAATATTCCATGGTCCAGAACT	Construction of a markerless *spa* knockout mutant using the pKOR1 vector system [6]
Spa-del	GTCGAGATCTATAAAAACAAACAATACACAACG	
Spa-del_attB2	GGGGACCACTTTGTACAAGAAAGCTGGGATCAGCAAGAAAACACACTTCC	
Spa-del rev	AAAAGATCTAACGAATTATGTATTGCAATA	
MprF_USA300_fw	CAGATATCAATATGACAAAAG	Amplification of *mprF* in USA300
MprF_USA300_rev	CTTAAATATTCTTATCTGTACC	Amplification of *mprF* in USA300
MprF_USA300_600	GTCATTTTTCTTACCATTATTC	Sequencing of *mprF* in USA300
MprF_USA300_1200	GTGCTTGTTTATTACTTTTAC	Sequencing of *mprF* in USA300
MprF_USA300_1800	GTTAGGTGATGAAAATGCC	Sequencing of *mprF* in USA300
MprF_USA300_2200	GATGGTTGCCAGAGTTAG	Sequencing of *mprF* in USA300
MprF_USA300_800rev	CTTCTTAGCTGATGTACC	Sequencing of *mprF* in USA300

1. Iordanescu, S. and M. Surdeanu, *Two restriction and modification systems in Staphylococcus aureus NCTC8325.* J Gen Microbiol, 1976. **96**(2): p. 277-81.
2. Peschel, A., et al., *Staphylococcus aureus resistance to human defensins and evasion of neutrophil killing via the novel virulence factor MprF is based on modification of membrane lipids with l-lysine.* J Exp Med, 2001. **193**(9): p. 1067-76.
3. Jones, T., et al., *Failures in clinical treatment of Staphylococcus aureus Infection with daptomycin are associated with alterations in surface charge, membrane phospholipid asymmetry, and drug binding.* Antimicrob Agents Chemother, 2008. **52**(1): p. 269-78.
4. Wang, R., et al., *Identification of novel cytolytic peptides as key virulence determinants for community-associated MRSA.* Nat Med, 2007. **13**(12): p. 1510-4.
5. Prassler, J., et al., *HuCAL PLATINUM, a synthetic Fab library optimized for sequence diversity and superior performance in mammalian expression systems.* J Mol Biol, 2011. **413**(1): p. 261-78.
6. Bae, T. and O. Schneewind, *Allelic replacement in Staphylococcus aureus with inducible counter-selection.* Plasmid, 2006. **55**(1): p. 58-63.
7. Bruckner, R., *A series of shuttle vectors for Bacillus subtilis and Escherichia coli.* Gene, 1992. **122**(1): p. 187-92.
8. Ernst, C.M., et al., *The lipid-modifying multiple peptide resistance factor is an oligomer consisting of distinct interacting synthase and flippase subunits.* MBio, 2015. **6**(1).

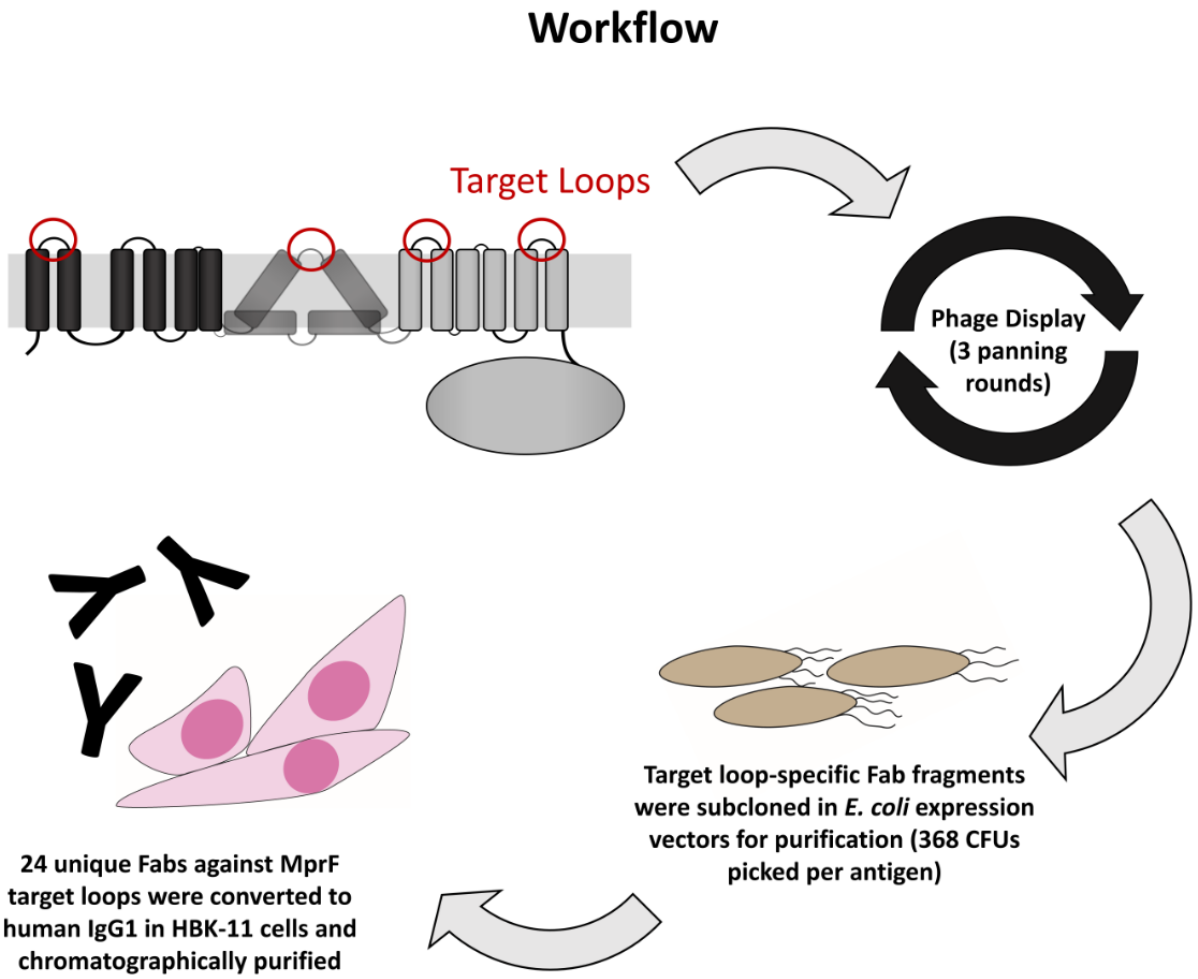

Figure 1 - figure supplement 1: Workflow for the development of multiple peptide resistance factor (MprF)-specific monoclonal antibodies (mABs). Biotinylated MprF peptide loops were incubated with the HuCal phage display library expressing single-chain human Fab fragments (Prassler et al., 2011), antigen-binding phages were enriched in three iterative panning rounds, bound antigen-specific phages were isolated, and respective Fab fragments were subcloned in *E. coli* expression vectors to yield His-tagged Fab fragments. Twenty-four unique Fabs against 4 MprF-derived peptides were converted to human IgG by cloning in an IgG1 expression vector system for production in human HKB11 cells, and IgGs were purified via protein A chromatography

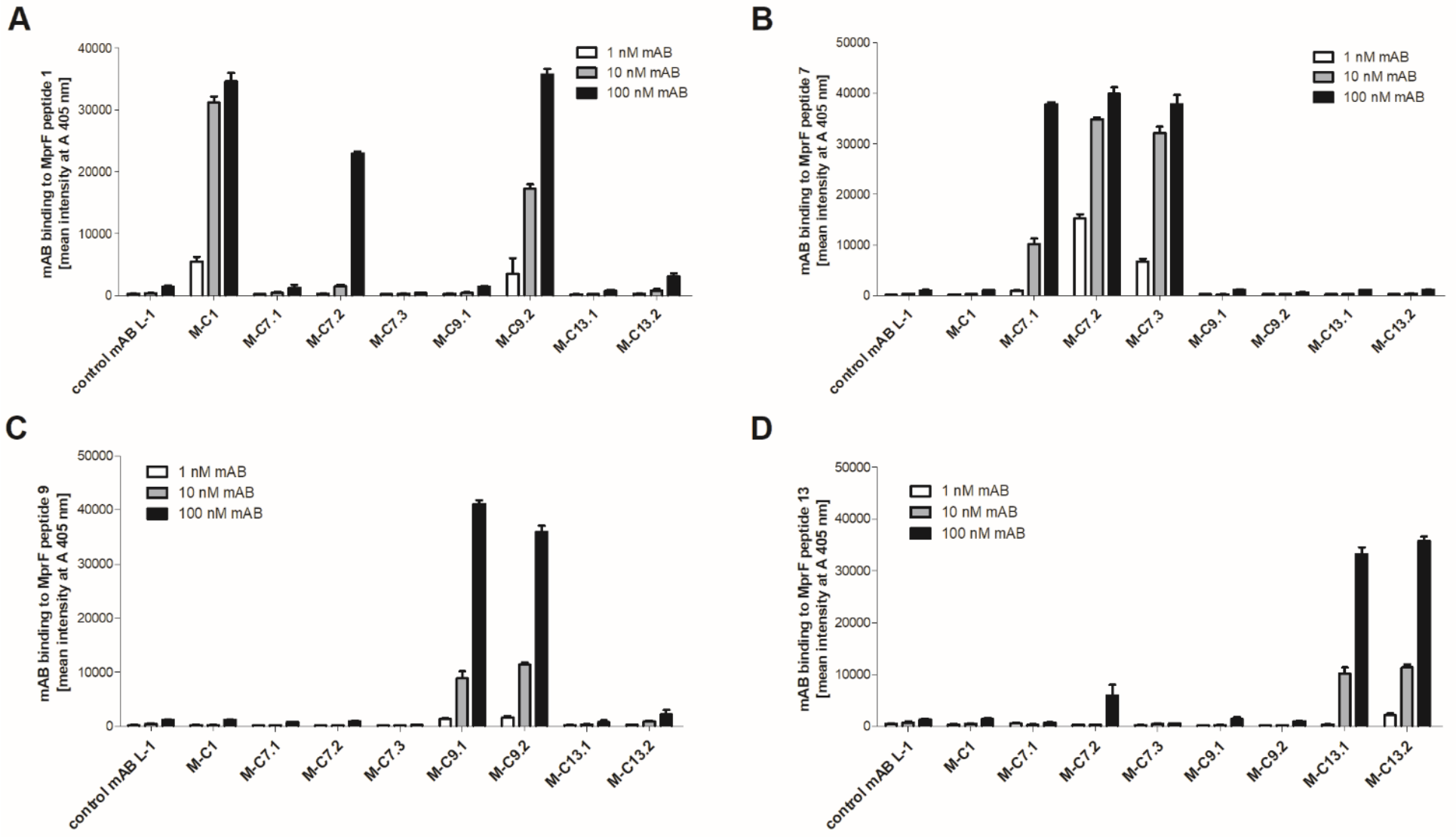
A
mAB binding to MprF peptide 1 [mean intensity at A 405 nm]
40000
30000
20000
10000
0
1 nM mAB
10 nM mAB
100 nM mAB
control mAB L-1
M-C1
M-C7.1
M-C7.2
M-C7.3
M-C9.1
M-C9.2
M-C13.1
M-C13.2
B
mAB binding to MprF peptide 7 [mean intensity at A 405 nm]
50000
40000
30000
20000
10000
0
1 nM mAB
10 nM mAB
100 nM mAB
control mAB L-1
M-C1
M-C7.1
M-C7.2
M-C7.3
M-C9.1
M-C9.2
M-C13.1
M-C13.2
C
mAB binding to MprF peptide 9 [mean intensity at A 405 nm]
50000
40000
30000
20000
10000
0
1 nM mAB
10 nM mAB
100 nM mAB
control mAB L-1
M-C1
M-C7.1
M-C7.2
M-C7.3
M-C9.1
M-C9.2
M-C13.1
M-C13.2
D
mAB binding to MprF peptide 13 [mean intensity at A 405 nm]
50000
40000
30000
20000
10000
0
1 nM mAB
10 nM mAB
100 nM mAB
control mAB L-1
M-C1
M-C7.1
M-C7.2
M-C7.3
M-C9.1
M-C9.2
M-C13.1
M-C13.2

Figure 1 – figure supplement 2: Specific binding of selected monoclonal antibodies (mABs) to cyclic multiple peptide resistance factor (MprF)-derived target peptides analyzed by ELISA. Biotinylated cyclic peptides corresponding to the MprF loops 1, 7, 9, or 13 were incubated with eight anti-MprF IgGs or the control mAB L-1 in phosphate-buffered saline (PBS). (A–D) show binding of mABs at increasing concentrations to cyclic MprF loops 1, 7, 9, and 13, respectively. The means and standard error of the mean (SEM) of mean intensity measured at A 405 nm in three biological replicates are shown.

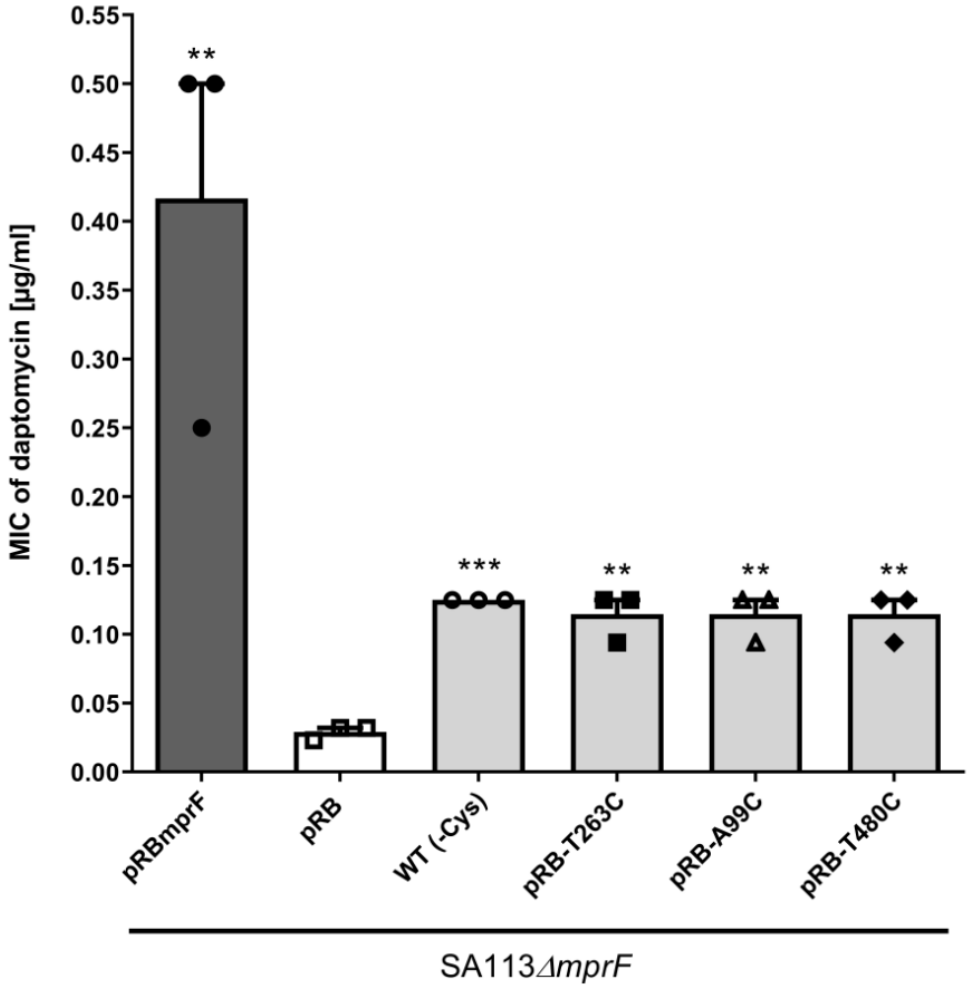

Figure 2 – figure supplement 1: Effects of cysteine replacement and insertion on multiple peptide resistance factor (MprF) function, assessed by measuring daptomycin susceptibility. Minimal inhibitory concentrations (MICs) of daptomycin against the indicated *S. aureus* strains are shown. The *mprF* deletion mutant with empty pRB474 plasmid served as a negative control, whereas cysteine depleted *mprF*-expressing variants show a fourfold increased daptomycin MIC while wild-type *mprF*-expressing positive control shows a tenfold increased MIC. The means + standard error of the mean (SEM) of results from three independent experiments are shown. Values that are significantly different from the values determined for *S. aureus* SA113Δ*mprF* bearing pRB474 (pRB), calculated by Student's paired t-test, as indicated (**p < 0.01; ***p < 0.0001).

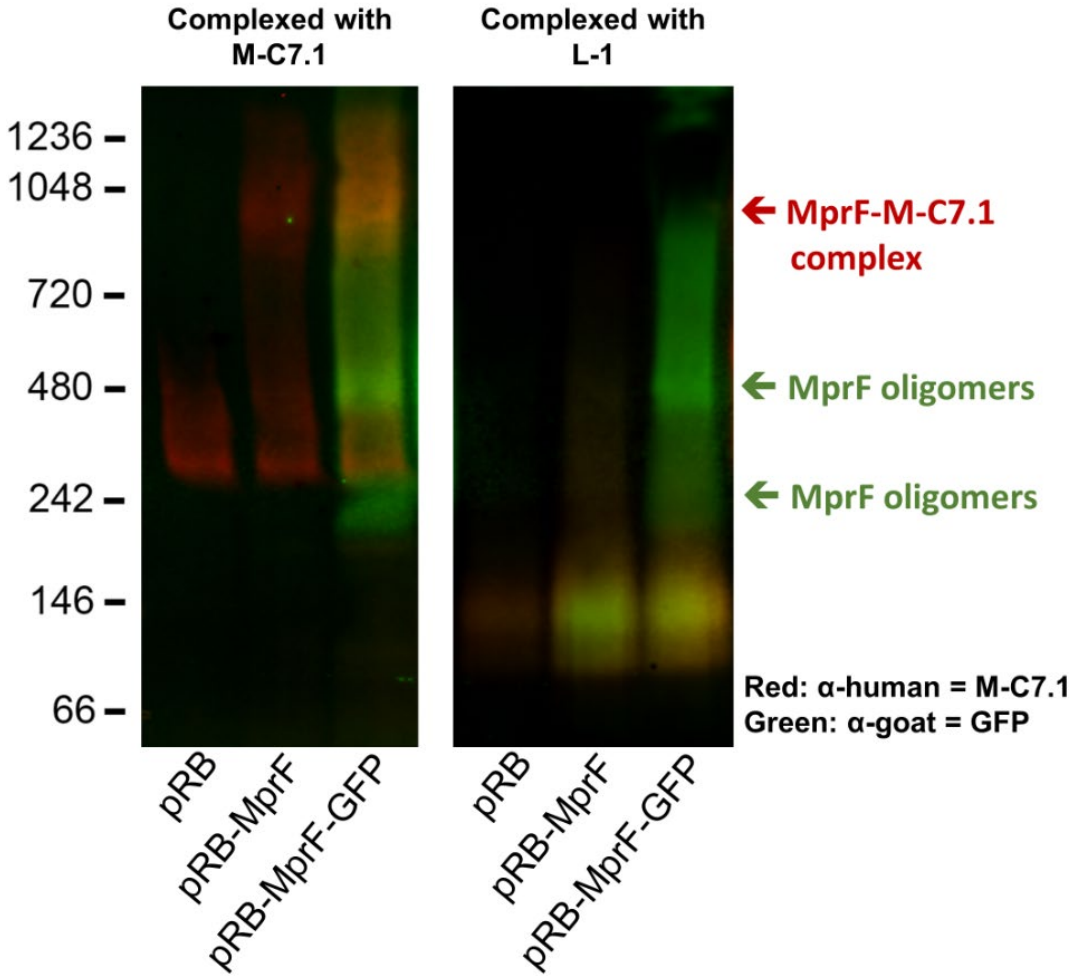

Figure 2 – figure supplement 2: Detection of M-C7.1 binding to multiple peptide resistance factor (MprF). An overlay of single channels from Figure 2A showing antihuman IgG binding to M-C7.1 in red and an antigoat IgG binding to the primary anti-GFP IgG in green. SA113Δ*spa*Δ*mprF* expressing the empty vector (pRB) served as negative control. Molecular masses in kDa of marker proteins are given on the left of the blot. Arrows mark the MprF–M-C7.1 complex at 900 kDa and the MprF oligomers at 250 and 500 kDa as previously described (Ernst et al., 2015). Further explanations are found in figure legend of Figure 2A.

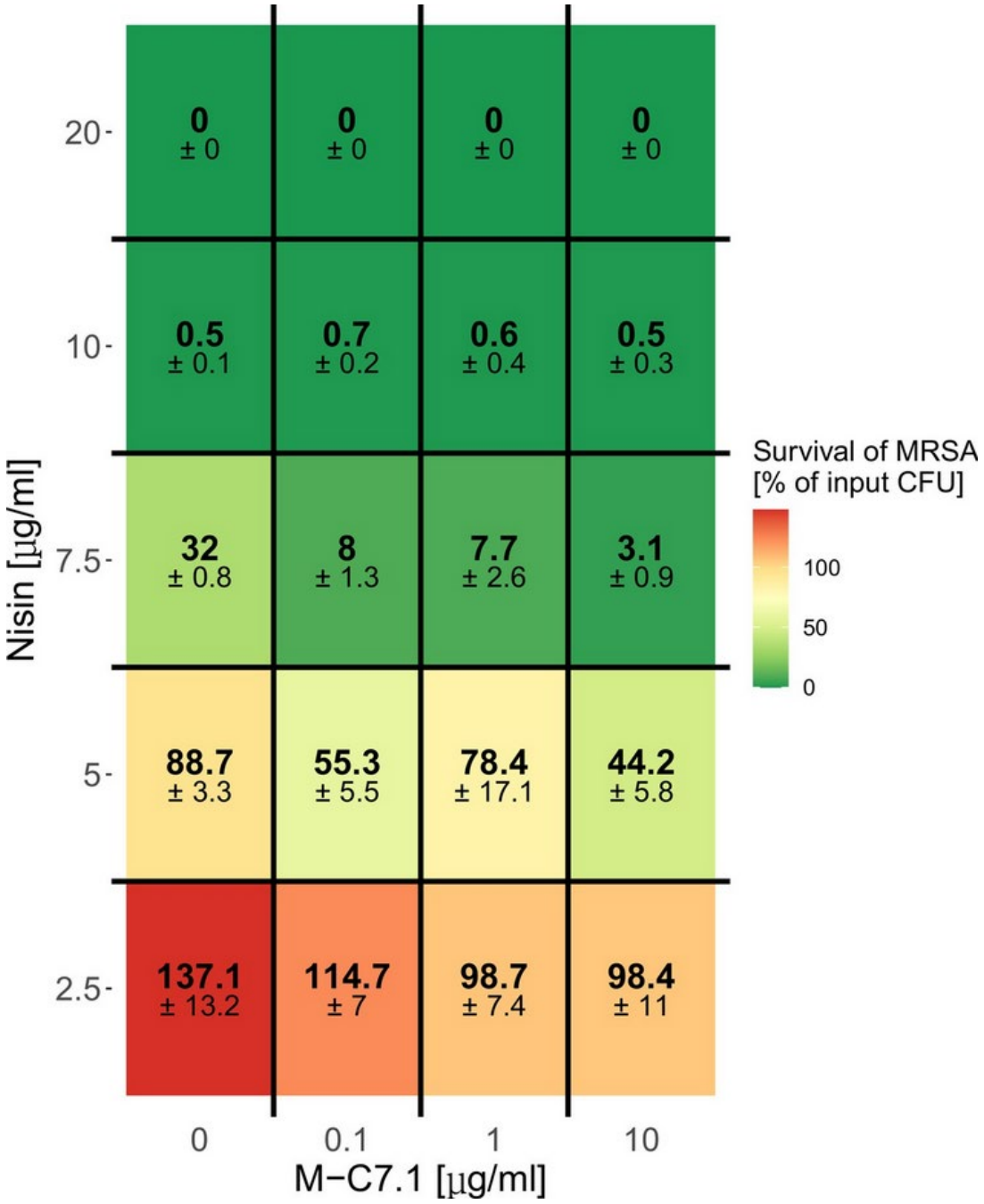

Figure 3 – figure supplement 1: Dose-dependent support of M-C7.1 of *S. aureus* killing by nisin. Survival of *S. aureus* USA300 in the presence of increasing concentrations of nisin and increasing concentrations of M-C7.1. Surviving colony-forming units (CFUs) of samples were analyzed after 2 hr incubation ('killing'), the control CFU (0 µg/ml nisin) ('input') was set to 100%. Percentages of surviving CFUs are indicated and underlaid with a color scale. The means + standard error of the mean (SEM) of results from three independent experiments are shown.

Chapter 4

Prokaryotic phospholipid translocation by ubiquitous PplT domain proteins

Janna N. Hauser[1,2,3], Arnaud Kengmo Tchoupa[1,2,3], Susanne Zabel[4], Kay Nieselt[3,4], Christoph M. Ernst[1,5], Christoph J. Slavetinsky[1,2,3,6#], Andreas Peschel[1,2,3#]

[1]Interfaculty Institute of Microbiology and Infection Medicine Tübingen, Infection Biology Section, University of Tübingen, Germany.
[2]German Center for Infection Research (DZIF), partner site Tübingen, Germany.
[3]Cluster of Excellence EXC2124 Controlling Microbes to Fight Infection, University of Tübingen, Germany
[4]Institute for Bioinformatics and Medical Informatics, University of Tübingen, Germany
[5]Current address: Department of Molecular Biology, Massachusetts General Hospital, Harvard Medical School, Boston, MA, USA
[6]Pediatric Surgery and Urology, University Children's Hospital Tübingen, University of Tübingen, Germany.
[#]Equally contributing corresponding authors.
Correspondence to: Christoph J. Slavetinsky and Andreas Peschel, Interfaculty Institute of Microbiology and Infection Medicine, Infection Biology Section, University of Tübingen, Auf der Morgenstelle 28, 72076 Tübingen, Germany

Preprint: bioRxiv. 2022:2022.03.11.483950. doi: 10.1101/2022.03.11.483950

Abstract

Flippase proteins exchanging phospholipids between the cytoplasmic membrane leaflets have been identified in Eukaryotes but remained largely unknown in Prokaryotes. Only MprF proteins that synthesize aminoacyl phospholipids in some bacteria have been found to contain a domain that translocates the produced lipids. We show here that this domain, which we named 'prokaryotic phospholipid translocator' (PplT), is widespread in Bacteria and Archaea, encoded as a separate protein or fused to different types of enzymes. We also demonstrate that the *Escherichia coli* PplT protein interacts with many phospholipid-synthetic enzymes and deletion of pplT impaired bacterial growth and membrane fluidity. Thus, PplT domain proteins appear to be general prokaryotic lipid flippases with critical roles in cellular homeostasis.

Introduction

Most of the basic processes and enzyme systems involved in growth and maintenance of prokaryotic cells have been explored in the past. Major mechanisms of membrane lipid synthesis and turnover have also been described thoroughly [1, 2]. However, 'flippase' proteins that facilitate the translocation of phospholipids from the inner leaflet, the site of synthesis, to the outer leaflet of the cytoplasmic membrane, have remained largely unknown. We speculated that such flippases might be among the conserved membrane proteins of unknown function found in many prokaryotic taxa. Phospholipid flippases may not be essential for cell viability, which might explain why they have not been identified in previous screening approaches for prokaryotic proteins with crucial function for cellular integrity. Flippases have been characterized in eukaryotic cells [3] but the responsible proteins do not seem to have obvious homologs in prokaryotes.

Flippase reactions are particularly difficult to study because the flipping process is fast and hard to monitor as the lipids remain in place and adapt only their orientation. Nevertheless, a prototype flippase has been identified in prokaryotic MprF proteins that synthesize and then translocate aminoacyl phosphatidylglycerol (Aa-PG) lipids such as lysyl-phosphatidylglycerol (Lys-PG) or alanyl-phosphatidylglycerol (Ala-PG) [4, 5]. Those lipids reduce the negative net charge at the outer surface of cytoplasmic membranes, thereby diminishing the binding of cationic antimicrobial molecules such as bacterial bacteriocin and host defensin peptides [6]. To achieve protection against such molecules, it is critical for microorganisms to efficiently translocate Lys-PG or Ala-PG, once these lipids have been formed by the MprF synthase domain at the inner surface of the cytoplasmic membrane. The synthase domain cooperates with the flippase domain in a dynamic fashion to deliver the lipid products to the translocation channel [7]. The two domains function together even if expressed as separate proteins [8]. The flippase domain of MprF consists of eight transmembrane sections [8] and contains a motif

that is accessible from both sides of the cytoplasmic membrane [9]. It has been proposed that this part moves during the lipid translocation process or that it is in the center between two larger cavities that form the lipid translocation channel [9]. The structure of the *Rhizobium tropici* MprF protein with bound Lys-PG molecules captured in the process of translocation has recently been elucidated by cryo-electron microscopy [7]. It gives rise to a mechanistic model that proposes a process with Lys-PG entering an inner protein cavity, which transiently opens a gate to an outer cavity, from which Lys-PG is subsequent released to the outer membrane leaflet [7]. The extent to which the flippase domain found in MprF proteins is present in Bacteria and Archaea, and if it may play a more general role in phospholipid translocation, has remained unknown.

The flippase domain of MprF proteins exhibits a conserved architecture with low sequence identity. It is referred to as cl04219, pfam03706, or UPF0104 in the NCBI Conserved Domain Database (CDD) [10] and as IPR022791 in the InterPro protein signatures database [11]. We show here that proteins consisting of this domain alone or in combination with various enzymatic domains are found in almost all of the major groups of Bacteria and Archaea, most likely to accomplish the translocation of membrane lipids. The corresponding *Escherichia coli* protein interacts with most of the phospholipid-biosynthetic enzymes and it is encoded in the vicinity of a cardiolipin (CL) synthase. Its inactivation is not lethal but affects membrane fluidity and the fitness of *E. coli*. We suggest naming the corresponding flippase domain 'prokaryotic phospholipid translocator' (PplT), which is likely to fulfill a general membrane homeostatic function in prokaryotes.

Results

PplT domain proteins are widespread in most groups of prokaryotes. MprF-related proteins are found in many different bacterial taxa [12]. Notably, we found that the two functional domains of MprF occur in different combinations. The Lys-PG synthase domain, for instance, occurs sometimes without the Lys-PG flippase domain [12]. On the other hand, the flippase domain is often encoded without a Lys-PG synthase or in combination with other enzymatic domains. Systematic evaluation of microbial genomes for the presence of this domain, referred to as PplT (cl04219), revealed an almost universal occurrence in most phyla of Bacteria (Fig. 1A) and in several Classes of Archaea (Fig. 1B). Indeed, blastp searches uncovered that the PplT domain is even found in bacterial species, which do not produce Aa-PGs, such as *E. coli* and many other Enterobacteriaceae [13, 14]. Thus, PplT may have a broader role in prokaryotes than previously thought. It should be noted that most prokaryotes with a *pplT* homolog encode only one protein with a PplT domain in their genome (Fig. S1).

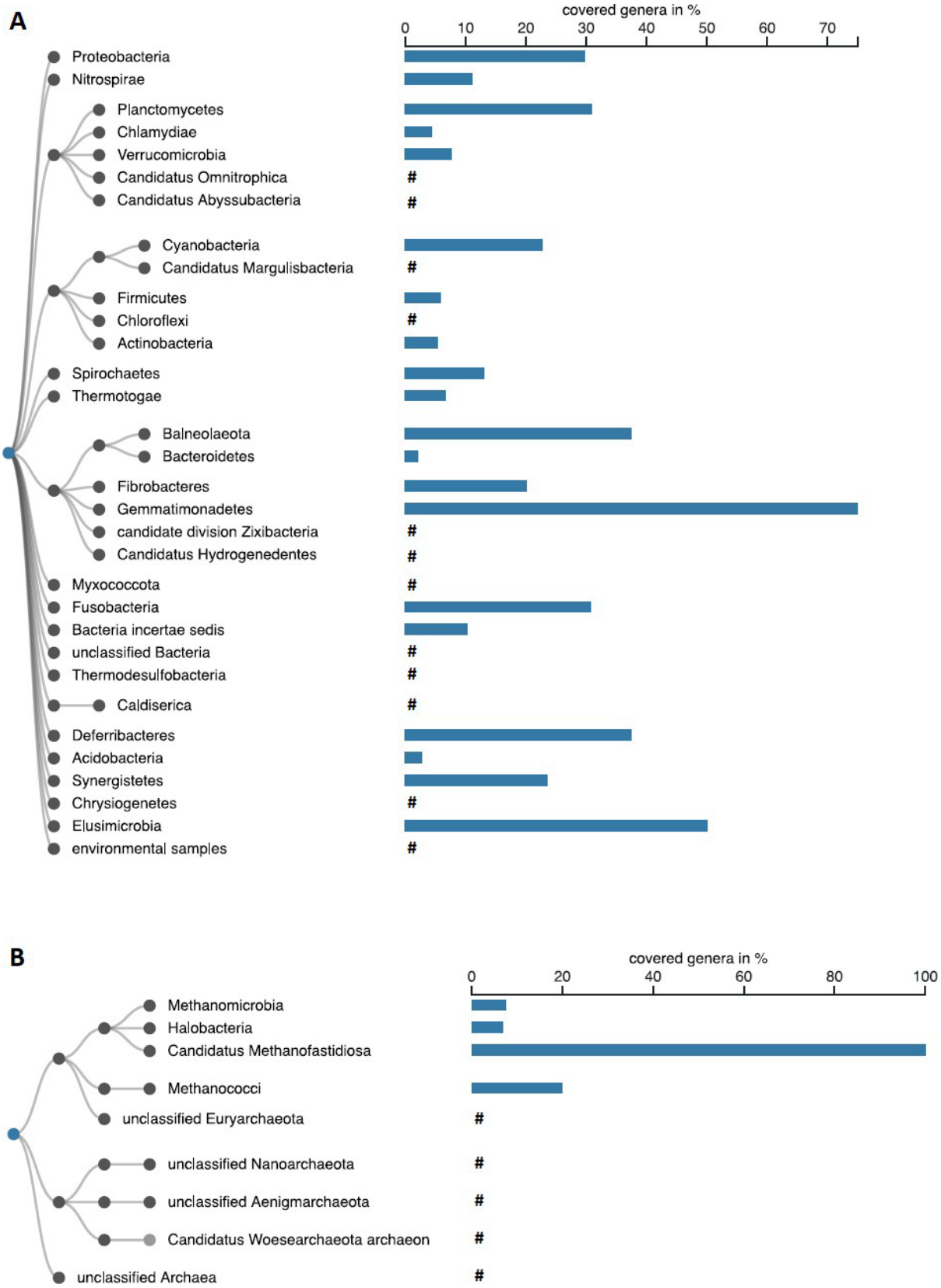

Figure 1: Distribution of the PpIT domain amongst taxa of the Bacteria (A) and Archaea (B) superkingdoms. The taxonomy was collapsed to the phylum rank. Dark grey leaf nodes indicate collapsed nodes. The bar chart indicates the fraction of genera of a particular Phylum (Bacteria) or Class (Archaea) carrying a PpIT homolog within the subtree rooted at the respective taxon. #, taxa include pplT genes but percentages of covered genera could not be calculated due to incomplete assignment of the genome on genus level.

PplT occurs as a separate protein in many different bacterial phyla including Proteobacteria, Actinobacteria, Firmicutes, Bacteroidetes, Planctomycetes, and Thermotogae as well as archaeal phyla including Euryarchaeota and Crenarchaeota. Moreover, PplT is found connected to other types of proteins in addition to Lys-PG or Ala-PG synthases (Fig. 2). The Conserved Domain Architecture Retrieval Tool [15] lists 148 different architectures of PplT domain-containing proteins. The most prevalent architectures include combinations with Aa-PG synthase domain (cl41273) of MprF proteins, glycosyl transferase domains (family A, cl11394; or family B, cl10013), or protein kinase domains (cl21453) (Fig. 2). MprF proteins were most often found in genomes of Cyanobacteria, Actinobacteria, Firmicutes, and Proteobacteria. A C-terminal or N-terminal family-B glycosyltransferase domain was found attached to PplT proteins from Actinobacteria, Nitrospirae, and Chloroflexi or Acidobacteria, respectively, while a family-A glycosyltransferase domain was found at the N-terminus of PplT in Archaea of the Euryarchaeota phylum. Several Actinobacteria encode a protein kinase domain, N-terminally fused to PplT. Further, less frequently occurring combinations were found with enzymatic domains such as dehalogenase-like hydrolases (cl21460), O-antigen ligases (cl04850), S-adenosylmethionine-dependent methyltransferase (cl17173), or phosphotransferases (cl37506), to name a few (Fig. 2). These findings suggest that PplT-containing proteins may have multiple roles, presumably in the synthesis, modification, and translocation of different types of membrane lipids or in membrane-linked signal transduction processes. In several bacterial and archaeal taxa, only a minority of the genera appear to encode PplT proteins in their genomes (Fig. 1) suggesting that PplT proteins may be important only in certain habitats or that some bacteria may use other transport systems, that could translocate phospholipids along with other types of cargo molecules.

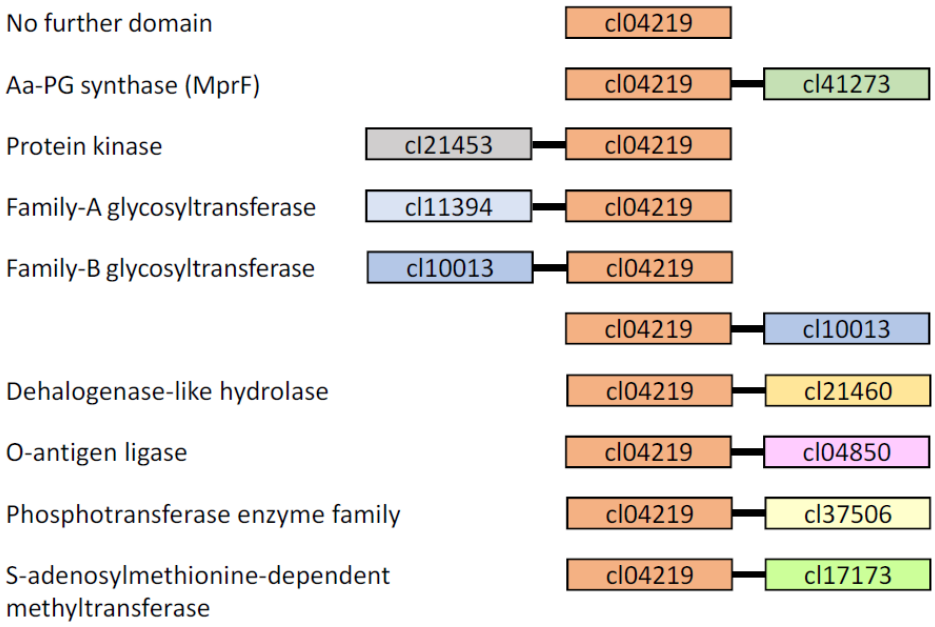

Figure 2: PplT domain protein architectures. Combinations of the PplT domain (cl04219) with other protein domains found in Bacteria and Archaea. The 10 most commonly occurring domain combinations are shown, as revealed by the Conserved Domain Architecture Retrieval Tool [15]. The domains are not drawn to scale.

The *E. coli* PplT is encoded together and interacts with lipid-synthetic enzymes. In order to study potential functions of PplT proteins not linked to other protein domains, we focused on the *E. coli* homolog, a protein of unknown function with the generic name YbhN, we suggest to rename PplT. *pplT* is not essential in *E. coli*, mutations in this gene are included in the Keio collection, a transposon mutant library [16], albeit without a reported phenotype. *pplT* is encoded in an operon together with the CL synthase gene *clsB* in *E. coli* and other Enterobacteriaceae including the genera *Shigella*, *Klebsiella* and *Pantoea* (Fig. 3A), which is in agreement with the role of PplT in lipid synthesis and translocation.

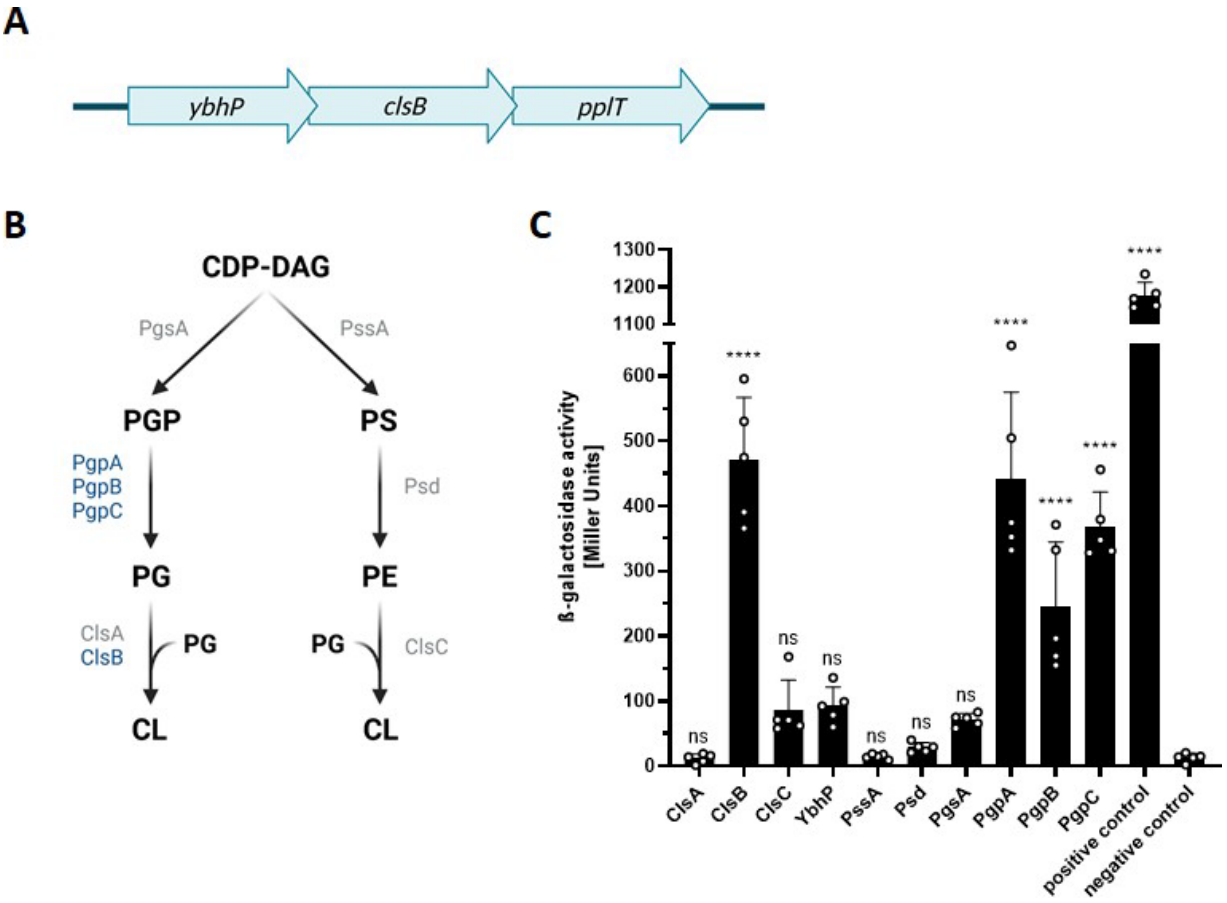

Figure 3: Genetic context and interaction partners of PplT in *E. coli*. (A) PplT is encoded in an operon together with YbhP, a protein of unknown function, and the cardiolipin synthase ClsB in Enterobacteriaceae, including the genera *Escherichia*, *Shigella*, *Klebsiella*, and *Pantoea*. The genes of the operon are not drawn to scale. (B) Schematic representation of the phospholipid synthesis pathways in *E. coli*. Cytidine diphosphate diacylglycerol (CDP-DAG), phosphatidylglycerol-3-phosphate (PGP), phosphatidylglycerol (PG), cardiolipin (CL), phosphatidylserine (PS), phosphatidylethanolamine (PE). Enzymes are marked in blue or grey, if they interacted with PplT or not, respectively. (C) Interaction studies with PplT and lipid-biosynthetic enzymes using the bacterial two-hybrid system and β-galactosidase assay for quantification. Data represent means plus SD of five biological replicates. Statistical significances were determined by two-way ANOVA followed by Dunnett's test in comparison to the negative control (ns, not significant; ****, P < 0.0001). Figures A and B were created with BioRender.com.

Phospholipid-biosynthetic proteins have been found to form large multicomponent complexes in bacteria such as *S. aureus* [17, 18]. To analyze a role of PplT in such complexes, its potential interaction with several phospholipid-biosynthetic proteins was studied in the bacterial two-hybrid system [8, 19, 20]. The genes to be analyzed were cloned in *E. coli* expression plasmids, resulting in C-and N-terminal fusions of potential interaction partners or PplT with the

complementary adenylate cyclase fragment T18 or T25, respectively. Interaction of T18 with T25 results in the production of cAMP, leading to expression of β-galactosidase, which was quantified. *E. coli* does not produce aminoacyl phospholipids but, in addition to phosphatidylglycerol (PG) and CL, phosphatidylserine (PS) and phosphatidylethanolamine (PE) [2]. PplT was found to interact with the proteins PgpA, PgpB, and PgpC, involved in PG synthesis and with the CL synthase ClsB, encoded in the same operon as PplT (Fig. 3A, B, C). Hence, PplT interacts with the majority of PG and CL biosynthetic enzymes in *E. coli* (Fig. 3C), which supports a role of PplT in phospholipid metabolism.

PplT shapes *E. coli* membrane fluidity and fitness. Although *pplT* is not essential in *E. coli*, its ubiquitous presence in most of the prokaryotic taxa suggests an important role in basic cellular functions. *pplT* was deleted in the uropathogenic *E. coli* (UPEC) strain CFT073. The mutant had the same phospholipid pattern as the wild type (WT) indicating that PplT has no obvious impact on the overall lipid composition (Fig. 4A, B). However, the mutant showed a significant increase in membrane fluidity compared to that of the WT strain, as analyzed by monitoring changes in fluorescence polarization of bacteria stained with 1,6-diphenyl-1,3,5-hexatriene (DPH) (Fig. 4C) [21, 22]. This finding supports the notion that PplT contributes to membrane homeostasis. The phenotype could be reverted back to WT level by complementation with a plasmid-encoded *pplT* copy (Fig. 4C). The *pplT* mutant also exhibited a growth defect compared with the WT in the late logarithmic phase and it did not reach the cell density of WT cultures (Fig. 5). This phenotype was pronounced at 37°C (Fig. 5A) but not observed at 42°C (Fig. 5B), which agrees with a role of PplT in membrane fluidity, a process that depends on temperature. When co-cultivated over several days, the WT grew better than the *pplT* mutant (Fig. 5C, D), demonstrating a competitive fitness benefit conferred by PplT.

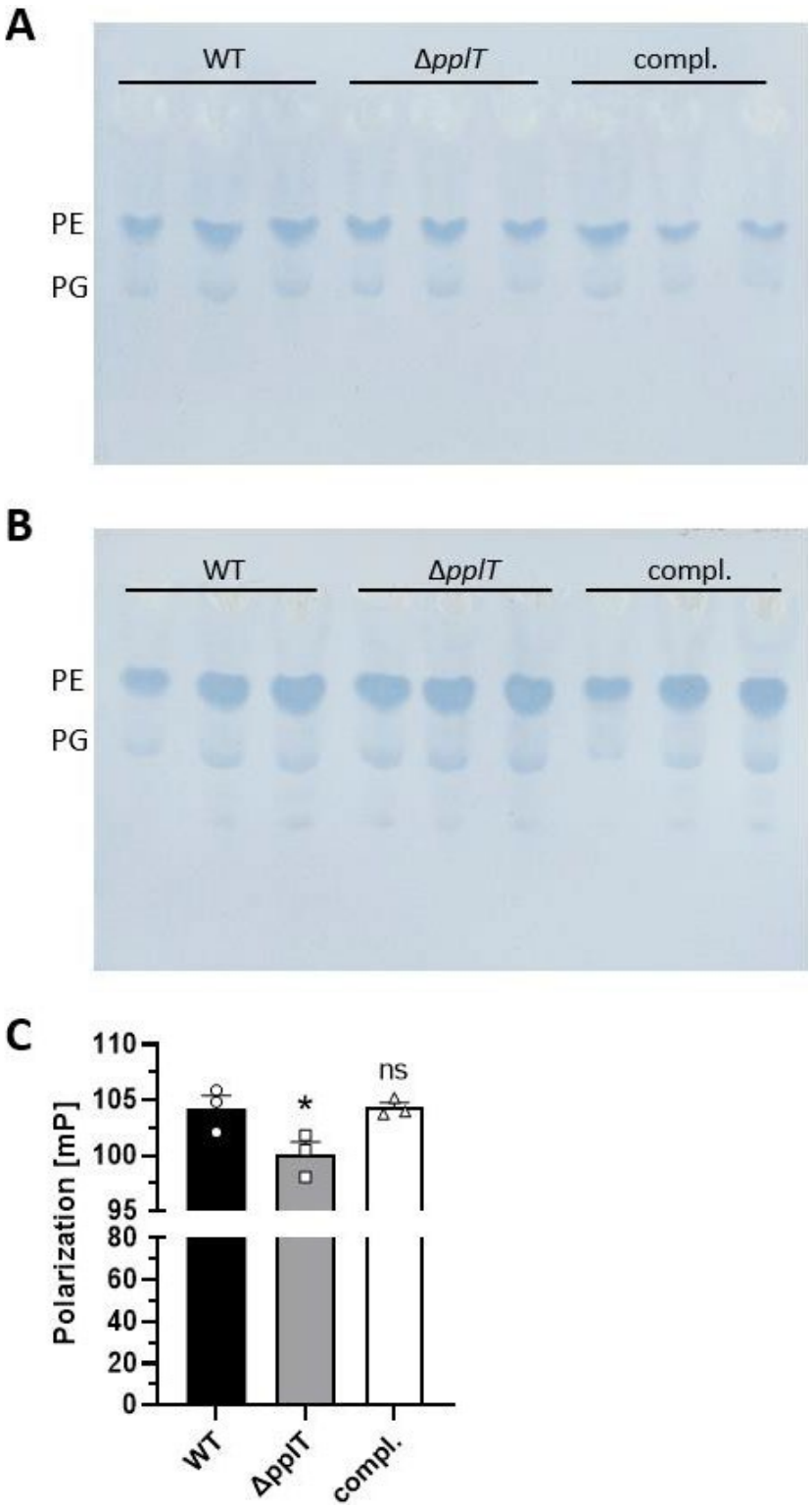

Figure 4: Impact of PplT on cell membrane lipid pattern and fluidity. Detection of phospholipids of *E. coli* CFT073 WT, *pplT* mutant and complemented mutant at exponential (A) or stationary (B) growth phase. Total lipids were isolated, separated via thin-layer chromatography and stained using molybdenum blue spray reagent. PE and PG spots are indicated, concentrations of the minor lipids PS and CL are too low to be detectable. Three biological replicates are represented. (C) Membrane fluidity analyzed via DPH staining. Bacterial cells were stained during exponential growth with DPH and polarization was measured. Means of three biological replicates with SEM are shown. Data were compared to the WT and statistically analyzed by one-way ANOVA (ns, not significant; *, $P < 0.05$).

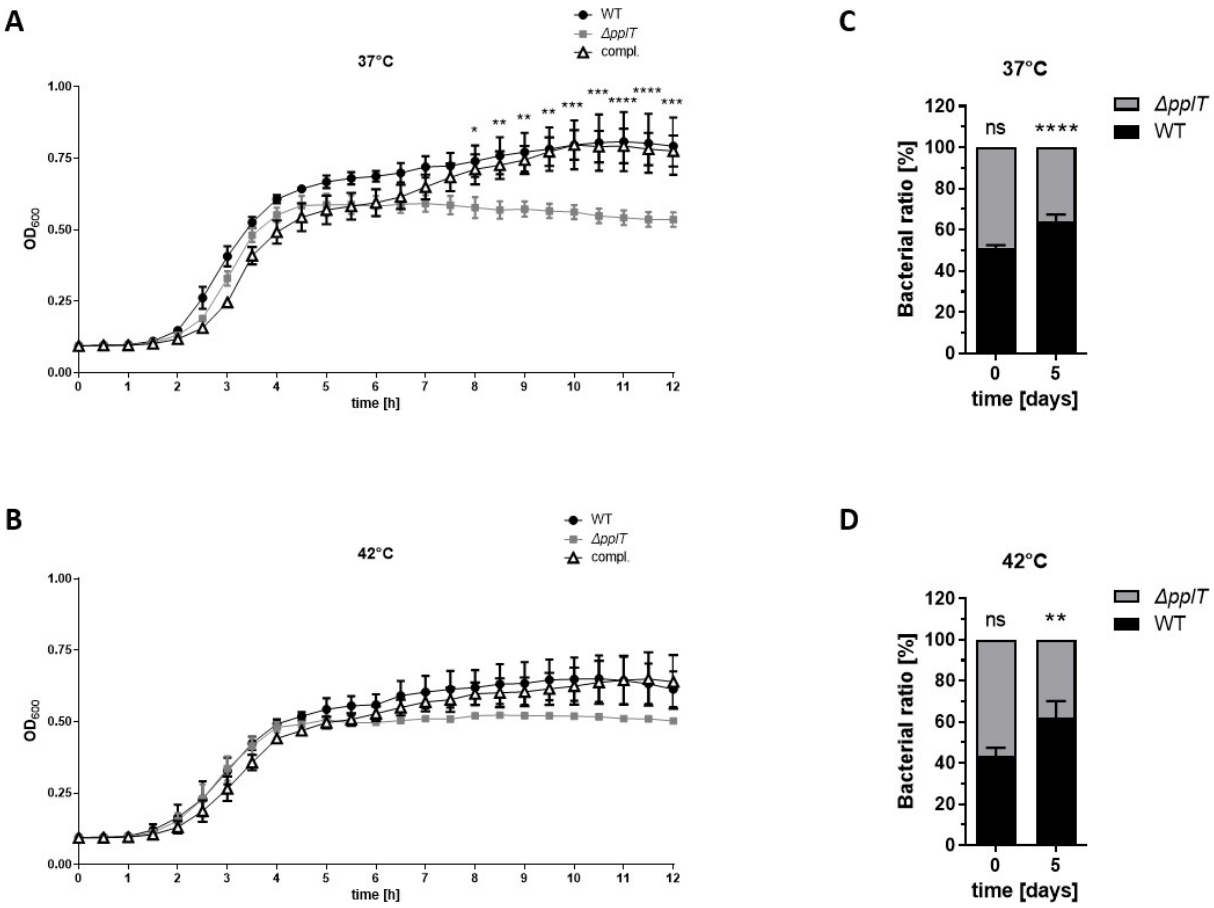

Figure 5: The *E. coli pplT* mutant exhibits a growth deficit compared to the WT. Growth curves of *E. coli* CFT073 WT, *pplT* mutant and complemented mutant at 37°C (A) or 42°C (B). Means of three biological replicates plus SEM are shown. The difference in growth between WT and *pplT* mutant was statistically analyzed by two-way ANOVA (*, P < 0.05; **, P < 0.01; ***, P < 0.0005; ****, P < 0.0001). Competition assay of WT and the *pplT* mutant over five days at 37°C (C) or 42°C (D). Means of three biological replicates with SD are shown. Data were statistically analyzed by two-way ANOVA and compared to the WT at the appropriate timepoint (ns, not significant; **, P < 0.01; ****, P < 0.0001).

Discussion

Phospholipids are synthesized at the inner leaflet of the cytoplasmic membrane but they need to be translocated to the outer leaflet to form a stable bilayer [1]. Phospholipids can flip spontaneously but this process is rather inefficient [23]. Appropriate membrane homeostasis therefore depends on dedicated flippases that translocate lipids. While such transporters are known for eukaryotic cells, their presence and nature in prokaryotes has remained largely unclear. ABC transporters translocating the lipid-bound precursors of peptidoglycan or teichoic acids have been identified [24, 25]. However, these molecules are usually highly specific and are unlikely to have a major impact on phospholipid translocation. Nevertheless, the lipid A translocating ABC transporter MsbA of *E. coli* has also a minor affinity for phospholipids [25]. The only dedicated bacterial phospholipid flippase described to date is the integral-membrane domain of MprF proteins, which connects the synthesis of aminoacyl phospholipids with their translocation [4, 5]. We show here that the flippase domain of MprF, named the PplT domain,

can be found as a separate protein or combined in modular proteins with other domains of diverse function, which supports a general role of PplT in bacterial and archaeal cells.

The PplT protein modulates the membrane fluidity and fitness of *E. coli*. The observed effects were moderate, which may be based on the fact that the lipid A flippase MsbA has also some basic phospholipid translocation capacity [25] and may compensate for the lack of PplT to some degree. *msbA* is essential though [16, 26], which precludes its simultaneous inactivation with *pplT*. The residual capacity of MsbA cell wall precursor flippases to translocate phospholipids may also explain why several bacterial species do not seem to encode obvious PplT orthologs. Membrane fluidity is strongly affected by temperature, which may explain the temperature-dependent impact of PplT in *E. coli*. It should be noted though that PplT domain proteins are also found in thermophilic microorganisms such as Thermotogae and archaeal extremophiles, suggesting that the translocation of certain lipids may require dedicated flippases even at high temperatures. The frequent combination of PplT with other enzymatic protein domains also suggests that certain modified lipids, potentially those with bulkier head groups, may be particularly dependent on cognate translocation machineries. Lipid translocation is a very dynamic process, which is difficult to monitor directly. Therefore, evidence for the flippase function of PplT proteins remains in part indirect. However, the fact that PplT interacts directly with most of the phospholipid-biosynthetic proteins of *E. coli* strongly underscores its central role in membrane homeostasis. Likewise, MprF proteins have been found to interact with larger phospholipid-biosynthetic protein complexes in *S. aureus* [17, 18].

It remains unclear how wide or narrow the substrate specificities of PplT domain proteins may be. Since *E. coli* does not produce aminoacyl phospholipids, PplT may translocate some or all of the *E. coli* phospholipids PG, CL, PS, and PE. These molecules differ in the net charge of their head groups, which has been found to be a major determinant for substrate recognition by the PplT domain of the *R. tropici* MprF [7]. Although the PplT domain of the *S. aureus* MprF is linked to synthesis of the cationic phospholipid Lys-PG, MprF has been found to also translocate the zwitterionic phospholipid Ala-PG [27], indicating that PplT proteins may have broader substrate specificities. In agreement with this assumption, a few point mutations have been shown to alter the function and probably substrate specificity of the *S. aureus* MprF [28].

It should be noted that most prokaryotic genomes with a PplT homolog contain only one PplT protein and only a minority encodes two (19.89%) or more (1.60%) of them, suggesting that one flippase is usually sufficient for most of the membrane-forming phospholipids. The presence or absence of certain conserved, charged amino acids in transmembrane segments of PplT domains may help to predict the substrate specificities of these proteins in the future.

Archaea have different phospholipids compared to bacterial ones, with monolayer-membrane forming isoprenoid lipids [29]. The broad presence of PplT proteins in Archaea suggest that these proteins can also flip such lipids, which are much bulkier than bacterial phospholipids

and contain two head groups, one at each end. It remains unclear if the PplT domain only facilitates the exchange of phospholipids between the inner and outer leaflet of cytoplasmic membranes or if it can translocate phospholipids in an energy-dependent fashion to generate asymmetric lipid patterns. Some of the transmembrane domains of MprF seem to be related to the proton-motif force-dependent major facilitator protein superfamily [30] and some studies found Lys-PG to be unevenly distributed between the two membrane leaflets [4], suggesting that PplT may use energy to translocate its substrate lipids.

Membrane homeostasis is an important fitness factor for all kinds of organisms. PplT proteins may therefore become attractive targets for future anti-fitness drugs to combat major human pathogens. In support of such a strategy, monoclonal antibodies directed against extracellular portions of the PplT domain of the *S. aureus* MprF have recently been shown by inhibiting the Lys-PG exposure at the outer leaflet of the membrane and therefore sensitize *S. aureus* to cationic antibiotics [9].

Materials and Methods

Occurrence and architecture of PplT in bacterial and archaeal taxa. In order to determine the distribution of PplT across the taxonomy a blastp search within NCBI's non-redundant protein database [31] was performed using the PplT/YbhN protein sequence of *E. coli* (old: NP_752801.1; new: WP_000045478.1) as a query and an E-value cutoff of 0.05. Blast hits originating from the superkingdoms Bacteria and Archaea were investigated separately. For each, the subtree of the NCBI taxonomy rooted at the respective superkingdom was thinned out for those taxa that possess a PplT homolog. The BLAST search and subsequent taxonomic visualization was performed with BLASTphylo [https://github.com/Integrative-Transcriptomics/BLASTphylo]. We used NCBI's Conserved Domain Architecture Retrieval Tool (CDART) [15] to identify different domain architectures that include a PplT domain. We used MicrobesOnline[32] to identify *pplT*'s operon structure in other Enterobacteriaceae.

Bacterial strains, mutagenesis, and maintenance. *E. coli* UPEC strain CFT073 (DSM103538) (Tab. S1) was used for *pplT* mutagenesis and analysis [33]. *pplT* was deleted in the chromosome of CFT073 as described previously [34]. Briefly, *E. coli* CFT073 was transformed with helper plasmid pKD46 encoding the Lambda-Red recombinase (Tab. S2) and incubated at 30°C on LB agar supplemented with ampicillin. The kanamycin resistance cassette with chromosomal DNA regions flanking *pplT* was amplified by PCR with primers pplT_KO_5 and pplt_KO_6 (Tab. S3) using pKD13 as template (Tab. S2). After arabinose-induced Lambda Red expression in *E. coli* CFT073 containing the helper plasmid, the PCR fragment was transferred by electroporation and cells were plated on kanamycin-containing LB agar for primary selection. After verification of the chromosomal *pplT* deletion by PCR (Tab. S3) and sequencing, mutants were streaked to single colonies on LB agar without antibiotics

at 37°C twice for curing of the temperature-sensitive helper plasmid. The loss of the helper plasmid pKD46 was confirmed by PCR (Tab. S3). The *pplT* deletion mutant was complemented by a *pplT* gene amplified from *E. coli* K12 and cloned in the *E. coli*/*S. aureus* shuttle vector pRB474 [35] (Tab. S2). All bacterial strains were grown in LB medium (Carl Roth) with appropriate antibiotics unless otherwise noted (Tab. S1).

Bacterial two-hybrid assay. To identify potential interaction partners of PplT, the commercially available bacterial two-hybrid kit (BATCH kit, Euromedex) was used [8, 19, 20] and the proteins to be studied were cloned as described previously [8]. The *pplT* gene was cloned in the high-copy number plasmid pUT18C, the potential interaction partners in the low copy-number plasmid pKT25 leading to C-terminal or N-terminal fusion with the adenylate cyclase fragments T25 or T18 of *Bordetella pertussis*, respectively (Tab. S2). The constructs were used to co-transform chemically competent *E. coli* BTH101. The resulting transformants were tested in a 96-well format for β-galactosidase activity, to quantify the protein-protein interaction as described previously [8] with slight modifications. Briefly, bacterial cells were grown at 30°C overnight in LB, supplemented with 0.5 mM isopropyl-β-D-thiogalactopyranoside (IPTG), 25 µg/ml kanamycin and 100 µg/ml ampicillin. 100 µl of the overnight cultures were used to measure the optical density at 600 nm (OD_{600}) in a 96-well microtiter plate (F-bottom, Falcon), another 100 µl were transferred into a deep 96-well plate (U-bottom, Sarstedt) and mixed with 1 ml buffer Z (60 mM Na_2HPO_4, 40 mM NaH_2PO_4, 10 mM KCl, 1 mM $MgSO_4$, 50 mM β-mercaptoethanol). To lyse the cells, 40 µl sodium dodecyl sulfate (0.1%) and 80 µl chloroform were added and mixed vigorously. After incubation at room temperature to allow phase separation, 100 µl of the aqueous phase were transferred into a 96-well microtiter plate (F-bottom, Falcon) and mixed with 20 µl o-nitrophenyl-β-D-galactopyranoside (4 mg/ml) to start the enzymatic reaction. The reaction was measured continuously for 1 h in a CLARIOStar plate reader (BMG Labtech) at OD_{420} and OD_{550}. The β-galactosidase activity in Miller Units was calculated by the formula: $1000*((OD_{420}-(1.75*OD_{550}))/(t*v*OD_{600}))$, where t is reaction time in minutes and v the reaction volume in milliliter.

Isolation of polar lipids. Polar lipids were extracted from bacteria grown to exponential or stationary phase using the Bligh-Dyer procedure [36]. Briefly, phospholipids were extracted by a mixture of sodium acetate buffer (20mM, pH 4.8), chloroform, and methanol (1:1:1 [by volume]), vacuum dried, and dissolved in chloroform-methanol (2:1 [by volume]). For detection of phospholipid patterns, appropriate amounts of polar lipid extracts were spotted onto silica gel high-performance thin-layer chromatography (HPTLC) plates (silica gel 60 F254, Merck) using a Linomat 5 sample application unit (CAMAG) and developed with chloroform:methanol:water (65:25:4 [by volume]) in an automatic developing chamber ADC 2

(CAMAG). Phospholipids were selectively stained with molybdenum blue spray reagent (1.3% in 4.2 M sulfuric acid, Sigma-Aldrich).

Measurement of the membrane fluidity. To measure the membrane fluidity of *E. coli* CFT073 WT and mutants, we used the method of fluorescence polarization upon staining with 1,6-diphenyl-1,3,5-hexatriene (DPH) as described previously [21, 22], with some modifications. Briefly, bacterial cultures grown to exponential phase were adjusted to an OD_{600} 1 and treated with a subinhibitory concentration of polymyxin B (30 µg/ml) for 30 min at 37°C for outer membrane permeabilization purposes. Bacteria were then stained with 8 µM DPH for further 30 min. After washing with PBS, DPH-stained bacteria were transferred to 96-well microtiter plate (F-bottom, black, Greiner) and fluorescence polarization was measured at an excitation wavelength of 360-10 nm, and emission wavelength of 450-10 nm in a CLARIOStar plate reader (BMG Labtech). Polarization values inversely correlate with membrane fluidity.

Bacterial growth assay. Temperature-dependent growth differences were analyzed in 96-well microtiter plate format. To this end, overnight cultures grown in LB with appropriate antibiotics were adjusted to OD_{600} 0.05 in fresh LB and 100 µl of the cell suspensions were transferred to a 96-well microtiter plate (F-bottom, Falcon) and growth was measured at OD_{600} in 30 min intervals at either 37°C or 42°C in an Epoch2 plate reader (BioTek).

To investigate growth differences of WT and *pplT* mutant in cocultivation, overnight cultures were adjusted to the same colony forming unit in fresh LB and used to inoculate a coculture, which was incubated in a shaking incubator at either 37°C or 42°C. Cells were passaged every 24 h in fresh LB for five days. To measure the numbers of live cells of the two competing strains, appropriate dilutions of the suspensions were spotted on LB agar plates with or without kanamycin. After incubation of the agar plates at appropriate temperatures, colonies were counted and ratios were calculated.

Statistics. Statistical analyses were performed with the Prism 8.4.2 package (GraphPad Software) and Group differences were analyzed for significance with one-way or two-way ANOVA. A P value of ≤0.05 was considered statistically significant.

Acknowledgement

We thank Anne Berscheid for providing plasmids pKD13 and pKD46, Cordula Gekeler and Ulrike Redel for technical support and Jennifer Müller for her contributions to the BLASTphylo project. This work was financed by Grants from Deutsche Forschungsgemeinschaft (DFG) SFB766 (to A.P.) and TRR261, project ID 398967434 (to K.N. and A.P), the German Center of Infection Research (DZIF) (to A.P. and C.S.). C.S. was also supported by the intramural Experimental Medicine program of the Medical Faculty at the University of Tübingen. The authors acknowledge project support (C.S.) and infrastructural support (C.S., K.N., A.P.) by the DFG Cluster of Excellence EXC2124 CMFI, project ID 390838134.

References

1. Zhang YM, Rock CO. Membrane lipid homeostasis in bacteria. Nat Rev Microbiol. 2008;6(3):222-33. doi: 10.1038/nrmicro1839. PubMed PMID: 18264115.
2. Dowhan W, Bogdanov M. Eugene P. Kennedy's Legacy: Defining Bacterial Phospholipid Pathways and Function. Front Mol Biosci. 2021;8:666203. Epub 2021/04/13. doi: 10.3389/fmolb.2021.666203. PubMed PMID: 33842554; PubMed Central PMCID: PMCPMC8027125.
3. López-Marqués RL. Lipid flippases in polarized growth. Curr Genet. 2021;67(2):255-62. Epub 2021/01/04. doi: 10.1007/s00294-020-01145-0. PubMed PMID: 33388852.
4. Ernst CM, Staubitz P, Mishra NN, Yang SJ, Hornig G, Kalbacher H, et al. The bacterial defensin resistance protein MprF consists of separable domains for lipid lysinylation and antimicrobial peptide repulsion. PLoS Pathog. 2009;5(11):e1000660. Epub 2009/11/17. doi: 10.1371/journal.ppat.1000660. PubMed PMID: 19915718; PubMed Central PMCID: PMCPMC2774229.
5. Ernst CM, Peschel A. Broad-spectrum antimicrobial peptide resistance by MprF-mediated aminoacylation and flipping of phospholipids. Mol Microbiol. 2011;80(2):290-9. Epub 2011/02/11. doi: 10.1111/j.1365-2958.2011.07576.x. PubMed PMID: 21306448.
6. Peschel A, Jack RW, Otto M, Collins LV, Staubitz P, Nicholson G, et al. Staphylococcus aureus resistance to human defensins and evasion of neutrophil killing via the novel virulence factor MprF is based on modification of membrane lipids with l-lysine. J Exp Med. 2001;193(9):1067-76. Epub 2001/05/09. doi: 10.1084/jem.193.9.1067. PubMed PMID: 11342591; PubMed Central PMCID: PMCPMC2193429.
7. Song D, Jiao H, Liu Z. Phospholipid translocation captured in a bifunctional membrane protein MprF. Nat Commun. 2021;12(1):2927. Epub 2021/05/20. doi: 10.1038/s41467-021-23248-z. PubMed PMID: 34006869; PubMed Central PMCID: PMCPMC8131360.
8. Ernst CM, Kuhn S, Slavetinsky CJ, Krismer B, Heilbronner S, Gekeler C, et al. The lipid- modifying multiple peptide resistance factor is an oligomer consisting of distinct interacting synthase and flippase subunits. mBio. 2015;6(1). Epub 2015/01/30. doi: 10.1128/mBio.02340-14. PubMed PMID: 25626904; PubMed Central PMCID: PMCPMC4324311.
9. Slavetinsky CJ, Hauser JN, Gekeler C, Slavetinsky J, Geyer A, Kraus A, et al. Sensitizing Staphylococcus aureus to antibacterial agents by decoding and blocking the lipid flippase MprF. Elife. 2022;11. Epub 2022/01/20. doi: 10.7554/eLife.66376. PubMed PMID: 35044295.

10. Yang M, Derbyshire MK, Yamashita RA, Marchler-Bauer A. NCBI's Conserved Domain Database and Tools for Protein Domain Analysis. Curr Protoc Bioinformatics. 2020;69(1):e90. Epub 2019/12/19. doi: 10.1002/cpbi.90. PubMed PMID: 31851420; PubMed Central PMCID: PMCPMC7378889.
11. Blum M, Chang HY, Chuguransky S, Grego T, Kandasaamy S, Mitchell A, et al. The InterPro protein families and domains database: 20 years on. Nucleic Acids Res. 2021;49(D1):D344-d54. Epub 2020/11/07. doi: 10.1093/nar/gkaa977. PubMed PMID: 33156333; PubMed Central PMCID: PMCPMC7778928.
12. Roy H, Ibba M. Broad range amino acid specificity of RNA-dependent lipid remodeling by multiple peptide resistance factors. J Biol Chem. 2009;284(43):29677-83. doi: 10.1074/jbc.M109.046367. PubMed PMID: 19734140; PubMed Central PMCID: PMCPMC2785599.
13. Cronan JE, Jr., Rock CO. Biosynthesis of Membrane Lipids. EcoSal Plus. 2008;3(1). Epub 2008/09/01. doi: 10.1128/ecosalplus.3.6.4. PubMed PMID: 26443744.
14. Furse S, Wienk H, Boelens R, de Kroon AI, Killian JA. E. coli MG1655 modulates its phospholipid composition through the cell cycle. FEBS Lett. 2015;589(19 Pt B):2726-30. Epub 2015/08/15. doi: 10.1016/j.febslet.2015.07.043. PubMed PMID: 26272829.
15. Geer LY, Domrachev M, Lipman DJ, Bryant SH. CDART: protein homology by domain architecture. Genome Res. 2002;12(10):1619-23. Epub 2002/10/09. doi: 10.1101/gr.278202. PubMed PMID: 12368255; PubMed Central PMCID: PMCPMC187533.
16. Baba T, Ara T, Hasegawa M, Takai Y, Okumura Y, Baba M, et al. Construction of Escherichia coli K-12 in-frame, single-gene knockout mutants: the Keio collection. Mol Syst Biol. 2006;2:2006.0008. Epub 2006/06/02. doi: 10.1038/msb4100050. PubMed PMID: 16738554; PubMed Central PMCID: PMCPMC1681482.
17. García-Lara J, Weihs F, Ma X, Walker L, Chaudhuri RR, Kasturiarachchi J, et al. Supramolecular structure in the membrane of Staphylococcus aureus. Proc Natl Acad Sci U S A. 2015;112(51):15725- 30. Epub 2015/12/09. doi: 10.1073/pnas.1509557112. PubMed PMID: 26644587; PubMed Central PMCID: PMCPMC4697411.
18. Weihs F, Wacnik K, Turner RD, Culley S, Henriques R, Foster SJ. Heterogeneous localisation of membrane proteins in Staphylococcus aureus. Sci Rep. 2018;8(1):3657. Epub 2018/02/28. doi: 10.1038/s41598-018-21750-x. PubMed PMID: 29483609; PubMed Central PMCID: PMCPMC5826919.
19. Karimova G, Gauliard E, Davi M, Ouellette SP, Ladant D. Protein-Protein Interaction: Bacterial Two-Hybrid. Methods Mol Biol. 2017;1615:159-76. Epub 2017/07/02. doi: 10.1007/978-1-4939-7033- 9_13. PubMed PMID: 28667611.

20. Griffith KL, Wolf RE, Jr. Measuring beta-galactosidase activity in bacteria: cell growth, permeabilization, and enzyme assays in 96-well arrays. Biochem Biophys Res Commun. 2002;290(1):397-402. Epub 2002/01/10. doi: 10.1006/bbrc.2001.6152. PubMed PMID: 11779182.
21. Chen Y, Reinhardt M, Neris N, Kerns L, Mansell TJ, Jarboe LR. Lessons in Membrane Engineering for Octanoic Acid Production from Environmental Escherichia coli Isolates. Appl Environ Microbiol. 2018;84(19). Epub 2018/07/22. doi: 10.1128/aem.01285-18. PubMed PMID: 30030228; PubMed Central PMCID: PMCPMC6146996.
22. Gohrbandt M, Lipski A, Grimshaw JW, Buttress JA, Baig Z, Herkenhoff B, et al. Low membrane fluidity triggers lipid phase separation and protein segregation in living bacteria. Embo j. 2022:e109800. Epub 2022/01/18. doi: 10.15252/embj.2021109800. PubMed PMID: 35037270.
23. Kol MA, de Kroon AI, Killian JA, de Kruijff B. Transbilayer movement of phospholipids in biogenic membranes. Biochemistry. 2004;43(10):2673-81. Epub 2004/03/10. doi: 10.1021/bi036200f. PubMed PMID: 15005602.
24. Swoboda JG, Meredith TC, Campbell J, Brown S, Suzuki T, Bollenbach T, et al. Discovery of a small molecule that blocks wall teichoic acid biosynthesis in Staphylococcus aureus. ACS Chem Biol. 2009;4(10):875-83. Epub 2009/08/20. doi: 10.1021/cb900151k. PubMed PMID: 19689117; PubMed Central PMCID: PMCPMC2787957.
25. Eckford PD, Sharom FJ. The reconstituted Escherichia coli MsbA protein displays lipid flippase activity. Biochem J. 2010;429(1):195-203. Epub 2010/04/24. doi: 10.1042/bj20100144. PubMed PMID: 20412049; PubMed Central PMCID: PMCPMC2888566.
26. Karow M, Georgopoulos C. The essential Escherichia coli msbA gene, a multicopy suppressor of null mutations in the htrB gene, is related to the universally conserved family of ATP-dependent translocators. Mol Microbiol. 1993;7(1):69-79. Epub 1993/01/01. doi: 10.1111/j.1365- 2958.1993.tb01098.x. PubMed PMID: 8094880.
27. Slavetinsky CJ, Peschel A, Ernst CM. Alanyl-phosphatidylglycerol and lysyl-phosphatidylglycerol are translocated by the same MprF flippases and have similar capacities to protect against the antibiotic daptomycin in Staphylococcus aureus. Antimicrob Agents Chemother. 2012;56(7):3492-7. Epub 2012/04/12. doi: 10.1128/aac.00370-12. PubMed PMID: 22491694; PubMed Central PMCID: PMCPMC3393434.
28. Ernst CM, Slavetinsky CJ, Kuhn S, Hauser JN, Nega M, Mishra NN, et al. Gain-of-Function Mutations in the Phospholipid Flippase MprF Confer Specific Daptomycin

Resistance. MBio. 2018;9(6). Epub 2018/12/20. doi: 10.1128/mBio.01659-18. PubMed PMID: 30563904; PubMed Central PMCID: PMCPMC6299216.

29. Caforio A, Driessen AJM. Archaeal phospholipids: Structural properties and biosynthesis. Biochim Biophys Acta Mol Cell Biol Lipids. 2017;1862(11):1325-39. Epub 2016/12/23. doi: 10.1016/j.bbalip.2016.12.006. PubMed PMID: 28007654.
30. Wang SC, Davejan P, Hendargo KJ, Javadi-Razaz I, Chou A, Yee DC, et al. Expansion of the Major Facilitator Superfamily (MFS) to include novel transporters as well as transmembrane-acting enzymes. Biochim Biophys Acta Biomembr. 2020;1862(9):183277. Epub 2020/03/25. doi: 10.1016/j.bbamem.2020.183277. PubMed PMID: 32205149; PubMed Central PMCID: PMCPMC7939043.
31. O'Leary NA, Wright MW, Brister JR, Ciufo S, Haddad D, McVeigh R, et al. Reference sequence (RefSeq) database at NCBI: current status, taxonomic expansion, and functional annotation. Nucleic Acids Res. 2016;44(D1):D733-45. Epub 2015/11/11. doi: 10.1093/nar/gkv1189. PubMed PMID: 26553804; PubMed Central PMCID: PMCPMC4702849.
32. Dehal PS, Joachimiak MP, Price MN, Bates JT, Baumohl JK, Chivian D, et al. MicrobesOnline: an integrated portal for comparative and functional genomics. Nucleic Acids Res. 2010;38(Database issue):D396-400. Epub 2009/11/13. doi: 10.1093/nar/gkp919. PubMed PMID: 19906701; PubMed Central PMCID: PMCPMC2808868.
33. Welch RA, Burland V, Plunkett G, 3rd, Redford P, Roesch P, Rasko D, et al. Extensive mosaic structure revealed by the complete genome sequence of uropathogenic Escherichia coli. Proc Natl Acad Sci U S A. 2002;99(26):17020-4. Epub 2002/12/10. doi: 10.1073/pnas.252529799. PubMed PMID: 12471157; PubMed Central PMCID: PMCPMC139262.
34. Datsenko KA, Wanner BL. One-step inactivation of chromosomal genes in Escherichia coli K- 12 using PCR products. Proc Natl Acad Sci U S A. 2000;97(12):6640-5. Epub 2000/06/01. doi: 10.1073/pnas.120163297. PubMed PMID: 10829079; PubMed Central PMCID: PMCPMC18686.
35. Bruckner R. A series of shuttle vectors for Bacillus subtilis and Escherichia coli. Gene. 1992;122(1):187-92. PubMed PMID: 1452028.
36. Bligh EG, Dyer WJ. A rapid method of total lipid extraction and purification. Can J Biochem Physiol. 1959;37(8):911-7. Epub 1959/08/01. doi: 10.1139/o59-099. PubMed PMID: 13671378.

Supplemental Material

Table S1: Bacterial strains.

Strain	Characteristics
E. coli CFT073	Uropathogenic wild type strain [33]
E. coli CFT073 Δ*pplT*	*pplT* chromosomal deletion mutant, *pplT* gene was replaced by kanamycin resistance cassette, Kan^R. This study.
E. coli CFT073 Δ*pplT* pRB*pplT*	*pplT* deletion mutant complemented by plasmid-encoded *pplT* version. This study.

Table S2: Plasmids.

Plasmid	Characteristics
pRB474*pplT*	*pplT* gene cloned in *E. coli*/*S. aureus* shuttle vector pRB474 [35], Amp^R.
pKD13	Template for Kanamycin resistance cassette. Amp^R, Kan^R [34].
pKD46	Lambda Red helper plasmid, Lambda Red expression inducible by L-arabinose. Amp^R [34].
pKT25-*clsA*	*clsA* gene encoded on low copy number plasmid pKT25 (Euromedex), fused to the C-terminal end of the adenylate cyclase fragment T25. This study.
pKT25-*clsB*	*clsB* gene encoded on low copy number plasmid pKT25 (Euromedex), fused to the C-terminal end of the adenylate cyclase fragment T25. This study.
pKT25-*clsC*	*clsC* gene encoded on low copy number plasmid pKT25 (Euromedex), fused to the C-terminal end of the adenylate cyclase fragment T25. This study.
pKT25-*ybhP*	*ybhP* gene encoded on low copy number plasmid pKT25 (Euromedex), fused to the C-terminal end of the adenylate cyclase fragment T25. This study.
pKT25-*pssA*	*pssA* gene encoded on low copy number plasmid pKT25 (Euromedex), fused to the C-terminal end of the adenylate cyclase fragment T25. This study.
pKT25-*psd*	*psd* gene encoded on low copy number plasmid pKT25 (Euromedex), fused to the C-terminal end of the adenylate cyclase fragment T25. This study.
pKT25-*pgsA*	*pgsA* gene encoded on low copy number plasmid pKT25 (Euromedex), fused to the C-terminal end of the adenylate cyclase fragment T25. This study.
pKT25-*pgpA*	*pgpA* gene encoded on low copy number plasmid pKT25 (Euromedex), fused to the C-terminal end of the adenylate cyclase fragment T25. This study.
pKT25-*pgpB*	*pgpB* gene encoded on low copy number plasmid pKT25 (Euromedex), fused to the C-terminal end of the adenylate cyclase fragment T25. This study.
pKT25-*pgpC*	*pgpC* gene encoded on low copy number plasmid pKT25 (Euromedex), fused to the C-terminal end of the adenylate cyclase fragment T25. This study.

pKT25-zip	Leucine zipper of GCN4 fused to the C-terminal end of the adenylate cyclase fragment T25. BATCH system kit, Euromedex.
pUT18C-*pplT*	*pplT* gene encoded on high copy number plasmid pUT18C (Euromedex), fused to the C-terminal end of the adenylate cyclase fragment T18. This study.
pUT18C-zip	Leucine zipper of GCN4 fused to the C-terminal end of the adenylate cyclase fragment T18. BATCH system kit, Euromedex.

Table S3: Primers.

Primer	**Sequence 5' → 3'**	**Usage**
pplT_KO_5	ATGCACATACTAAAGAACTTAACTATACTT CACATCGCCGCTTCATTTTTTGTAGGCTGG AGCTGCTTCG	Amplification of kanamycin resistance cassette from pKD13 with overhang homolog to the chromosomal *pplT* surrounding; for construction of the chromosomal *pplT* deletion mutant in *E. coli* CFT073.
pplT_KO_6	GAAACGCAGGATCGGGTAGAAACTGAAA ACACGGGGGTAAAACCCTGATGATTCCGG GGATCCGTCGACC	
pKD46_gone_1	CCCGTGCGTTTGATGACGATG	Primers to confirm the curing of the helper plasmid pKD46.
pKD46_gone_2	GGATTCATTGTCCTGCTCAAAGTCC	
pRB_pplT_BamHI_fw	AAATTATggatccCAGAGGAGGTCGGCTGA TGAGTAAATCAC	Cloning of *pplT* into pRB474 for plasmid-based complementation of the *pplT* deletion mutant.
pRB_pplT_EcoRI_rev	AAATTATgaattcAACTAAACTTCACATCGCC GCTTC	
pplT_up	ggttcgttgtgcttttatagg	Sequencing primers to verify the chromosomal pplT deletion mutant.
pplT_down	cttcccggcgctgg	
ClsA_BamHI_for	TAATCggatccTATGACAACCGTTTATACG	Cloning of *clsA* from *E. coli* CFT073 into pKT25 for bacteria two-hybrid.
ClsA_EcoRI_rev	ACGTTgaattcTTACAGCAACGGGCTG	
ClsB_BamHI_for	TCATTggatccTATGAAATGTAGCTGGCGCG	Cloning of *clsB* from *E. coli* CFT073 into pKT25 for bacteria two-hybrid.
ClsB_EcoRI_rev	ACTCAgaattcTCAGGGTTTTACCCCCGTG	
ClsC_BamHI_for	GTCTGTggatccTATGATGAAGAAAACGCCCAC	Cloning of *clsC* from *E. coli* CFT073 into pKT25 for bacteria two-hybrid.
ClsC_EcoRI_rev	CGCGTgaattcTTACAATAACCATTCCACGG	
YbhP_BamHI_for	GAAAATggatccTATGCCCGATCAAACAC	Cloning of *ybhP* from *E. coli* CFT073 into pKT25 for bacteria two-hybrid.
YbhP_EcoRI_rev	ACATTgaattcTCATAAATGAATCTCCGC	
PssA_BamHI_for	CATCCggatccTATGAAAATGACAAAACTGG	Cloning of *pssA* from *E. coli* CFT073 into pKT25 for bacteria two-hybrid.
PssA_EcoRI_rev	CAGGGgaattcTTACTGCGTGGTACCG	
Psd_BamHI_for	CACTGTggatccGATGTTGTCAAAATTTAAGCG	Cloning of *psd* from *E. coli* CFT073 into pKT25 for bacteria two-hybrid.
Psd_KpnI_rev	TGTGAgaattcTTACAGGATGCGGCTAATTAATC	
PgsA_BamHI_for	GCTACggatccCTTGTTAAATTCATTTAAAC	Cloning of *pgsA* from *E. coli* CFT073 into pKT25 for bacteria two-hybrid.
PgsA_EcoRI_rev	ATGGAggtaccTTAGACCTGGTCTTTTTTG	
PgpA_BamHI_for	GTCATggatccTATGCAATTTAATATCCCTAC	Cloning of *pgpA* from *E. coli* CFT073 into pKT25 for bacteria two-hybrid.
PgpA_EcoRI_rev	AACGAgaattcTCACTGATCAAGCAAATCTG	

PgpB_BamHI_for	AAGGAggatccTATGACCATTTTGCCACGCC	Cloning of *pgpB* from *E. coli* CFT073 into pKT25 for bacteria two-hybrid.
PgpB_EcoRI_rev	CACAAgaattcCTACGACAGAATACCCAGC	
PgpC_BamHI_for	GAGGCggatccCATGCGTTCGATTGCC	Cloning of *pgpC* from *E. coli* CFT073 into pKT25 for bacteria two-hybrid.
PgpC_EcoRI_rev	CAGCGgaattcTTAACTTTCTTGTTCTCGTTG	
pUT18_PplT_BamHI_for	CCCTGggatccGATGAGTAAATCACACCCGCG	Cloning of *pplT* from *E. coli* CFT073 into pUT18C for bacteria two-hybrid.
PplT_EcoRI_rev	ATACTgaattcTCACATCGCCGCTTCATTTTTC	
pKT25 fw_2	CAACTTCCGCGACTCGGCG	Sequencing primer to verify insert of pKT25.
pKT25 rev	gattaagttgggtaacgccag	
pUT18C for	CGTCACCCGGATTGCGGC	Sequencing primer to verify insert of pUT18C.
pUT18C rev	cggggctggcttaactatgc	

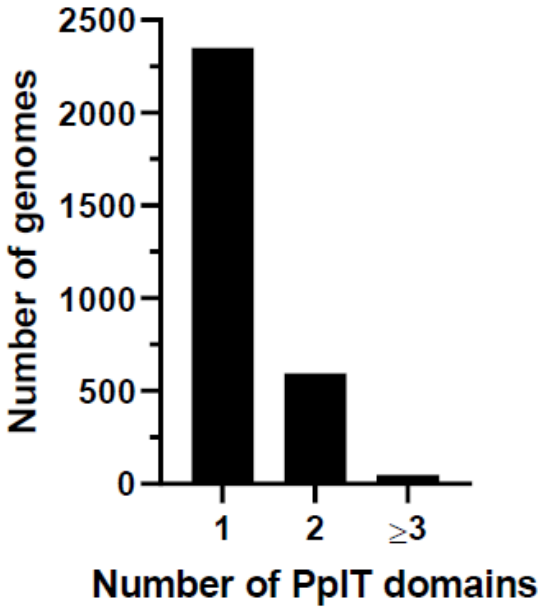

Figure S1: Most PplT containing genomes of prokaryotes harbor only one homolog. Number of genomes with one, two or more genes encoding PplT domains are shown.

Appendix

Protocol substituted cysteine accessibility method (SCAM)

Sensitizing Staphylococcus aureus to antibacterial agents by decoding and blocking the lipid flippase MprF; Elife. 2022 Jan 19;11:e66376. doi: 10.7554/eLife.66376

Reagents

- N*-(3-Maleimidylpropionyl) Biocytin (MPB) 10 mM in DMSO
  Nα-(3-Maleimidylpropionyl)Biocytin (MPB), 25mg; ThermoFisher M1602
- 4-Acetamino-4'-Maleimidylstilbene-2,2'-Disulfonic Acid (AMS) 10 mM in DMSO
  4-Acetamido-4'-Maleimidylstilbene-2,2'-Disulfonic Acid, Disodium Salt (AMS), 25mg; ThermoFisher A485

Buffer A		**for 100 ml**
HEPES	100 mM	2.38 g
sucrose	250 mM	8.56 g
$MgCl_2$	25 mM	2.5 ml of 1 M stock solution
KCl	0.1 mM	100 µl of 100 mM stock solution

→ adjust pH 7.5 with 1 M KOH (ca. 6 ml)
→ sterile filtration, store at 4°C

Buffer IP1 / IP2		**for 100 ml**
Tris-HCl	50 mM	5 ml of 1 M stock solution
NaCl	150 mM/1M	876.6 mg/5.844 g
EDTA	1 mM	200µl of 0.5 M stock solution
Thesit	2%	2 ml; added in 500 µl portions
SDS	0.4%	400 mg

→ pH 8.1 with NaOH/HCl

Solubilisation buffer		**for 100ml**
Tris-HCl	50 mM	5 ml of 1 M stock solution
EDTA	1 mM	200 µl of 0.5 M stock solution
SDS	2%	2 g; buffer can be carefully warmed in the microwave to solve the SDS

Further stock solutions

- $MgSO_4$ 1 M (12.04 g/100 ml)
- $MgCl_2$ 1 M (20.33 g/100 ml)
- KCl 100 mM (0.0746 g/10 ml)
- EDTA 0.5 M, pH 7.5; (14.61 g/100 ml + first ca. 40 NaOH-pllts.)
- β-ME 2 M (β-Mercaptoethanol) (3.5 ml for 25 ml Stock)
- Glycin HCl 0.1 M, pH 2.2
- Tris-HCl 1 M, pH 9 (15.76 g/100 ml)
- MPB 10 mM (5.236 mg/1 ml DMSO)
- AMS 10 mM (5.36 mg/1 ml DMSO)
- Proteinase inhibit. 1 pellet dissolved in 5 ml water, aliquoted and stored at -20°C

O/N culture

1	O/N culture in 10ml TSB + appropriate AB, 37°C shaking incubator

Main culture and labelling

1	Inoculate 100ml TSB + AB in Flask to OD_{600} = 0.1 Grow for 2:15h (OD_{600} ≈ 0.75) at 37°C with shaking			
2	**From now work on ice!** Harvest cells in 2 x 50 ml Falcon; 10 min, 4700 rpm, 4°C Prepare tubes for step 6-12; cool down UZ			
3	Resuspend cell pellet in 700µl Buffer A + 0.7 µl $MgSO_4$, 0.04 µl lysozyme, 7 µl protease inhibitor, 0.7 µl DNase, 1.4 µl EDTA (pH 7.5) and 2.1 µl Lysostaphin. avoid bubbles (would damage membrane)			
4	15min on ice, afterwards 45min at 37°C			
5.1	Labelling outside: + 7.5 µl 10 mM MPB Incubate for 20 min on ice quench reaction: +7.5µl 2 M β-ME		5.2	Blocking outside: 7.5 µl 10 mM AMS Incubate for 20 min on ice do not quench reaction
6	Add samples to 0.5 ml pre-cooled glass beads in 1.5ml flat-bottom screw cap tube			
7	Bead mill 35 s at 6 m/s once			
8	-		8.1	Labelling inside: + 7.5 µl 10 mM MPB Incubate for 6 min on ice quench reaction: +7.5 µl 2 M β-ME
9	Centrifuge 1 min, 1000xg, 4°C Transfer supernatant into new 1.5 ml tube, avoid beads (as possible)			
10	Centrifuge 2 min, 10 000xg, 4°C Transfer 420µl (bzw. equal volumes) supernatant into 1.5 ml Ultracentrifugation tube. **TARE!**			
11	Ultracentrifuge 35 min, 38 000xg, 4°C. Remove supernatant completely, pellet should be mostly yellow/translucent			
12	Freeze pellet at -80°C ON			

Immunoprecipitation

1	Thaw samples on ice. (~40min)
2	+100 µl buffer A (pH 7.5) + 0.02 M β-ME, vortex at 1400 rpm, 1h, 4°C
3	+ 100 µl solubilisation buffer vortex at 1400 rpm, 30 min, 4°C

	keep for 30 min at 37°C vortex at 1400 rpm, 30 min, 4°C
4	+ 300 µl buffer IP1, vortex shortly Centrifuge max speed, 10min, 4°C
5	Prepare Magnetic FLAG beads: Keep beads and rack on ice. Take 12.5 µl FLAG bead slurry per sample. Pipette into 1.5ml tube, remove liquid. Wash 2 times with 2 x volumes of buffer IP1 Remove buffer, add 1.5 x volumes (slurry) buffer IP1 and transfer 20 µl beads per sample into 1.5 ml tube
6	Load beads with FLAG-tagged protein: Add supernatant (from step 4) on top of magnetic beads. Incubate 2.5 h rotating at 4°C.
7	Wash 4 x with 100 µl IP buffer; 2 x with IP1, 2 x with IP2
8	Elution: Remove the buffer and add 30 µl of 0.1 M glycine HCl pH 2.2 Incubate 2 x 8 min on ice, mix between the 2 x 8 min by pipetting up and down
9	Prepare 1.5 ml tubes with 3 µl 1 M Tris-HCl (pH 9). Transfer the eluate (from step 8) to the prepared tubes.
10	Store at 4°C. (best avoid)

Preparation of SDS gels (8x)

1	Clean glass equipment with ethanol, assemble gel preparation appliance
2	Prepare **separative gel**: H_2O 15,9ml 1,5M Tris-HCl (pH 8,8) 10ml 10% SDS solution 200µl 30% acrylamide 13,3ml APS 400µl TEMED 16µl Mix by inverting the Falcon tube carefully. Infuse the gel mixture between the glass plates, avoid bubbles. Cover the surface with isopropanol. Let the gel solidify completely (~20min)
3	Remove isopropanol from the gel surface
4	Prepare **stocking gel**: H_2O 13,6ml 1M Tris-HCl (pH 6,8) 2,5ml 10% SDS solution 200µl 30% acrylamide 3,4ml APS 200µl

	TEMED 20µl Mix by inverting the Falcon tube carefully. Infuse the gel mixture between the glass plates on top of the separative gel, avoid bubbles. Insert the pocket former into the wet gel. Let the gel solidify completely
5	Wrap always 2 gels into a wet paper towel and pack the gels into a small garbage bag. Store the gels at 4°C. Gels are usable for ~1 month

Antibodies

1st AB: Streptavidin (800nm) 1:5000 **+ anti-FLAG** 1:10000

Thermo Fisher: Streptavidin Protein, DyLight 800 conjugate, 21851

Sigma-Aldrich: Monoclonal ANTI-FLAG® M2 antibody produced in mouse, F3165-.2MG

2nd AB: anti-mouse (700nm) 1:10000

Li-COR IRDye 680RD goat anti-mouse secondary antibody

SDS PAGE

1	12 µl sample + 4 µl 4 x SDS sample buffer → 45°C, 5 min
2	Inject samples on SDS Gel (5 µl page ruler and all of the sample)
3	15 mA per Gel, 15 min
4	35 mA per Gel, 45-60 min

Western Blot

1	Activate membrane (Immobilion FL PVDF) in methanol, soak whatsmann paper in westernblot buffer	
2	Layers for semidry turbo blot (BioRad): **Top** 4. Whatman paper (soaked in 1x Westernblot buffer) 3. SDS gel 2. Activated membrane 1. 1x Whatman paper (soaked in 1x Westernblot buffer) **Bottom**	
3	Blotting: 30 min, 25 V	
4	Take off gel (should be empty)	
5	Blocking membrane: Incubate membrane for 25 min in blocking buffer (Thermo); 10 ml per membrane	Can be done over night
6	Wash 2-3 x with 1 x TBST	Can be done over night
7	1st antibody: Streptavidin 1:5000 + αFLAG 1:10000 (2 µl Strep + 1 µl αFlag in 10 ml TBST per membrane) for 1:20 h slewing	
8	Wash 3 x 5 min with 1 x TBST	Can be done over night

9	2nd antibody: anti-mouse 1:10000 (1 µl in 10 ml TBST per membrane) for 1 h slewing	Can be done over night
10	Wash 3 x 5 min with 1 x TBS (not TBST)	Can be done over night
11	Detection by LICOR: 1. Put Membrane on field 2. Moisturize membrane with ddH_2O 3. Put rubber cover on top, roll with roller, close lid. 4. Start Image Studio → Janna_Cys Adjust size of membrane. 2 channels (700nm and 800nm), Preview, Start.	

Contributions to publications

Chapter 1 – Prokaryotic Phospholipid Translocation in Cytoplasmic Membranes (ready for submission)
I wrote the manuscript and generated all figures. Andreas Peschel and Christoph J Slavetinsky edited the manuscript.

Chapter 2 – Gain-of-Function Mutations in the Phospholipid Flippase MprF Confer Specific Daptomycin Resistance
I provided the strain pRB-P314L, determined the impact of calcium addition on cross-resistance to calcium-independent antibiotics (Fig. S1) and validated the T345A findings by determining the impact of T345A, V351E, and S337L on cytochrome c binding (Fig. 3B) and cross-resistance to antibiotics (Fig. 4A).

Chapter 3 – Sensitizing Staphylococcus aureus to antibacterial agents by decoding and blocking the lipid flippase MprF
For this publication, I constructed the strains WT(-Cys), pRB-T263C, pRB-A99C, pRB-T480C, performed and analyzed SCAM (Figure 2B) and functionality testing of MprF under cysteine replacement (Figure 2 – figure supplement 1), investigated the dose dependency of M-C7.1 and nisin on killing of S. aureus (Figure 3 – figure supplement 1), wrote, reviewed and edited the manuscript (in parts or complete).

Chapter 4 – Prokaryotic Phospholipid Translocation by ubiquitous PplT domain proteins (preprint)
I constructed all strains, performed and analyzed all experiments by myself except for the bioinformatic analysis (Figure 1 and Figure S1) and membrane polarization (Figure 4C). I wrote, reviewed and edited the manuscript (in parts or complete).

Curriculum vitae

removed